

University of Southampton Research Repository

Copyright © and Moral Rights for this thesis and, where applicable, any accompanying data are retained by the author and/or other copyright owners. A copy can be downloaded for personal non-commercial research or study, without prior permission or charge. This thesis and the accompanying data cannot be reproduced or quoted extensively from without first obtaining permission in writing from the copyright holder/s. The content of the thesis and accompanying research data (where applicable) must not be changed in any way or sold commercially in any format or medium without the formal permission of the copyright holder/s.

When referring to this thesis and any accompanying data, full bibliographic details must be given, e.g.

Thesis: Author (Year of Submission) "Full thesis title", University of Southampton, name of the University Faculty or School or Department, PhD Thesis, pagination.

Data: Author (Year) Title. URI [dataset]

University of Southampton

Faculty of Engineering and Physical Sciences

Civil, Maritime and Environmental Engineering

Engineering Analysis of 19th Century British Merchant Ships

by

Sophie Annabel Mary Cannon

Thesis for the degree of Doctor of Philosophy

September 2019

Abstract

Abstract

Faculty of Engineering and Physical Sciences

Civil, Marine and Environmental Engineering

Thesis for the degree of Doctor of Philosophy

Engineering Analysis of 19th Century British Merchant Ships and Shipbuilding

by

Sophie Annabel Mary Cannon

Previous analysis of the evolution of 19th Century British merchant ships has been primarily qualitative. This research aims to develop a method to quantitatively analyse historic ship performance and to challenge present conceptions of ship design in the 19th Century. Literature indicates that this was a period of change, with the transformation from wooden sailing ships to steel steam ships. A parametric study of existing hull data demonstrates the potential to carry out a diachronic study of changes to ship design and performance. However, there is insufficient data to draw conclusions on performance factors such as ship speed. This is countered by the creation of a new dataset, based on a velocity prediction program (VPP) designed to calculate the sailing performance of historic ships. With few examples of these vessels remaining, the VPP must work with minimal input data. Regression-based methods used in initial ship design have therefore been identified and validated using CFD, forming the basis of the VPP. The input data comes from lines plans and builder's half models from maritime museums around Britain. With the correct methodology, a large amount of information can be extracted from these sources. Tests show that 3D scanning of half models can be used to create a lines plan, which can be converted into digital models. This allows a new set of hull data to be generated. Where available, sail plans are used to calculate sail areas, with regression lines to provide estimates where there is no sail plan. Weights and centres are estimated in a similar way based on survey reports.

61 British ships from throughout the 19th Century were digitised. The parameters extracted are used to generate a set of speeds under different conditions using the VPP. A second parametric analysis was carried out with the new data, enabling narratives to be visualised where it was previously impossible. This shows that advances in performance were driven by hull form, and the historic understanding of hydrodynamics and its impact on design may be traced. Comprehension of the evolution of these ships has also been challenged. Tonnage laws are often credited with causing changes to hull form and performance, but the data indicates that any effect they had was more gradual and less than previously suggested. The same appears to be true for the repeal of the Navigation Acts, as British ships had been gradually improving prior to this. The view of different ship types is also questioned. The dataset indicates that East Indiamen, often treated as obsolete, were capable of reaching speeds equal to some ships of the 1850s. It is also shown that average windjammers had greater capacity and upwind sailing performance than clippers.

The understanding of the evolution of 19th Century British merchant ships has been advanced by the creation of a new methodology for determining the performance of historic ships. Along with the generation of a new dataset, this provides a fresh view of a topic that has been extensively commented on qualitatively and can now be analysed quantitatively.

Abstract

Contents

Contents.....	i
Table of Figures.....	iv
List of Tables	viii
Research Thesis: Declaration of Authorship	xi
Acknowledgements.....	xiii
Nomenclature	xv
List of Abbreviations	xvi
Glossary.....	xvii
Timeline.....	vii
Chapter 1: Introduction	1
1.1 Research Question	2
1.2 Aims and Objectives.....	3
1.3 Novelty.....	4
1.4 Overview of Thesis	4
Chapter 2: Background and Literature Review.....	7
2.1 Evolution of Merchant Shipping in the 19 th Century	7
2.2 Naval Architecture in the 19 th Century	12
2.3 Analysis of 19 th Century Merchant Ships	17
2.4 Availability of Information	20
2.5 Parameter Based Performance Analysis.....	23
2.6 Digital Reconstruction of Hull Forms	25
2.6.1 3D Scanning.....	26
2.7 Velocity Prediction Programs.....	27
2.8 Resistance Estimation of Historic Ships	29
2.8.1 Full-Scale Replicas	30
2.8.2 Regression Based Methods.....	31
2.8.3 Computational Fluid Dynamics	34
2.8.4 Contemporary Trial Data.....	35
2.9 Hydrodynamic Side Force Estimation Methods.....	35
2.9.1 Resistance Due to Leeway	39

Contents

2.10 Propulsion Forces	40
2.10.1 Sail Propulsion	40
2.10.2 Steam Propulsion.....	41
2.11 Heeling/Righting Moments.....	42
2.12 Summary.....	42
Chapter 3: Parametric Analysis of Existing Data	45
3.1 Variation of Hull Dimensions	46
3.2 Variation of Performance with Time	53
3.3 Summary.....	55
Chapter 4: Development of a Velocity Prediction Program	57
4.1 Cutty Sark and Storm Cloud.....	57
4.2 Hydrodynamic Resistance Estimation	58
4.2.1 Comparison of Resistance Methods with Historic Data	63
4.2.2 Comparison of Resistance Methods with CFD	64
4.2.3 Sensitivity of CFD to mesh density	66
4.2.4 Resistance Sensitivity.....	67
4.3 Hydrodynamic Side Force Estimation.....	69
4.3.1 Added Resistance Due to Side Force	70
4.3.2 Comparison of Hydrodynamic Side Force Methods for Different Vessels	70
4.3.3 Comparison of Hydrodynamic Side Force Methods with CFD.....	72
4.3.4 Hydrodynamic Side Force Sensitivity.....	75
4.4 Sail Force Estimation	75
4.5 Righting and Heeling Moments	77
4.5.1 Effect of Heel Angle on Hydrostatics	77
4.5.2 Effect of Heel Angle on Resistance and Hydrodynamic Side Force	78
4.5.3 VCG Sensitivity.....	80
4.6 Velocity Prediction Program Design	81
4.6.1 VPP Sensitivity	86
4.7 Summary.....	88
Chapter 5: Selection and Digitisation of Primary Data.....	91
5.1 Selection of Ships for Analysis	91
5.2 Creation of Digital Hull Models.....	93
5.2.1 Modelling from a Lines Plan	93
5.2.2 Modelling from a Half-Model	95
5.2.3 Post-processing of the Scanned Data	97

Contents

5.2.4	Resistance Comparisons	100
5.2.5	Reliability of Scanned Hull Forms.....	102
5.3	Calculation of Sail Areas.....	105
5.4	Estimate of Centre of Gravity.....	110
5.4.1	Structure	111
5.4.2	Rig.....	114
5.4.3	Machinery and Coal	115
5.4.4	Cargo, Crew and Ballast	116
5.5	Summary	119
Chapter 6:	Modelled Data and Case Studies	121
6.1	Re-analysis of Data.....	121
6.2	The Driving Forces behind Change.....	128
6.2.1	Hull vs. Sails.....	128
6.2.2	Changes to Understanding Hydrodynamics.....	130
6.2.3	Impact of the Tonnage Laws	137
6.2.4	International Influence	141
6.3	Technical Impact	143
6.3.1	The Effect of Rigs.....	143
6.3.2	The Decline of the East India Company	148
6.3.3	Clippers and Windjammers.....	153
6.4	Summary	157
Chapter 7:	Conclusions and Future Work.....	159
7.1	Conclusions	159
7.2	Future Work	160
References	163
Appendix A	VPP Calculations.....	173
A.1	Holtrop Resistance Estimation.....	173
A.2	Fung Resistance Estimation	174
A.3	Kijima (1990) Side Force Estimation	177
A.4	Victory Sail Force Estimations	177
Appendix B	Ship Data	180
Appendix C	Gantt Chart.....	242

Table of Figures

Figure 1: Diagram showing how Alexander Hall of Aberdeen intended to reduce tonnage according to the 1836 rule using an extended (Aberdeen) bow (MacGregor, 1988, p. 106)	9
Figure 2: Chapman's bow wave (Q-P). Hull moving from right to left (Stoot, 1959, p. 35)	14
Figure 3: Scott Russell's wave-line theory bow (Scott Russell, 1860b, fig. 1).....	15
Figure 4: C_B with V_S for various ship types (Watson and Gilfillan, 1977, p. 284).....	24
Figure 5: Force balance required for VPP	28
Figure 6: Breakdown of different resistance estimation methods.....	29
Figure 7: Series hull shapes supplied by the Wolfson Suite 2016 PowerPrediction Software (Wolfson Unit, 2016) and body plan of the <i>Cutty Sark</i> (Lubbock, 1924, p. 31).....	30
Figure 8: Accuracy and cost of manoeuvring prediction methods (ITTC, 2008, p. 146)	39
Figure 9: Spread of ships included in the dataset over time	46
Figure 10: Variation in L/B ratio for sailing and steam ships.....	48
Figure 11: L/B envelopes for sail and steam data, including standard deviation (σ) and averages.	49
Figure 12: Variation of length with time	50
Figure 13: Variation of beam with time.....	50
Figure 14: Variation in B/T ratio with time	51
Figure 15: Variation of L/T with time.....	52
Figure 16: Variation in $L/\nabla^{1/3}$ with time	53
Figure 17: Variation of maximum (highest) recorded V_S with time	54
Figure 18: Variation of Froude number with time.....	55
Figure 19: Hull model of <i>Cutty Sark</i>	58
Figure 20: Hull model of <i>Storm Cloud</i>	58
Figure 21: R_T estimations from <i>MAXSURF Resistance</i>	59
Figure 22: Comparison of Fung and Holtrop methods and Tonry et al. (2014) for <i>Cutty Sark</i>	61
Figure 23: Breakdown of resistance components for the Holtrop method	62
Figure 24: Breakdown of resistance components for the Fung Method	62
Figure 25: Towing set up for trials of <i>HMS Greyhound</i> (Froude, 1874).....	63

Contents

Figure 26: Comparison of Holtrop and Fung methods with data from trials of <i>HMS Greyhound</i>	64
Figure 27: Comparison of CFD results with regression based estimates for <i>Cutty Sark</i>	65
Figure 28: Comparison of CFD results with regression based estimates for <i>Storm Cloud</i>	65
Figure 29: Varying mesh density against R_T and time steps required for $V_S = 11$ kn.....	66
Figure 30: Change in average actual time per time step with varying mesh density.....	67
Figure 31: Variation of R_T with changes in parameter at $V_S = 6$ kn.....	68
Figure 32: Variation of R_T with changes in parameter at $V_S = 15$ kn.....	68
Figure 33: Comparison between S_H estimation methods at $V_S = 15$ kn.....	69
Figure 34: Proposed method of estimating R_λ	70
Figure 35: Variation between Inoue and Kijima (1990) for different vessels ($V_S = 15$ kn $\lambda = 15^\circ$)....	71
Figure 36: Comparison of S_H from CFD with estimated S_H for <i>Cutty Sark</i> at $V_S = 11$ kn.....	72
Figure 37: Comparison of S_H from CFD with estimated S_H for <i>Cutty Sark</i> at $V_S = 15$ kn.....	73
Figure 38: Estimated R_λ compared to R_λ from CFD for <i>Cutty Sark</i> at $V_S = 11$ kn.....	74
Figure 39: Estimated R_λ compared to R_λ from CFD for <i>Cutty Sark</i> at $V_S = 15$ kn	74
Figure 40: Variation S_H with changes in parameter at $V_S = 15$ kn	75
Figure 41: Full rigged ship (top) and Barque (bottom)	76
Figure 42: Effect of ϕ on R_T for <i>Cutty Sark</i>	78
Figure 43: Effect of ϕ on S_H for <i>Cutty Sark</i> at $V_S = 11$ kn	79
Figure 44: Effect of ϕ on $R_T + R_\lambda$ for <i>Cutty Sark</i> at $\lambda = 5^\circ$	79
Figure 45: Effect of changing VCG on output heel angle ($V_T = 25$ kn, $\gamma = 130^\circ$, $\theta = 50^\circ$)	80
Figure 46: Diagram showing sail angles used in the VPP	83
Figure 47: Flow Chart describing the VPP	84
Figure 48: Polar performance diagram for <i>Cutty Sark</i> at $V_T=20$ kn, $\theta=50^\circ$	85
Figure 49: Variation in λ with γ for <i>Cutty Sark</i> at $V_T=20$ kn, $\theta=50^\circ$	86
Figure 50: Variation in ϕ with γ for <i>Cutty Sark</i> at $V_T=20$ kn, $\theta=50^\circ$	86
Figure 51: Variation of V_S with changes in parameter ($V_T = 25$ kn, $\gamma=140^\circ$, $\theta=50^\circ$)	87
Figure 52: Structured point cloud with curves constructed from the lines of <i>Cutty Sark</i>	94
Figure 53: Comparison between modelled sections (red) and original lines plan (black).....	95
Figure 54: Model rendered with Gaussian curvature to indicate hull fairness	95

Contents

Figure 55: Half model design for <i>Cutty Sark</i>	96
Figure 56: <i>Cutty Sark</i> half model	96
Figure 57: STL file from scanning the <i>Cutty Sark</i> half model in the dark using <i>Sense™</i> scanner	97
Figure 58: Scanned hull (red) adjusted to fit original lines plan (black)	98
Figure 59: Lines projected onto the half model mesh.....	99
Figure 60: Comparison of <i>Cutty Sark</i> digital model (green) with scaled projected scan lines (red)	99
Figure 61: Comparison between particulars for scan post-processing methods.....	100
Figure 62: Comparison of R_T for the scanned models relative to the original	101
Figure 63: Difference between V_s of <i>Cutty Sark</i> between the original and the scanned models ..	102
Figure 64: MacGregor's comparison of lines and model of <i>Schomberg</i> (Image: Brunel Institute) ..	103
Figure 65: V_s for lines based models and scan based models in sailing condition 1.....	105
Figure 66: Marked up sail plan of the <i>Cutty Sark</i> (Sail Plan courtesy of the Brunel Institute)	106
Figure 67: Sail area estimation of sailing vessels.....	108
Figure 68: Sail area estimation of steam-powered vessels	109
Figure 69: Vertical centre of sail area above load waterline.....	110
Figure 70: Longitudinal centre of sail area from aft perpendicular	110
Figure 71: Principal scantlings for <i>Acasta</i> (1845) (Courtesy of Lloyd's Register)	112
Figure 72: Structural model of <i>Acasta</i> based on the Lloyd's Register survey report	112
Figure 73: Structural weight estimations based on survey reports	114
Figure 74: Estimates of mast mass based on plans and survey reports.....	115
Figure 75: Machinery mass from literature compared to NHP	116
Figure 76: Relationship between Δ and NRT for cargo estimate	117
Figure 77: Stowage of Tea (Stevens, 1894, p. 669)	118
Figure 78: Modelled L/B compared with literature.....	121
Figure 79: Variation of $L/\nabla^{1/3}$ ratio with time including modelled data.....	122
Figure 80: Variation of C_p with time using modelled data.....	123
Figure 81: Change in C_{ws} with time	124
Figure 82: Maximum V_s in a 30 kn wind	125
Figure 83: Average speeds for sailing vessels in a 30 kn wind at 5-year intervals	126

Contents

Figure 84: Maximum F_n in a 30 kn wind.....	126
Figure 85: Measure of stability with time.....	127
Figure 86: Changes to C_{RT} against time at a V_s of 5 kn.....	129
Figure 87: Changes to C_{RT} against time at a V_s of 10 kn.....	130
Figure 88: Changes to C_T against time ($V_s = 10$ kn, $\gamma = 130^\circ$, $\theta = 40^\circ$)	130
Figure 89: i_E with time.....	132
Figure 90: Change in position of LCB with time	132
Figure 91: Variation in C_F and C_W with time at $V_s = 5$ kn.....	134
Figure 92: Variation in C_F and C_W with time at $V_s = 10$ kn between 1840 and 1900.....	135
Figure 93: Variation of B/D ratio with time for sailing ships.....	136
Figure 94: Variation of L/B ratio with time for sailing ships	136
Figure 95: Variation of tonnage/ ∇ ratio with time for sailing ships	138
Figure 96: Effect of tonnage laws on B/D	139
Figure 97: Average B/T and B/D ratios for sailing ships compared with Salisbury's value (Salisbury, 1966, p. 338)	139
Figure 98: Effect of tonnage laws on L/D	140
Figure 99: Effect of tonnage laws on i_E with a 5-year average line for sailing ships.....	141
Figure 100: Increasing V_s of British ships in relation to American clippers ($V_T = 30$ kn).....	143
Figure 101: V_s of ship-rigged vessels relative to barque-rigged downwind ($V_T = 15$ kn, $\gamma = 130^\circ$)	144
Figure 102: V_s of ship-rigged vessels relative to barque-rigged upwind ($V_T = 15$ kn, $\gamma = 70^\circ$).....	144
Figure 103: Comparison between ship and barque-rigs for <i>Wendur</i> (1884) ($V_T = 15$ kn, $\theta = \text{Variable}$).....	145
Figure 104: Differences in C_T between ship and barque-rigged vessels ($V_s = 10$ kn, $V_T = 15$ kn, $\gamma = 130^\circ$, $\theta = 40^\circ$).....	146
Figure 105: Differences in C_{RT} between ship and barque-rigged vessels at $V_s = 10$ kn	146
Figure 106: C_{HS} of ship-rigged vessels relative to barque-rigged at $\lambda = 5^\circ$	147
Figure 107: C_{AS} of ship and barque-rigged vessels at $V_s = 5$ kn ($V_T = 20$ kn, $\gamma = 130^\circ$, $\theta = 40^\circ$).....	148
Figure 108: L/B ratio comparison between East Indiamen and other sailing merchant ships	149
Figure 109: V_s of East Indiamen compared to other merchant ships ($V_T = 30$ kn)	150

Contents

Figure 110: C_{RT} of East Indiamen compared to other sailing merchantmen.....	151
Figure 111: Comparison of the East Indiaman, <i>Farquharson</i> (Left), and the West Indiaman, <i>Neilson</i> (Right) – Not to scale	151
Figure 112: Comparison between average upwind V_S , downwind V_S and cargo capacity.....	154
Figure 113: L/B averages from literature and modelled data in relation to downwind V_S	155
Figure 114: Variation of F_n and speed during the clipper and windjammer eras.....	156
Figure 115: Variation of C_{RT} and downwind C_T during the clipper and windjammer eras at 5 kn .	156
Figure 116: Variation of stability relative to length.....	157
Figure 117: Comparison of S_H from CFD with estimated S_H for <i>Storm Cloud</i> at V_S = 11 kn	178
Figure 118: Comparison of S_H from CFD with estimated S_H for <i>Storm Cloud</i> at V_S = 15 kn	178
Figure 119: Estimated $R_T + R_\lambda$ compared to $R_T + R_\lambda$ for <i>Storm Cloud</i> at V_S = 11 kn	179
Figure 120: Estimated $R_T + R_\lambda$ compared to $R_T + R_\lambda$ for <i>Storm Cloud</i> at V_S = 15 kn.....	179

List of Tables

Table 1: Summary of Regression Methods for Resistance Estimation.....	32
Table 2: Limits for the Fung Regression Analysis. Minimum and maximum data from (Fung and Leibman, 1995)	33
Table 3: Limits for the Holtrop-Mennen method. Minimum and maximum data from (Wolfson Unit 2016)	34
Table 4: Summary of manoeuvring prediction methods.....	38
Table 5: Parameter limits of the vessels used for the Kijima (1990) and Inoue (1981) Equations ..	38
Table 6: Allowable limits for the Fung Regression Analysis for <i>Cutty Sark</i> , <i>Storm Cloud</i> and <i>SS Great Britain</i>	59
Table 7: Limits for the Holtrop-Mennen method for <i>Cutty Sark</i> , <i>Storm Cloud</i> and <i>SS Great Britain</i> (Red = out of limits)	60
Table 8: Number of ships that meet the parameter requirements for the Holtrop method based on existing data	61
Table 9: Summary of mesh densities used for CFD tests on <i>Cutty Sark</i>	67
Table 10: Percentage of ships in database that meet the limitations of the Kijima method.....	70

Contents

Table 11: Summary of vessels used to compare hydrodynamic side force estimation methods	71
Table 12: Effect of changing heel angle on hydrostatics	78
Table 13: Iteration sizes used in the VPP	81
Table 14: Hydrostatic input for the VPP with data for <i>Cutty Sark</i>	81
Table 15: Final selection of ships (NMM=National Maritime Museum Greenwich, BI=Brunel Institute, GRM=Glasgow Riverside Museum, LRF=Lloyd's Register Foundation).....	92
Table 16: Wind conditions for comparing speeds of scans against original.....	102
Table 17: Average difference between parameters of lines and scan based models	104
Table 18: Summary of mass items	119
Table 19: Parameter differences between East Indiamen and other ships prior to 1840	152

Contents

Research Thesis: Declaration of Authorship

Print name: Sophie Annabel Mary Cannon

Title of thesis: Engineering Analysis of 19th Century British Merchant Ships

I declare that this thesis and the work presented in it are my own and has been generated by me as the result of my own original research.

I confirm that:

1. This work was done wholly or mainly while in candidature for a research degree at this University;
2. Where any part of this thesis has previously been submitted for a degree or any other qualification at this University or any other institution, this has been clearly stated;
3. Where I have consulted the published work of others, this is always clearly attributed;
4. Where I have quoted from the work of others, the source is always given. With the exception of such quotations, this thesis is entirely my own work;
5. I have acknowledged all main sources of help;
6. Where the thesis is based on work done by myself jointly with others, I have made clear exactly what was done by others and what I have contributed myself;

None of this work has been published before submission

Signature:

Date:

Contents

Acknowledgements

Firstly I would like to thank my supervisors, Dr Steve Boyd and Dr Julian Whitewright for their guidance, support and encouragement during this research.

I am also grateful to the Leverhulme Trust for providing the funding that made this research possible.

I would also like to thank the Greenwich National Maritime Museum and Glasgow Museums for allowing me access into their model stores to gather data, the Brunel Institute for their help with obtaining plans from their extensive collection, Lloyd's Register Foundation for access to their archives and the Newcastle University Maritime Special Collection for allowing me to view their copies of Scott Russell's *Modern System of Naval Architecture*.

Finally I would like to thank my family and friends for all their support, in particular my partner Steven for looking after me and supporting me.

Contents

Nomenclature

α	Angle of Attack on Sails	D_x	Drag Force
β	Apparent Wind Angle	F_n	Froude Number
γ	True Wind Angle	h_B	Depth of Bulbous Bow
Δ	Displacement (Mass)	i_E	Half Angle of Entrance
η	Engine Efficiency	L, L_{WL}	Waterline Length
θ	Sail Bracing Angle	L_{BP}	Length between Perpendiculars
λ	Leeway Angle	L_x	Lift Force
ρ_A	Density of Air	LCB	Longitudinal Centre of Buoyancy
ρ_W	Density of Water	LCF	Longitudinal Centre of Flotation
σ	Standard Deviation	LCG	Longitudinal Centre of Gravity
τ	Trim	n	Number of Masts
ϕ	Heel Angle	r'	Non-dimensional Turning Rate
A_{20}	Transom Area	R_λ	Added Resistance Due to Leeway
A_{APP}	Wetted Surface Area of Appendage	R_F	Frictional Resistance
A_{BT}	Area of Bulbous Bow	R_R	Residuary Resistance
A_M	Midship Sectional Area	R_T	Total Resistance
$A_{S,T}$	Total Sail Area	R_V	Viscous Resistance
$A_{S,X}$	Sail Area of Individual Sail Types	R_w	Wave-making Resistance
WSA	Wetted Surface Area	R_n	Reynold's Number
A_{WP}	Waterplane Area	S_A	Aerodynamic Side Force
B, B_M	Beam at Midships	S_H	Hydrodynamic Side Force
B_{20}	Transom Beam	T, T_M	Draught at Midships
C_{AS}	Coefficient of Aerodynamic Side Force	T_{20}	Transom Draught
C_B	Block Coefficient	T_E	Engine Thrust
C_D	Coefficient of Drag	T_F	Draught Forwards
C_F	Coefficient of Frictional Resistance	T_{LCF}	Draught at LCF
C_{HS}	Coefficient of Hydrodynamic Side Force	T_T	Total Thrust
C_L	Coefficient of Lift	∇	Displacement (Volume)
C_P	Prismatic Coefficient	VCG	Vertical Centre of Gravity
C_{RT}	Coefficient of Total Resistance	V_A	Apparent Wind Speed
C_T	Coefficient of Sail Thrust	V_S	Ship Speed
C_w	Coefficient of Wave-making Resistance	V_T	True Wind Speed
C_{WP}	Waterplane Area Coefficient	Y'	Non-dimensional Hydrodynamic Side Force
C_{ws}	Wetted Surface Area Coefficient	Y'_λ	Linear Hydrodynamic Derivative of Side Force
C_M	Midship Section Coefficient	$Y'_{\lambda\lambda}$	Non-linear Hydrodynamic Derivative of Side Force
D_M	Moulded depth		

List of Abbreviations

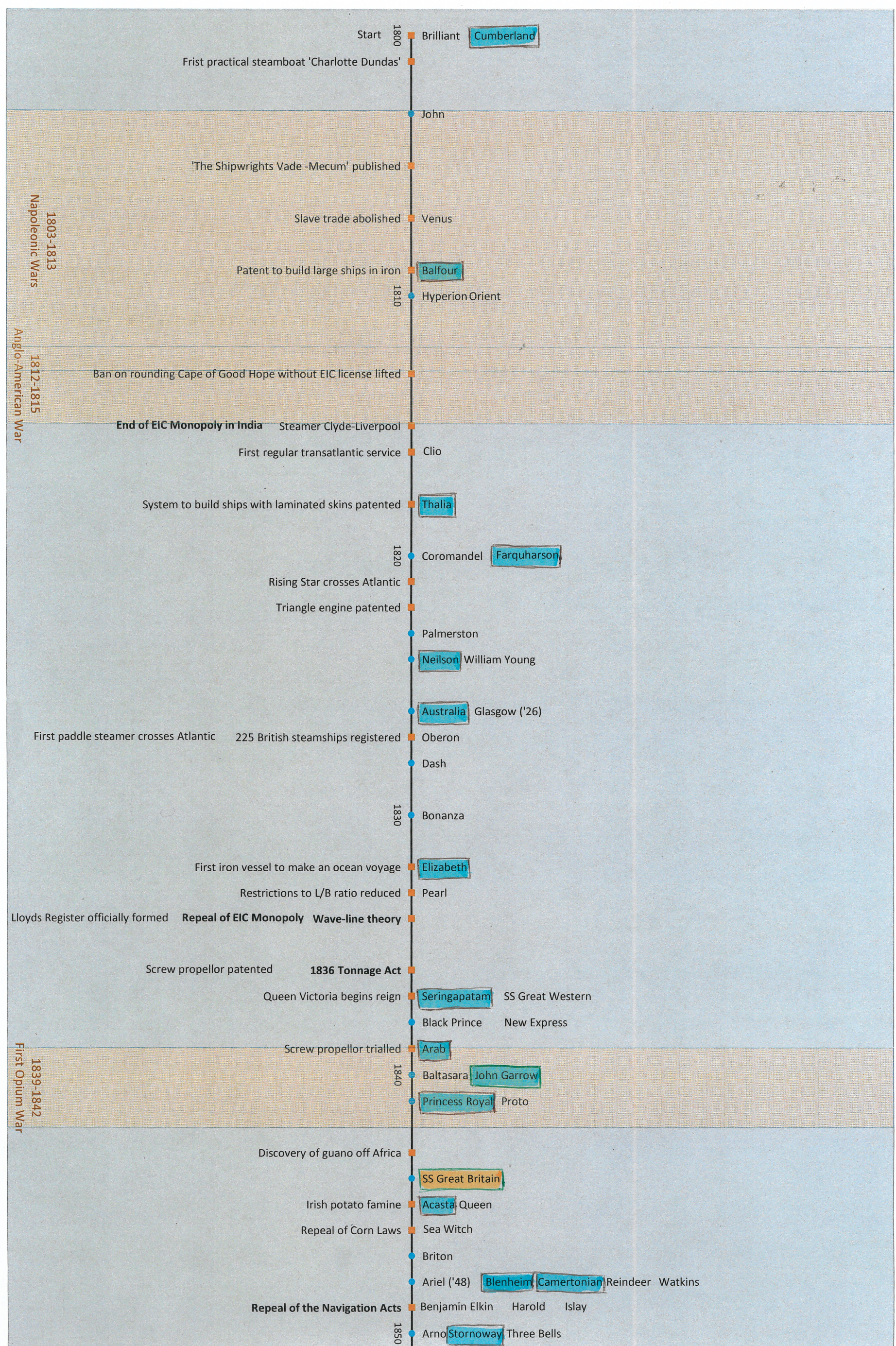
3D	Three-Dimensional
B/D	Beam-Depth Ratio
B/T	Beam-Draught Ratio
BI	Brunel Institute
CE	Centre of Effort
CFD	Computational Fluid Dynamics
EHP	Effective Horsepower
EIC	East India Company
GRM	Glasgow Riverside Museum
HM	Heeling Moment
IHP	Input Horsepower
INA	Institution of Naval Architects
ITTC	International Towing Tank Conference
L/B	Length-Beam Ratio
$L/\nabla^{1/3}$	Length-Displacement Ratio
LCB	Longitudinal Centre of Buoyancy
LCF	Longitudinal Centre of Flotation
LCG	Longitudinal Centre of Gravity
LR	Lloyd's Register
LRF	Lloyd's Register Foundation
MNL	Merchant Navy Lists
NHP	Nominal Horsepower
NMM	National Maritime Museum Greenwich
NRT	Net Register Tonnage
PMM	Planar Motion Mechanism
RANSE	Reynold's Averaged Navier Stokes Equation
RINA	Royal Institution of Naval Architects
RM	Righting Moment
RORO	Roll-On Roll-Off Vessel
SS	Screw Steamer
TransINA	Transactions of the INA
VCG	Vertical Centre of Gravity
VPP	Velocity Prediction Program
WSA	Wetted Surface Area

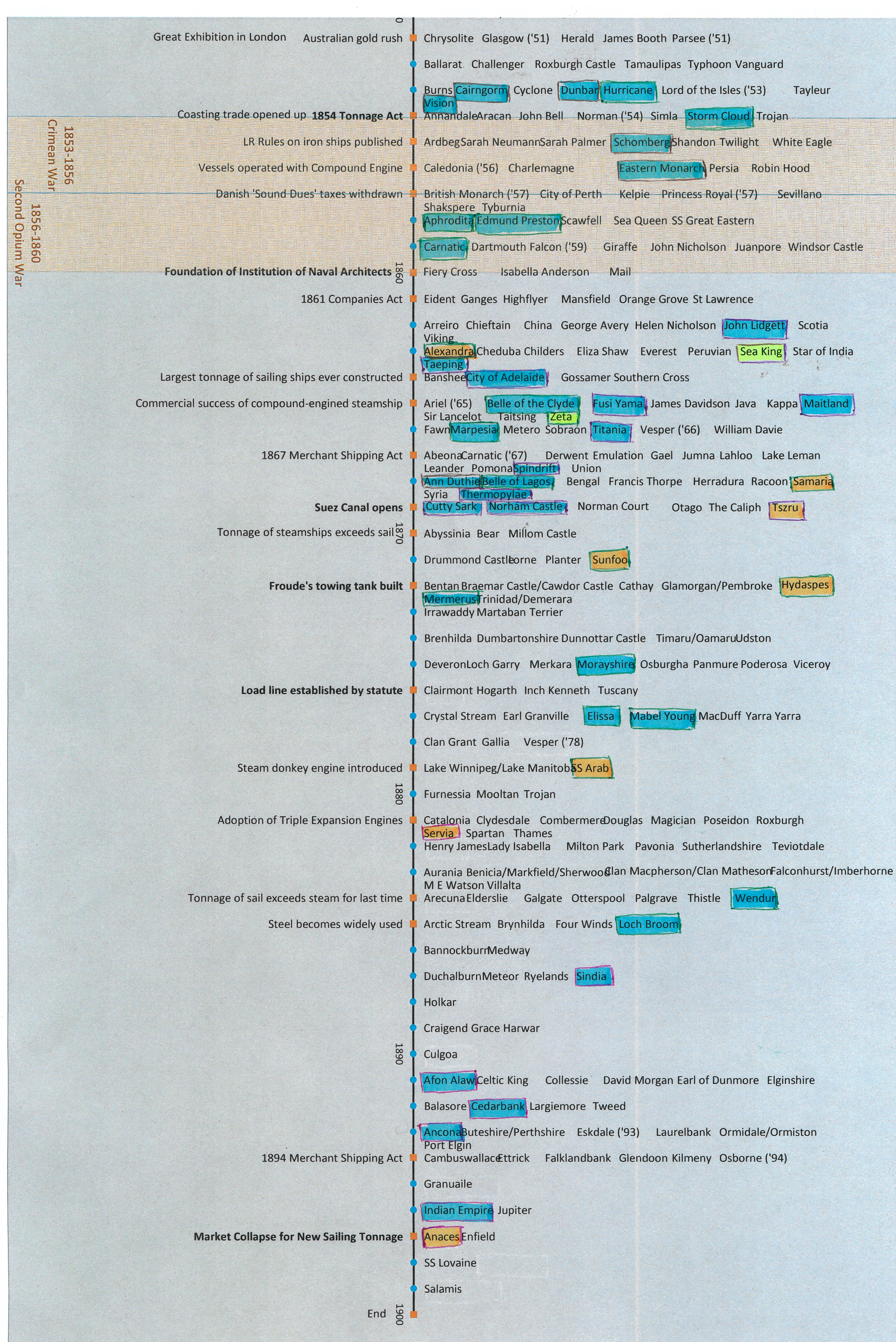
Glossary

Term	Symbol	Description
Angle of Attack	α	The angle between the apparent wind angle and the sail
Apparent Wind	V_A, β	The speed/direction that the wind is coming from relative to the vessel having accounted for ship speed
Ballast		Additional weight that is placed in the ship for improved stability. The ballast condition refers to the condition where there is no cargo on the vessel.
Barque Rig		Normally three masts, with square sails on the fore and main mast and fore-and-aft sails on the aft mast
Beam	B	The width of the ship, usually measured at the waterline
Bermudan Rig		A modern set up consisting of triangular sails
Block Coefficient	C_B	The ratio between the displaced volume of a ship and a cuboid with sides equal to the length, beam and draught of the vessel
Bow		The front end of a ship
Bracing Angle	θ	The angle of the sails of a square rigged ship relative to the bow
Buttock Plane		Plane running parallel to the vertical centre plane of the vessel
Deck beam		Transverse structural member supporting the deck
Depth of Hold	D_H	The internal depth of the ship
Displacement Mass	Δ	The mass of water displaced by the hull
Displacement Volume	∇	The volume of water displaced by the hull
Draught	T	The distance between the baseline of the vessel and the waterline
Driver		A quadrilateral fore-and-aft sail supported by a boom at the bottom and a gaff boom at the top.
Fore Mast		The foremost mast of a ship
Frame		Transverse structural member supporting the outer planking/panels
Free Surface		The surface of the water
Freeboard	FB	The distance between the waterline and the deck edge
Froude Number	Fn	The ratio between the ship speed and the square root of length multiplied by gravitational acceleration
Headsail		A sail, usually a jib, positioned forward of the fore mast
Heel Angle	ϕ	The angle between the upright axis of the ship compared to the perpendicular to the waterline
Jib		A triangular fore-and-aft sail. A type of staysail
Keel		A longitudinal structure at the base of the ship
Keelson		Stringer running along the centreline above the keel
Leeway	λ	The angle between the direction of travel and the direction in which the vessel is pointing

Contents

Term	Symbol	Description
Length Between Perpendiculars	L_{BP}	The length between the forward perpendicular, usually situated where the bow meets the load waterline, and the aft perpendicular, usually positioned at the aft of the sternpost or the centre of the rudder stock
Length Overall	L_{OA}	The total length of the ship including parts above the waterline
Main Mast		The middle, or largest mast of a ship
Midship Section Coefficient	C_M	The ratio of the midship section area to a rectangle with sides equal to the beam and draught of the vessel
Mizzen Mast		The aftermost mast of a ship
Moulded Depth	D_M	The depth of the ship from the baseline or top of keel to the deck edge
Non-dimensional		A measure that does not take size into account and can therefore be compared with others more readily
Polar Performance Diagram		A diagram showing how sailing vessel speed varies with wind direction
Port		Left hand side facing the bow
Prismatic Coefficient	C_P	The ratio between the displaced volume of a ship and a prism with length equal to the ship and cross section area equal to the midship section. Sometimes known as fineness coefficient
Register Length		The length of the ship for the purpose of calculating tonnage
Schooner Rig		Fore-and-aft rigged, occasionally with a square sail on the fore mast
Section Plane		A plane running parallel to the midship section of the vessel
Ship Rig		Normally three masts. Square sails on every mast.
Spanker		See "Driver"
Starboard		Right hand side facing the bow
Staysail		A triangular sail fixed to the "stays" supporting the masts
Stern		The aft end of a ship
Stringer		Structural member often running fore-and-aft
Stunsail		A light wind sail which flies outside the square sails
Sway		The motion of the ship in a lateral direction
Trim	τ	The difference between the draught at either end of the vessel
True Wind	V_T, γ	The speed/direction that the wind is coming from relative to the vessel
Turning Rate	r	The rotational speed of the ship around the vertical axis
Waterline Plane		A plane running parallel to the level waterline of the vessel
Waterplane Area Coefficient	C_{WP}	The ratio of the waterplane area to a rectangle with sides equal to the length and beam of the vessel
Wetted Surface Area	WSA	The surface area of the hull below the waterline
Wetted Surface Area Coefficient	C_{ws}	The ratio between the wetted surface area and the square root of the displaced volume and length





Chapter 1: Introduction

"In any pre-industrial society, from the upper Palaeolithic to the nineteenth century A.D., a boat or (later) a ship was the largest and most complex machine produced." (Muckelroy, 1978, p. 3). Even during the industrial revolution, ships were central to the economy, growing larger and more complex than ever. The relationship between ships and the economical, social and political environments mean that ships can be used to show the narrative of a changing society (Adams, 2013, p. 22). It was during the 19th Century that the process of globalisation began in earnest, with ships playing a vital role in the transport of goods, people and ideas. Colonialism reached its peak, driving an increased emphasis on international connectivity. The opening up of world trade affected more than just the economy; changing priorities stimulated technological improvements in both sailing ships and the new steam ships (Greenhill, 1980, p. 3). The science of naval architecture was developing at a faster rate than ever, with a growing influence on ship design and forming the basis of the understanding we have today (MacGregor, 1988, pp. 15–20). The size of ships increased dramatically as wood was replaced by first iron and then steel (MacGregor, 1988, pp. 130–135). Both shipping and ships evolved beyond recognition during this century of change, yet there is no comprehensive quantitative study on how ship design and performance actually evolved in the 19th Century.

Much of our knowledge of the past is only theoretical. An archaeologist or historian will attempt to interpret evidence using the tools available, with the knowledge that one new find may disprove their hypothesis. The more evidence there is for a theory, the less likely it is that this will happen. Increasing the number of available tools, therefore, will strengthen an argument. This often requires an inter-disciplinary approach to obtain a greater understanding of a subject.

Archaeological and historical studies tend to focus on the social and physical aspects of ship design. The tendency to investigate individual vessels or events also leads to information being portrayed as a series of discrete points in history (Dolwick, 2008, p. 16). There are only a few studies that have attempted to quantify historic ship performance, with many using replica vessels to obtain data (e.g. Couser, Ward and Vosmer, 2009; Poveda, 2012; Tanner, 2013; Tonry *et al.*, 2014). This approach is often expensive, time consuming and may still include significant errors (Macarthur, 2009, p. 173). There is also scope to further investigate the development of ship design over time, with the most complete works being primarily descriptive in nature (MacGregor, 1988; Gardiner and Greenhill, 1993a). Existing archaeological methods, both experimental and theoretical, currently lack the detail required to develop a quantitative and diachronic approach for estimating changes in performance. Without this there is often an assumption that change is linear between known points, which is not necessarily the case (Adams,

Introduction

2013, pp. 50–51). In order to examine a range of ships and ship types, there is therefore a need for a methodology to approach the problem in a repeatable, reliable and inexpensive manner.

Naval architecture may offer a way of quantifying historic ship performance in a way that can be used to consider change over time. The tools used in initial ship design to estimate the performance of a vessel before it is built could theoretically be used in reverse. Maritime museums around the UK hold a vast store of information in the form of ship plans and builder's half models. Additional sources such as Lloyd's Register provide basic information on ship dimensions. If information on the shape of ships can be harnessed from these sources by digitising hull forms, these initial design tools may be employed and the outputs examined by means of a parametric analysis. Using these parameters, ship speed may also be estimated through a velocity prediction program (VPP), providing information about an aspect of performance for merchant ships that is often neglected in favour of cargo capacity. The issue is that there is no standard approach for reverse-engineering historic ships and carrying out the subsequent performance analysis. Although naval architects make it their business to study ships, there is still limited understanding of the study of historic ships. This means processes need to be updated by combining an understanding of the history of naval architecture and ship design with modern techniques. This would also provide an invaluable tool for archaeologists and historians for understanding historic ships, people and the sea.

1.1 Research Question

There have been several claims about how the changing economic and political environment in the 19th Century has had an effect on ship design and performance (MacGregor, 1988, pp. 13–15; Mendonça, 2013, p. 1726). Updates to legislation were often a reaction to economic, social and technological changes and are often considered directly responsible for the evolution of ships (McDowell, 1952, chap. 9).

This research will address the following questions:

- Can these changes be measured by means of an engineering analysis?
- How can this be achieved?
- Can this be used to either support or disprove archaeological and historical hypotheses?

This research will provide analysis based on a quantitative rather than a qualitative narrative using methods that have not previously been applied to historic ships on a large scale.

1.2 Aims and Objectives

The aim of this research is to develop an understanding of the evolution of ships in a diachronic manner, while using easily accessible engineering techniques to quantify performance in a repeatable way. This means that the evolution of ship design and performance will be considered as a process, as opposed to synchronically as a series of individual points. This research will help to establish the current best approach for analysing historic ship design. The information extracted from this will then enable a greater understanding of how ship design is influenced and allow the effect of certain historic events to be quantified in terms of ship performance. This research will lead to improved procedures for data analysis in maritime archaeology.

In order to achieve this, the following objectives are required:

- Carry out a parameter based analysis on existing hull data to determine the advantages, limitations and challenges of using this method;
- Identify what tools can be used to successfully analyse ship performance, in particular hydrodynamic forces;
- Develop a method for applying these tools for historic ships, with respect to estimating ship speed in a repeatable manner;
- Investigate different hull digitisation methods in order to extract additional data from extensive collections of ship models and plans held by museums across the country;
- Identify suitable vessels to help understand change across the century. The tools identified will then be applied to these ships;
- Use a series of case studies to assess the developed methodology and use the data generated from the selected vessels to show how both ships and the understanding of design changed:
 - Determine whether the cause of change is driven by aerodynamic or hydrodynamic forces;
 - Investigate the effect of the understanding of hydrodynamics on ship design and performance;
 - Investigate the extent to which tonnage laws affected design;
 - Investigate the impact of international influence on design, specifically the influence of the USA;
 - Determine the difference between ship rigged and barque rigged vessels in terms of speed reduction;
 - Assess differences between East Indiamen and other merchant ships of the time;

Introduction

- Examine the concept of the “zenith of sail” in relation to clippers and windjammers.

1.3 Novelty

Previous studies on historic ships do not include detailed quantitative analyses that could be used to help understand the evolution of ship design and technology. The structured engineering performance analysis of multiple ships spanning a large period of time has not been carried out in as much detail before. This research will include the justification of using modern techniques for historic craft, which are often used with little appreciation for how they work. A parametric analysis of pre-existing and newly modelled data will examine the evolution of ships in a quantitative manner, using more data points and parameters than have previously been considered for historic ships. A VPP designed to estimate the sailing performance of a wide variety of ships enables objective data to be generated and facilitates the examination of multiple ships and ship types throughout time. The methodology developed will offer an inexpensive supplement to experimental maritime archaeology with a greater degree of certainty than has previously been obtained.

1.4 Overview of Thesis

This thesis will begin with an overview of merchant shipping in the 19th Century, including a description of the development of naval architecture at the time. This will be followed by a review of previous studies on historic ship performance and the availability of data with respect to 19th Century British merchant ships. A discussion on ways in which parametric data can be used to infer performance is provided, as well as methods in which further parameters can be extracted from plans and ship models. The second part of the literature review covers the design of a VPP for estimating historic ship speed, with an analysis of the ways in which individual force components may be calculated.

The third chapter covers a parametric analysis on the data discussed in the literature review. Basic hull parameters from over 1000 ocean-going merchant ships are examined with respect to the state of merchant shipping at the time. The results from this are two-fold: there is evidence that hull data can be used to both trace the development of design and tie in the narrative of the socioeconomic environment, but there are also large gaps in the data that may confirm any inferred performance changes. This indicates that more hull data is required.

One piece of information that was found to be inconclusive from the parametric analysis was the ship speed. This was found to be lacking in quantity, with inconsistencies in the source material. One way to counter this is the creation of a VPP to calculate speed under controlled conditions.

Introduction

This is covered in Chapter 4, where methods of estimating each individual force component is examined and tested. Sensitivity analyses are carried out on each component and then on the VPP as a whole. This shows not only the accuracy of the VPP, but also defines how reliable the input data, and consequently the digital models required for the input, needs to be.

Chapter 5 deals with the selection and creation of digital models of the ships used to perform a reanalysis of the parametric data, including the estimation of sailing performance from the VPP. 3D scanning procedures and the potential effect of scanning accuracy are discussed. Methods of estimating weights and centres for the righting moments of the ships are defined in this section. For ships where the structural report and sail plan are missing, methods of estimating sail areas and structural mass based on other vessels are also discussed.

With the VPP developed in Chapter 4 and the new data generated using the methods described in Chapter 5, the next chapter covers a reanalysis of the data, incorporating newly modelled data, with respect to a number of case studies identified within the literature review. These case studies cover aspects influencing ship design, such as the development of naval architecture and tonnage laws, as well as the variation between different ship types, such as windjammers and clippers. This quantitative evidence shows that common perceptions about the development of ships in the 19th Century are not always completely accurate.

The final section of the thesis summarises the work that has been covered and highlights areas in which the research could be continued. The further work will cover increasing the accuracy of the VPP, including improved methods of calculating sail forces for large sailing ships. With the methodology developed in this thesis, it will also be possible to examine other ship types from different eras in the same manner.

Introduction

Chapter 2: Background and Literature Review

The role and evolution of ship design and performance in the industrial revolution is a subject that has been extensively commented upon, but has not been quantitatively examined in detail. Changes in society can be linked to changes in ship design, and so examining the evolution of ships alongside narratives from literature is crucial (Adams, 2013, p. 49). Analysing the performance characteristics of ships and boats is a relatively recent concept. In the past, ship design was based mainly on experience and instinct, leaving little in the way of technical records of how a vessel may have performed (Clowes, 1962, pp. 2–3). With an emerging trend for experimental maritime archaeology, there have been several attempts to reverse-engineer historic ships and retrospectively evaluate performance. If this concept of experimental archaeology is combined with principles of naval architecture, then there is a potential to apply engineering measures to investigate the evolution of ships in a quantitative manner. This section will provide an overview of the main developments in merchant shipping and relevant developments in naval architecture in the 19th Century, review some of the problems associated with studies on the subject, and examine how some naval architecture design tools may be applied.

2.1 Evolution of Merchant Shipping in the 19th Century

Prior to the 19th Century, British merchant shipping was tied up under a series of Navigation acts dating back to 1381, restricting trade to English and then later British ships (Corlett, 1975, p. 1; MacGregor, 1980a, p. 11). In the 17th Century the East India Trading Company (EIC) was formed and claimed a monopoly on Eastern trade, creating the first real British merchant service (Corlett, 1975, pp. 1–2). The EIC was to dominate British trade for the next 200 years. During this time, ships had evolved to carry as much cargo as possible. Speed only became the most important factor when required to fight or evade other vessels (Kelly and Ó Gráda, 2018, p. 3). Unlike other merchant vessels, the ships of the EIC, the East Indiamen, were heavily armed as a deterrent to pirates (McGowan, 1980, p. 23). When operating under normal circumstances, because of the strict navigation laws and no real competition, there was no requirement to outrun other ships (MacGregor, 1988, p. 63). Ships at the beginning of the 19th Century were remarkably similar in hull form to those of the 16th Century, albeit larger (McGowan, 1980, p. 5).

Going into the 19th Century, the nature of ship design was beginning to change. As a result of the Napoleonic wars, from 1813 Britain found itself in a depression that lasted until the middle of the century (MacGregor, 1984a, p. 10). A direct result of this was the end of the ban on rounding the Cape of Good Hope without an EIC licence and the repeal of the EIC monopoly in India. An act of parliament in 1823 permitted independent British ships to trade with every country covered by

Background and Literature Review

the EIC charter with the exception of China (MacGregor, 1984a, p. 161). This was extended to include China in 1834, causing an unsteady economic environment as demand for privately owned ocean going ships peaked and then subsequently collapsed due to over-supply (MacGregor, 1984a, pp. 10–11). The high demand for goods like tea in Britain made the Eastern trade an attractive opportunity for ship owners, who felt they could guarantee high profits from these popular luxuries (Hersh and Voth, 2011). In addition to the economic impacts of the repeal of the EIC monopoly, there was now a greater incentive to build faster ships as competition between ship owners flourished (MacGregor, 1979, p. 20), although the steady trade to and from India to support the colonies would have reduced the impact of this. The legacy of the East Indiamen themselves continued in the form of the ‘Blackwall Frigates’, named after the area in London in which they, and previously nearly all East Indiamen, had been built (Lubbock, 1922, p. 24; Kemp, 1978, pp. 199–200).

A change in tonnage laws in 1836 had a direct effect on the design of ships; prior to this, depth had been assumed to be half of the breadth of a ship, leading to many deep ships with full ends, in an attempt to increase cargo carrying capacity while avoiding the costs associated with a large tonnage (Lubbock, 1914, p. 105; Corlett, 1975, p. 2; Greenhill, 1980, p. 12). The new tonnage calculations considered cross sectional area at three points, thus favouring long ships with fine ends (Lubbock, 1914, pp. 105–106; MacGregor, 1988, p. 98). These characteristics are now well known to have a positive effect on the speed of a ship (Watson, 1998, p. 74). Despite ship builders of the day already understanding the relationship between length and speed (Steel, 1805, p. 145), the fact that this shape was only adopted in some vessels after the tonnage laws and not earlier after the repeal of the monopoly in India, indicates that the main incentive was still to obtain maximum cargo capacity. This is supported by drawings from shipyards, as shown in Figure 1, providing details on how to design a vessel specifically to circumvent the new tonnage laws (MacGregor, 1988, pp. 106–107). This led to the development of what quickly became known as the ‘Aberdeen bow’, which enabled the capacity of the ship to be maintained by extending the length of the ship above the measurement point, which was at half the midship depth (*Registry Act (5 & 6 Will. IV C.56)*, 1835). What is not currently evident is how long it took for these changes to become mainstream and potentially improve ship performance.

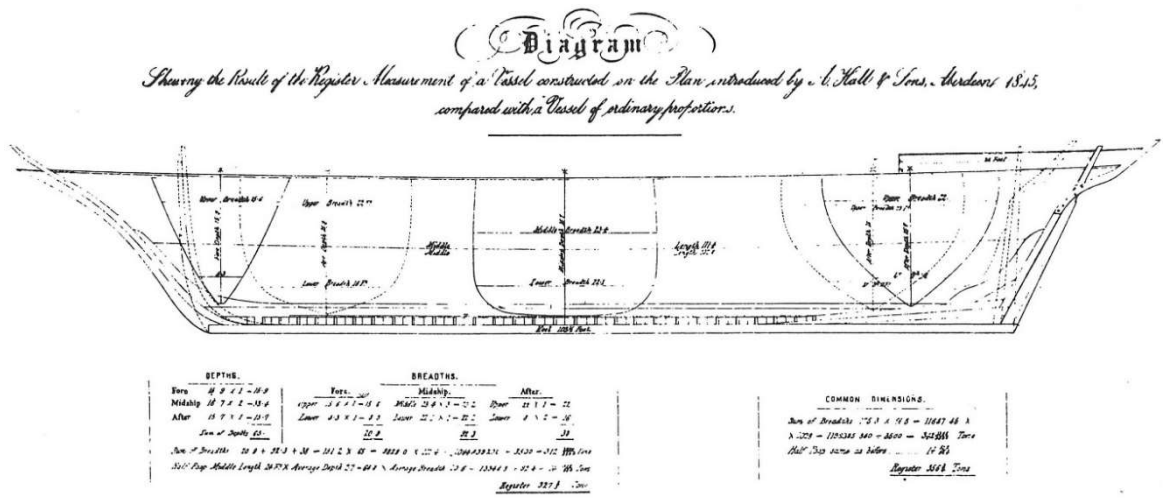


Figure 1: Diagram showing how Alexander Hall of Aberdeen intended to reduce tonnage according to the 1836 rule using an extended (Aberdeen) bow (MacGregor, 1988, p. 106)

Internationally, at the beginning of the 19th Century, the newly independent United States of America (USA), unhappy with the British dominance over trade, were beginning to develop new ships designed for speed which could later be used to operate in the low-volume, high-value China trade (Geels, 2002, p. 1264). During the Napoleonic wars, these ships reached new technological heights as they traded with both France and Britain, for which speed was required to escape patrols from both sides (Davis, 2009, p. 181). In addition to this, the British ban on the slave trade in 1806 encouraged foreign slavers to build ships designed to outrun British vessels that enforced the ban amongst ships of all nations (MacGregor, 1988, p. 14). Emigration to the USA after the Napoleonic wars led to the first regular transatlantic voyages being established in 1818 (Corlett, 1975, p. 3; Griffiths, 1985, p. 9; Geels, 2002, p. 1265). Before this, passengers would have had to wait to find a ship willing to take them, which would only leave once full (Griffiths, 1985, p. 9). This helped to establish the practice of designing ships to operate in a specific trade. The climate in the North Atlantic proved to be a particular obstacle to regular voyages all year round, and so the ships used in this trade needed to be able to withstand heavy seas, whilst maintaining their course (MacGregor, 1984a, p. 164).

Increasing ability of steam powered ships, which had been in use on inland waterways in both Britain and the USA since the turn of the century, assisted regular transatlantic travel with the first steam powered crossing in 1819 (Brock and Greenhill, 1973, p. 13). The development of the screw propeller in the mid-1830s helped to bring Britain back into competition with the USA, who had until then dominated the transatlantic route (Corlett, 1975, p. 4). Even as steam technology was advancing in the Atlantic trade, sailing ships were seeing improvements in the Eastern trade, where steam ships had not yet reached levels of efficiency to compete due to inefficient engines and a lack of coaling stations on the way to Asia (Sichko, 2011, p. 5). This was generally seen as a

Background and Literature Review

low-volume, high-value trade, with cargoes such as tea from China, which were in high demand in Britain (McDowell, 1952, p. 109). The main commodity that the British Empire had to offer in return was opium from India, which would ultimately cause wars between Britain and China (Whipple, 1980, pp. 24–25). As the ships were essentially smuggling opium into China, the small, fast American style of ship design became popular, therefore introducing a use for the clipper ships in Britain (Lubbock, 1914, p. 4; Corlett, 1975, p. 5).

A series of events towards the middle of the century were to bring about perhaps the biggest change to British merchant shipping. A temporary lift of the Navigation Acts occurred as a result of the Irish famine in 1845 and the Corn Laws were subsequently repealed in 1846, allowing foreign ships to bring in grain (MacGregor, 1984a, p. 11). The Navigation Acts against the USA were permanently lifted in 1849 (Lubbock, 1914, p. 106; MacGregor, 1979, p. 12), leaving a direct competition between Britain and the USA. It is commonly claimed that this had an almost instantaneous effect on British ship design, from the moment the first American ship arrived in London (Lubbock, 1914, pp. 107–108; McDowell, 1952, p. 110; Whipple, 1980, pp. 70–71), although it is possible that the development of the finer lined British clipper ships had begun several years before as a response to other influences such as tonnage laws (MacGregor, 1979, p. 12, 1988, p. 154, 183).

In 1854, tonnage laws were updated again to calculate internal volume using more sections, the number of which varied depending on the size of the ship (*Tonnage Act (17 & 18 Vict. C.104)*, 1854), the earliest form of the system used today (MacGregor, 1988, p. 151). Although harder to calculate, it followed a similar form to the 1836 law, but the increased number of sections allowed for a more accurate estimate of volume (MacGregor, 1988, p. 151). Around this time a shortage of wood in Britain led to the construction of composite ships from wood and iron, meaning that larger, stronger ships could be built (Geels, 2002, p. 1268). This, possibly combined with the American civil war, propelled Britain to the forefront of maritime technology (Greenhill, 1980, p. 33; MacGregor, 1984b, p. 172).

The period between 1850 and 1870 is commonly known as the clipper ship era, named after the famous tea clippers that raced to bring the first tea of the season to the UK from China. Although an excess of tonnage following the termination of the Crimea war in 1856 led to reduced orders for new builds, clipper ships were still being built (MacGregor, 1988, p. 202). Between 1856 and 1866, in response to an increased interest in sailing ships driven by events such as the Great Exhibition in 1851 (MacGregor, 1988, p. 130), a monetary incentive was offered to the first clipper home, initially as a premium of £1 per ton on the freight and in 1866 as a prize of £1000 (*The Pall Mall Gazette*, 1866). It seems likely that, even after the incentive was scrapped, the interest

Background and Literature Review

around the tea races kept speed as the primary design goal for many years to come. Particularly towards the end of this period, it was not uncommon for newspapers to closely follow the progress of the tea clippers (*Glasgow Herald*, 1868; MacGregor, 1988, pp. 190–191). These are a primary source of much of what we currently know about contemporary opinions of clippers, although they were prone to exaggeration when describing the ships (MacGregor, 1988, p. 154). The media attention surrounding the tea clippers may be responsible for the assumption that they were one of the greatest technological advances of the 19th Century.

The opening of the Suez Canal in 1869 is often credited with the rise of the steam ship, as they were no longer required to go around the Cape of Good Hope, which had previously been impractical due to a lack of coaling stations (Fletcher, 1958, p. 558). The shortcut the canal afforded steam ships was not open to sailing ships, due to unfavourable winds and a requirement for a steam tug to assist them (Geels, 2002, p. 1269; Sichko, 2011, p. 4; Mendonça, 2013, p. 1734). In addition to this, advances in engine efficiency and understanding of iron structures enabled steam power to be used for most trades, and within two years of the canal opening, the tonnage of steam ships built in Britain had overtaken sail (Fletcher, 1958, p. 560).

Around this time, research activity in ship design itself was flourishing, with the formation of societies such as the Institution of Naval Architects (INA) in 1860 (now the Royal Institution of Naval Architects). This encouraged the sharing and testing of new ideas and theories, many of which are still in use today. Safety in shipping also became a topic of interest in the 19th Century. Lloyd's Register (LR) had first introduced design rules in 1835 in an effort to improve ship safety (Lloyd's Register Foundation, 2017). These rules would have been optional, however, and so the effect was limited. The enforcement of the Plimsoll mark in 1876 was another significant point in history, where ships were required to have a certain freeboard (Lavery, 2019, p. 237). It is currently uncertain what effect this had on ship design, although it would have meant a reduction in the cargo carrying capabilities of many vessels. As with the changes in tonnage law, it is likely that there would have been some alteration to hull form to accommodate this reduction. The capsizing of *HMS Captain* in 1870, in which 480 lives were lost (Sandler, 1973, p. 63) was also a trigger for increased investigation into ship stability. The court marshall following the incident found that the stability of the hull had been insufficient (Sandler, 1973, p. 64). For the decade after the sinking of *HMS Captain* a number of papers were published on how such disasters could be prevented from happening again and the best methods of increasing stability (Barnaby, 1871; Wildish, 1872; Porter, 1879). The culmination of these arguments was that either the freeboard or the beam of ships should be increased (Barnaby, 1871, p. 64).

Towards the end of the century, as steam ships finally became a viable option for carrying cargo, a final breed of sailing ships emerged: the windjammers. These were much larger than the clippers that preceded them and were built for capacity over speed (Lubbock, 1953b, pp. 9–10; Geels, 2002, p. 1270). As steam ships had taken much of the regular and perishable cargoes away from them, sailing ships were left with bulk cargoes with no time restrictions, such as jute or grain (McDowell, 1952, p. 118; Lubbock, 1953b, pp. 9–10; Geels, 2002, p. 1270). The advantage of the sailing ship over the steam ship was in that there were minimal operating costs, and so in addition to being a cheap way to transport goods, if no cargo could be found then they could wait in remote places for very little cost (Allen, 1980, p. 21). They could also be operated as floating warehouses (Lubbock, 1953b, p. 10; Greenhill, 1980, p. 35). Unlike the clippers, which had thrived in the public spotlight, the windjammers favoured function over form, and so are often not treated with the same romantic descriptions (McDowell, 1952, p. 118; Mendonça, 2013, p. 1734).

Modern perceptions of the mechanisms behind changes to design will claim that advances in merchant ships are fed directly from military developments (Chatfield, 1946, p. xxxviii). However, in terms of the design process behind warships and merchant ships, there were considerable differences. For example, warships were not subjected to the same protectionist based legislation as their merchant counterparts. In addition to this, where merchant ships were usually built for capacity, warships were often designed as floating gun platforms, which meant that stability was of much greater import for the latter (Wildish, 1872, p. 74). The argument that military technology drives merchant technology is also not upheld during the 19th Century; several of the best known advances had been in common use in merchant ships before they were adopted by the admiralty, for example the screw propeller (Kemp, 1978, p. 158). The influence of warship design on merchant vessels must therefore be treated with caution.

At the close of the century, steam ships had developed to a point that they no longer required auxiliary sail propulsion. Sailing ships were still operational, but only made up around 20% of British tonnage afloat (Mendonça, 2013, p. 1727) and the building of new sailing tonnage for ocean-going trades had almost entirely ceased. Ship design had changed beyond recognition over the course of 100 years, yet there is still little understanding of the evolution of ships in relation to the changing conditions. By understanding this, not only will we have a better archaeological understanding of ship design in the 19th Century, but also potentially an insight into how future events may influence ship performance.

2.2 Naval Architecture in the 19th Century

In addition to the political and economic environment, an understanding of the scientific environment in the 19th Century helps to identify influences on ship design and performance.

Background and Literature Review

Although there was already a history of trying to apply science and mathematics to ship design, it was during the 19th Century that the basis of modern naval architecture was formed (Molland, Turnock and Hudson, 2011, pp. 1–3). There are several contemporary pieces of literature that provide an insight into the development of naval architecture as a science in the 19th Century. The contents of these sources, described in this section, indicate a changing understanding of theoretical hydrodynamics, in particular hull resistance, as well as an increasing dependence on scientific input into ship design.

The first piece of evidence of what naval architecture looked like in the 19th Century comes from David Steel's *Shipwright's Vade Mecum* (1805). This is essentially a handbook for shipbuilders and gives advice on the ideal construction of a vessel. There are a few interesting points to note from this text concerning the design of ships. The first of these is in relation to the positioning of the "Midship-bend," or the point of the maximum beam of a vessel. The text states that, although it is known that a fine bow appears to give less resistance (Steel, 1805, p. 145), the maximum beam should be placed in the forward part of the ship, hence causing a bluffer bow. The reason for this that Steel gives, is because experience had shown that greater buoyancy towards the bow allowed the column of water ahead of the vessel to be opened fully, enabling the rest of the ship to travel through with less resistance. He also notes that it allows the ship to "lift easier in a heavy sea," indicating that the resistance will be reduced by going over a wave rather than through it (Steel, 1805, p. 152). Although this may be true to some extent with the frictional resistance, there are many other forces at work that Steel appears to be unaware of, for example the impact of wave-making resistance and its dependence on bow shape.

Another text that would have been available to shipbuilders in the early 19th Century was the works of the Swedish naval architect, Fredrik Henrik af Chapman, originally translated into English in 1813 (Chapman, 1968). Several of Chapman's conclusions are based on real vessels he had examined, many of which would have been British ships, giving a reasonable idea of the state of naval architecture at the turn of the century. His theories on resistance, which were tested with models, are well reasoned, if not quite correct, and he attempts to relate the geometry of ships to his findings. His belief is that there are two primary resistance components: one arising from the velocity of the ship, and one due to the pressure of a wave pushed along in front of the vessel ahead of the point of greatest breadth, as shown in Figure 2. Although he fails to come to a conclusion on the best hull form as a result of his theory, the conclusions drawn from his experimental results may have influenced later designs (Kemp, 1978, p. 122). The notable conclusions are: at low speeds the angle of the bow is not important; resistance is lowest when the ship is symmetrical fore-and-aft; when a bow wave is formed a blunt bow will create more resistance than a sharp bow (Chapman, 1968, pp. 82–83). Another geometrical detail credited to

Chapman is the advice that the longitudinal centre of buoyancy (LCB) should be positioned 1-2% forwards of the centre of the waterline (Wildish, 1872, p. 69). It is difficult to see where this would fit within the conclusions of his experiments, however, as if a ship is symmetrical fore-and-aft, it would follow that the LCB would be at amidships. This confusion over his conclusions may be the reason that the idea of a finer lined ship took time to be accepted by naval architects (Kemp, 1978, p. 122).

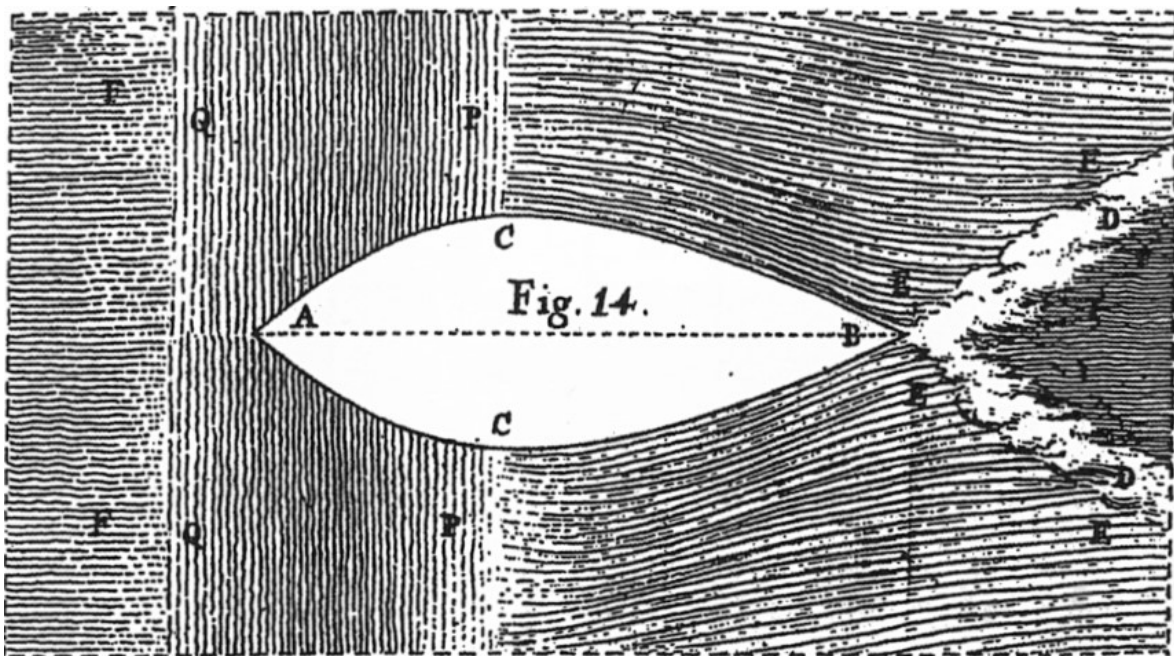


Figure 2: Chapman's bow wave (Q-P). Hull moving from right to left (Stoot, 1959, p. 35)

One of the main issues facing naval architects in the 19th century was the question of how to determine the resistance of a ship, and hence what the best design was for reducing resistance. Isaac Newton's theories of the existence of a solid of least resistance had been discounted (Ferreiro and Pollara, 2016, p. 416), and at the turn of the century it was believed that the resistance was proportional to the square of the velocity (Ferreiro, 2007, p. 129). In order to understand this, the motion of fluid around the hull needed to be understood. Steel (1805, p. 152) treats the situation by describing a column of water that must be opened at the bow and then sucked back in again at the stern, hence producing resistance as the hull moves the water to the side. This idea was still in evidence in 1853 as shown by a paper in the transactions of the INA (TransINA) by John Bourne (1867). He describes experiments carried out during his career that indicate that friction is a greater cause of resistance than the lateral motion of water, which he admits is generally accepted by 1867 when the paper was written. The wetted surface area (WSA), driven by the midship section and the length, was found the greatest influencer of this. Because of this he suggests a semi-circular midship section as preferable. In both Steel's book and Bourne's paper, it is agreed that a longer, sharper vessel will have less resistance, the primary

change in opinion between the sources being the significance attached to this form due to a lack of understanding of the relationship between resistance and speed.

In 1834 John Scott Russell began to develop his wave-line theory in an attempt to develop the form of least resistance originally described by Isaac Newton (Scott Russell, 1860a, pp. 184–186; Ferreiro and Pollara, 2016, p. 418). Initially formed of parabolic curves, by 1844 Russell had developed the “ideal” hull form to consist of a bow formed from a sine wave, as illustrated in Figure 3, a stern 2/3rd the length of the bow in a cycloidal shape and any additional length of hull formed by a parallel midbody. The length of the bow and stern were dependent on the required speed (Ferreiro and Pollara, 2016, p. 421). The reasoning behind the theory was that water particles, treated as a large number of tiny, spherical balls, would be able to roll smoothly along the surface with minimal changes to the angle, so as to prevent a “violent collision” between the particle and the surface of the hull (Scott Russell, 1860a, pp. 191–192). The derived hull form was not necessarily practical when applied to a real ship, yet the concept of a hollow bow and the proportions of the entrance and run were adopted by some ship designers, a feature that is particularly noticeable in some extreme clippers (Scott Russell, 1861; Ferreiro and Pollara, 2016). Scott Russell’s wave-line theory remained prominent until the introduction of streamline theory by William Macquorn Rankine in the mid-1860s (Ferreiro and Pollara, 2016, p. 435).

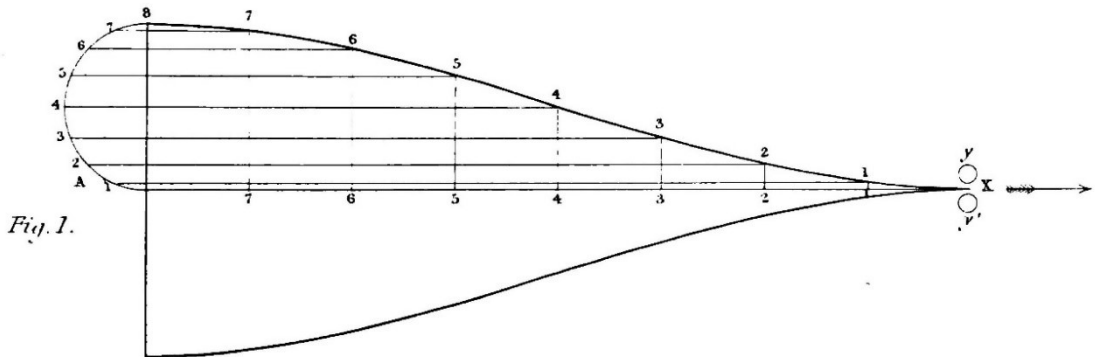


Figure 3: Scott Russell's wave-line theory bow (Scott Russell, 1860b, fig. 1)

In the 1870s, ten years after the formation of the INA, the theories that are still accepted today concerning resistance began to appear in textbooks and papers on naval architecture, namely the consideration of friction and wave-making resistance as the more significant components (Froude, 1877; White, 1877, p. 431; Rawson and Tupper, 2001b, p. 413). The thinking changed from how a ship moves through water, to how the water moves past the ship (Rankine, 1870, p. 177; White, 1877, p. 431). This led to the identification of the important features of a ship with regards to resistance: wetted surface area, length and hull roughness affect the frictional resistance, and the length of entrance affects the wave-making resistance. A third component is also discussed, the

Background and Literature Review

eddy-making resistance, which is the resistance induced due to the wake of the vessel. This component calls for a gradual termination to the stern, as opposed to a full stern that ends abruptly. The work of William Froude and later his son, Robert Edmund, stand out in this area. W. Froude was the first to correctly identify the effects of scaling on the resistance components, meaning that theories of resistance could be tested meaningfully at model scale, with methods fundamentally the same as used in modern model tests (Rawson and Tupper, 2001b, p. 415; Molland, Turnock and Hudson, 2011, pp. 1–2). Some of these experiments allowed W. Froude to identify how the wave system generated by the hull affects the resistance, indicating that a long, thin ship was not necessarily the solution to a fast ship (W. Froude, 1877). Although this had been claimed before (Scott Russell, 1861), this was the first time that it could be scientifically proven.

Advances in stability during the 18th and 19th Centuries, were primarily driven by French scientists, who sought a comprehensive understanding on the subject (Reed, 1885, p. xiv), with the concept of the metacentre first introduced in 1746 by Bouguer (Woolley, 1860, p. 12). In Britain, meanwhile, research into stability was focused on the practical aspects, not necessarily considering the capabilities of a vessel beyond its normal operational range. It is suggested that in the first part of the Century, when sail power was dominant, the approach to stability was to ensure that the righting moment was as large as possible, meaning that detailed calculations were not always used and a greater margin of error was allowable (Wildish, 1872, p. 74; Reed, 1885, p. xvii). It is claimed in one paper from 1872, that there were only three instances where the metacentric height of a sailing ship was recorded (Wildish, 1872, p. 73). According to Scott Russell, up until an Act of Parliament in 1833, legislation was actually set in a way that penalised more stable ships (Scott Russell, 1864). It is unclear which Act he is referring to, but his description indicates that many shipbuilders and designers did not take the greatest care with the stability of their vessels. The concept of a long, thin ship being beneficial to speed also had an inverse effect on ship stability, with claims that this reduction in stability may have directly caused the loss of a number of vessels (Reed, 1885, p. xvii).

It appears from this review of the understanding of naval architecture in the 19th Century, that there are three phases of development; empirical, developmental and modern. The empirical phase covers the first 35 years, until Scott Russell begins his investigations into wave-line theory. During this phase ship design was based primarily on observations and experience. This includes the works of Steel and Chapman, the empirical nature of which are shown by the conclusions that a blunt bow produces the least resistance. The developmental phase is where a greater amount of experimentation occurs, led by Scott Russell. During this time improvements were made in reducing the frictional resistance of ships. The developmental phase ends with the modern phase, beginning between 1860 and 1870 with the work of Rankine on streamlines, Froude's model tests

and discoveries concerning wave making and a greater emphasis on the accurate calculation of stability. This phase signifies the period in which the understanding of hydrodynamics as we know today began to take shape.

2.3 Analysis of 19th Century Merchant Ships

Considering the extensive changes to merchant shipping throughout the 19th Century, there have been remarkably few studies in the area. Most studies tend to be descriptive and limited to individual examples (Ransley *et al.*, 2013, p. 173). Perhaps the largest piece of research was carried out by the maritime historian David MacGregor, who published several books on the subject of ship design throughout his life. MacGregor (1980a, 1984a, 1984b, 1988) discusses the changes to the design and performance of sailing ships over the course of a century. This discussion is centred on a series of lines plans copied from builders' records or models. The importance of the speed-length ratio, the prismatic coefficient (C_p) and the underdeck tonnage coefficient in relation to performance are discussed (MacGregor, 1988, p. 20). The latter of these could be considered as a parallel to the block coefficient (C_b), and is calculated using the tonnage of the vessel and the registered dimensions, all of which are generally available for a ship. However, this measure could be misleading as the internal layout is likely to vary between ships and changes in tonnage calculation method makes this an inconsistent measurement and not necessarily indicative of fine lines. C_p is known to be an important factor in defining the speed that a ship could reach, however MacGregor considers it primarily as a geometric description of how fine a ship is without fully understanding the relationship between C_p and ship speed. The speed-length ratio, defined by MacGregor as the maximum ship speed divided by the square root of the waterline length (MacGregor, 1988, p. 20) is a useful method of comparing ship performance where the speed of the vessel is known as it provides an idea of how efficient a hull might be. MacGregor (1988, p. 20) defines a fast vessel as one with a speed-length ratio greater than 1.25 ($F_n=0.37$). For the majority of ships discussed, however, there is no record of the speed, and so it is often estimated based on the length. The usefulness of this is questionable, as there is no evidence that these ships were actually capable of obtaining these speeds (MacGregor, 1988, p. 92,156,194). This means that several of the speeds presented are only a function of length and the categorisation as a "fast" ship is apparently based on whether it looks like it should be. Despite concerns about the analysis methods, however, the collection of plans accumulated by MacGregor and held at the Brunel Institute in Bristol is a valuable resource for this research.

One of the most utilised information from the 19th Century is the tonnage of ships built or registered in the UK (Mitchell and Deane, 1971, pp. 220–222). This data can be broken down further to show trends, for example, the number of sailing ships and steam ships (Mendonça,

Background and Literature Review

2013, pp. 1727–1729). However, how useful is tonnage for measuring technological development? Hughes and Reiter (1958) use a breakdown of tonnage built in the UK between 1814 and 1860 to investigate variations in cargo carrying capacity between wood and iron, and paddle and screw propelled steam ships. Although this is a good way of showing the relative cargo carrying capacity of different ship types through time, it must be remembered that tonnage rules changed significantly throughout the century, so there is no consistent measure (Bristol Record Society, 1950, pp. 10–13). Despite the unreliability of the measurement, some details are clearly shown by the study, including that steam ships became generally accepted around 10 years earlier than thought, and iron vessels made up the bulk of steam tonnage around 15 years earlier than previously thought (Hughes and Reiter, 1958, p. 365).

The improvement of sailing ships occurring in parallel with the rise of the steam ship is one of the better known phenomena that occurred during the 19th Century. It is commonly believed that the threat of the new encouraged improvement of old technology in order to compete. This has been dubbed the “sailing ship effect”. It is unlikely, however, that this was the primary mechanism in the rise of the sailing ship (Mendonça, 2013, pp. 1734–1735). For several decades, both types of ship would have had their own operational benefits and would not necessarily have been in direct competition. Mendonça (2013) presents an argument against the existence of the sailing ship effect based on average tonnage, which is defined as a vessel’s “usefulness”. Although this provides some evidence to disprove the sailing ship effect, increases in the capacity only indicates improvement in construction technology, which would enable larger vessels to be built. What is not taken into account is the other important performance aspect for merchant ships: speed. Tonnage does not show the shape of the vessel, which has a significant influence on the ship speed. Therefore, an alternative measurement is required to obtain a complete understanding of technological improvements in ships.

A recent study on 19th Century ship performance estimated the hull resistance of four merchant ships with the intention of comparing hull efficiency, i.e. the hull resistance (Tonry *et al.*, 2014). This study was primarily aimed at comparing the tea clippers *Cutty Sark* and *Thermopylae*, who famously raced each other in 1872. Although the method used appears to be sound, there are a few points in which the overall results are questionable. Firstly, the considerably different sizes of the ships have not been considered, leading to the perhaps obvious conclusion that the larger ships have a greater resistance. An East Indiaman, although large for its time, has been included. Despite operating on the same route as the tea clippers, East Indiamen would have been employed as both cargo and passenger ships and could fight when required (MacGregor, 1980a, p. 196). These characteristics make it a very different vessel from a clipper, and so it is called into question how useful the inclusion of an East Indiaman is in this study. For a true comparison of

Background and Literature Review

hull forms, non-dimensional values for ship speed and resistance would have clarified the differences between the hull forms, particularly where the East Indiaman was presented at a different speed. Secondly, it would be expected that an increase from 6.4 to 9 ms⁻¹ would cause a significantly higher increase in resistance than is presented (70.5 kN to 76.6 kN), even with the omission of wave-making resistance.

The idea of using ship speed to determine changing performance has been investigated in a discussion paper for the Centre for Economic Policy Research (Kelly and Ó Gráda, 2018). The discussion is focused around logs from various European East India Trading Companies and the transatlantic packets that operated in the early 19th Century. This data appears to show an increase in expected speed of British ships between 1750 and 1830. The issue with the methodology used lies in the multiple sources of potential error that may arise from using voyage logs only, particularly with daily logs. The first of these, which has been highlighted by the authors, is related to the lack of reliability in measuring longitude at the time. This means that the distance recorded may not be correct. A similar issue is related to the measurement of wind conditions; the Beaufort scale was not developed until the end of the period considered (Macarthur, 2009, p. 173), and so the data has been corrected to account for this (CLIWOC, no date). Despite the efforts of the organisation who collated the data, it is still possible that a degree of misinterpretation exists, which, when combined with the fact that the wind speed and direction would have been an average for an entire day, increases the potential error. The ship speed would also be an average, meaning that there is no certainty that the vessels would have been capable of obtaining those speeds under the given conditions.

The other issue with this paper lies with the data selection. The authors have omitted ships where the data is considered to be unreliable, including examples where recorded ship speed is “implausibly high”. When looking at change in speed over time it seems unusual to omit certain data points based on their speed, particularly when this “implausibly high” speed includes 10 kn, or where the ship speed is more than half of the wind speed. Considering that there are examples of replicas of similar ships obtaining these speeds under sail, the assumption is met with some scepticism (Pokorný, 2017).

Overall, previous research into the design of 19th Century merchant ships has been primarily speculative. Tonnage is one of the most common measurements, although there are issues with consistency and it is mostly related to the cargo carrying aspect of performance. The research that has considered ship speed appears to have been carried out with little consideration for the historical context, or is too reliant on contemporary recording methods, which contain many uncertainties. This research intends to cover these gaps by looking at alternative measures and a

way to consistently estimate ship speed in a scientific manner to establish change in performance over time.

2.4 Availability of Information

Perhaps the greatest challenge regarding historic vessels is the available information that can be used for performance analysis from an engineering perspective, which may be lacking due to missing evidence in the archaeological record or from historical sources. Surviving examples of merchant vessels in their original form even from as recent as the early 20th Century are rare; those that do survive have often been upgraded to modern standards. Much of the available data is too sparse for a comparison of ships over time and a certain amount of interpretation is required. This means that there will almost always be some form of uncertainty in a reverse-engineered design (Steffy, 1994, p. 241).

There are several ways in which modern techniques and knowledge may be applied to account for the lack of solid evidence or useable information that may be associated with using historic sources. In the more extreme cases where there is no trace of the craft in question, adaptations of similar vessels may be required (McGrail, 2009, pp. 21–23). One such example is detailed in a paper on a project to investigate an ancient Egyptian seagoing vessel from around 1500BCE (Couser, Ward and Vosmer, 2009). The full-scale reconstruction produced was based on a river craft from the same era, of which there were relief carvings and minimal remains. A number of modern naval architecture techniques were used to adapt the base model into a sea-going vessel. This included strength and stability calculations that would not have been available to the ancient Egyptians. A similar approach was taken in research on Polynesian voyaging canoes (Finney, 1977). With no trace of the originals, common features of modern canoes were used to create a representative “parent” canoe. In more recent history, there has been an increase in the quantity of information available for a variety of vessels and vessel types. This means that it may be possible to find similar ships as well as sources such as iconography to fill in any gaps (McGrail, 2009, pp. 21–23). These hypothetical reconstructions are often used for the purpose of acquiring an estimate of the lines plan and other information such as hydrostatics and sailing performance for the vessel in question (Tanner, 2018, p. 143).

In addition to the physical characteristics of a vessel, external design influences are not always clearly recorded or interpreted. A recent publication investigating the purpose of rams in ancient Mediterranean galleys suggests that ancient designers knew of the hydrodynamic advantages of an extension to the bow, and only later considered that it may be used as a weapon (Murray *et al.*, 2017). An earlier paper by one of the authors also claims that this hydrodynamic advantage was only discovered at the beginning of the 20th Century (Ferreiro, 2011, p. 354), calling into

Background and Literature Review

question where the evidence is for the new claim. The experimental procedure used in proving the hypothesis is also questionable, as the hull form used appears to be a generic canoe shape, not that of the vessel in question and little consideration has been taken to how the changes in hull form required to fit the “cutwater” may influence the outcome. The result is therefore showing only that adding an appendage and increasing the overall fineness of a vessel makes it more hydrodynamically efficient. With no evidence supporting how this may have been discovered by boat builders in around 900 BCE, the conclusions reached are questionable. It is therefore vital to assess the results of an engineering analysis in relation to other sources, including those related to the social context, that may support or contradict a theory.

In the case of 19th Century ships, some of the information required for a performance prediction can already be found from documents such as build records and logbooks. This removes a degree of uncertainty in the design. Maritime museums around the UK hold a large collection of information, much of it from the 19th Century. These include ship plans, structural reports and models. In addition to this, there are various archives containing contemporary newspaper reports, which document the public interest in merchant shipping. A few logbooks for merchant ships also survive, although many have been lost or destroyed, and the information varies in quality (Wilkinson, 2009). There are also a number of other contemporary sources that provide details that can be useful for the reconstruction of historic ships. Examples of this include guides on cargo loading and stowage, that would have been used by ship’s masters to calculate how much cargo they can carry (Stevens, 1894).

Some consideration needs to be given to the types of ship model available. These can be divided roughly into two types: display models and builders’ models (Lavery and Stephens, 1995, pp. 10–14). Display models were often made after the construction of the ship and were given to the owner or used by the builder as an advertisement. These models would be finished to a high standard, but the hull shape may not necessarily be representative of the full-scale ship as they were intended for show only (Lavery and Stephens, 1995, p. 14). Builders’ models, however, would normally be made before construction to show the hull shape of a vessel and would usually be an accurate representation of the vessel (Whipple, 1980, p. 57). Occasionally the as built and as designed vessel may differ, but without further sources to show alterations, the model is often the best source of hull information alongside a lines plan.

Lloyd’s Register of Shipping, published by the organisation of the same name, also provides information on some British merchant ships from 1764. However, the amount of information available varies throughout the 19th Century. Early registers include details such as the name of the vessel, the tonnage, the age and the draught. After the official formation of LR in 1834, the

Background and Literature Review

age is replaced with the year of build and the draught is removed altogether. Later, changes are made to reflect updates to tonnage laws and in the mid 1860's the register length (length of keel and stem), beam and depth of hold are included (Lloyd's Register Foundation, 2016). After the introduction of the Plimsoll mark in 1876, details of the moulded depth and freeboard are listed for some vessels, allowing the reader to obtain an estimate of the draught. All of the registers contain a classification awarded by LR for those ships surveyed by them, based on factors such as material and construction method. Early classifications were very subjective, as there was no set survey method (Lloyd's Register Foundation, 2017) and surveyors were generally biased towards the more traditional vessels (MacGregor, 1984a, p. 19). Structural survey reports are also available from LR after 1834, with only a few surviving from before this date (Royal Museums Greenwich, no date).

Online databases such as the Clydeships database (Caledonian Maritime Research Trust, 2019) provide summaries of the information available for a large number of ships, generally related to the area in which they were built. These provide details such as name, official number, main particulars and tonnage. However, these databases are intended for looking up individual vessels and so gathering data from them is time consuming. This is particularly challenging where the ship does not have a unique official number, which is the case for ships lost or broken up before 1855 (Owens, 2015), and shares a name with several other vessels. These databases are also almost exclusively for ships built in Scotland or the North of England. If the official number is known, some details may also be obtained from the Merchant Navy Lists, particularly towards the end of the century. Similarly, wreck reports may contain useful details, such as loading conditions and draught.

The number and total tonnage of ships built in Britain and Ireland is commonly employed as a means of showing the development of ships with time (MacGregor, 1984b; Ville, 1993; Mendonça, 2013). This data may be found for most of the 19th Century and early 20th Century in the *Abstract of British Historical Statistics* by Mitchell and Deane (1971). The individual tonnages of ships may be found in various locations, including Lloyd's Register of shipping and the Merchant Navy lists, making it one of the most readily available pieces of information. The difficulty lies in the presence of multiple tonnage laws and calculation methods used during the 19th Century. There is usually some reference to which tonnage has been used, but in some cases it remains unclear, particularly when the "new register" tonnage was superseded in 1854 (MacGregor, 1988, p. 25).

As the 19th Century progressed, interest in ship performance increased as new technologies developed and speed became more important (MacGregor, 1988, p. 153). Steam ships in

particular were the subject of several studies to identify the characteristics that were most important for efficiency and speed (Fyfe, 1907, p. 3). These studies were accompanied by attempts to understand the science behind ship design, with many of the concepts discovered still in use today. In addition to providing the scientific background to ship design described in Section 2.2, these contemporary studies provide us with valuable performance data, particularly from the latter part of the century. Fortunately, as the experiments were relatively new, reports often contained detailed descriptions of the procedures used and so some idea of the reliability of results can be obtained (Du Bosque, 1896). Although these studies contain a reasonable amount of useful information, they do not necessarily give an overview of general ship design and performance at the time, as there was usually more interest in experimental ships, leading to an amount of bias in the available data (MacGregor, 1984a, p. 21).

Despite being relatively recent history, there is a variable level of technical information available on 19th Century British merchant ships. Much of the data that is available is in the form of models and plans, and so needs to be extracted. For accurate comparisons, the method of extraction will need to be consistent. When combined with details from survey reports and databases, there should be enough detail to infer something of the performance of these ships using modern engineering analysis methods.

2.5 Parameter Based Performance Analysis

The sources described in Section 2.3 provide some of the particulars of the vessels considered in this research. Previous studies on hull optimisation have highlighted the importance of some of the principal hydrostatics in relation to ship performance. Regression based resistance estimation methods use these particulars, usually in a non-dimensional form, showing a strong link between hull geometry and resistance.

Watson and Gilfillan (1977) review some typical ship design methods based on existing data. This involves considering typical relationships between principal dimensions for different ship types. The relationships between different hull parameters are considered and comment is made on how these have varied with time. For example, it is noted that between 1962 and the time the paper was published in 1977, the typical length-beam ratio (L/B) of ships decreased, citing a desire to reduce hull costs as the reason (Watson and Gilfillan, 1977, p. 282). The beam-depth ratio (B/D) was also noted to have reduced, owing apparently to a change in stability requirements during this time (Watson and Gilfillan, 1977, p. 283).

Although these relationships show some information about performance, i.e. the ability of a ship to achieve its requirements, the interpretation is dependent on knowing more about what

different ship types are typically capable of achieving. The only measure that appears to be directly compared to performance is the block coefficient, C_B , as it is dependent on the principle ship dimensions and has a significant effect on ship speed (Watson and Gilfillan, 1977, p. 284; Schneekluth and Bertram, 1998, p. 25). This indicates that the overall form of the ship has the most important effect on performance. The comparison between C_B and ship Froude number (Fn) shown in Figure 4 clearly shows different ship types lying in distinct areas of the graph and highlights the relationships between C_B and ship performance. Fn is a non-dimensional measure of speed given by equation 1, where ship speed (V_s) in ms^{-1} is non-dimensionalised using the square root of length (L) and gravitational acceleration (g).

$$Fn = \frac{V_s}{\sqrt{gL}} \quad (1)$$

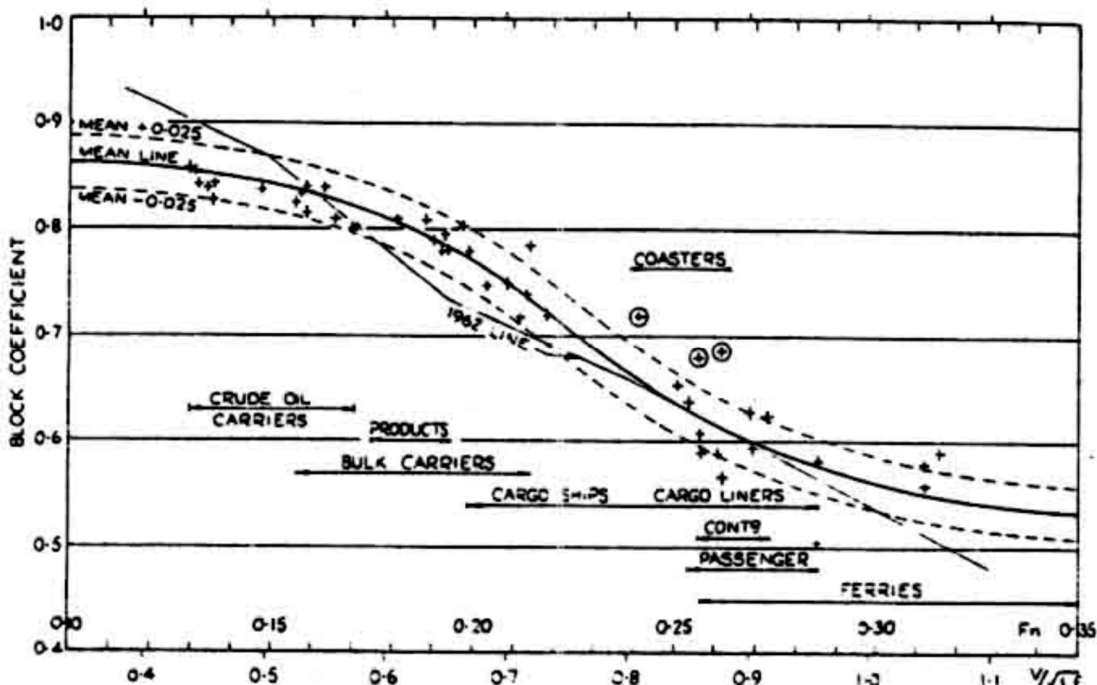


Figure 4: C_B with V_s for various ship types (Watson and Gilfillan, 1977, p. 284)

Day and Doctors (1997) developed a genetic algorithm to investigate the effect of parametric changes to a hull on total resistance. Using constant hull displacements, the main parameters considered are length-displacement ratio ($L/\nabla^{1/3}$), L/B , beam-draught ratio (B/T), C_P and C_B . An optimum for each parameter was found over a range of speeds. Although this study shows an unrealistic set of conditions that do not take into account stability and strength requirements, it does show how different parameters affect the speed of a vessel. The key result that may be derived from this research, is that the variation in parameters has an inconsistent and highly variable effect on the speed (Day and Doctors, 1997, p. 253).

At the early design stages of a ship when an approximation of the hull parameters is required, it is sometimes possible to employ a design lane. These can be developed either from systematic hull form analysis or from using data from actual ships (Toby, 1997, p. 161). If the required speed and approximate length of the vessel is known, then these design lanes can give the user an idea of the most efficient hull proportions for that vessel. As these design lanes are generally based on experience, they should incorporate all operational requirements and offer a realistic design. Conversely, they may also allow an insight into the average performance of a particular ship type.

All of these examples show that there is a potential to infer some performance information from the principal particulars. However, although the dependence of the speed-length ratio on certain parameters can be shown, it is noted that the importance of an individual parameter is not necessarily constant (Fung, 1987, p. 78). This indicates that several parameters would need to be examined at once to infer any information about ship performance without knowing the speed beforehand. In addition to this, the highest quality information is found where there is a variety of data available, something that is not currently possible for 19th Century merchant ships given the available information. This research will address this through digital reconstructions of hull forms from lines plans and models to increase the size of the dataset in a consistent format.

2.6 Digital Reconstruction of Hull Forms

The ability to extract hull parameters from existing designs is an important part of this research as with more data, a full parametric analysis could be carried out. As the available technical information of 19th Century ships is often incomplete, a digital model would help to obtain some of this knowledge, including details such as hull displacement, form coefficients and WSA. In addition to this, a digital model may be used in conjunction with some initial design calculation to generate an estimate of ship speed. These methods will be discussed in Sections 2.7 to 2.11.

Maritime museums around the country have collections of lines plans and half models, many of which are from the 19th Century. These resources may be employed to generate digital models of the ships they represent. There are several ways of doing this, including a manual input of offsets or a lines plan into a specialist ship design program or providing a 3D scan of a model or full-scale ship. For the results to be useful, the digital model needs to be as accurate as possible, without compromising computing cost. A part of this research will be dedicated to assessing the suitability of different digital modelling methods.

For creating a 3D model of an existing ship, there are two main factors to be considered: the sort of data available and the purpose of the model. For 19th Century merchant ships the data is mostly available as lines plans and half models. Lines plans are the easiest to read as they are

defined by set measurements; however, the quality of useful information is dependent on the detail given. It often requires a good knowledge of ship design to create an accurate model. Much of the design data available is in the form of builder's half models held in museum archives. Half models are, as the name suggests, scale models of ships cut along the centreline that were historically used by shipbuilders as a way of designing boats and ships in three dimensions (Whipple, 1980, p. 57; MacCarthaigh, 2008). These models are harder to extract data from, as it requires some form of 3D scanning to be useful in this context. The result of this is often a point cloud or surface mesh, which then needs to be converted into surfaces. An alternative method is to use the scan surface to generate a lines plan (Menna, Nocerino and Scamardella, 2011, p. 250).

There are program suites dedicated solely to ship design, such as the Wolfson Unit's *Shipshape*, which works using curves based on cubic splines and offsets. *Delftship* and *MAXSURF Modeler* primarily use Non-Uniform Rational Basis Spline (NURBS) surfaces (Delftship Marine Software, 2016; Bentley Systems Incorporated, 2017). Other programs which are not ship design orientated, such as *Rhinoceros 3D (Rhino)* which uses NURBS surfaces to form solids, have also been found to be good for modelling ships.

In order to create a digital model from a lines plan, curves or surfaces based on splines are more suitable, as many ship designs are based around splines. This means that with a set of given points from the plan it should be easier to produce a faired surface. When using a point cloud or mesh this becomes more complex, and so curves must be fitted to the data before a surface can be formed. Due to personal preference and the range of available features, the *MAXSURF* suite was chosen as the primary software for this research. Some of the useful features that may be exploited are the ability to put a scaled background image in the different ship views and multiple methods of fitting a surface around given curves or markers. It is also possible to import surfaces and curves from *Rhino*, which was found to be better for modelling from scanned data. For directly modelling a hull form within *MAXSURF*, a point cloud or lines plan is the most useful data source.

2.6.1 3D Scanning

3D scanning is a term that is used to describe all methods of extracting information from an object in three dimensions. Used extensively for mapping terrain, many methods can also be applied to smaller objects. These techniques offer a way of creating a digital version of an object, making it easier to take measurements and keep a record of the object (Webster, Sims and Means, 2015). A 3D scan would provide a series of known points along the surface of the hull positioned relative to a predefined origin, which can then be interpreted as either a point cloud or a surface mesh.

There are several forms of 3D scanning, including photogrammetry, laser scanners and white light scanners. These are all contactless methods, meaning that they will not damage the surface that they are recording (Emam, Khatibi and Khalili, 2014, p. 353; Jiang *et al.*, 2016, p. 211). Light scanners themselves come in two forms; those that use markers to assist tracking and positioning, and those that do not (Dickinson *et al.*, 2016, p. 210).

Several scanning techniques could be employed to capture information from models. A number of factors need to be considered, including accuracy, processing cost and portability. The last of these is related to the location of available models in museum archives; it needs to be possible to take the scanner to the model. The accuracy and processing cost are interlinked and a compromise between them is normally required. As the scanned models will need to be scaled up to obtain the final hydrostatics for the ship, any errors will also be scaled. The majority of half models for 19th Century merchant ships appear to be 1:48 scale (1/4 inch per foot), meaning any deviation from the actual surface will be 48 times larger. As most ship hulls are smooth, anomalies that may cause problems later on may be removed by including more data points. Conversely, increasing the number of data points will increase the time to process the scan, and an increased number of data points may have the effect of increasing the surface complexity.

The digital reconstruction of hull forms will enable previously unknown hydrostatic data to be extracted and the creation of a new VPP aimed at historic ships allows new performance data to be generated. The digital models will not only provide more information to carry out a parameter based analysis of the data, but will also provide enough information to generate a velocity prediction, giving an insight into the performance of 19th Century British merchant ships in a way that has not been done before. This approach provides a more consistent view of the evolution of ships than the studies described in Section 2.3.

2.7 Velocity Prediction Programs

There are previous studies which investigate the performance of ships from the past, specifically sailing performance, which encompasses the resistance and propulsion capabilities of the vessel (Gifford, 1995, pp. 126–127; Grant *et al.*, 2001; Couser, Ward and Vosmer, 2009, pp. 8–10). These, however, are based on real sailing trials of existing vessels or archaeological reconstructions, which is impractical when investigating a wide variety of ships. Other studies treat performance as the ability of a ship to carry cargo (Hughes and Reiter, 1958; Mendonça, 2013). As the 19th Century progressed, the requirement for faster ships increased as competition increased (Greenhill, 1980, p. 26) and so speed, along with cargo capacity, may be used as a measure of performance. A VPP may be used to generate an estimate of the speeds a sailing ship is capable of under a given set of conditions.

Background and Literature Review

A VPP is usually based on balancing forces and moments from the hull and sails. It is usual to consider only the longitudinal forces and the transverse forces and moments acting on the vessel, omitting dynamic effects (Claughton, Wellicome and Shenoi, 1998; Marchaj, 2000). The output is the speed that may be obtained by a sailing vessel at a given wind speed and direction.

Depending on the complexity of the VPP, information such as leeway angle, heel angle and required sail trim may also be extracted. Figure 5 summarises the corresponding hull and sail forces and moments.

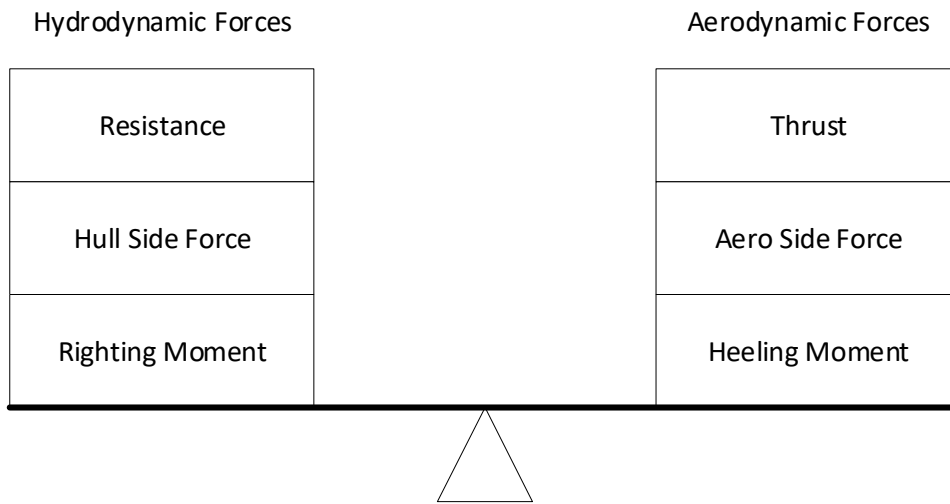


Figure 5: Force balance required for VPP

The individual force components required to calculate these results could alone show certain characteristics of the hull and sails. The hull resistance, for example, gives an idea of the efficiency of the hull (Tonry *et al.*, 2014, p. 1). However, care needs to be taken when comparing the resistance of different hull forms, as it is heavily dependent on size. Resistance alone does not take into account some of the more extreme design changes that occurred during the 19th Century, such as changes to propulsion systems. It would also omit some of the other important outputs that can be obtained from a VPP, such as the leeway angle. This is dependent on the side force from the hull and sails, and has a significant effect on the course keeping abilities of a ship. The heel is also a useful measure, as it has implications for both crew comfort and safety. Prior to the introduction of the Plimsoll mark in 1876, there was no legal minimum freeboard and therefore it may not have necessarily taken a large heel angle for a vessel to flood or capsize (Barnaby, 1871, p. 64).

The force components used in the VPP can come from a variety of sources. The most common of these are from model test data and series data (Claughton, Wellicome and Shenoi, 1998; De Jong, 2008). For VPPs concerning historic ships this is usually based on tank tests (Grant *et al.*, 2001; De Jong, 2008; Palmer, 2009b, p. 320), or where the aim is to obtain a polar performance diagram only, full scale trials on a replica ship (Finney, 1977; Palmer, 2009b, p. 324). The downside of this

is that they are limited to one particular ship or ship type. This research aims to create a VPP that can be used for a wide variety of ships. The following sections review some of the methods that may be used for calculating the individual components required for a VPP.

2.8 Resistance Estimation of Historic Ships

The first step in determining the speed of a vessel is to estimate the hull resistance. This is the force acting against the thrust and hence is used to determine forward ship speed. The determination of total resistance requires combining a number of individual resistance components dependent on the calculation method. As shown in Figure 6, there are several ways of approaching this problem: the use of computational fluid dynamics (CFD) to simulate the various resistance components; the use of standard series data; experimental calculation using scale models; theoretical estimation; or a combination of the above (Molland, Turnock and Hudson, 2011, p. 188).

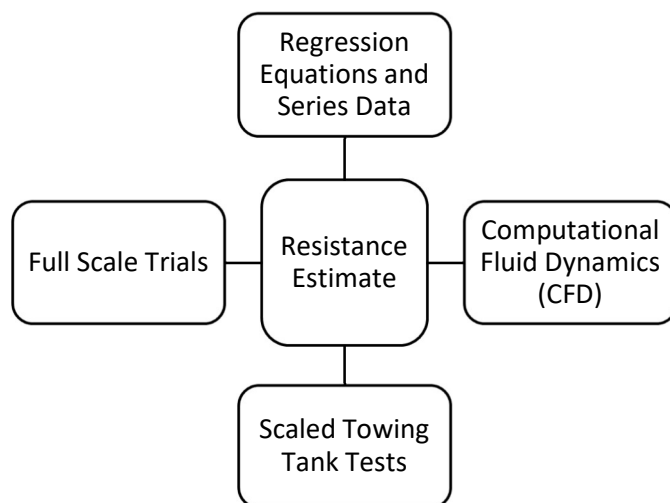


Figure 6: Breakdown of different resistance estimation methods

For historic ships, there is scope for exploiting computational methods. Modern performance analysis is often concerned with hull optimisation, usually for the purposes of meeting environmental regulations (Molland, Turnock and Hudson, 2011, p. 3). The optimisation process acts as a feedback loop, with iterations until the design meets the requirements. This process may be adapted by removing the feedback loop, enabling individual details of ship performance to be calculated for an existing design.

The major disadvantage of using modern evaluation techniques is the reliance on geometry. Ships today vary from those in the 19th Century in both size and shape. Many analysis methods use modern assumptions, for modern ships. For example, the empirical series data and regression formulae derived from towing tank tests and used in algorithms for performance prediction programs are often divided into “families” and come with a warning that they may not provide

exact results (Bentley Systems Incorporated, 2013, p. 3). Care should be taken, therefore, to ensure that the given hull parameters are within the range specified for each method (Fung, 1987, p. 78; Molland, Turnock and Hudson, 2011, p. 191). Some examples of the geometry typical to these families can be seen in Figure 7, along with the body plan of the *Cutty Sark* to highlight the difference in hull shape. Whilst some of this modern geometry may bear a resemblance to later steam ships or the bulk-carrying windjammers, this may not hold true for earlier sailing ships. It is therefore necessary to consider the suitability of a method for multiple ship types, something that has not yet been explored in detail.

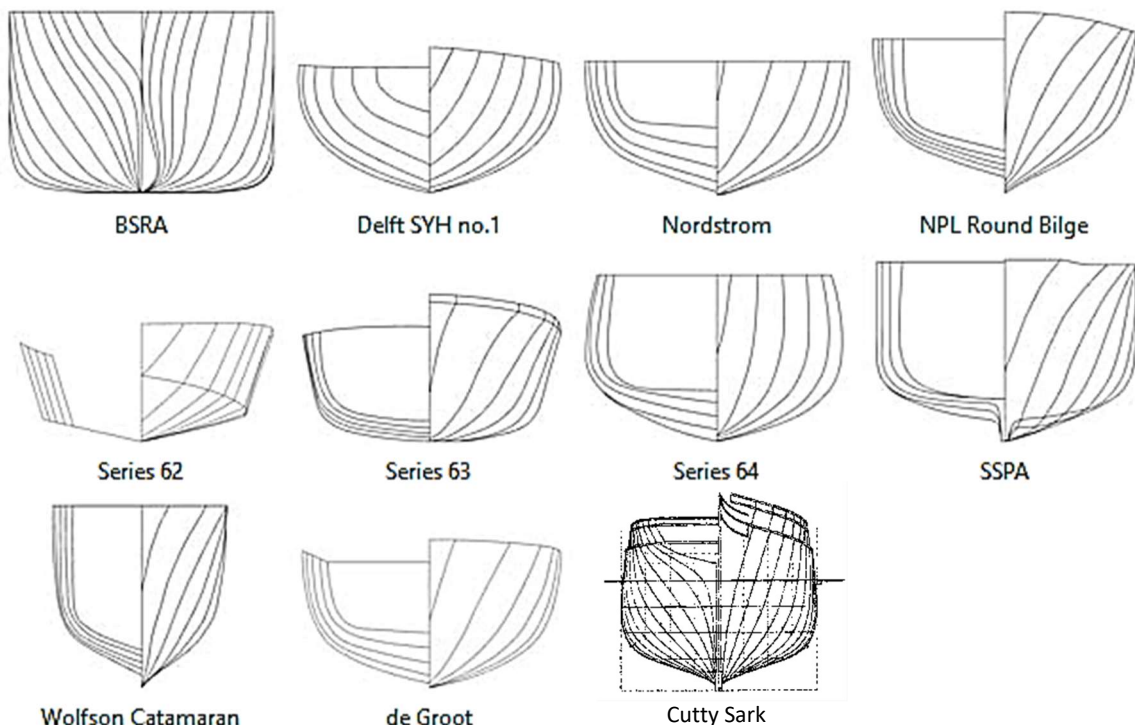


Figure 7: Series hull shapes supplied by the Wolfson Suite 2016 PowerPrediction Software (Wolfson Unit, 2016) and body plan of the *Cutty Sark* (Lubbock, 1924, p. 31)

Considerations must also be taken with regard to the nature of historic ships in computational models and simulations. The hull roughness, for example, is often much greater than would be normal for a modern ship that many of the computational methods are tailored to (Palmer, 2009a, p. 32). This would also need to be considered when using model testing. However, as this factor will need to be calculated for all methods it is proposed that in order to make a direct comparison hull roughness should be omitted from the resistance estimation.

2.8.1 Full-Scale Replicas

Building a full-scale reconstruction of a vessel is perhaps the most obvious way to evaluate performance. There are advantages in understanding how the vessel is built that cannot necessarily be found from examining the archaeological record (Macarthur, 2009, p. 176; Bischoff *et al.*, 2014, p. 24) or creating a computer model. The main downside stems from the high costs

involved (McGrail, 2009, p. 21; Tanner, 2018, p. 143). To look at multiple vessels of any large size would require several decades and a vast pool of resources.

Tools and materials have an impact on the reliability of information that can be extracted from full scale reconstructions (Bischoff *et al.*, 2014, p. 25). The use of tools and materials available for the correct period may increase the authenticity of the design in terms of construction and measured performance. Some examples of replicas have sought to achieve this, such as the hypothetical Egyptian vessel described by Couser *et al.* (2009). The Polynesian canoe *Hokule'a*, however was unable to use authentic materials (Finney, 1977, p. 1278) and so there is a question of how useful performance results may be from a historical point of view, as it is essentially a modern boat. This is often a downside to using full-scale reconstructions when a compromise between cost and authenticity is required. Health and safety requirements also provide a barrier as ships are generally not allowed to operate unless fitted with modern amenities such as an engine, sewage disposal and electric lighting (Macarthur, 2009, p. 169). Despite the reduced confidence in performance results, however, a balance must be drawn between safety and authenticity, as the builders of the 1977 replica *Pride of Baltimore* discovered when she capsized and sank in 1986 (Davis, 2009, p. 180).

A certain level of confidence in the performance of a reconstruction may be obtained due to the complex nature of the environment and difficulties in modelling accurate wind and sea conditions. Scale model tests are carried out in conditions that are not necessarily characteristic of the operating environment. This, added to potential scaling errors being eradicated, means that the full-scale reconstruction has an advantage over a model (Tanner, 2018, p. 143).

2.8.2 Regression Based Methods

A common method of hull resistance estimation uses mathematical models or regression equations based on empirical data, which have the advantage of being easily computerised (Moody, 1996, p. 73). Alternatives include tabulated or graphical ship data, which are less suited for computerisation due to the need for interpolation (Moody, 1996, p. 74). In this section, the use of mathematical models based on regression analyses is explored.

Table 1 details some of the more commonly used regression methods for estimating hydrodynamic resistance in ship design. These mostly calculate total resistance (R_T) by means of combining the frictional resistance (R_F) with a 'residuary' resistance (R_R). The exception is the Holtrop method which, by applying a form factor to R_F , calculates the wave-making and viscous resistances (R_W , R_V). The Fung and Holtrop methods are considered in the most detail as they appear to be the most suitable for historic ships based on vessel type and parameter limits.

Table 1: Summary of Regression Methods for Resistance Estimation

Method	No. Models (Observations)	Aimed at:	Resistance Components	Correlation Factor
Holtrop	334	Tankers, general cargo and container ships, fishing vessels, tugs, frigates	R_R, R_W, R_F, R_V	Constant (calculated by method)
Van Oortmerssen	93 (970)	Small Ships (trawlers/tugs)	R_R, R_F	User specified
Series 60		Single Screw Merchant	R_R, R_F	User specified
Delft (I,II,III)	39	Yacht Canoe Hull	R_R, R_F	N/A
Compton	6	Small High Speed Transom Stern	R_R, R_F	Fixed (0.0004)
Fung	739 (>10000)	High Speed Transom Stern	R_R, R_F	Fixed (0.0005)

The Fung method is based on 10672 resistance data points from 739 models from the David Taylor Model Basin (Fung and Leibman, 1995, p. 152). This was intended for the estimation of resistance of high speed transom stern hull forms, with the aim of providing a reliable estimation for larger vessels. The speed range covered by this method is from a Froude number of 0.15 to 0.9, which satisfactorily covers vessels such as *Cutty Sark*, capable of reaching speeds of over 17 kn ($F_n = 0.346$) and often averaging over 14 kn ($F_n = 0.285$) (Lubbock, 1924, pp. 11–15). The method is used to calculate the residuary resistance of the vessel (Fung and Leibman, 1995, p. 162). Total resistance is then calculated using the frictional resistance defined by the International Towing Tank Conference (ITTC) 1957 friction line, given by:

$$C_F = \frac{0.075}{(\log_{10} Rn - 2)^2} \quad (2)$$

$$R_F = C_F \frac{1}{2} \rho_W WSA \cdot V_s^2 \quad (3)$$

Where C_F is the coefficient of frictional resistance, Rn is the Reynold's number and ρ_W is water density.

The allowable parameter limits for the Fung method are shown in Table 2 and are based on the volumetric displacement (∇), waterline length (L), LCB, WSA, mass displacement (Δ), half angle of entry (i_E), midship sectional area (A_M), waterplane area (A_{WP}) and the transom area, beam and draught (A_{20}, B_{20}, T_{20}). It should be noted that the units are in feet and UK tons.

Table 2: Limits for the Fung Regression Analysis. Minimum and maximum data from (Fung and Leibman, 1995)

Parameter	Fung Minimum	Fung Maximum
$\Delta/(L/100)^3$	16.239	359.180
LCB	0.481	0.591
$C_{ws} = WSA/(\Delta L)^{0.5}$	14.324	23.673
i_E (°)	2.600	31.730
L/B	2.520	17.935
B/T	1.696	10.204
$C_p = V/LA_M$	0.526	0.774
A_{20}/A_M	0.000	0.740
$C_M = A_M/BT$	0.556	0.994
B_{20}/B	0.000	1.000
$C_{wp} = A_{wp}/LB$	0.662	0.841
T_{20}/T	0.000	0.770

The Holtrop method is based on data from 334 models, and is suitable for a greater range of speeds ($Fn = 0.05$ to 0.85), which incorporates all likely speeds for the ships considered (Holtrop, 1984, p. 272; Wolfson Unit, 2016). There are also a limited number of parameters required for the analysis as shown in Table 3, which may improve its suitability for use with historical sources. The method of calculating resistance differs slightly from the Fung method; where Fung uses residuary resistance and frictional resistance to get the total resistance, Holtrop relies on wave-making resistance and frictional resistance with a corresponding form factor (Holtrop and Mennen, 1982, p. 166). Both methods employ the ITTC'57 friction correlation line and allow for the inclusion of appendage resistance. In both cases, if further detail was required, the ITTC'78 friction coefficient line could be swapped in, which allows for the inclusion of air drag and hull roughness (Molland, Turnock and Hudson, 2011, p. 87).

The approach to transom induced drag is the first way in which the methods differ; in Fung, transom resistance is a component of residuary resistance. In Holtrop, it is considered as a component of the total resistance, alongside appendage resistance and an allowance for bulbous bows, a feature which is not catered for in the Fung method, but was beginning to be explored as a method of reducing resistance towards the end of the century (Ferreiro, 2011, p. 348). The approach to transom drag in Fung perhaps makes it less suitable as a universal solution for historic ships, most of which would not have had a transom stern in the modern sense. This may mean that resistance is underestimated where a transom is not present, as two of the terms included in the equation are entirely dependent on transom dimensions. The other main difference between the methods is the way in which the model-ship correlation allowance is included, as both are based on model tests. The Holtrop model-ship correlation coefficient is designed to vary according to the geometry of the vessel (Holtrop and Mennen, 1982, p. 166),

meaning that, along with the limited number of input parameters, it is more adaptable to suit a large number of ship types (MARIN, 2010, p. 8). By calculating the correlation coefficient independently, it may also be adapted to include hull roughness, which is often of importance for historic ships. Fung assumes that the correlation coefficient remains constant (Fung and Leibman, 1995, p. 159). The full methods for both Holtrop and Fung can be found in Appendix A.

Table 3: Limits for the Holtrop-Mennen method. Minimum and maximum data from (Wolfson Unit 2016)

Parameter	Holtrop Minimum	Holtrop Maximum
C_P	0.550	0.850
C_B	0.450	0.840
C_{WP}	0.630	0.950
L/B	3.900	9.500
B/T	2.000	4.000
LCB	-2.000	3.000
Fn	0.050	0.850

2.8.3 Computational Fluid Dynamics

CFD is a method often used in modern ship design and analysis (Weymouth, Wilson and Stern, 2005; Zou, Larsson and Orych, 2010; Tezdogan *et al.*, 2015). This tool enables naval architects to simulate the flow around a given hull form and calculate the pressure and shear forces on individual elements across the surface. These forces are then combined to obtain total resistance. The benefit of this method is that it can produce a relatively accurate result without the need for manufacturing a towing tank model. As it models the flow around the hull form, CFD can be applied to any vessel. The downside of this is that there is still a considerable computing time involved, with modelling each vessel to the standards required as well as the simulation time for each speed. Even a relatively simple simulation assuming calm water can take in excess of 12 hours to run (Tonry *et al.*, 2016, p. 2).

CFD has the potential to provide a result comparable with a full-scale reconstruction. It has advantages due to reduced cost and dependence on available material. Increased complexity of simulations is also a possibility as overall time is reduced compared to full scale trials (Tanner, 2018, p. 143). This enables potentially more vessels to be analysed in the same time at a fraction of the cost required for a full-scale reconstruction. To match the complexity of the environment, however, this advantage may be lost due to the computationally intensive process involved in modelling the free surface (Tonry *et al.*, 2014, p. 2). It should be noted though, that repeatability is increased as a variety of models can be tested under the same conditions. Thus, if CFD is to be applied to the problem, there must be a balance between simulation time and complexity of the model.

A common method for solving the flow around a hull is by using a Reynolds-Averaged Navier-Stokes Equation (RANSE) based solver, which bypasses the need for a complex direct numerical solver for turbulent flow. This is a mathematical model, which accounts for unsteady flow without resolving it, which would be computationally demanding. The downside of this is that the physical accuracy of the solution is dependent on the accuracy of the mathematical model (Çengel and Cimbala, 2010, pp. 878–879).

There are several examples where CFD has been compared with alternative methods, including experimental and mathematical methods. Research into using CFD for manoeuvring calculations have been shown to be 5% accurate in deep water compared to experimental data (Zou, Larsson and Orych, 2010, p. 428). This comparison with experimental data for calculating hull forces indicates that CFD would be a suitable method for analysing historic hull forms where experimental data is limited.

2.8.4 Contemporary Trial Data

Towards the end of the 19th Century, the relatively new science of naval architecture was beginning to gain momentum. As discussed in Section 2.2, an understanding of the different components that made up total hull resistance of a ship was being developed. In the 1870s, William Froude's tests on planks led him to understanding how total resistance could be divided into frictional and residuary components, the latter of which would remain constant between model and full-scale ship. Subsequent tests justified the use of models to estimate ship resistance (Molland, Turnock and Hudson, 2011, pp. 1–2). The result of this advancement was an increasing number of performance trials being carried out both on models and ships, with particular attention given to the shape of the vessel. Several sets of data, including hull parameters, were subsequently published (Fyfe, 1907, pp. v–vi).

These sets of data not only provide an insight into the understanding of naval architecture in the late 19th and early 20th century, but also provide an opportunity to compare results from modern techniques, as described above, with actual trial data that would otherwise be nearly impossible to obtain. As there are very few existing 19th century vessels that still operate, obtaining new data would involve the costly manufacture of towing tank models.

2.9 Hydrodynamic Side Force Estimation Methods

Hydrodynamic side force is an important measure when creating a VPP as it is required to balance the lateral force produced by sails. The side force is also an important component in manoeuvring simulations, as it is required to determine the turning capabilities of a vessel. Previous work on the latter of these is likely to provide the most suitable estimation method for obtaining the side

Background and Literature Review

force generated by the hull, as modern sailing simulations tend to assume a canoe hull body and keel, which is not applicable to a majority of historic ships (De Ridder, Vermeulen and Keuning, 2004). The alternative method of obtaining side force is by means of a model test, which would not be practical in this research.

Empirical or semi-empirical methods for estimating manoeuvring characteristics generally employ the same base method, known as the Mathematical Manoeuvring Group (MMG) method, with the difference between them being in the hydrodynamic derivatives used. In order to obtain the hydrodynamic side force from these methods, it is necessary to use a linearized approach on the assumption that forward speed is constant (Fossen, 2011, p. 140). This allows the sway and yaw model to be decoupled from surge. Although yaw moment and side force remain coupled, it is assumed that in the case of large sailing ships the yaw moment is negligible if the ship is sailed correctly. The side force can therefore be calculated from:

$$Y'(\lambda, r') = Y'_\lambda \lambda + Y'_r r' + f_Y(\lambda, r') \quad (4)$$

where Y' is the non-dimensional form of hydrodynamic side force, Y'_λ and Y'_r are the sway and yaw derivatives respectively, and $f_Y(\lambda, r')$ represents the non-linear term based on the leeway angle (λ), and the dimensionless turning rate (r') (Inoue, Hirano and Kijima, 1981, p. 113). If we assume that yaw moment is negligible as under normal sailing conditions the ship should not be yawing, this is reduced to an equation of the form:

$$Y'(\lambda) = Y'_\lambda \lambda + f_Y(\lambda) \quad (5)$$

Assuming that f_Y is dependent on λ^2 , $\lambda r'$ and r'^2 , this can be presented as:

$$Y'(\lambda) = Y'_\lambda \lambda + Y'_{\lambda\lambda} \lambda |\lambda| \quad (6)$$

Given the hydrodynamic derivatives Y'_λ and $Y'_{\lambda\lambda}$, the side force may then be estimated. Some of the methods of obtaining these coefficients are described below. There are two main approaches used: treating the hull form as a low aspect ratio wing on its side or using slender body theory (Horn, 2000, p. 5). There have been several attempts to obtain the regression formulae to calculate these derivatives.

Inoue et al (1981) found that the lateral force on the hull could be estimated using only length (L), beam (B), draught (T), C_B and trim (τ). The hydrodynamic derivatives, presented by Skogman (1985, p. 208) and defined in equations (7) and (8), are based on the regression analysis of 10 different models representing a variety of modern hull forms (general cargo, oil tanker, car carrier and RORO). This method is one that treats the hull form as a low aspect ratio wing and the measurements were extracted from rotating arm tests. Unlike most other methods, Inoue et al

include the non-linear term $f_Y(\lambda, r')$ in the equation of motion, allowing larger leeway angles to be considered.

$$Y'_\lambda = \left(-0.5\pi k - 1.4C_B \frac{B}{L} \right) \left(1 + \frac{2\tau}{3T} \right) \quad (7)$$

$$Y'_{\lambda\lambda} = -6.6(1 - C_B) \frac{T}{B} + 0.08 \quad (8)$$

Where k is the hull aspect ratio ($k = 2T/L$).

An updated version of the Inoue method is presented by Kijima et al (1990), which obtains the hydrodynamic derivatives based on 13 ships in the load, half load and ballast conditions. The authors note that the method is most suitable for conventional hull forms, in particular regarding the stern shape, which has been noted by others to be an important factor in manoeuvrability (Clarke, Gelding and Hine, 1983, pp. 59–60; Lee and Shin, 1998, p. 633; Horn, 2000, p. 6). As this work is an extension of the study by Inoue et al (1981) it also considers the non-linear derivatives, although the earlier paper was based on fewer models and Kijima has included extra terms to improve accuracy (Horn, 2000, p. 91). The linear term of both methods are the same and include a term to account for trim. The non-linear derivative of the Kijima method is given in equation (9). In 2000 this method was adapted to account for stern shape, introducing terms based on coefficients of the aft half of the vessel (Noor, 2009, p. 45). As these new terms are relatively complicated to derive for those unfamiliar with naval architecture, this method is not ideal for this analysis and so is not presented here.

$$Y'_{\lambda\lambda} = -2.5(1 - C_B) \frac{T}{B} + 0.5 \quad (9)$$

Clarke et al (1983), applies linear theory to the problem and proposes empirical models based on the acceleration and velocity derivatives. The authors consider a range of previous attempts to estimate the linear derivatives, including Inoue (1981), Wagner-Smitt (1970) and Norrbin (1971), the last two of which are based on the same data set as each other (Clarke, Gelding and Hine, 1983, p. 52; Horn, 2000, p. 89). These apply the low aspect ratio wing theory with the derivatives measured from Planar Motion Mechanism (PMM) experiments. The aim of Clarke's paper is to explain some of the differences between these previous attempts to obtain empirical formulae by carrying out multiple linear regression analyses on both rotating arm and PMM experiments. The linear nature of this method reduces the range of leeway angles that may be considered. This means that at higher angles, hydrodynamic side force will be underestimated. Another set of regression coefficients is presented by Shin and Lee (1998), aimed at low-speed, blunt ships with a stern bulb. These are based on the same hydrostatics as previous studies, though with the

Background and Literature Review

inclusion of the stern bulb area for estimating yawing moment. A summary of the methods described are provided in Table 4.

Table 4: Summary of manoeuvring prediction methods

Method	No. of Models (Observations)	Experiment Type	Base Theory	Accounts for Stern	Accounts for Trim	Suitable for:
Norrbin	(30)	PMM	Low Aspect Ratio Wing	No	No	
Wagner Smitt	(30)	PMM	Low Aspect Ratio Wing	No	No	
Inoue	10 (24)	Rotating Arm/Oblique Tow	Low Aspect Ratio Wing	No	Yes	Typical Merchant Hull Forms
Clarke	(72)	PMM/Rotating Arm	Slender Body		No	
Kijima (1990) (2000)	13 (29)	Rotating Arm/Oblique Tow	Low Aspect Ratio Wing	No	Yes	Conventional Forms
Lee & Shin		PMM	Low Aspect Ratio Wing	Yes	No	Low-Speed Blunt Ships with Stern Bulb

Based on the above discussion, the two most suitable methods appear to be those by Inoue and Kijima (1990). These both incorporate a non-linear term, which is important when considering larger angles of leeway. As with the Holtrop method for estimating hull resistance, both of these methods are best suited for conventional hull forms. From examination of the model particulars used by Kijima, most of which were used in both studies, it can be seen that these hull forms had a relatively shallow draught compared to vessels from the 19th Century. The minimum and maximum parameters of the range of ships scaled to a length of 2.5m are given in Table 5.

Table 5: Parameter limits of the vessels used for the Kijima (1990) and Inoue (1981) Equations

	Min	Max
L (m)	2.5	2.5
B (m)	0.367	0.555
T (m)	0.1	0.183
C_B	0.522	0.835

The main issue with the use of regression analysis for estimating hydrodynamic side force is related to the number and variety of hull forms used. Most are based on a small selection of hull forms with a wide variety of geometries, which makes it harder to identify trends due to the scatter of data (McTaggart, 2016, p. 7), and there is some variation in curve fitting methods (Clarke, Gelding and Hine, 1983, p. 54). Resistance methods contain a much larger quantity of data and therefore more confidence can be placed in the regression equations. As can be seen in Figure 8, the use of empirical methods for estimating any manoeuvring characteristics comes at

the cost of accuracy (ITTC, 2008, p. 146). This indicates that a validation of the methods is required. An advantage of using a manoeuvring model to estimate hydrodynamic side force for the VPP is that at a later stage additional terms for yaw may be added to allow the simulation of sail performance in a wider variety of conditions.

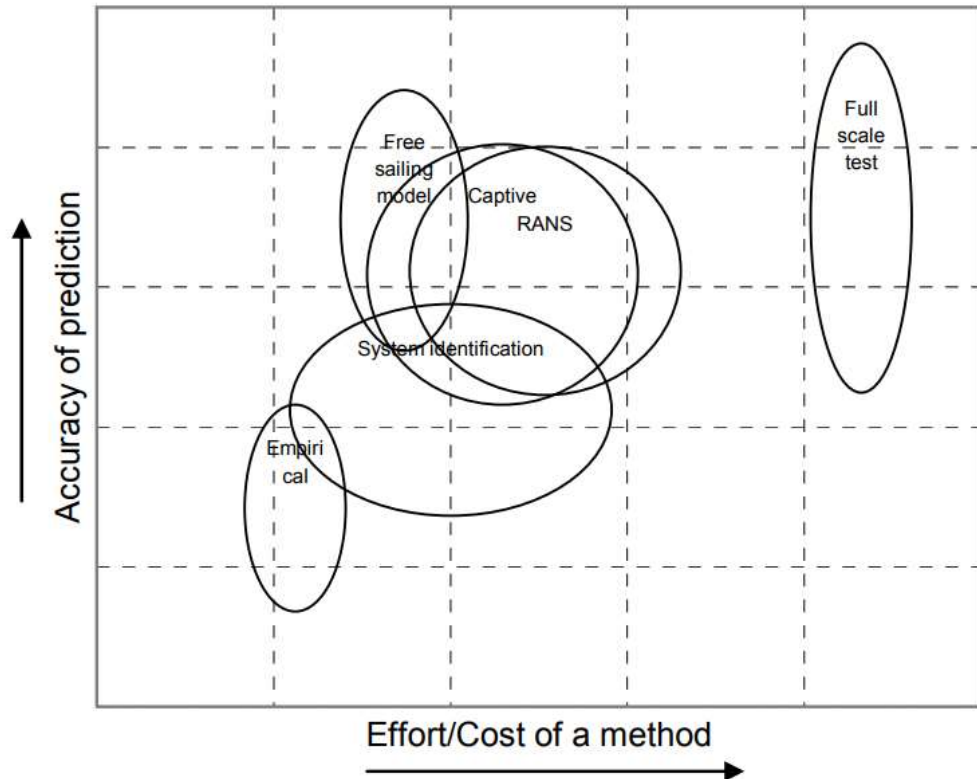


Figure 8: Accuracy and cost of manoeuvring prediction methods (ITTC, 2008, p. 146)

2.9.1 Resistance Due to Leeway

As the angle of leeway increases, it is to be expected that the resistance in the fore-and-aft direction will increase. This is the added resistance due to leeway (R_L). Longo and Stern (2002) show that, for a Series 60 hull form, the increase in resistance is linear with the increase in leeway, meaning that the added resistance may be added directly on to the total resistance. The only example of a regression-based analysis of the added resistance due to leeway is in the Delft yacht hull series, which, as has previously been discussed, would be unsuitable for most large historic hull forms (De Ridder, Vermeulen and Keuning, 2004). An equation is also suggested by Skogman (1985, p. 209) for estimating the added resistance of a kite assisted research vessel, however it is noted that there is a large amount of scatter in the data from which the regression curve is obtained. It is also unclear as to which units should be used. Other literature that covers the topic suggests calculating added resistance, or the hydrodynamic derivatives for resistance, by means of model testing (Fujiwara *et al.*, 2005, p. 135).

2.10 Propulsion Forces

In addition to the hydrodynamic forces, propulsion forces (thrust and aerodynamic side force) also need to be known in order to obtain an estimate of ship speed. In the case of 19th Century ships, the propulsion may be provided from sails, steam driven paddles or screw propellers, or a combination. Sails provide a thrust, aerodynamic side force and heeling moment that will need to be counteracted by forces from the hull to reach a state of equilibrium. Steam driven ships will generate almost entirely thrust when travelling in a straight line under engine, for which only R_T is required for equilibrium. However, as nearly all steam powered ships in the 19th Century were fitted with auxiliary sails, it is also important to consider the sailing properties of these vessels (Brock and Greenhill, 1973, p. 17; Allington, 2004, p. 125).

2.10.1 Sail Propulsion

There is currently a good understanding of the sail forces generated by modern rigs (Marchaj, 2000; Whitewright, 2011, p. 3). However, there have been minimal studies on the mechanics of traditional sailing rigs. Modern yachts are often Bermudan rigged, which work by generating lift and drag forces as air passes over the sail. The majority of ships in the 19th Century, however, would have been square rigged, which offer significantly different lift and drag coefficients.

Although a small number of the sails, such as headsails, staysails and spankers operate in a similar manner to modern sails, with lift as the primary driving force (Radhakrishnan, 1997, p. 506), the main force acting on the square sails would have been drag (Radhakrishnan, 1997, p. 504). This difference in sail type means that modern VPPs would not be appropriate for most historic ship types.

Contemporary estimations for sail power cannot be considered as a reliable option for calculating sail force, as even towards the end of the century, the force components acting on the sails were considered “undeterminable” (Kemp, 1891, p. 95). It would appear that sailing rigs were designed more as a matter of experience and general understanding of the physics behind sail propulsion and the speeds that could be obtained in similar vessels as opposed to actual calculation.

Despite being considered an obsolete technology, there are still examples of square-rigged ships being built, often for sail training organisations. As there is little or no base data for sailing performance, it is usual in this case for the designer to conduct wind tunnel tests (Deakin, 1997, pp. 70–71). As time is often limited, a set of common rig setups are tested, so vessel performance can be calculated for given conditions. These tests produce a set of data that may be used in a VPP for that vessel. The downside of this method is that it is vessel specific.

To look at several different rigs, a more flexible method would be required. A student project looking at creating a simulation of *HMS Victory* developed a series of regression equations for individual sails based on a series of wind tunnel tests (Leszczynski *et al.*, 2005, pp. 94–95). This was so that a greater variety of sail conditions could be considered within the simulation. The equations developed in the project include the effects of blockage and aerodynamic drag, which means they would not need to be calculated separately. A potential issue with using these regression equations is related to the age of the vessel in question. *HMS Victory* was designed and built in the mid-18th Century. In the late 18th to early 19th Century many new rig types were emerging and replacing the old ones (MacGregor, 1980a, pp. 39–47). However, as the sails were modelled individually, it should be possible to model some of the newer rigs based on this data. Despite this, it is only likely to provide valid information for primarily square-rigged vessels, such as ship or barque rigged, and not fore-and-aft rigged vessels such as schooners. The only way to combat this lack of reliability would be to create a new regression method based on a large systematic study of historic sailing rigs, which is outside the scope of this research.

2.10.2 Steam Propulsion

The propulsion force generated by steam-powered vessels is almost exclusively thrust. Both aerodynamic side force and heeling moment should be negligible when the vessel is travelling in a single direction. The primary issues to be tackled in order to calculate propulsive power are related to engine and propulsor efficiency. As steam ships were limited by the amount of fuel they could carry, efficiency was always a matter of concern for 19th Century engineers. Scott Russell provides a good overview of the issues facing ship designers, including ways to estimate the potential output of propulsive mechanisms (Scott Russell, 1864). Records of trials and designers' handbooks provide some insight into how engine efficiency was treated and calculated for a number of ships (Fyfe, 1907). The most commonly recorded engine power is the nominal horsepower (NHP), which is based on geometry rather than actual power output, and so should be treated with the same caution as tonnage. A few sources supply the indicated horsepower (IHP), which is more useful, as this is the actual power supplied by the engine. To estimate the speed of a vessel, however, the effective horsepower (EHP) is required, which is equivalent to the IHP after efficiency losses have been accounted for.

Given the quantity of contemporary work on steam propulsion and efficiency, it may be possible to estimate EHP, or at least IHP, based on a statistical analysis. Fyfe (1907), for example, presents a handbook to aid steam ship designers in the early 20th Century using data collected from various trials and tank tests, many of which are 19th Century examples.

2.11 Heeling/Righting Moments

In addition to the forward and lateral force balance of the hull and sails, it is usual to consider the lateral moments in a VPP (Claughton, Wellicome and Shenoi, 1998; Marchaj, 2000). These equate to the heeling moment from the sails and righting moment developed by the hull. Heeling moment may be calculated based on the force on the sails applied at the centre of effort, which can be estimated from the sail geometry. Righting moment, however, is dependent on the stability characteristics of the hull, for which underwater geometry and vertical centre of gravity (VCG) are key.

Obtaining the VCG is often harder in older vessels as weights and centres of the hull, rigging and cargo are required. Ideally the VCG of a vessel would be found by conducting an inclining experiment on a complete and accurate reconstruction (Tanner, 2013a, p. 140). This is not practical most of the time and so an estimate is required. Several 3D modelling programs now allow an input of the material used to help estimate weight and centre. This may require a lot of detail in the model, which could be challenging dependent on records, and would result in an increased processing time. Factors such as construction material, structure and cargo loading (Poveda, 2012) will need to be taken into account. This may be easily changed and adjusted in a computer model where it cannot on a physical model, something that remains true for any element of performance analysis (Rawson and Tupper, 2001a, p. 36).

Previous studies that have considered the stability of a historic ship have calculated the weights and centres of a vessel by assigning each individual element, such as planks, a density and allowing a margin for other unknown fittings, for example fastenings (Poveda, 2012, p. 4; Tanner, 2013b, p. 87). The ships under consideration for these studies were both under 30 m in length, but many ships from the 19th Century were more than twice this. It would therefore be very time consuming to calculate the weight and centre of even an individual ship in this way. A proposed solution to this problem is to consider uniform density across larger structural members, such as the hull shell and frames to obtain an estimate of the weight and centre of gravity of the lightship hull. Estimated crew and cargo weights and centres can then be included. In several cases, the overall displacement is known and so it should be possible to equate the estimate with known information to show how reliable this method is.

2.12 Summary

A great deal of change occurred in merchant shipping throughout the 19th Century. There is a transition between sailing ship types, from the East Indiamen, to clippers and finally to windjammers. During this time steam propulsion also becomes a viable option and the primary shipbuilding material transitions from wood to iron and steel. In addition to this, there are a

Background and Literature Review

number of pieces of legislation that have been cited as the reason for some significant changes to hull shape. The understanding of hydrodynamics evolved from an empirical viewpoint, based on observation and experience, to the form that it takes today, where scientific theory plays a significant part. These narratives form the ideal bases for a series of case studies that will be carried out in Chapter 6 to determine the value of the methodologies developed in this research.

Despite this, there has been little research into the effect that political and economic events and processes had on the evolution of ship performance. The few attempts that have been made to quantify historic ship performance have focused mainly on individual vessels and their sailing performance. The most common method is through full-scale reconstructions, which is an expensive solution and often has issues with modern standards. The use of modern engineering analysis techniques to estimate historic ship performance has not been investigated thoroughly.

Limited data is available for ships from the era, although this is often incomplete or does not permit a complete performance analysis, for example where tonnage is used as a measure. Given the correct hull parameters, it should be possible to infer the change in ship performance over time; however, it is unlikely that there is enough available data to achieve this. An assessment of existing data will therefore be made in Chapter 3 to examine the extent to which it can be used.

With enough information, it should be possible to obtain the approximate speed and sailing characteristics of a vessel in a given condition using a combination of numerical and statistical analysis combined in a VPP. This will enable vessels with a variety of available data to be compared to each other, hence allowing a narrative of how performance changed over time. In order to obtain enough information, however, a method of digitising hull forms is required, either through 3D scanning of half models or reconstruction from a lines plan. 3D scanning methods that could be used for this have been identified and will be examined in greater detail in Chapter 5. As there has been no previous work on a VPP suitable for a variety of historic ship types, it is proposed that a modular approach is taken. This will mean that if an alternative method for calculating an individual force component is required, it should be possible to change the program accordingly without the need to rewrite large sections of the code. This will be of particular importance with regards to the propulsion forces as these are perhaps the most complicated to replicate.

Tools that could potentially be used for this research have been investigated in detail. For resistance estimation, the use of regression equations and CFD are possibilities. A comparison between two different regression methods and CFD will be carried out in Chapter 4, with the potential of an additional comparison with contemporary trial data. Regression methods for calculating hull side force have also been identified and will be assessed in a similar manner. A

Background and Literature Review

limited review of approaches for estimating propulsion forces and heeling and righting moments has also been covered, but will require some further testing.

Chapter 3: Parametric Analysis of Existing Data

The discussions in Sections 2.3 and 2.5 on the available data on 19th Century British merchant ships and parametric analyses have highlighted the potential to infer performance from data found in literature. Over the course of this research, data has been collected on over 1000 ships, from a number of the sources described, including books, databases and wreck reports. Around 310 of these have either a lines plan or builders half model known to be in existence. The rest of the data comes primarily from leading literature on the subject of 19th Century merchant ships (Lubbock, 1953a, 1953b; MacGregor, 1980a, 1984a, 1984b, 1988).

Not all sources were able to draw on complete records (MacGregor, 1984a, p. 21), however, and so there is likely to be some geographical bias towards areas with better record keeping. This is particularly the case for those areas that drove the building of iron ships, as this was a new technology and hence better recorded (MacGregor, 1988, p. 130). These include the North of England and Scotland (MacGregor, 1988, p. 132). For the same reason there may also be some bias towards certain trades, for example the well-known tea trade, which sparked public interest at the time. In an attempt to minimise the effects of this, some limits have been applied. Where possible, the data has been restricted to ocean-going cargo and passenger vessels only. This means that they must have been built to operate beyond British waters, including the Channel and North Sea. Examples of ocean-going vessels include those trading to the Mediterranean, South America, or China. The dataset does not include whalers or cruise ships. They must also have been built and originally registered in the UK, which during this time period included Ireland. It must be noted that this dataset only makes up a very small portion of the ships built and registered in the UK in the 19th Century. Records on tonnage indicate that between 1814 and 1899, over 57,000 ships were registered in the UK (Mitchell and Deane, 1971, pp. 220–222).

There is also a variation in the availability of data with time; earlier records are unlikely to be as complete as later ones, particularly since the introduction of official numbers in 1855 (Owens, 2015). Figure 9 shows the number of ships in the dataset in five year intervals within the 19th Century, where it is clear that a large portion of the data occurs within the final 50 years. Despite the variation in data levels and the potential for bias, it is believed that even where the data is sparse, the ships selected are representative of typical ocean-going merchant ships based on descriptions of the vessels in question. The discrepancy between the number of sailing ships and steam ships is owing to a lack of literature on ocean-going steam ship dimensions, as much of the literature from this period focuses either on the development of the sailing ship, or the advances in machinery technology.

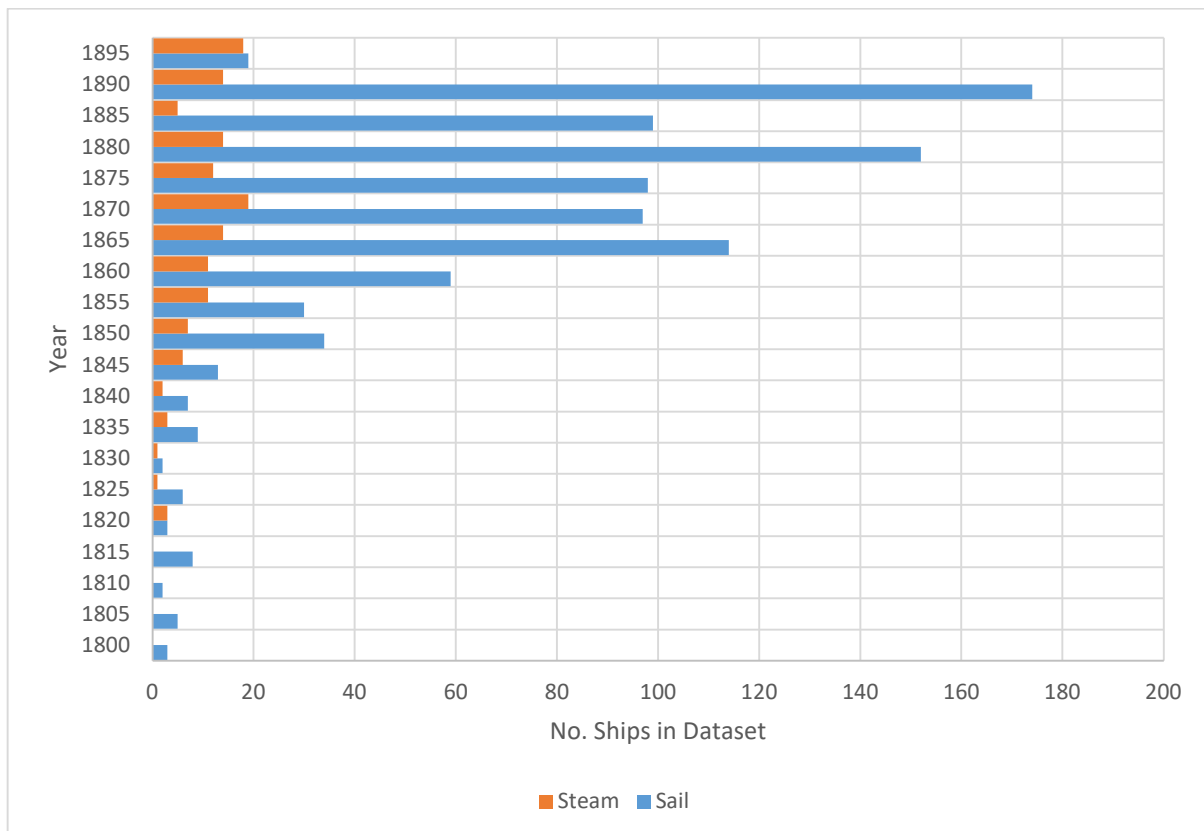


Figure 9: Spread of ships included in the dataset over time

3.1 Variation of Hull Dimensions

Of the gathered data, the most common ship dimensions presented are the length, beam and depth of hold, as these are the dimensions usually required for tonnage calculations. Length and beam are perhaps the most useful of these dimensions for inferring performance, as the depth of hold is dependent on the internal layout of the ship and does not necessarily represent the true size. There is some variation in the measurement of these dimensions as tonnage definitions varied, and records are not always clear which definition is used. The length is generally the distance between the fore part of the stem and the sternpost, which is approximately equal to the length between perpendiculars (L_{BP}) (MacGregor, 1988, pp. 271–273). The beam given in registration is generally the maximum (*Customs Act (3 & 4 Will. IV C.55)*, 1833; MacGregor, 1988, p. 273).

These primary dimensions may be examined using the length-beam (L/B) ratio, a non-dimensional ratio that does not take into account the size of the ship. This is important for comparing historic ships, particularly during this time period where the main construction materials vary, allowing for a huge variety in ship size, with an average increase in length of just under 200 ft from 83.44 ft to 281.98 ft between the first 20 years and the last 20 years of the 19th Century according to the dataset. This increase is likely to have been driven by a combination of factors, including an increase in world trade that called for larger cargo capacities, and a change from wooden

construction to iron and steel which enabled much larger vessels to be constructed (Geels, 2002, p. 1268). Figure 10 shows the variation of L/B ratio based on 936 sailing ships and 138 steam ships with time. Although the change in L/B with time has been discussed in relation to more modern vessels (Watson, 1998, p. 66), a graphical representation of it cannot be found. By plotting this data against time, it is possible to visualise the evolution of hull forms. The data for the sailing ships shows the clearest trend, with the average L/B increasing from 3.4 to 6.7 over the course of the century. As this dataset is comprised of the same ship types, the distinct change in dimensions indicates that there were significant changes to the way ships were designed during the 19th Century.

Previous research on 19th Century ship design provides some reasons for the features displayed in Figure 10. The first of these features is the reasonably unchanged L/B for the first 30 years or so. This is likely to be due to an Act of Parliament dating back to 1784, which limited the size of merchant ships to an L/B of 3.5 in an attempt to reduce smuggling (*Smuggling Act (Geo. III C.47)*, 1782; Benham, 1986, pp. 108–116; MacGregor, 1988, p. 14). Around half of the vessels during this time period appear to keep to this rule, however there are a number of exceptions. Many of these exceptions will be those ships which were exempted from the Smuggling Act, which included most long-distance trading vessels included in this dataset (*Smuggling Act (Geo. III C.47)*, 1782). A small number of ships that fail to comply with the rule may have been those which relied on the authorities turning a blind eye. The purpose behind the rule was to ensure that no ships would be fast enough to outrun revenue cutters, however, the majority of the vessels in this dataset were large, square-rigged vessels that posed no threat to the much smaller fore-and-aft rigged cutters, meaning that they were able to bend the rules to some extent (Benham, 1986, pp. 108–116). Despite the exceptions covering the majority of vessels included in this dataset, it appears from the data that the restriction of L/B probably did influence ship design.

According to Figure 10, after the smuggling act was reduced in 1833 to cover only fore-and-aft rigged vessels below 200 tons (MacGregor, 1988, p. 14), there appears to be an increase in the average L/B . This cannot be solely attributed to the removal of the limitation, however, as a change in tonnage law is also likely to have impacted vessel shape. The 1836 law changed the way tonnage was calculated, switching to a volume based method. However, the calculation only required three sections to be measured, and so enterprising shipbuilders found that this could be exploited to create maximum cargo capacity for a minimum tonnage (MacGregor, 1988, p. 98). This was achieved by creating hull forms with long, fine ends, which would reduce the capacity to some extent. This could be countered by increasing the length, which was only measured at half the depth and so introducing a sharp rake to the stem and stern helped to mitigate this. This means that a balance would need to be created between cargo capacity, length and tonnage. As

Parametric Analysis of Existing Data

there is currently limited information on the actual size of ships, other than the tonnage, more data would be required to examine this effect in detail.

There is a lot more variation in the steam ship data, particularly between 1845 and 1875. This may be because of the experimental nature of many of the steam ships, but also because in many cases it is harder to define their use. Due to poor engine efficiencies, many of them were employed in the coastal trade, especially in the early period of steam propulsion (Craig, 1980, p. 7). Despite efforts to remove the coastal ships from the data set, there may still be a number included, as fewer detailed accounts of steam ships have been found until late in the century and so the trade cannot always be determined. The most obvious feature of the steam ship data is that the L/B is consistently higher than for sailing ships. This may be due to the removal of cargo space in steam ships to accommodate the engine and coal. In order to extend the cargo space to a point where the steam ship is viable competition to sailing ships, the best dimension to increase would be the length. Although structural cost would increase, this is offset by the reduction in machinery and fuel costs as length has the least impact on resistance (Watson, 1998, p. 66). Another factor that may have led to steam ships being narrower is due to the position of the paddles in the earlier steam ships. It was often found that the wave profile generated by the hull created a hollow at the position of the paddle, which reduced the thrust (Gardiner and Greenhill, 1993b, pp. 16–17). The way to counter this was to increase the length of the ship as this reduced the amplitude of the waves around the paddle.

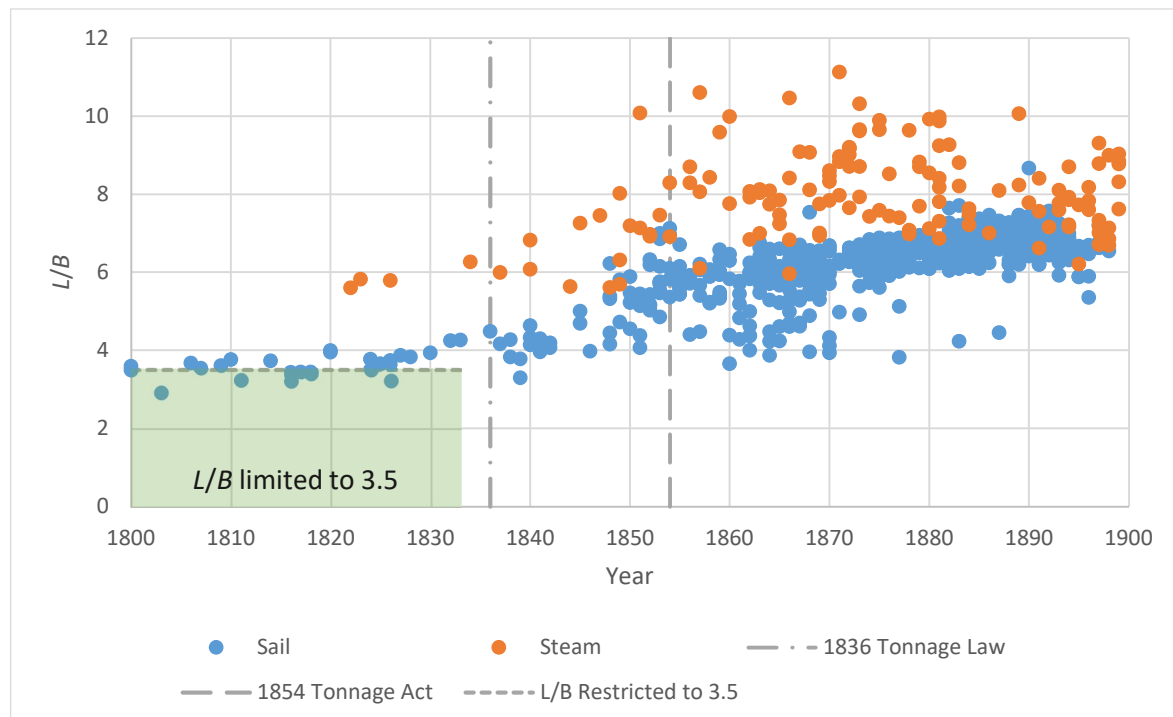


Figure 10: Variation in L/B ratio for sailing and steam ships

Parametric Analysis of Existing Data

The average values of L/B over time agree with the above discussion. This is shown in Figure 11, along with the standard deviation (σ) in five-year intervals. It is particularly clear in this figure that there was a greater variety of hull forms being created between 1845 and 1875 in both types of ship. As both sail and steam ships are built for similar purposes as ocean going cargo and passenger ships, this indicates that the variation may be due to a greater amount of experimentation. This variation reduces between 1875 and 1880, at which point the average sailing ship L/B appears to reach a level that it remains at for the next 20 years. This L/B ratio of around 6.5 appears to remain constant for ships throughout most of the 20th Century (Watson and Gilfillan, 1977, p. 282; Watson, 1998, p. 66).

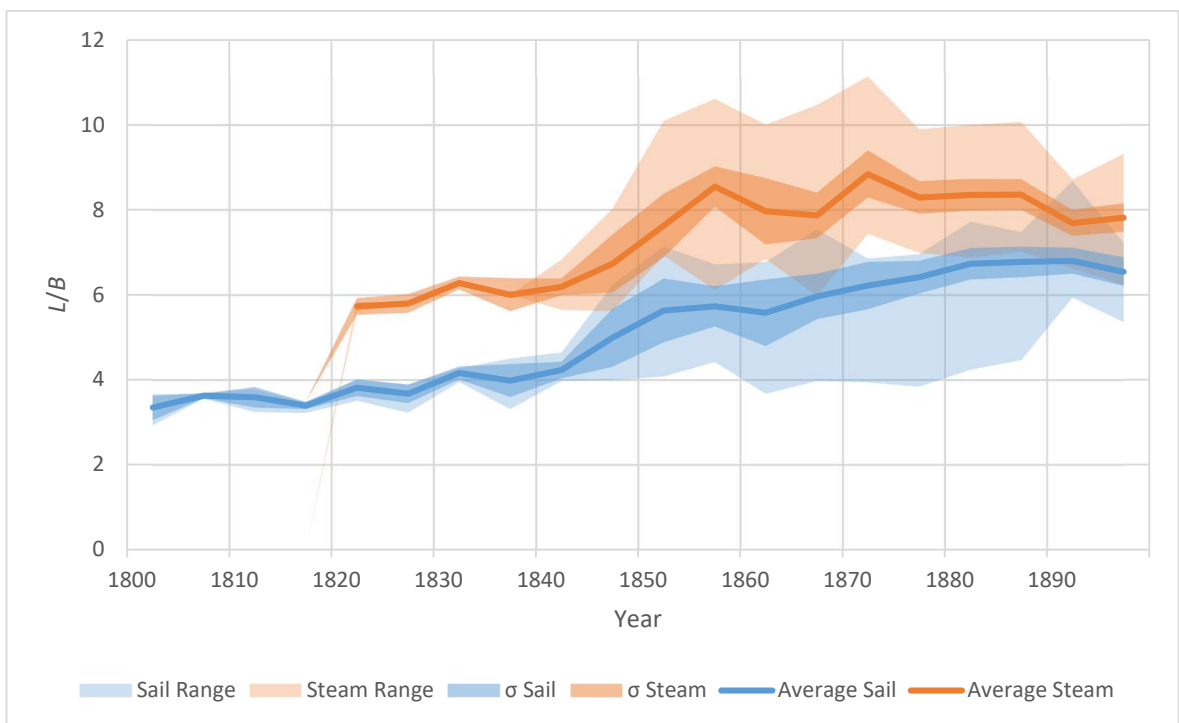


Figure 11: L/B envelopes for sail and steam data, including standard deviation (σ) and averages

The effectiveness of L/B as a measure can be found by considering the individual components of length (L) and beam (B). The variation in these particulars, shown in Figure 12 and Figure 13 respectively, indicate that, as discussed before, the average length of ships increased dramatically over the course of the century. It can also be seen that at the same time, there was also a more gradual increase in beam, which accounts for the overall increase in L/B . This increase in length is an important part of the development of ships in the 19th Century, and is likely to be visible in many aspects of the analysis as it has a significant impact on both hull resistance and stability, as well as the ability of the vessels to carry cargo and larger sail areas. With the increase in length there would have been changes to the stability characteristics of the vessels.

Parametric Analysis of Existing Data

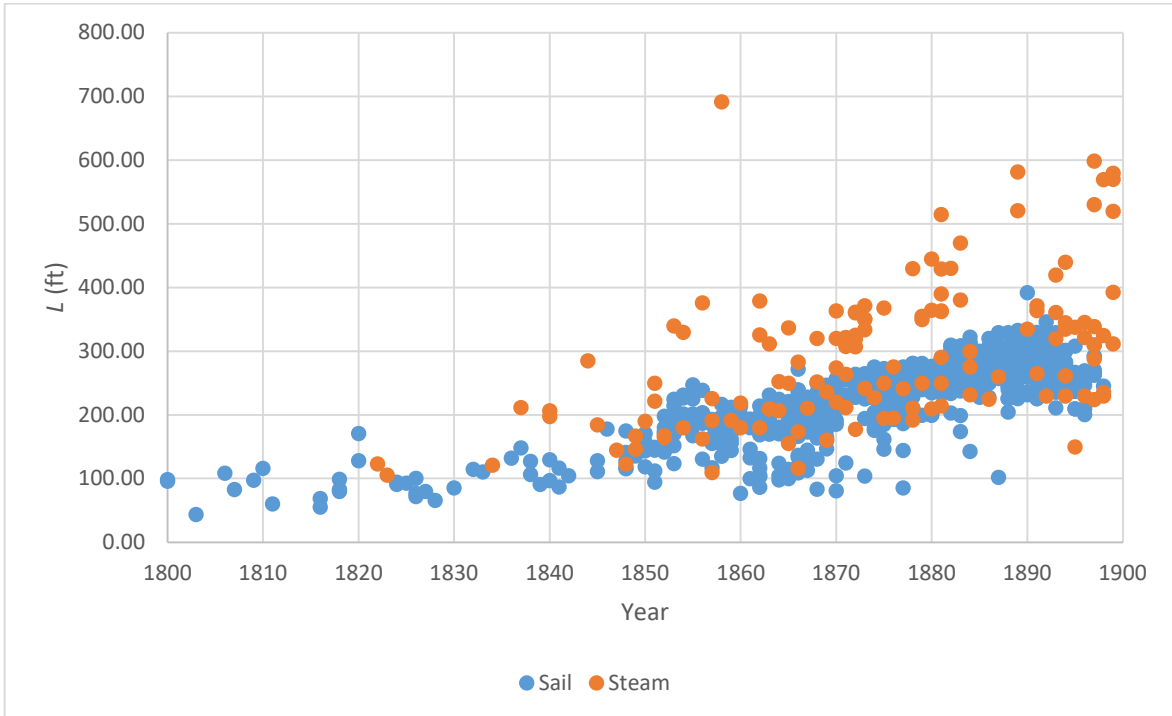


Figure 12: Variation of length with time

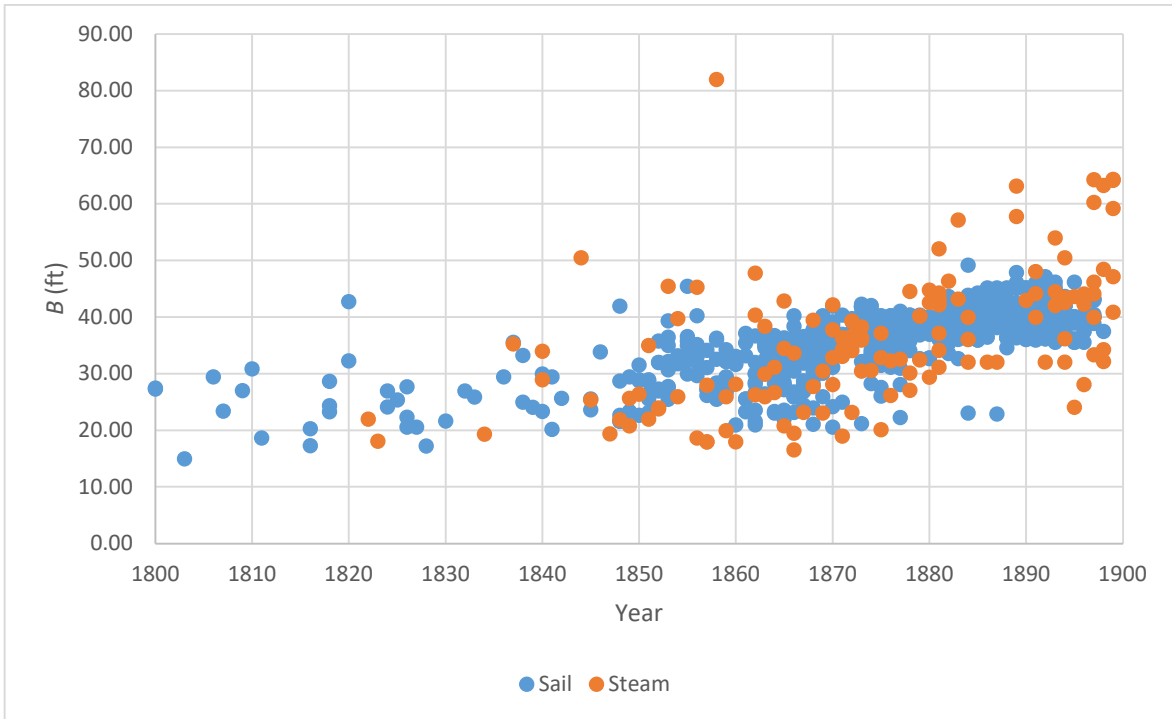


Figure 13: Variation of beam with time

Another dimension that has the potential to show how ship design changed is the load draught. This can be displayed by the beam-draught ratio, B/T , as shown in Figure 14. One of the most common claims about the depth, and as a consequence draught, is that prior to the 1836 tonnage law, ships were often built “deep and narrow” to account for the fact that the tonnage calculation assumed the depth to be half of the beam (White, 1877, p. 44; Salisbury, 1966, p. 338; MacGregor, 1988, p. 23). This was an important consideration for ship owners as many fees were dependent on the tonnage (Miller, 1980, p. 125; MacGregor, 1988, p. 99). However, the data

presented here indicates that there was not much change after the law was altered despite the claims that dimensions were altered as a result. This could suggest that, although deepening the hull was an obvious solution to get around the tonnage laws, it may not have been a priority to ship builders who may have had other practical considerations. One such reason to keep the draught lower could have been due to the tidal range in Britain. It has previously been noted that British ships often have flatter bottoms than other countries such as America, due to the need to prevent capsizing as the tide goes out (MacGregor, 1988, p. 44). However, there may still be some truth in the claims of deep hulls because the L/B increases, as shown in Figure 10 and Figure 11. If the B/T ratio remains constant, this means that the draught will effectively decrease relative to length. The result is that prior to the 1836 tonnage law, it may be better to refer to ships as "deep and short" (Salisbury, 1966, p. 338), shown by the variation of L/T in Figure 15, as opposed to "deep and narrow". Linking this to the tonnage law is difficult, however, as there is no clear reason to maintain the B/T ratio after 1836.

Figure 14 does give a good account of the availability of data. Up until 1834, draught was recorded in Lloyd's register, which accounts for the larger number of data points present prior to this date. Following this period, there is very little data for around 20 years, at which point the number of records increase in line with the number of vessels in the dataset. This means that there is little information about what may have happened during this period.

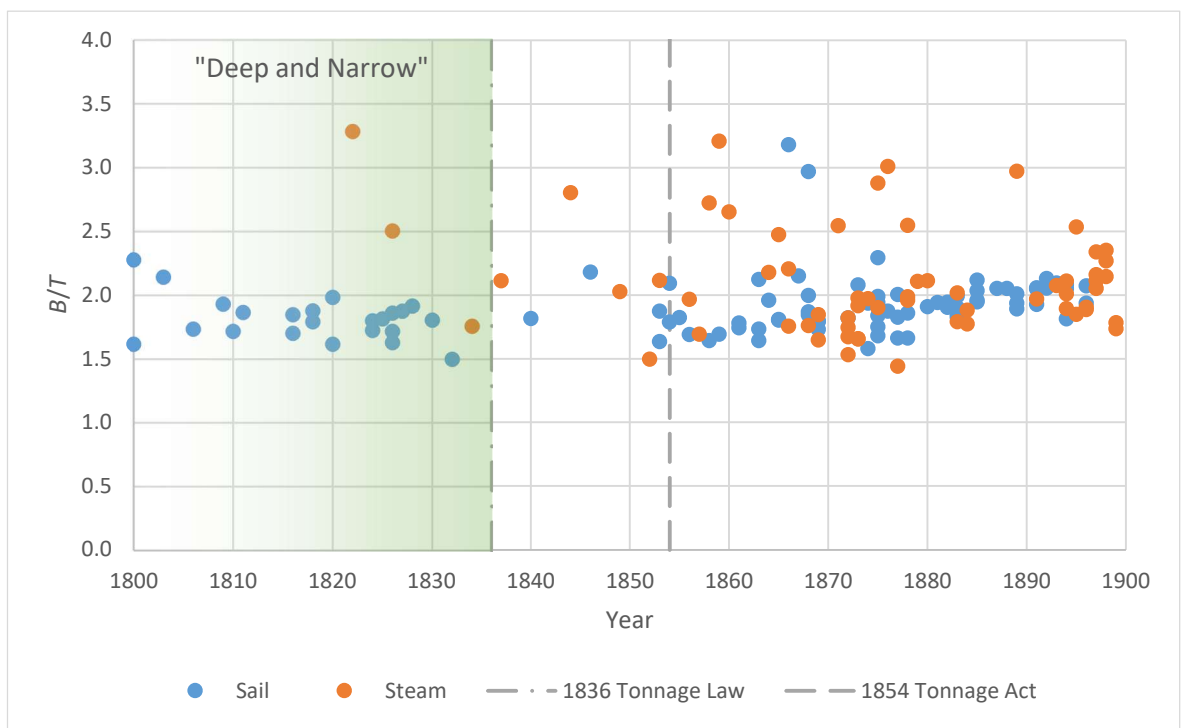


Figure 14: Variation in B/T ratio with time

Parametric Analysis of Existing Data

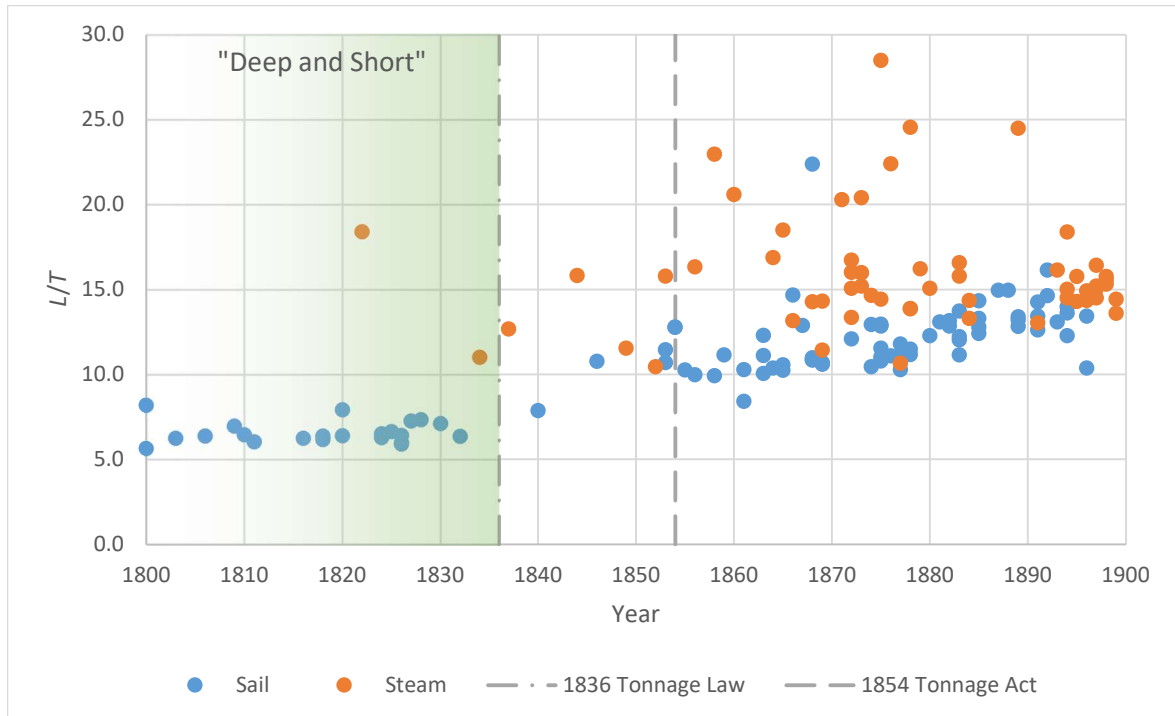


Figure 15: Variation of L/T with time

As described in Section 2.5, it is not possible to reliably infer ship performance from the principal dimensions alone. Although in general a long, narrow vessel will usually be capable of higher speeds than a short, wide one, there are other factors that affect the magnitude of the speed (Day and Doctors, 1997, p. 253; Schneekluth and Bertram, 1998, p. 2). One of these factors that affects both speed and capacity is the underwater hull form. There are a number of volumetric parameters relating ship dimensions to volumetric displacement (∇) that help to describe this, including the length displacement ($L/\nabla^{1/3}$) ratio, C_B and C_P . Figure 16 shows the variation in $L/\nabla^{1/3}$ for the currently available data. The trend for this value should resemble that for L/B as it would be expected that the narrower a ship becomes, the finer it would be. This would also be an indication of a hull form which is capable of higher speeds. However, there is clearly not enough data to determine any trend, unless it is to suggest that there is little or no change in the fullness of the ships.

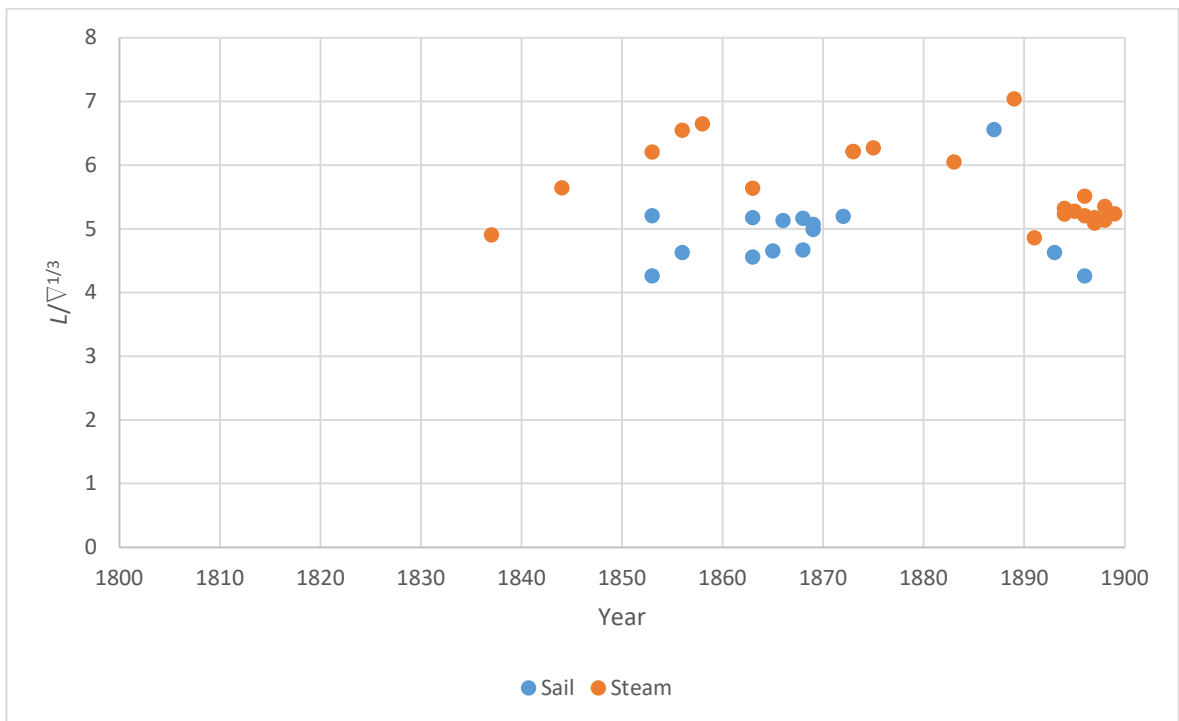


Figure 16: Variation in $L/V^{1/3}$ with time

The number of values found in literature for the hull coefficients, C_B and C_P , were found to be too few for any meaningful analysis, with 27 C_B values and only 7 for C_P . Another dimension that is key to understanding performance is the WSA. The frictional resistance of a hull is dependent on WSA and so to infer performance from a parametric analysis, it is important to consider this value. However, within the dataset there are only two instances in which WSA is given in literature. Given this, and the lack of volume data, it is clear that more data is required if performance is to be inferred from the hull parameters.

3.2 Variation of Performance with Time

The performance of a ship is dependent on a number of factors. For a 19th Century merchant ship speed and capacity were the most valuable considerations for a ship owner (Mendonça, 2013, pp. 1727–1728). In addition to this, running costs would have been an important factor, which were dependent on factors such as crew numbers (McGowan, 1980, p. 24) and fuel efficiency (Craig, 1980, p. 7). These are generally dependent on small-scale technological advances, for example changes to sail operation which are outside the scope of this research. Cargo capacity can be tracked to some extent through the tonnage of ships (Mendonça, 2013, p. 1728), meaning that at this stage this is the most accessible performance factor to investigate.

The data examined so far only deals with hull form. For a measure of ship performance that goes beyond hull shape, it is important to also consider propulsion. The simplest way to examine the ship as a complete system is to consider the ship speed, V_s . Data from literature varies for this measure, as each speed recorded is generally taken in different conditions. This is particularly true

Parametric Analysis of Existing Data

for sailing vessels, where the maximum recorded ship speed will usually be the average speed recorded over the course of a day. Not only will the wind conditions vary during the sample period, but it is unlikely to be the same between vessels. Figure 17 shows how much variation there is between the highest ship speed found reported in literature for individual vessels. The steam ships in particular show a wide variation. A majority of these values came from trial reports and so are likely to be reasonably accurate as the maximum speed achievable under engine. Therefore the variation is possibly due to the wide variety of trades that steam ships operated in. However, the steam data does not usually account for the presence of sails as auxiliary propulsion, which was a common occurrence in the 19th Century (Brock and Greenhill, 1973, p. 16). For sailing ships it may be argued that there is a speed increase with time, but as there are only a few data points and there is uncertainty about the reliability of the data, these results may not be comparable.

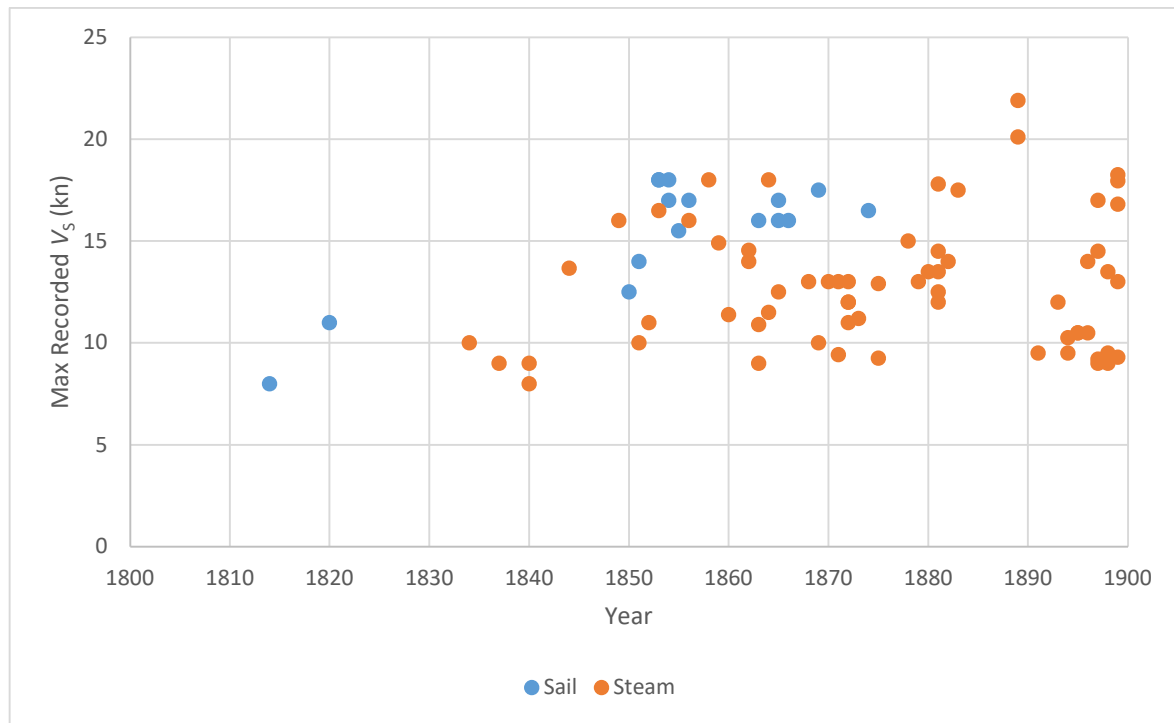


Figure 17: Variation of maximum (highest) recorded V_s with time

With the dimensional parameters previously described, efforts were made to keep them independent from ship size by presenting them in a non-dimensional form. For speed, however, the size of the ship is an important factor in the development of the performance, and so comparisons of the attainable speed may be carried out without correcting for the size. If the size of ship were to be accounted for, this could be achieved by using the Froude number, F_n , as defined in equation (1).

The variation of F_n in this dataset displays no clear trend, as shown in Figure 18. The dependence on ship speed accounts for this, as discussed above. In addition to this, the removal of the length,

which is known to have one of the greatest effects on speed, reduces the variation, indicating that the increase in length demonstrated across the century is one of the largest drivers for any increase in speed. The advantage of using F_n as a measure would be that it indicates the combined ability of a hull form and rig layout, irrespective of other factors that may influence the size, such as building material or cargo type.

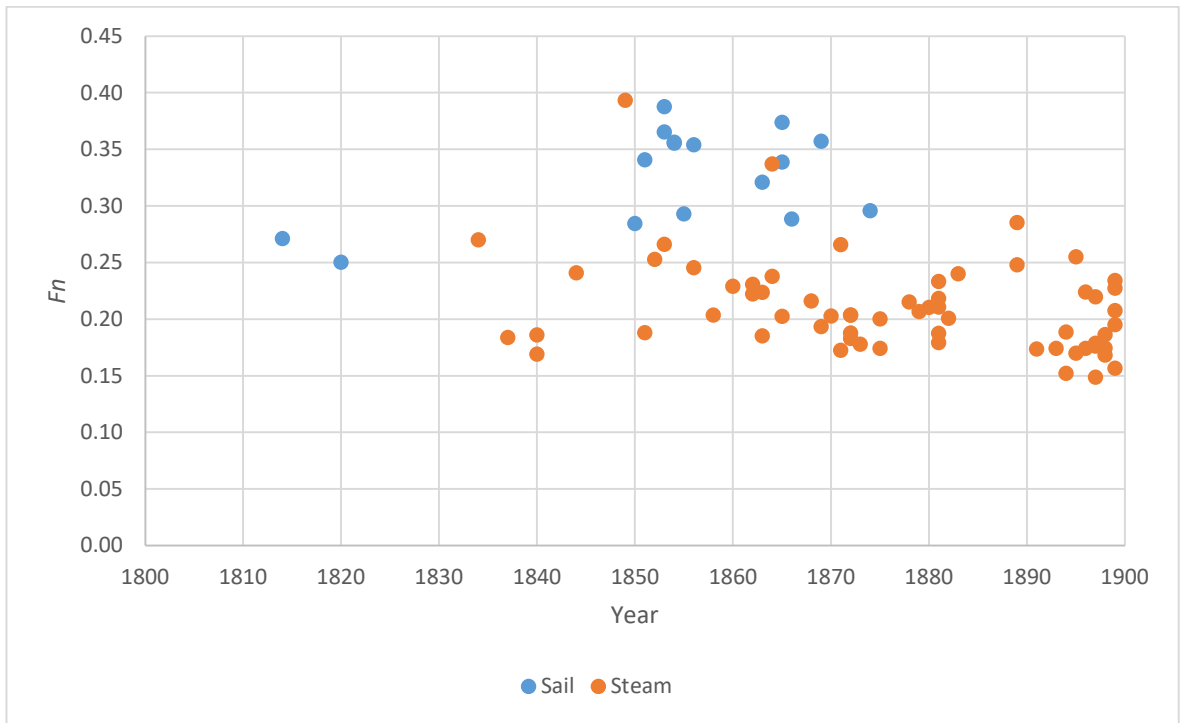


Figure 18: Variation of Froude number with time

3.3 Summary

The parametric analysis has highlighted two main issues that need to be examined further. The first is that the current data available does not allow for ship performance to be inferred with any degree of accuracy. The second point is that even if enough hull data was acquired, the only way to confirm the conclusions is by considering changes to speed over time. At this moment there is little consistency in the way speed is recorded and so there is no way to confirm if there is a change over the century. To solve this lack of consistency, a method is required to generate comparable speed data under the same conditions. The way to achieve this is through the creation of a VPP aimed specifically at historic ships. In addition to this, a number of ships will need to be digitally modelled in order to extract data that is otherwise unavailable, which will allow some of the more sparsely populated areas of the dataset to be filled, for example the length displacement ratio shown in Figure 16 or WSA. The creation of the VPP and the digital models will be discussed in Chapters 4 and 5.

The data collected for this analysis shows the potential for showing narratives using a parametric analysis. It has been shown that it is possible to some extent to show features of hull design

Parametric Analysis of Existing Data

relevant to changes in tonnage laws, supposedly making ships deeper and anti-smuggling legislation limiting the length-beam ratio. Whilst the former of these appears to have less of an impact on depth than supposed, the latter seems to have more of an impact considering that a large number of the ships in the dataset were exempt from this rule. With further data it should be possible to determine to what extent these regulations were affecting ship design, or whether there were other factors that can be shown by alternative parameters. Given more data, other narratives can also be considered, for example tracking the development of naval architecture or the influence of foreign shipping. In addition, there is also the potential to show variations between different ship types, such as East Indiamen, Clippers and Windjammers. The ability to predict speed will particularly benefit these comparisons. These topics will form a series of case studies to be considered in Chapter 6.

Chapter 4: Development of a Velocity Prediction Program

As discussed in Chapter 2, the analysis of 19th Century British merchant ships is a broad topic. It is necessary, therefore, to find a robust and repeatable method of obtaining performance characteristics that allows a comparison of a range of historic ship types. The methodology developed to assess this will need to be adaptable to account for the varying designs and levels of available data to allow a direct comparison to be made. This section covers the development of a VPP designed specifically for historic ships, using the *Cutty Sark* as a primary test case.

So far, studies on ships in this era have compared hull resistance or “hull efficiency” (Tonry *et al.*, 2014), or looked at contemporary data with measurements such as tonnage that were liable to change over time (Hughes and Reiter, 1958; Mendonça, 2013; Kelly and Ó Gráda, 2018). Although these are undoubtedly useful, they fail to incorporate other aspects of hull performance, in particular maximum ship speed, which was an increasingly important factor as demand for goods increased (MacGregor, 1988, p. 13). Only one study considered speed as a performance measure, but this was the average taken from voyage logs and any speed over 10 kn was dismissed as “implausibly high” (Kelly and Ó Gráda, 2018, p. 9). Previous VPPs that have been designed for historic ships have focused on individual ships or ship types, often obtaining the forces through experimentation (Grant *et al.*, 2001; De Jong, 2008; Palmer, 2009b, p. 320). However, the VPP created in this chapter needs to be able to calculate the performance of a wide variety of ships, and so more flexible methods are required. To achieve this, the use of regression methods is examined. CFD is used to justify the hydrodynamic forces calculated using these and the results are compared with contemporary literature where possible.

Due to the potential for errors in the process of hull digitisation, particularly with 3D scanning methods and the estimation of the VCG, it is important that we understand the effect of these errors on the output from the VPP. A sensitivity analysis was therefore carried out, examining the effect of changing dimensions on the individual hydrodynamic components and the VPP as a whole. This analysis will help to determine the limits of the VPP as well as the accuracy required to create a digital model of a vessel, which shall be discussed in the next chapter. It should be noted that in its current form, the VPP is designed to assess the as-launched clean hull condition for sailing in calm water. This means that the VPP should be overestimating the speed.

4.1 Cutty Sark and Storm Cloud

To verify the accuracy of alternative hull force estimation and digital reconstruction methods, a comparison needs to be made with a known design. For this purpose, an “ideal” model of the *Cutty Sark* was created based on lines taken off the ship in the 1920s, as the original lines have

Development of a Velocity Prediction Program

been lost (Lubbock, 1924, p. 31). *Cutty Sark* was chosen as it is one of the few 19th Century merchant ships still in existence, has detailed voyage data available and, being built in 1869, is from approximately the middle of the century. This digital model was also used to create a physical scaled half model, with a view to trialling different 3D scanning techniques. This enables a geometric comparison to be carried out to determine whether the scanning methods used for some of the data collection are suitable. The method used to construct this digital model will be discussed in more detail in Chapter 5. An image of the digital model is shown in Figure 19.

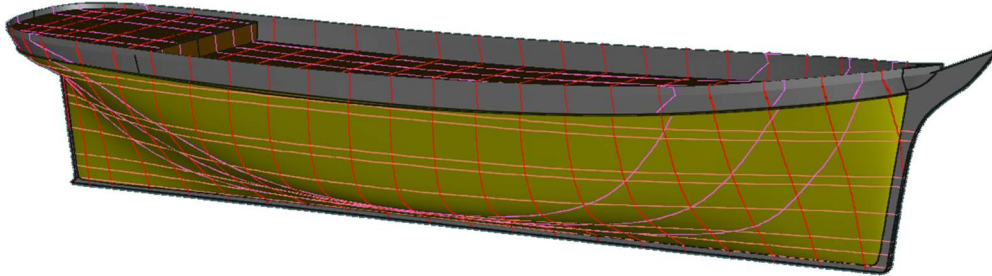


Figure 19: Hull model of *Cutty Sark*

In order to check that the results of the VPP development are representative of a variety of hull forms, another ship was modelled, *Storm Cloud* (Figure 20). This was an experimental hull design at the time of build in 1854 (MacGregor, 1988, pp. 167–168; Ferreiro and Pollara, 2016, p. 431) and is sufficiently different from *Cutty Sark* to justify its use as a comparison. Data from Brunel's *SS Great Britain* and a small number of other vessels have also been included as a comparison.

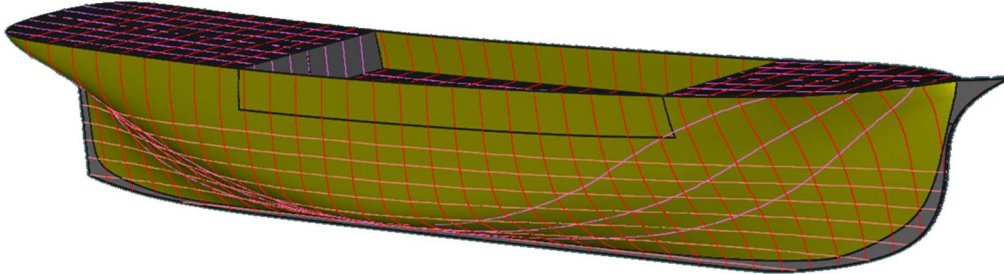
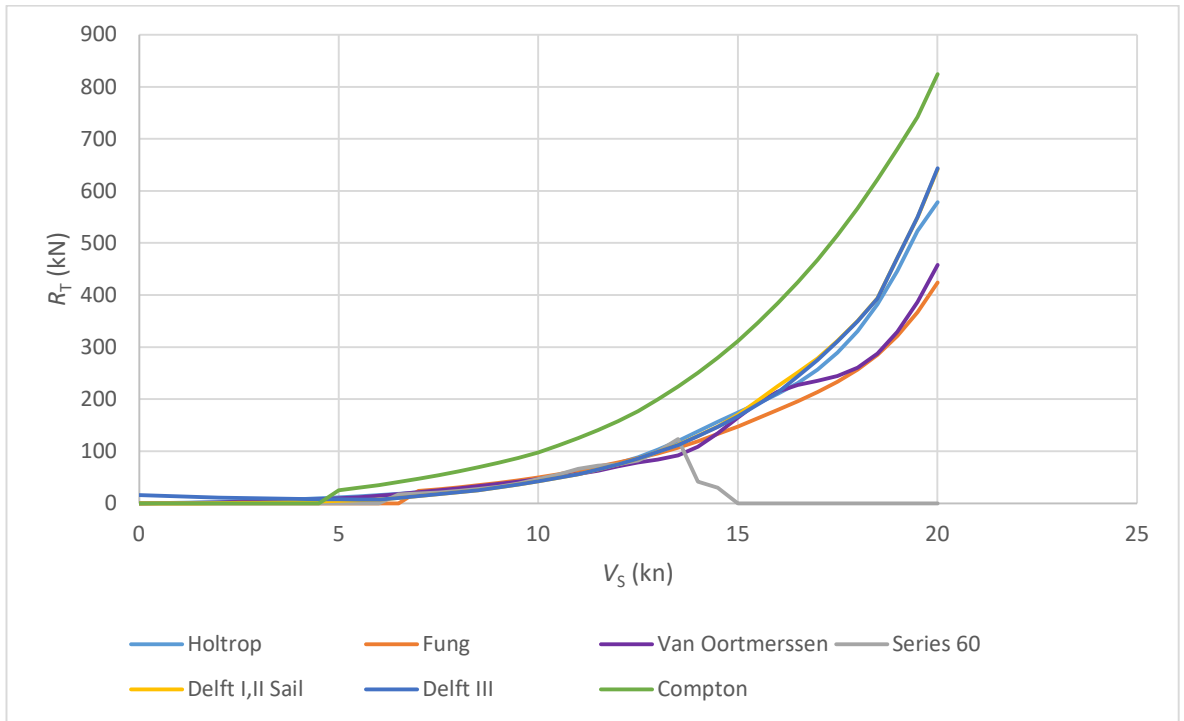


Figure 20: Hull model of *Storm Cloud*

4.2 Hydrodynamic Resistance Estimation

Initial estimates for the resistance of *Cutty Sark* were carried out using *MAXSURF Resistance*. As in other software, an idea is given of whether the vessel geometry fits within the required parameters for the regression analysis. Seven different methods were applied (Holtrop, Van Oortmerssen, Series 60, Delft I,II Sail, Delft III, Compton and Fung), with all but Fung's method falling outside of the parameter limits in at least one instance. These initial resistance results are shown plotted against ship speed in Figure 21. The Fung method and the Holtrop method, which only failed on the beam-draught ratio, were then coded and examined in detail using *MATLAB* in order to determine their suitability for use with historic hull forms.


 Figure 21: R_T estimations from MAXSURF Resistance

On closer inspection of the parameters used for the Fung analysis, it can be seen that the majority of the parameters for *Cutty Sark* and *Storm Cloud* lie in the lower half of the range of allowable values, as shown in Table 6. The more consistent the location of the parameters within the bounds, the more likely it is that the vessel is suitable for use within that analysis. For *SS Great Britain*, however, the greater variation hints that its geometry is not as suited to the Fung method.

 Table 6: Allowable limits for the Fung Regression Analysis for *Cutty Sark*, *Storm Cloud* and *SS Great Britain*

Parameter	<i>Cutty Sark</i>	<i>Storm Cloud</i>	<i>SS Great Britain</i>
$\Delta/(L/100)^3$	223.389	192.04	158.753
LCB	0.490	0.443	0.480
C_{ws}	16.613	16.367	15.269
i_E (°)	16.800	11.840	24.700
L/B	5.950	6.069	5.644
B/T	1.775	1.833	2.806
C_P	0.627	0.550	0.638
A_{20}/A_M	0.000	No data	No data
C_M	0.781	0.811	0.792
B_{20}/B	0.000	No data	No data
C_{WP}	0.737	0.697	0.790
T_{20}/T	0.176	No data	No data

It is noted that the Fung method may not be suitable for this research, as it is aimed at vessels that normally operate at an Fn of over 0.3, which lies within the upper range of speeds for these vessels, with an average reported maximum Fn of 0.24. To estimate resistance at the lower

Development of a Velocity Prediction Program

speeds seen during normal operating conditions, an alternative method should be considered. For this, the Holtrop method would appear to be suitable as it covers a wide variety of hull forms. Because of this and its availability in most performance prediction software, it is sometimes used to estimate resistance without an appreciation of its limits. One example where the Holtrop method is applied is in Tanner (2013a), where the vessel in that study does not meet the requirements for C_B or L/B , indicating that an alternative method may have been more appropriate. This highlights a need for an investigation into whether it is suitable for use for historic ships with geometry noticeably different to modern vessels.

Table 7 gives an indication of how the three ships considered fit within the limits of the Holtrop analysis. For *Cutty Sark* and *SS Great Britain* the correlation is good, with each parameter lying in approximately the same range for each ship. However, as was previously noted, the B/T ratio of the *Cutty Sark* lies outside the suggested limits. This could be an issue with several vessels from the early 19th Century, as tonnage laws restricted beam and length, but not draught, leading to many deep, but narrow ships until the rules were changed in 1836 (White, 1877, p. 47; MacGregor, 1988, p. 24). The extent to which this may be a problem becomes evident as data is gathered for a greater number of ships. Load condition is also important, as can be noted with *Cutty Sark*, here analysed with the load draught of 20 ft. Under normal operating conditions, it is likely that the ship would have a shallower draught, and so the beam-draught requirements would be satisfied, although in this research the vessels are considered in the load condition. The parameters for *Storm Cloud* fit less well, probably due to her unusual hull form and very fine entrance. With the exception of the LCB, which is much further aft than is usual, the parameters are not that far below the minimum.

Table 7: Limits for the Holtrop-Mennen method for *Cutty Sark*, *Storm Cloud* and *SS Great Britain* (Red = out of limits)

Parameter	<i>Cutty Sark</i>	<i>Storm Cloud</i>	<i>SS Great Britain</i>
C_P	0.627	0.550	0.638
C_B	0.488	0.444	0.505
C_{WP}	0.737	0.697	0.790
L/B	5.950	6.069	5.644
B/T	1.775	1.833	2.806
LCB	-0.988	-5.738	0.020

The initial data gathered for the parametric analysis in Chapter 3 indicates that for a majority of vessels, the beam-draught ratio is likely to cause the most issues with using the Holtrop method. Table 8 shows a summary of the number of ships that meet each requirement. It should be noted, that although only 35% of the ships meet the beam-draught requirement where it is known, 120/156 of these have a higher ratio than *Cutty Sark*, which strengthens the argument of using her as a test case.

Table 8: Number of ships that meet the parameter requirements for the Holtrop method based on existing data

Parameter	No. of Ships	Out of Total	Percentage
C_P	7	7	100%
C_B	27	27	100%
C_{WP}	14	14	100%
L/B	1026	1071	96%
B/T	55	156	35%
LCB	1	1	100%

The resistance estimations calculated using *MAXSURF Resistance* for *Cutty Sark*, shown in Figure 22, show that at lower speeds ($Fn < 0.25$, 12.5 kn), there is very little difference between the Fung and Holtrop Methods. Both methods also correspond reasonably well with the lower resistance value presented by Tonry et al. (2014), where CFD was used to estimate the hull efficiency of the *Cutty Sark*. However, as speed increases, there is an increasing difference between the two methods, even within the speeds that *Cutty Sark* was reportedly capable of achieving. It is also noted that the higher speed resistance does not correspond with the CFD results presented by Tonry et al. (2014), although in that case the resistance appears to be remarkably low. Validation of the results of the analytical resistance discussed above is required in order to provide confidence in their use for 19th Century merchant ships. This will be discussed in Section 4.3.

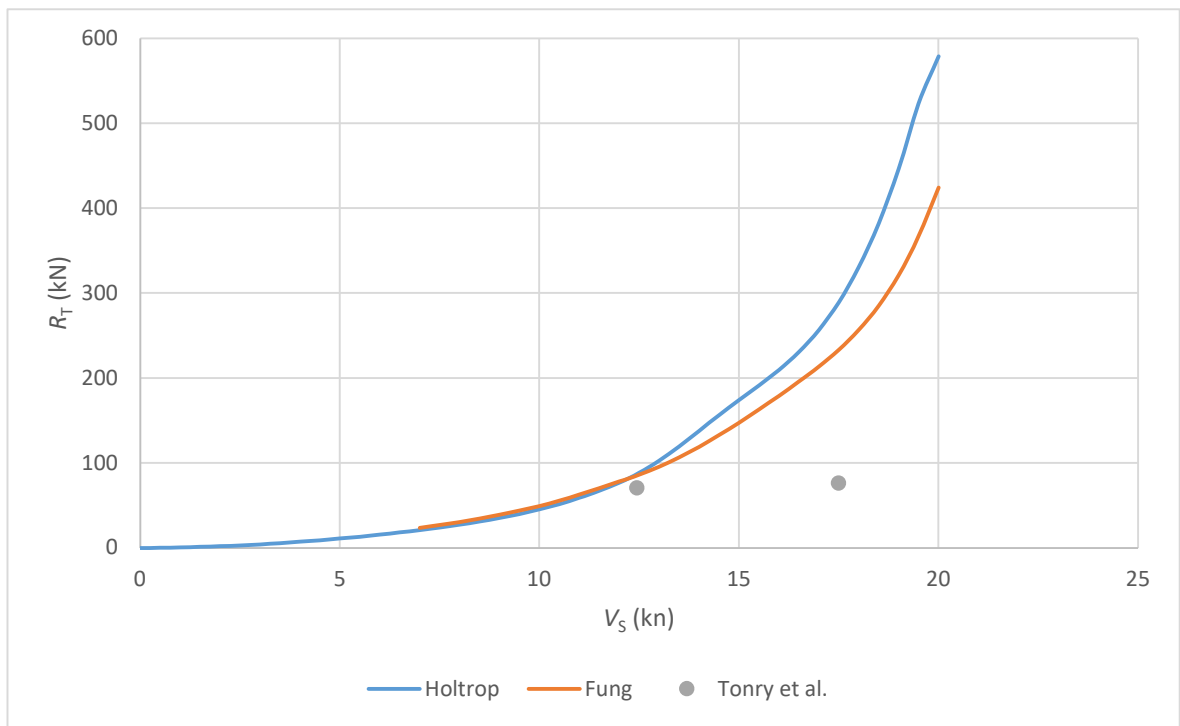

Figure 22: Comparison of Fung and Holtrop methods and Tonry et al. (2014) for Cutty Sark

Figure 23 and Figure 24 show the resistance breakdown for both methods. Despite the Holtrop method using wave-making resistance, R_W , and the Fung method using residuary resistance, R_R , it is clear that up until $Fn \approx 0.27$ (13 kn for *Cutty Sark*) frictional resistance, R_F , dominates for both methods. This corresponds with the comparison of resistance in Figure 22, where at this point the

Development of a Velocity Prediction Program

results begin to diverge. At lower speeds the results are similar as both methods use the ITTC'57 friction line to calculate frictional resistance, as shown in Section 2.8.2, equations 2 and 3.

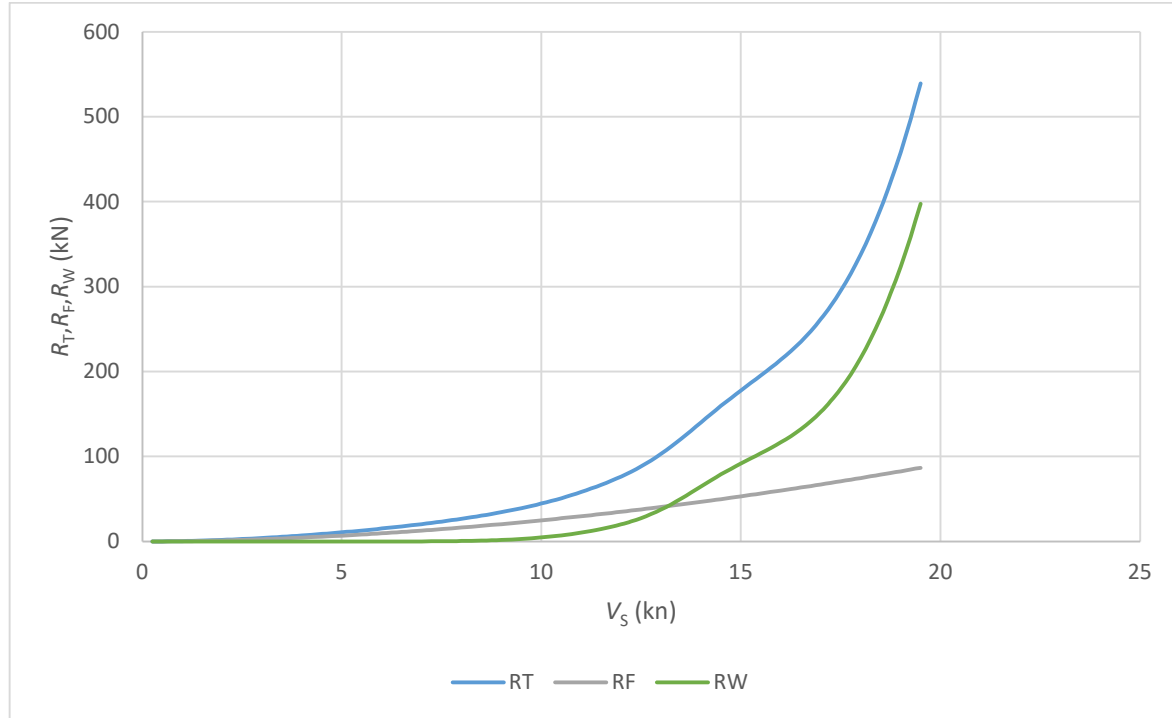


Figure 23: Breakdown of resistance components for the Holtrop method

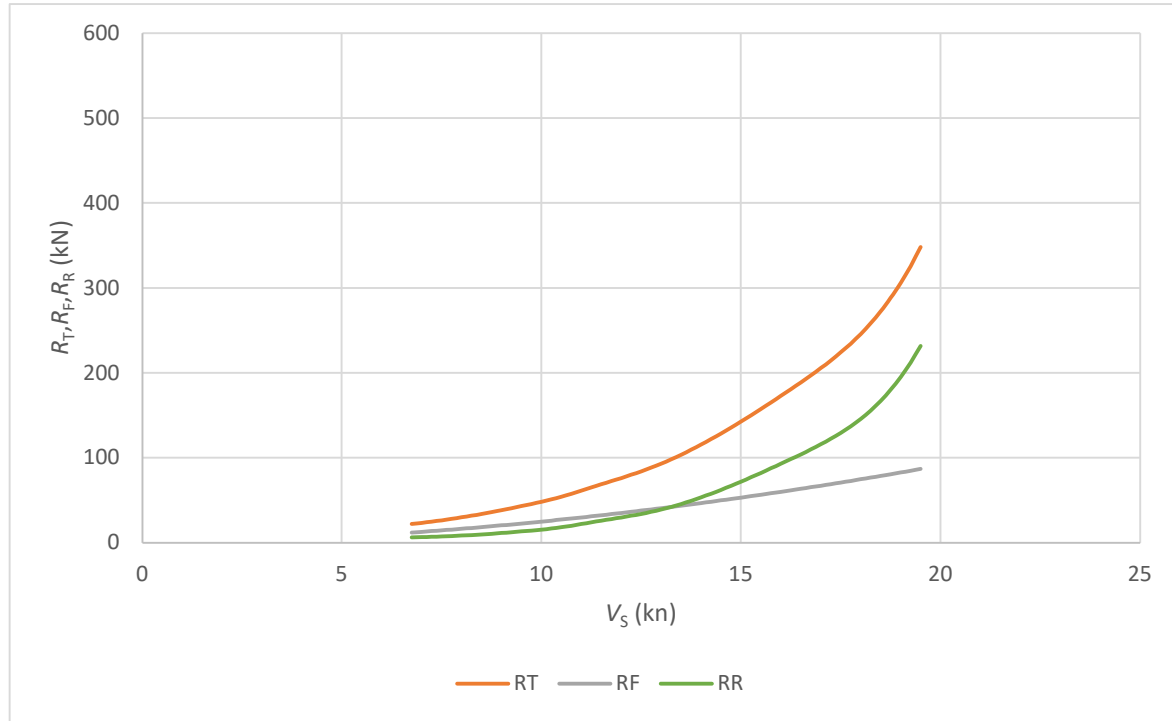


Figure 24: Breakdown of resistance components for the Fung Method

There are a few options available for validating these regression methods: carrying out tank tests, using trial data or using CFD. The first two may be achieved with contemporary data available from the late 19th Century, or with new tank tests, which would incur a large cost. Using CFD is computationally expensive, although there is scope to adjust the complexity of the simulation to

balance running time with accuracy. Historic data and CFD have been investigated to provide validation for the use of either the Holtrop or Fung methods for historic ship performance.

4.2.1 Comparison of Resistance Methods with Historic Data

As there is no known trial data for the *Cutty Sark* or *Storm Cloud*, and the source data for tank tests on *SS Great Britain* carried out in the 1970s could not be located, an alternative was required to compare prediction methods with trial data. As previously discussed, there are contemporary datasets that can be used. One of these was produced by W. Froude on *HMS Greyhound*, a British naval sloop, in full scale trials carried out to validate his towing tank tests (Froude, 1874; White, 1877, p. 453; Molland, Turnock and Hudson, 2011, pp. 1–2). The tests were carried out by towing *HMS Greyhound* behind another vessel, with a log line constantly paying out from *Greyhound* so as to measure the actual speed of the vessel, recorded on “a revolving cylinder charged with a long sheet of paper”, while a dynamometer fitted to the tow rope provided the towing force (Froude, 1874, p. 38). The tow set up is shown in Figure 25. Some of the results are available in graphical form in TransINA 1874 (Froude, 1874).

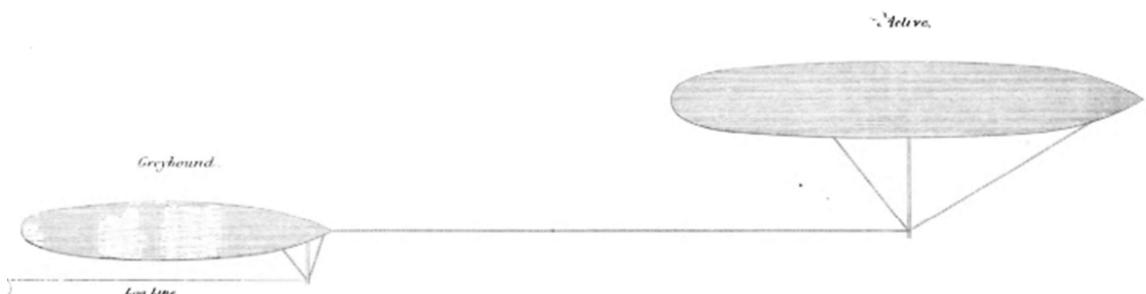


Figure 25: Towing set up for trials of *HMS Greyhound* (Froude, 1874)

If assumptions are made for the half angle of entry and the position of the LCB, a comparison with the discussed regression methods can be made. With the half angle of entry assumed to be 20° and the LCB at -0.5% aft of amidships, the results shown in Figure 26 are for the “normal” displacement condition. There is no clear answer to which method is more suitable. However, it is noted that although the trial data is initially closer to the Fung estimate, it follows nearly the same trend as the Holtrop method, hinting that at higher resistances it will bear more similarity to Holtrop. As assumptions had to be made with regards to the form of the ship, it is still desirable to have an alternative validation method.

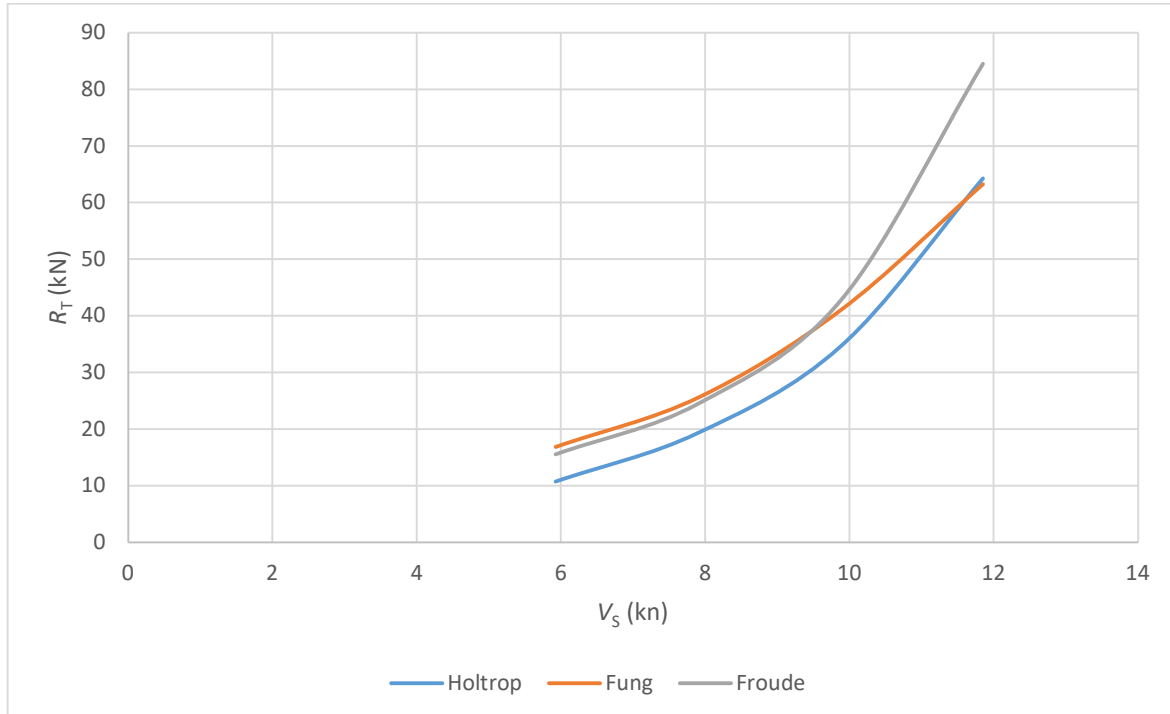


Figure 26: Comparison of Holtrop and Fung methods with data from trials of *HMS Greyhound*

4.2.2 Comparison of Resistance Methods with CFD

Another way of estimating hull resistance is to carry out a CFD analysis on the hull form. As no suitable tank test or full-scale trial data has yet been found as a comparison to the regression analysis methods, CFD results are essential to assess the suitability of other methods. For obtaining these results, a version of the digital model of *Cutty Sark* was analysed using the *EHP* (Estimating Hull Performance) add-on for *STAR CCM+*. This is a RANSE solver, which combines the full functionality of *STAR CCM+* as a platform for CFD with a user interface specifically aimed at setting up the analysis of ship hulls in calm water (Siemens PLM Software, 2016). The benefits of using this add-on are associated with a faster set up time, which would be essential if CFD were to become the main method of analysing resistance. The simulation is set up according to industry best practice and allows the user to input a range of speeds, which are then run as a batch analysis, with a report output at the end (Siemens PLM Software, 2016). The user is still able to make changes within the original interface, including adding additional force measurements in other directions, meaning that the hydrodynamic side force can also be calculated in this way.

Results from *EHP* using a reasonably coarse mesh (base cell size = 0.206 m) show similarities to the results from the Holtrop method, although at higher speeds there are some differences. Figure 27 shows this. It is clear that the Fung method is considerably underestimating the resistance, which is perhaps to be expected as it is aimed at vessels with a modern transom. A similar trend is shown with results generated for *Storm Cloud*, shown in Figure 28.

Development of a Velocity Prediction Program

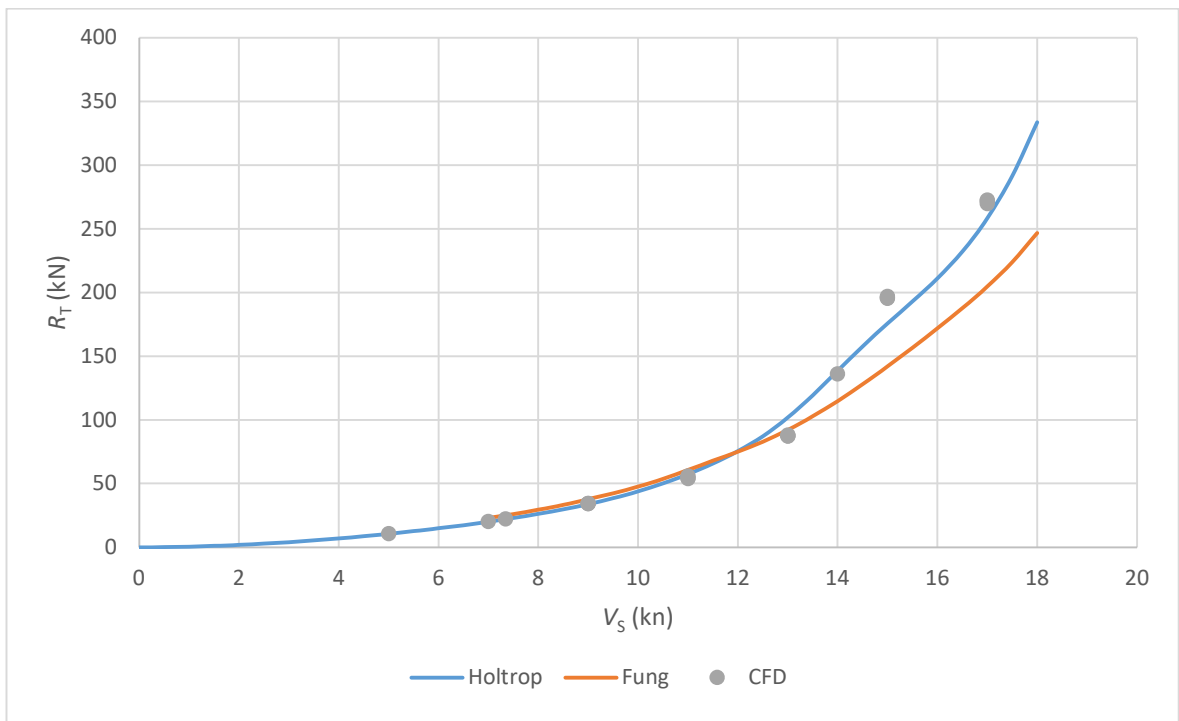


Figure 27: Comparison of CFD results with regression based estimates for *Cutty Sark*

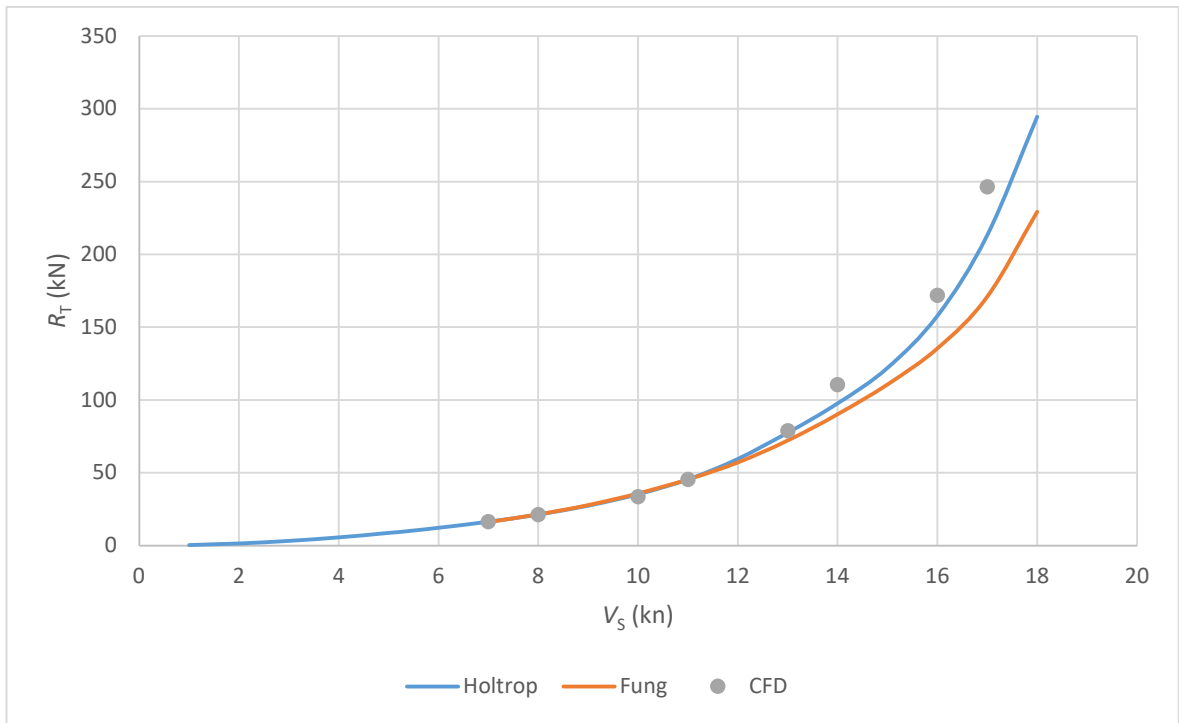


Figure 28: Comparison of CFD results with regression based estimates for *Storm Cloud*

Given the initial similarity between the CFD and Holtrop results, it appears that the Holtrop method is indeed a suitable way to estimate hull resistance for a historic vessel. It is noted that Holtrop does not show as much variation due to wave-making as the CFD suggests there should be. This has historically been a large problem with series and regression analysis methods (Van Oortmerssen, 1971, p. 397). Theoretically, the difference could be corrected by adjusting the constants used for predicting humps and hollows in the resistance curve; however, there is no

evidence to suggest that an altered formula would be appropriate for other hull forms. As the difference is reasonably small, it is argued that the Holtrop method is satisfactory.

Since the correlation between the resistance estimation and the CFD was so good, other forces required for the VPP will be explored in a similar manner. This applies particularly to hydrodynamic side force, for which added resistance due to leeway also needs to be estimated.

4.2.3 Sensitivity of CFD to mesh density

The density of the mesh is important to any CFD simulation, as it defines how accurate the results will be. The finer the mesh, the more detailed the surface on which the fluid is acting will be. However, this increases the number of calculations that need to be carried out and so increases the simulation time. This means that there needs to be a balance between computing time and accuracy. To determine the effect of mesh density, and whether a finer mesh is required to obtain an accurate result, further tests were carried out on *Cutty Sark* with a variety of densities. There appears to be no definitive benefit to increasing the mesh density as there is little change in resistance (Figure 29), but processing time increases drastically (Figure 30). This indicates that the results from the CFD are accurate, even where a lower mesh density was used. If CFD were used as the final method, since the variation in total resistance is small, the time to run the simulation is the best way of selecting mesh size. Based on time taken for each time step and number of steps required for each mesh density, a base element size of around 0.2 m would be best. For coarser meshes, slightly more variation in resistance is displayed, so even if the time required is less, the results may not be as accurate. This set up was used for the analysis of *Storm Cloud*.

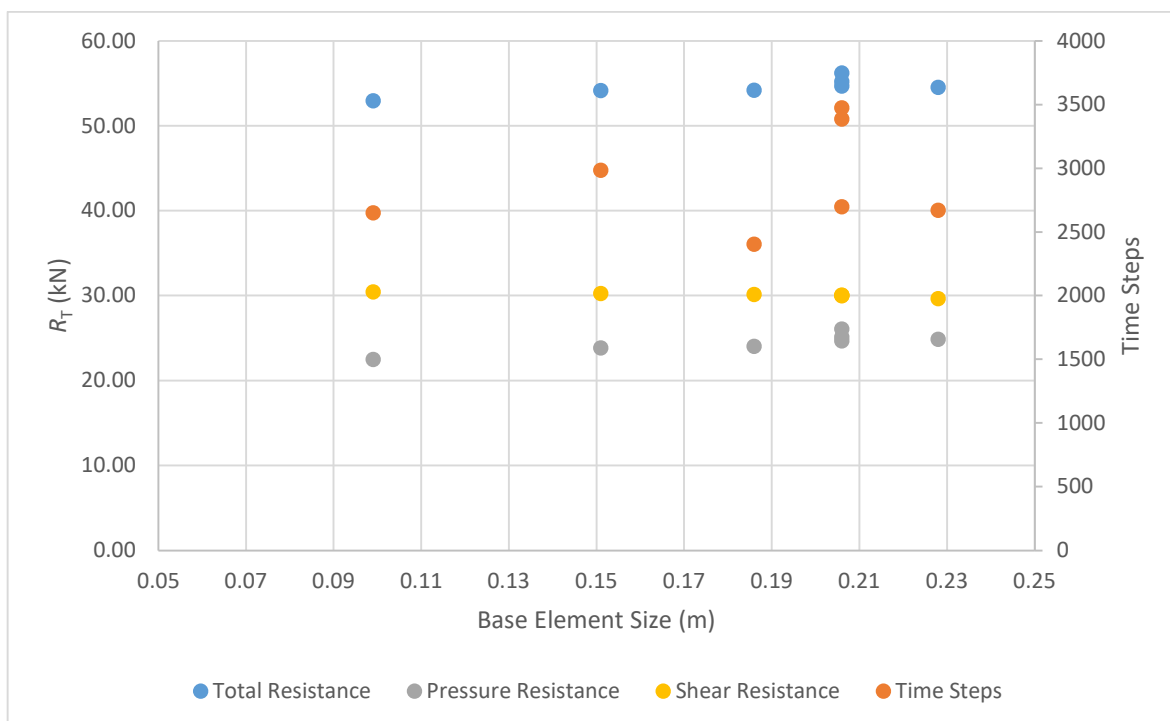


Figure 29: Varying mesh density against R_T and time steps required for $V_s = 11$ kn

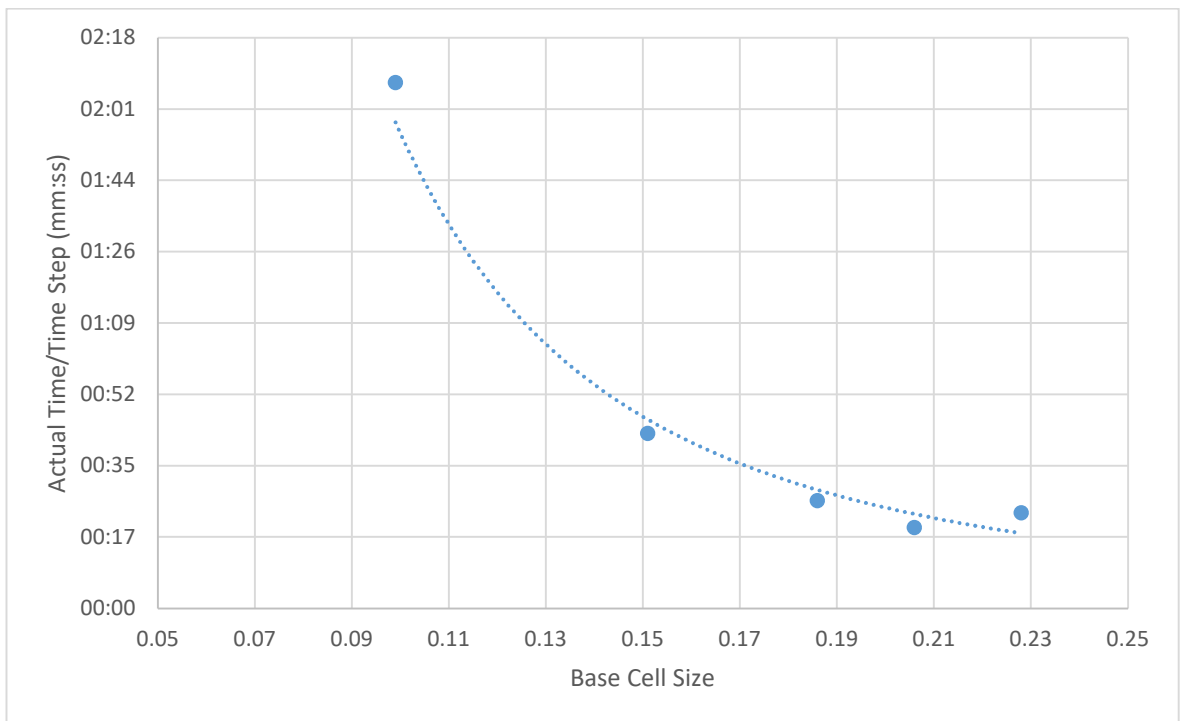


Figure 30: Change in average actual time per time step with varying mesh density

A summary of the mesh densities are given in Table 9, with the finest mesh at the top.

Table 9: Summary of mesh densities used for CFD tests on *Cutty Sark*

Base Cell Size (m)	Cells	Faces	Vertices
0.099	10924864	32775672	11184095
0.151	3496556	10492491	3622075
0.186	2195052	6583744	2285409
0.206	1716803	5149100	1794347
0.228	1348762	4045407	1415539

4.2.4 Resistance Sensitivity

The resistance calculation is perhaps the most important component of the VPP, as it is the primary force component for obtaining forward ship speed. There are 15 hull parameters required for the Holtrop method, which has been identified as the most suitable for this analysis. Although several of these will not be relevant to most of the vessels in question, for example, the bulbous bow dimensions, this still leaves several opportunities for errors to arise. In total eight parameters were identified to have a significant effect on the result.

For consistency, the sensitivity analysis has been carried out using *Cutty Sark* as a case study. Parameters were individually changed to see the effect caused by each. Figure 31 and Figure 32 show the results of this analysis for a ship speed of 6 kn and 15 kn respectively. It is clear that length is a dominating factor at all speeds. C_P also has a significant effect on resistance; however, the majority of this effect will be due to its dependence on the length as it is a ratio between the displaced volume and the prismatic volume formed by the midship sectional area and the length.

Development of a Velocity Prediction Program

This means that in real terms the effect of change in length is not as significant as is shown.

Assuming volume and midship section remain relatively constant, the change in length will be countered by the subsequent inverse change in C_P . The main difference between the two speeds is the effect of the WSA. This is considerably more significant at the lower speed as it determines frictional resistance, which was shown previously to be dominant at speeds lower than $Fn = 0.27$, or 13 kn in the case of *Cutty Sark*.

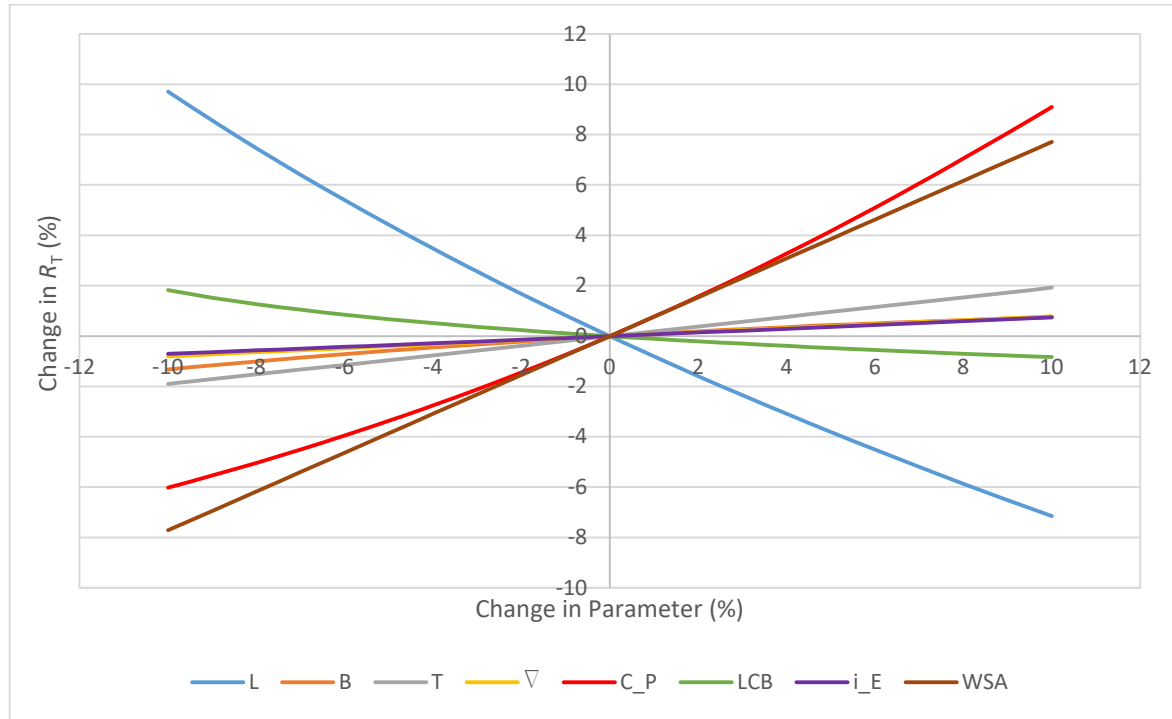


Figure 31: Variation of R_T with changes in parameter at $V_s = 6$ kn

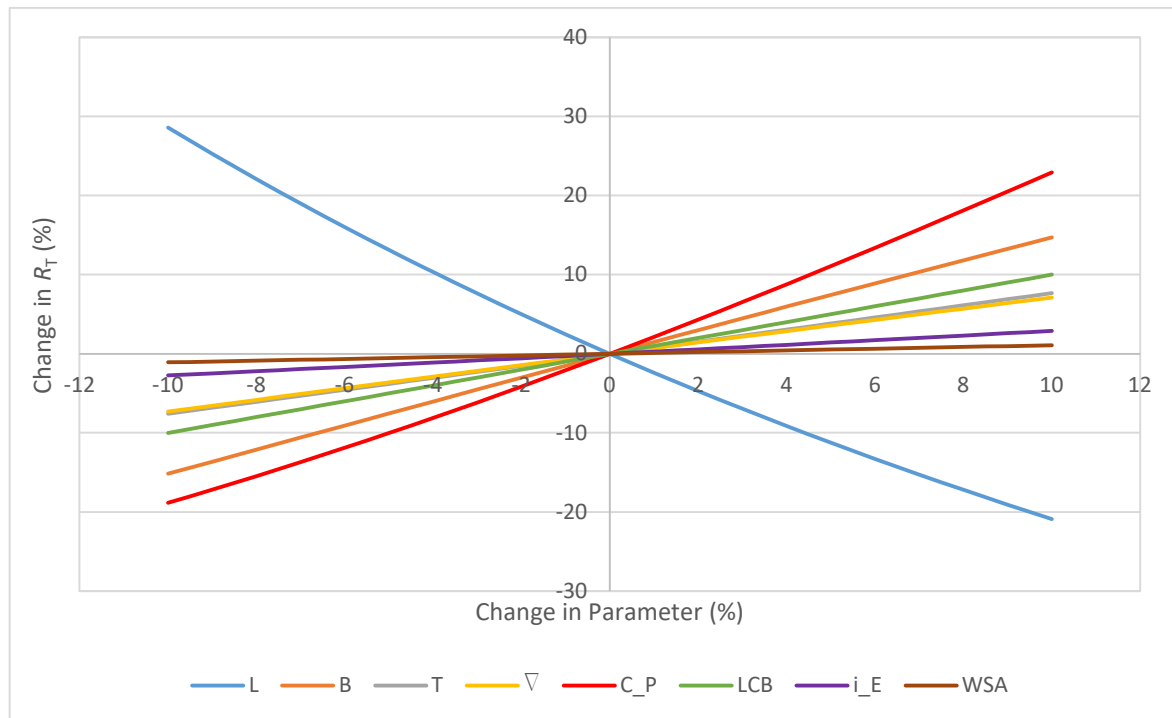


Figure 32: Variation of R_T with changes in parameter at $V_s = 15$ kn

4.3 Hydrodynamic Side Force Estimation

Hydrodynamic side force (S_H) is the lateral component of the force generated by the hull. It is particularly significant for vessels under sail, as it is required to balance the lateral force from the sails. As discussed in Section 2.9, there are a number of regression formulae for manoeuvring calculations that can estimate S_H . Particulars for *Cutty Sark* were input into a number of these regression equations, which were coded using *MATLAB*. The wide variation in results shown in Figure 33 indicates that, as with the resistance estimation, some form of validation is required. As no experimental data has been located for the hydrodynamic side force of historic ships, this validation requires the use of CFD. It should also be noted that only Inoue and Kijima's methods include a non-linear term, and so these were the methods applied to the validation. As both are based on the same set of data, a comparison of results for a number of different vessels has first been carried out to ascertain the differences between them. Kijima (2000) has not been included as this employs parameters that are harder to calculate, and where data on ships is limited, it may not be possible.

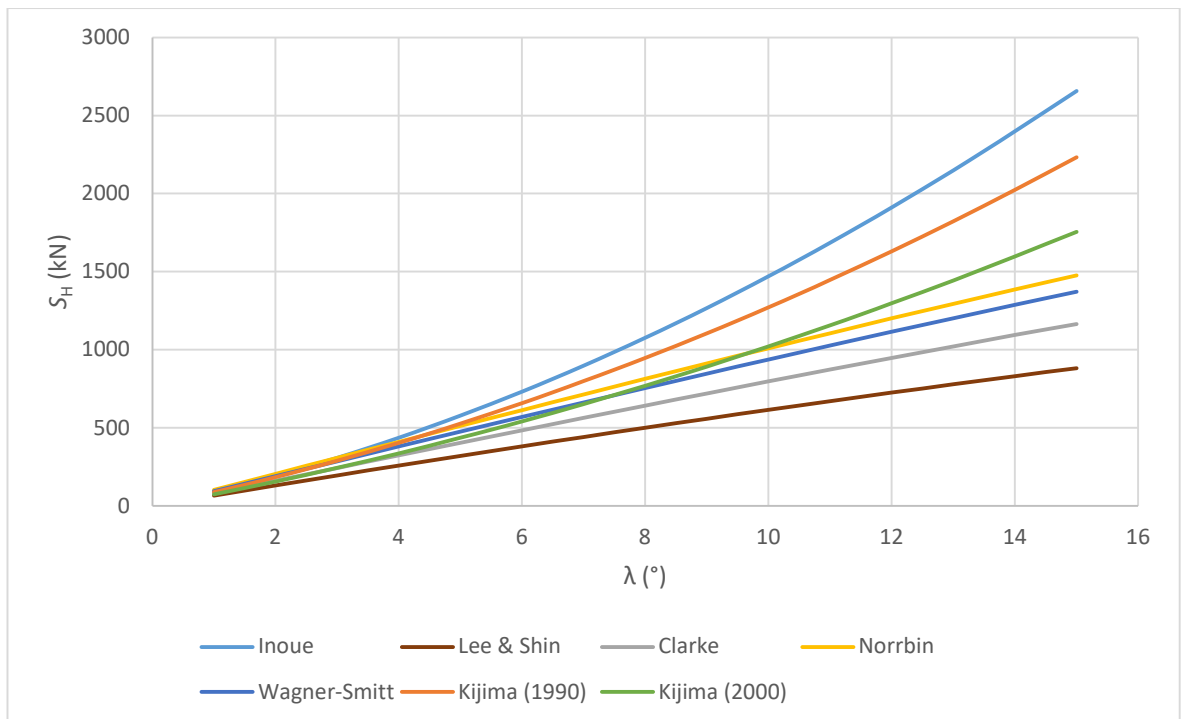


Figure 33: Comparison between S_H estimation methods at $V_s = 15$ kn

Although the Kijima and Inoue methods do not have explicit limitations, it is possible to compare the parameters of the models included in the method to the relative size of the ships in the larger database. This is shown in Table 10, with the number of ships that fall within the model dimensions scaled to a length of 2.5 m. It is noted that the greatest potential issue lies with the draught, T , which is similar to the case with the forward resistance estimation. This is not believed to be a major issue with the method, although it again highlights the need for a validation.

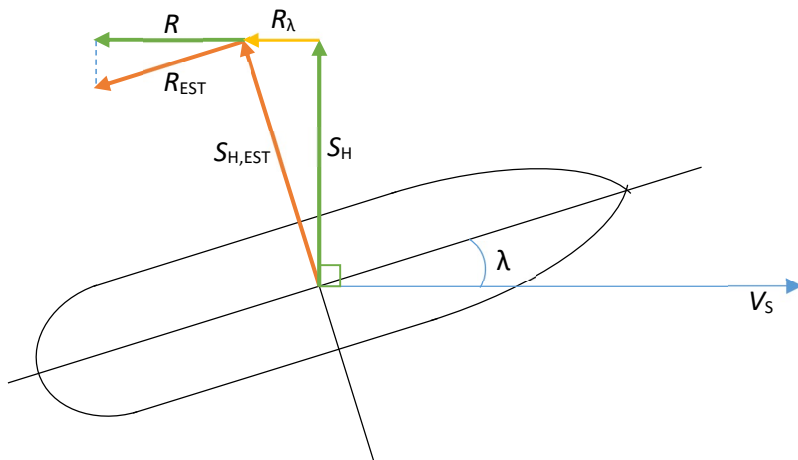
Table 10: Percentage of ships in database that meet the limitations of the Kijima method

Parameter	Number of Ships	Out of Total	Percentage
B	706	1071	66%
T	57	154	37%
C_B	7	7	100%

4.3.1 Added Resistance Due to Side Force

As was discussed in the literature review in Chapter 2, there is no generally accepted method for estimating added resistance due to leeway, R_λ . As it is impractical to undertake model tests to obtain the added resistance in this research, an alternative method based on trigonometry is proposed. The resistance estimation (R_{EST}) and the side force estimation ($S_{H,EST}$) are measured in the coordinates of the vessel. In the direction of travel, at a leeway angle λ , however, the total resistance is larger. As shown in Figure 34, this difference will be R_λ . This means that:

$$R_\lambda = S_{H,EST} \sin \lambda \quad (10)$$


Figure 34: Proposed method of estimating R_λ

Due to the linear nature of this estimation, it is likely to only be accurate for small leeway angles at a relatively low ship speed, although there are suggestions that the increase in resistance is linear for all angles (Longo and Stern, 2002, p. 563). Considering the lack of evidence or data to support this hypothesis, it is important to find a way to validate it, which will be done using CFD.

4.3.2 Comparison of Hydrodynamic Side Force Methods for Different Vessels

Due to the limited number of parameters required to calculate hydrodynamic side force using the Inoue (1981) and Kijima (1990) methods, it is possible to apply them to several ships at an early stage. In addition to the *Cutty Sark* and *Storm Cloud*, seven vessels could be found with enough hydrostatic information to provide an estimation without reconstructing the hull form. A summary of these vessels is provided in Table 11. The main purpose of comparing the results from

Development of a Velocity Prediction Program

these ships is to investigate the effect of different hull parameters on the difference between the methods. A plot of the side force calculated by each method at $V_s = 15$ kn and $\lambda = 15^\circ$ is shown in Figure 35. This is a high speed and a large angle for leeway and may not be representative of the vessels' capabilities, but indicates the differences between the methods clearly.

Table 11: Summary of vessels used to compare hydrodynamic side force estimation methods

	Year	Propulsion	Material	L (m)	L/B	B/T	L/T	C_B
<i>SS Great Western</i>	1837	Paddle	Wood	64.618	6.001	2.119	12.717	0.646
<i>SS Great Britain</i>	1843	Screw	Iron	85.356	5.545	2.853	15.821	0.514
<i>Himalaya</i>	1853	Screw	Iron	103.632	7.473	2.116	15.814	0.494
<i>Storm Cloud</i>	1854	Sail	Iron	60.960	6.069	1.831	11.112	0.444
<i>Persia</i>	1856	Paddle	Iron	114.605	8.356	1.957	16.348	0.482
<i>Sea King</i>	1863	Screw	Composite	67.056	6.769	1.757	11.892	0.579
<i>Cutty Sark</i>	1869	Sail	Composite	64.369	5.949	1.775	10.559	0.492
<i>Mermerus</i>	1872	Sail	Iron	80.530	6.638	1.823	12.103	0.572
<i>Elleric</i>	1897	Screw	Steel	103.327	7.338	2.053	15.067	0.796

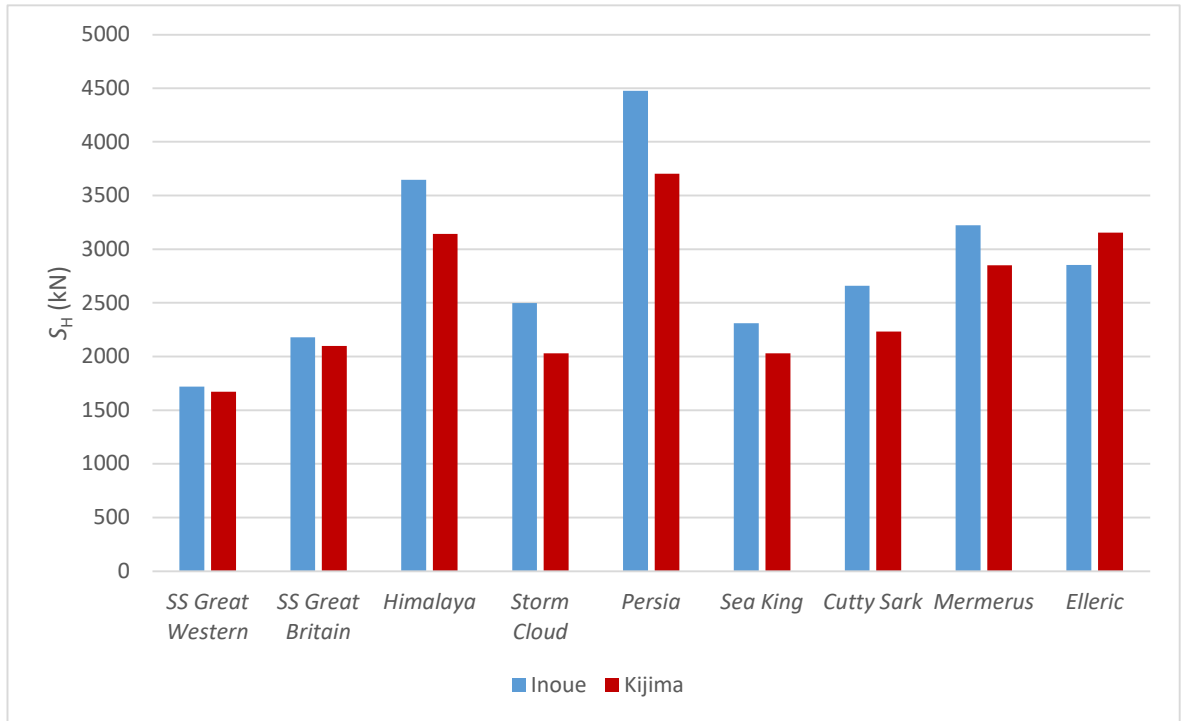


Figure 35: Variation between Inoue and Kijima (1990) for different vessels ($V_s = 15$ kn $\lambda = 15^\circ$)

It can be seen that for the majority of these hull forms, Inoue's method produces a higher side force estimation, with the difference appearing to be related to the beam as this varies in a similar manner. However, in the case of the steamer *Elleric*, this is clearly not the case. The parameter that may cause this difference could be the C_B , which is much higher for *Elleric* than for the other vessels.

These results agree with what might be expected based on the equations for the hydrodynamic derivatives. Both methods employ the same linear term, which is affected by length, beam,

Development of a Velocity Prediction Program

draught, trim and C_B , however the non-linear terms, based on C_B and B/T are different. This means that the differences between the two methods are dependent on the non-linear term. This will be due to the extra three models included by Kijima in the regression analysis.

4.3.3 Comparison of Hydrodynamic Side Force Methods with CFD

The use of CFD is required to validate both the estimated hydrodynamic side force for historic ships and the added resistance due to leeway. The *Cutty Sark* was again used for the CFD validation. Some alterations are required to the setup used for the resistance estimation. As the angle of flow had to be varied, a full-field domain was required as the assumption of symmetry is no longer valid. The resistance and the side force were obtained for a range of leeway angles between 5 and 15°. These were then compared with the estimated side force results from Inoue and Kijima (1990). As it was impractical to carry out this analysis at every ship speed interval, only 11 and 15 kn were considered. These are representative of normal operating speeds for *Cutty Sark* and are large enough to show a difference between the methods. The results for hydrodynamic side force at a V_s of 11 and 15 kn are shown in Figure 36 and Figure 37 respectively.

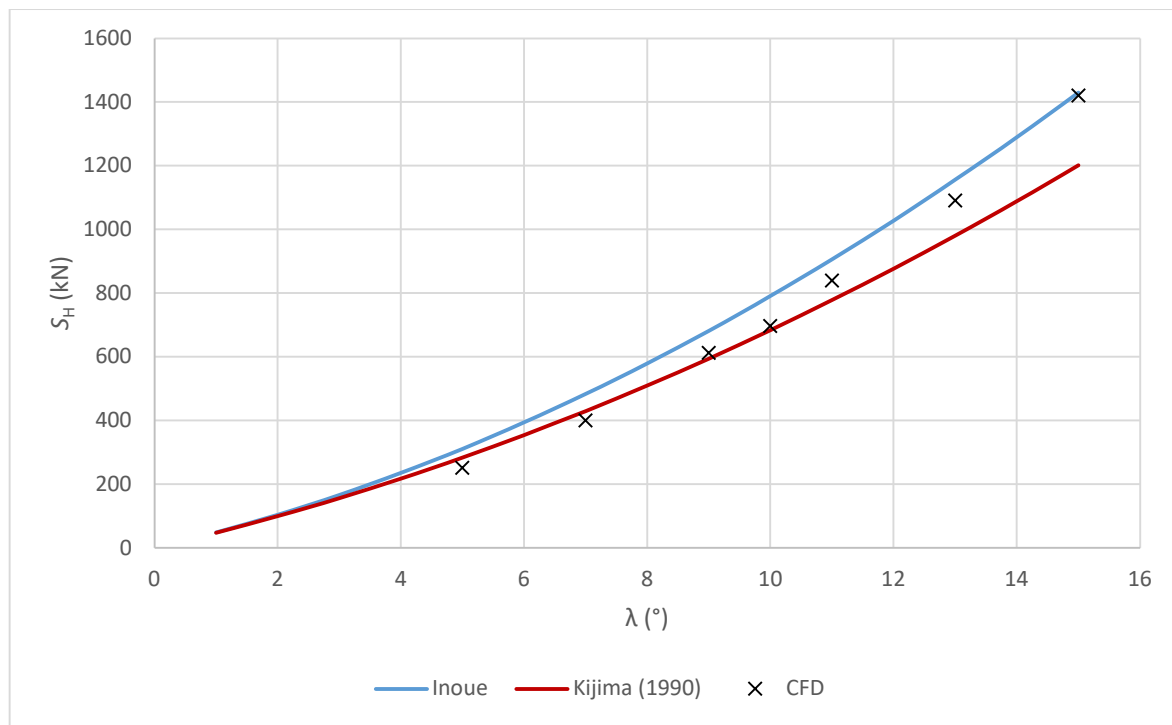


Figure 36: Comparison of S_H from CFD with estimated S_H for *Cutty Sark* at $V_s = 11$ kn

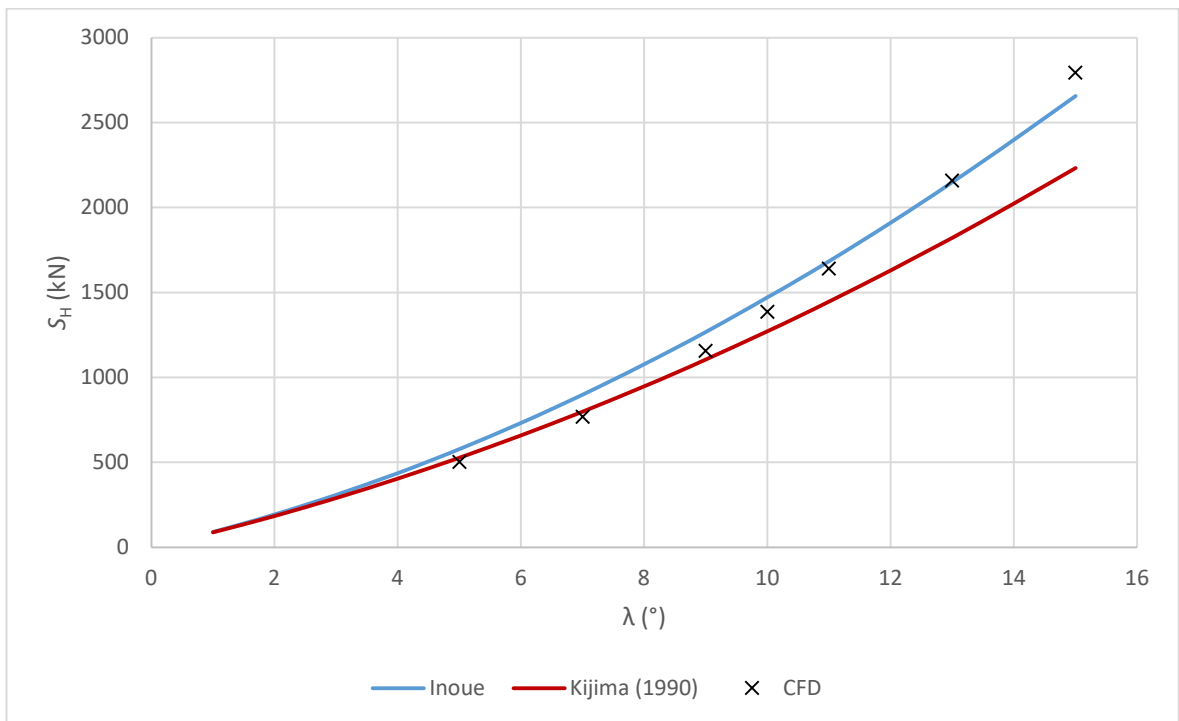


Figure 37: Comparison of S_H from CFD with estimated S_H for *Cutty Sark* at $V_s = 15$ kn

Although the values obtained from the CFD follow the general trend of both curves, it is currently impossible to define which prediction method would be suitable at this stage. For both speeds there seems to be a transition between the two methods at around $\lambda = 10^\circ$. Given this, the prediction method used for the analysis of historic ships may be better selected with a knowledge of the leeway in operation. Despite the differences, the methods are similar enough that an approximate angle may be obtained from the VPP using either method. This would then enable the correct method to be selected based on this approximate angle. Contemporary literature indicates that “good” examples of vessels should not exceed 8-12° when close-hauled, which would have the greatest leeway (White, 1877, p. 479). This suggests that the Kijima method is best based on the above results. The same analysis on *Storm Cloud* produced similar results and are shown in Appendix A.5.

In terms of added resistance, the CFD results also show a promising similarity to the prediction previously described. The results are shown in Figure 38 and Figure 39 for $V_s = 11$ and 15 kn respectively. In this case, it would appear that using the Inoue method for estimating R_λ is more accurate. However, for $\lambda < 10^\circ$ there is very little difference between the methods.

Development of a Velocity Prediction Program

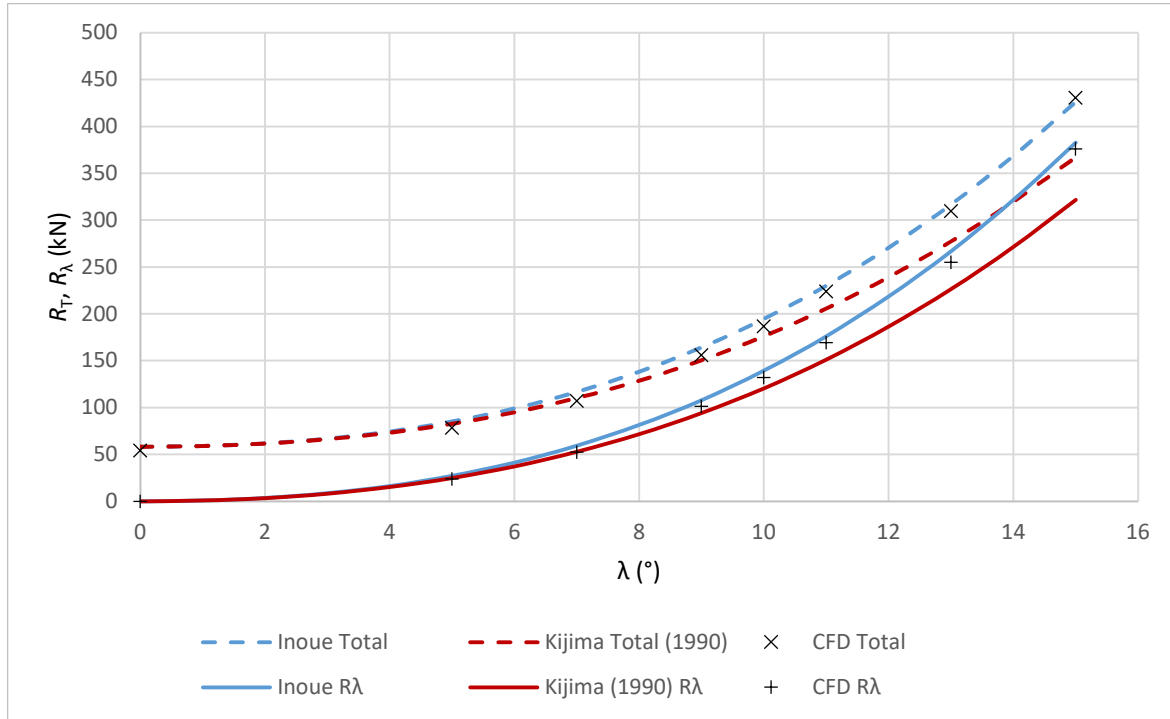


Figure 38: Estimated R_λ compared to R_λ from CFD for *Cutty Sark* at $V_s = 11$ kn

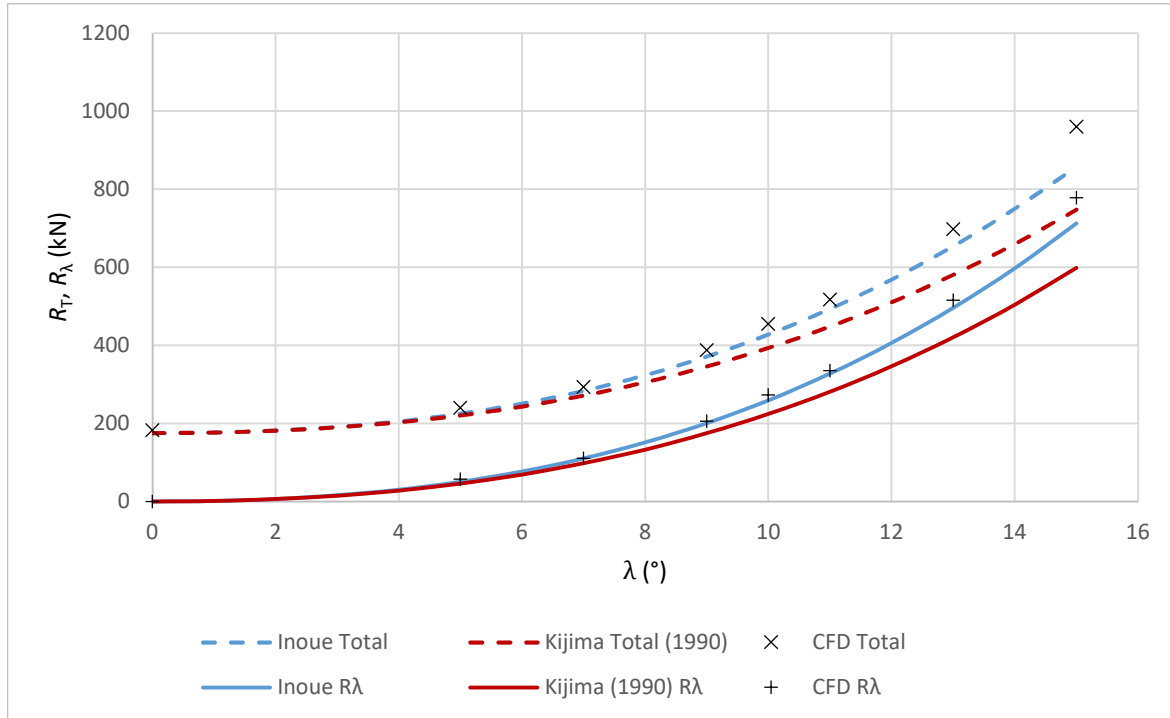


Figure 39: Estimated R_λ compared to R_λ from CFD for *Cutty Sark* at $V_s = 15$ kn

For *Storm Cloud*, the results shown in Appendix A.5 mostly agreed with those for *Cutty Sark*, although at 11 kn the results appear to favour the Kijima method more. These results are therefore compatible with the above discussion, and the trigonometric method of estimating added resistance given in Equation 10 is suitable for these angles.

4.3.4 Hydrodynamic Side Force Sensitivity

A sensitivity analysis was carried out for the hydrodynamic side force in a similar manner to the resistance. Both methods identified rely on only five parameters: L , B , T , C_B and τ . As C_B is dependent on the other parameters, its individual effect was measured using change in displaced volume, ∇ . The results displayed in Figure 40 for the Inoue method shows that the parameter that has the greatest effect on side force is the draught, T , which varies on an even keel. This will be because an increase in draught will cause the greatest increase in the projected area of the hull. As trim, τ , is related to draught, it also has a large impact. The next most important parameter is length, which also increases the projected area. Variations in beam and displacement, and hence C_B , cause minimal change to the overall side force. As the forces calculated by Kijima (1990) are usually smaller, it is expected that the effect shown by Inoue would be less.

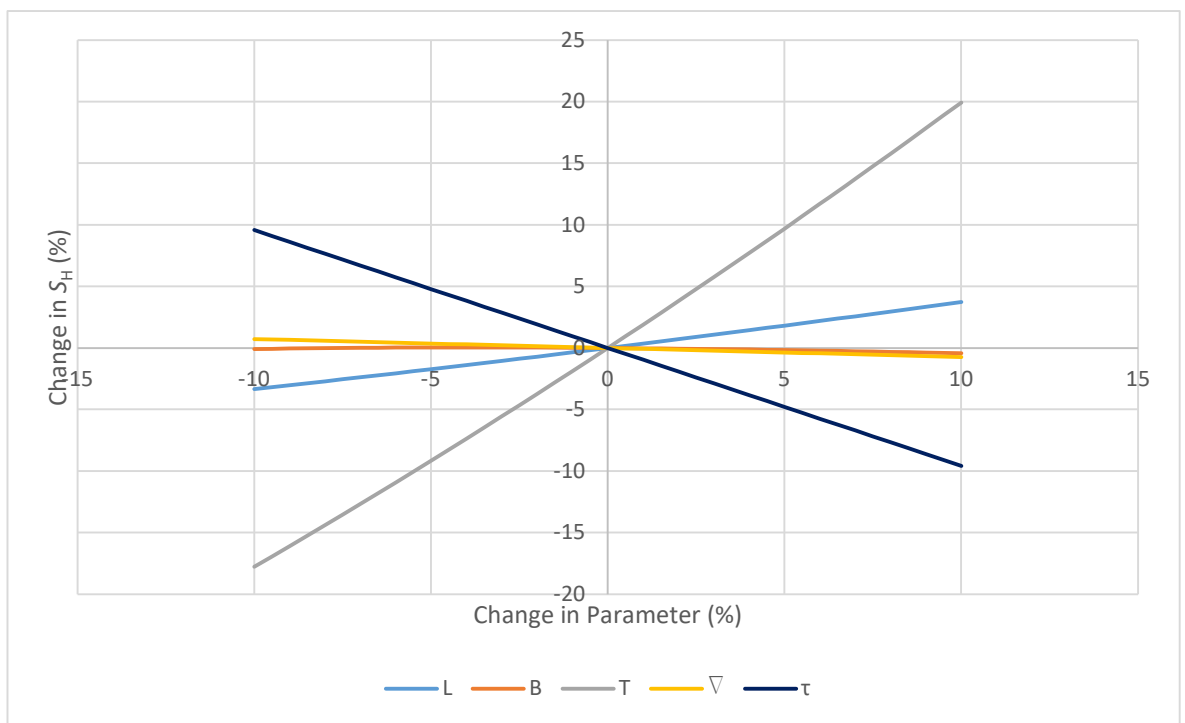


Figure 40: Variation S_H with changes in parameter at $V_s = 15$ kn

4.4 Sail Force Estimation

As discussed in Chapter 2, calculating sail forces for square-rigged vessels is an area that has not been examined much in literature (Radhakrishnan, 1997; Palmer, 2009b, p. 320). It is therefore proposed that the regression equations developed by students creating a simulation of the *HMS Victory* that were identified in Section 2.10 are used to calculate the aerodynamic lift and drag coefficients (Leszczynski *et al.*, 2005, pp. 94–95; Turnock *et al.*, 2006, p. 14). This means certain assumptions need to be made. The first of these is the assumption that sail shape is similar enough between the *Victory* and 19th Century vessels that the equations are suitable. The second major assumption is that blockage effects between the sails remain consistent for all rigs. Since

Development of a Velocity Prediction Program

blockage and aerodynamic drag are accounted for in the equations, there is no need to calculate these. In order to reduce errors, the majority of ships considered in this research will be either ship or barque rigged, as these are primarily square rigged, as shown in Figure 41. However, in order to include steam ships in the analysis, it may also be necessary to consider some with schooner or barquentine rigs, which are primarily fore-and-aft sails. It is expected that the error on these latter rigs will be greater. As triangular jibs are common in modern yachts, for these it would be possible to generate a more reliable estimate. However, this would involve mixing methods which is not felt to be appropriate in this case. As discussed in Section 2.10, these assumptions will not be entirely accurate as there will have been variation between sail shape, and blockage effects are likely to change with the number of masts. At this stage the main focus of the VPP is to help to understand the development of hulls, and so the lack of detail in the sailing model is not of primary importance, especially as it was not uncommon for ships to be re-rigged during their lifetimes. This means that the estimation is satisfactory for this purpose. An improvement on this methodology will be an area for further work outside of this research.

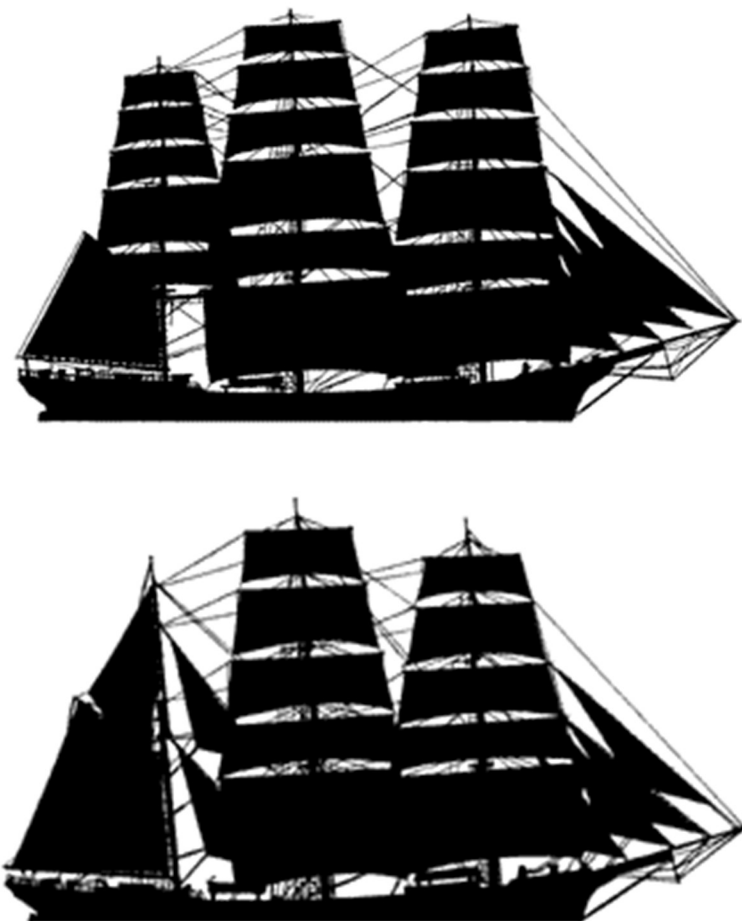


Figure 41: Full rigged ship (top) and Barque (bottom)

These equations, given in Appendix A.4, estimate the lift coefficient (C_L) and the drag coefficient (C_D) for each sail type using a given angle of attack (α). These may then be converted into the lift (L_x) and drag (D_x) forces using the sail areas of each sail type as shown in equation (11).

$$C_L, C_D = \frac{L_x, D_x}{1/2 \rho_A A_{S,x} V_A^2} \quad (11)$$

Where ρ_A is the density of air, $A_{S,x}$ is the sail area and V_A is the apparent wind speed. These forces may then be resolved into the frame of reference of the hydrodynamic forces to get sail thrust.

In terms of incorporating these equations into the VPP, certain boundary conditions have been applied as there are limits to their use even with *HMS Victory* (Leszczynski *et al.*, 2005, pp. 95–96). For example, the angle of attack has been set to zero in the case of the wind coming in front of the sails, which would alter the aerodynamic properties. In addition to this, as the equations do not allow for $\alpha = 0$, the VPP has been set that in these cases lift and drag go to zero and hence no thrust is generated. The full sail force equations are given in Appendix A.4.

4.5 Righting and Heeling Moments

The proposed method for calculating heel angle, ϕ , is by generating a lookup table for righting moments, RM , which may then be used to balance the heeling moment, HM , calculated based on sail area. Such a table can be created using a digital model in the *MAXSURF Stability* software using estimates of the weights and centres of the vessel. The methods of obtaining these estimates will be discussed in Chapter 5. By balancing the righting and heeling moments, it will be possible to identify the angle of heel at which a vessel sails. The main issue with this part of the VPP is determining the effect that the heel angle has on the overall speed, in particular the resistance component, which is dependent on the hydrostatic particulars. In order to determine whether this effect is significant, the impact of changing heel angle on the hydrostatics and resistance in CFD have been examined.

4.5.1 Effect of Heel Angle on Hydrostatics

As heel angle increases, the resistance will normally vary as hydrostatics change. The degree of this is dependent on the shape of the hull, in particular WSA as this drives the frictional resistance. In order to measure the change in hydrostatics, the digital model of the *Cutty Sark* was input into the *MAXSURF Stability* software at a set displacement and ϕ changed systematically. Table 12 shows the outcome of this analysis. It is clear from the data that there is no significant change of hydrostatics until around $\phi = 20^\circ$. This means that the effect on resistance should also remain small. This will be due to the relatively rounded hull shape of the *Cutty Sark*, a characteristic shared by many ships of that time. As it is unlikely that these vessels would often exceed $\phi = 20^\circ$,

Development of a Velocity Prediction Program

it is proposed that the effect of heel on *resistance* and hydrodynamic side force is negligible. This will be confirmed with CFD simulations at a variety of heel angles.

Table 12: Effect of changing heel angle on hydrostatics

ϕ (°)	0	5	10	15	20	25
L_{WL} (m)	65.316	65.324	65.336	65.351	65.370	65.393
B_{WL} (m)	10.880	10.910	10.999	11.146	11.341	11.070
T_{LCF} (m)	5.638	5.636	5.630	5.619	5.602	5.579
V (m ³)	1853.649	1853.648	1853.647	1853.645	1853.652	1853.679
C_p	0.611	0.612	0.613	0.615	0.618	0.623
LCB (m from aft)	32.007	32.008	32.008	32.009	32.009	32.008
T_F (m)	5.729	5.730	5.732	5.735	5.737	5.739
WSA (m ²)	968.880	969.139	969.938	971.373	973.711	993.121
C_B	0.460	0.460	0.460	0.462	0.465	0.478
C_M	0.759	0.757	0.756	0.757	0.760	0.770

4.5.2 Effect of Heel Angle on Resistance and Hydrodynamic Side Force

To test the assumption that heel has negligible effect on resistance, a set of simulations were run in CFD with the model at three angles of heel (5°, 10°, 20°) with a ship speed of 7, 11 and 15 kn.

This was done at three angles of leeway (0°, 5°, 10°). The higher heel angle was not included in the simulations with leeway as the bow wave would have gone over the deck and made the results unreliable. Figure 42 shows the outcome of the simulations with $\lambda = 0^\circ$. In general, there is only a small difference between the heeled and the upright simulations, indicating that heel does not affect resistance in a significant manner.

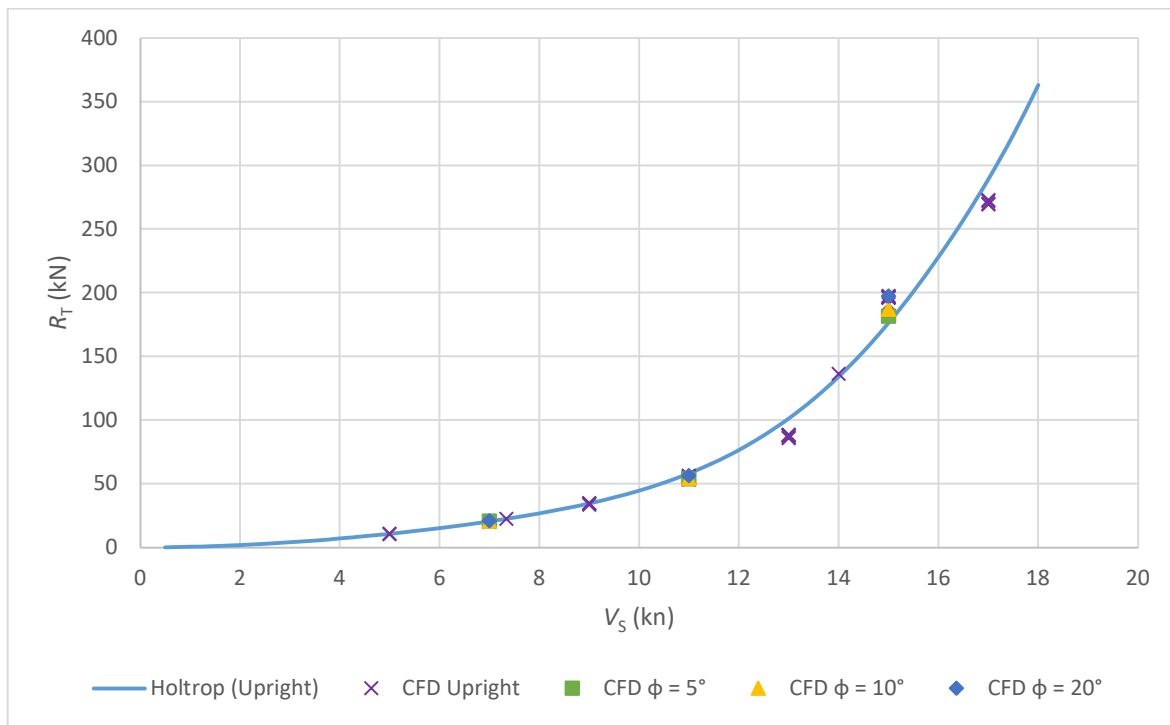


Figure 42: Effect of ϕ on R_T for Cutty Sark

Development of a Velocity Prediction Program

The results for the simulations with leeway also indicate that the assumption is valid and also show negligible effect of heel on the other hydrodynamic forces, although perhaps showing a preference for the Kijima estimation method. This could be due to the selection of leeway angle, as the transition point shown previously was around $10^\circ \lambda$. Figure 43 and Figure 44 show hydrodynamic side force and overall resistance respectively. In light of this, it is clear that the effect of heel on resistance is negligible for ships like *Cutty Sark*.

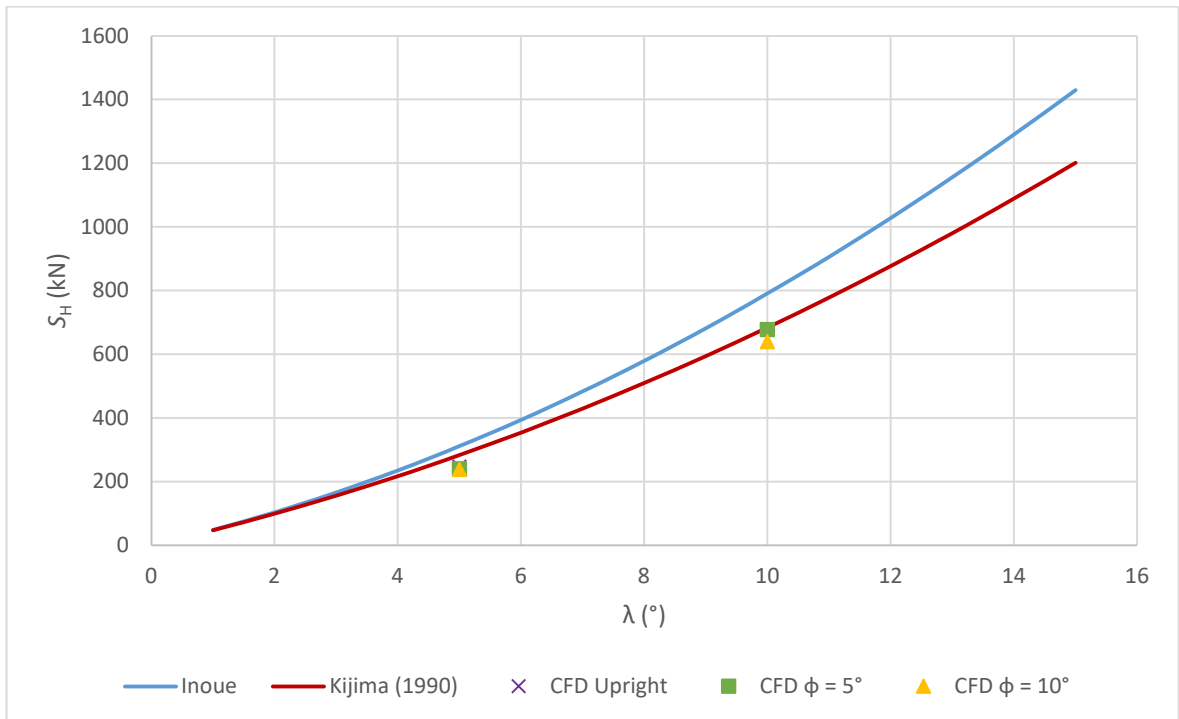


Figure 43: Effect of ϕ on S_H for *Cutty Sark* at $V_S = 11$ kn

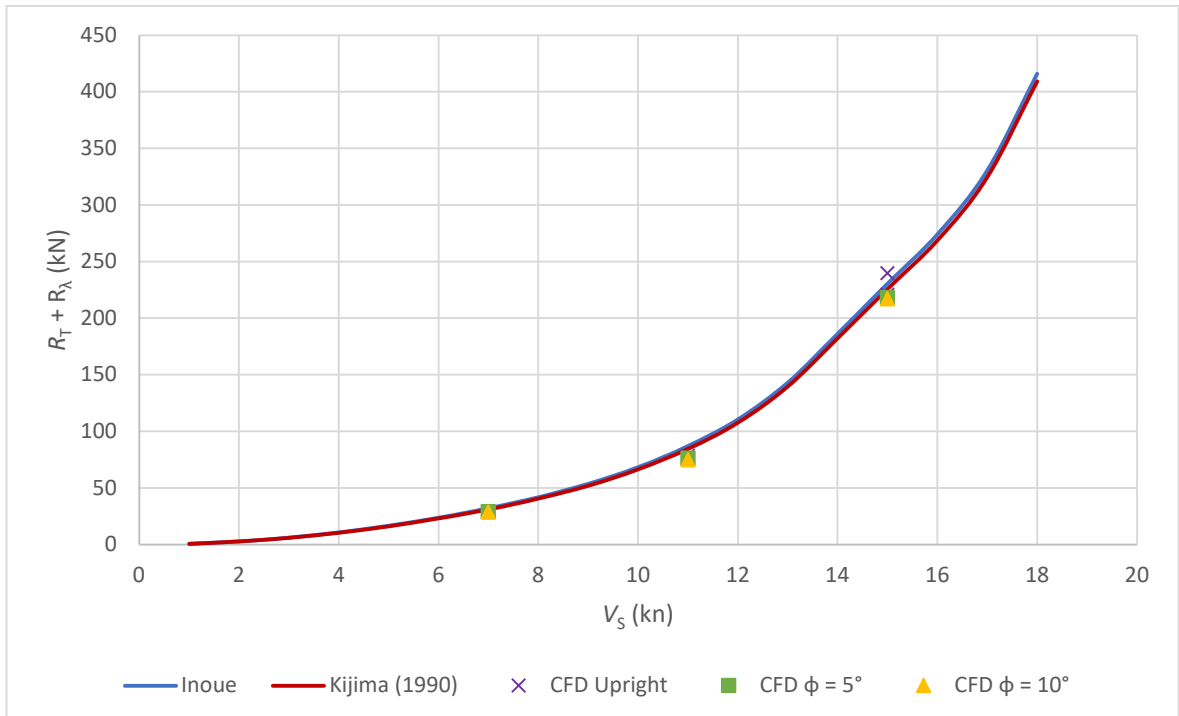


Figure 44: Effect of ϕ on $R_T + R_\lambda$ for *Cutty Sark* at $\lambda = 5^\circ$

4.5.3 VCG Sensitivity

Due to the level of available data on historic ships, the VCG used to calculate the righting moment needs to be based on a number of assumptions, which will be explained in Chapter 5. This means that it may not reflect the actual VCG of the vessel. The impact of this can be examined by changing the overall VCG calculated for *Cutty Sark* incrementally to generate new tables of righting moment and examining the heel angle output of the VPP.

Figure 45 shows the result of this analysis in a true wind speed, V_T , of 25 kn at a true wind angle, γ , of 130° and the bracing angle of the yards, θ , at 50°. It is clear that very small changes in VCG, where 1% is approximately equal to 50 mm, there is a significant effect on the heel angle of the vessel. As has previously been discussed, however, the heel angle was found to be negligible in relation to the hull resistance and side force, with its only implication being on the sail forces. This means that, despite providing a potentially unreliable angle of heel, error in calculating the VCG will only produce a negligible effect on the overall speed and leeway. The sensitivity analysis confirmed this, with the difference in speed over the course of a 10% variation in VCG amounting to 0.05 kn and leeway angle varying by 0.01°. The only foreseeable issue with the positioning of the VCG is the possibility that it may cause the vessel to exceed its freeboard, which would cause the VPP to fail. With the time available for this research, however, it is not possible to obtain a more accurate VCG.

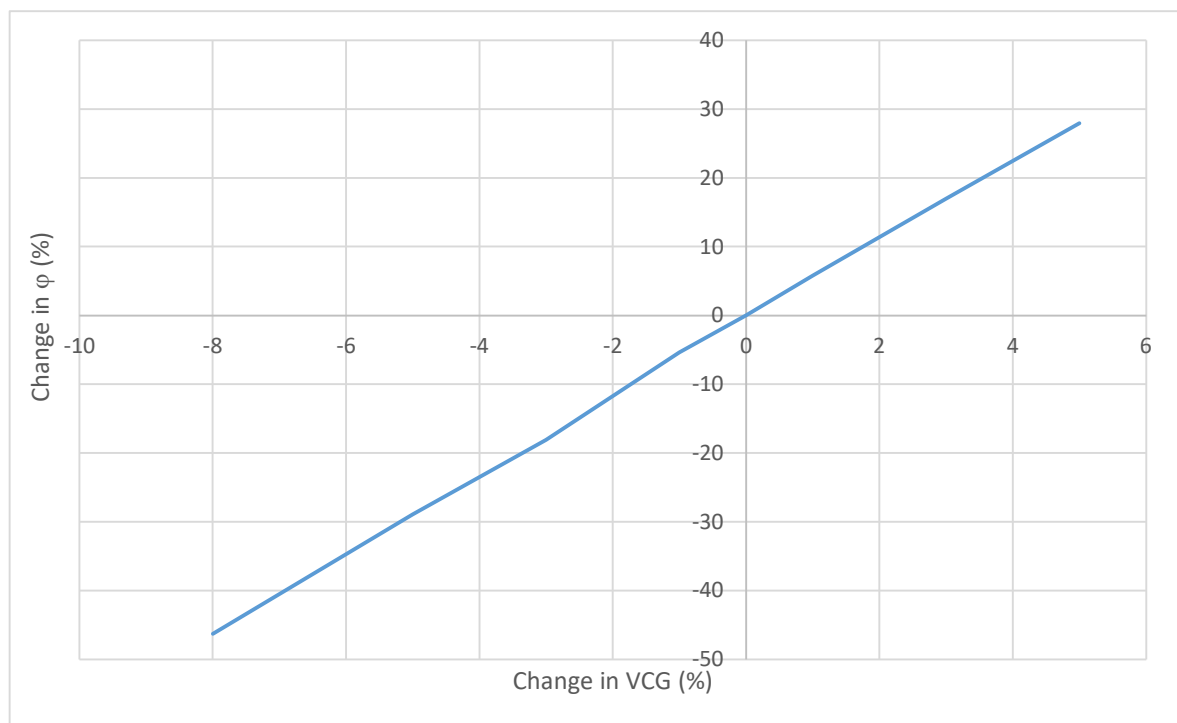


Figure 45: Effect of changing VCG on output heel angle ($V_T = 25$ kn, $\gamma = 130^\circ$, $\theta = 50^\circ$)

4.6 Velocity Prediction Program Design

The design for the VPP for this research is driven primarily by a need to be flexible, to cope with a wide variety of hull forms and sailing rigs as well as potentially limited input data. The modular approach to its design means that it should be possible to incorporate alternative methods at a later stage. The VPP has been written in *MATLAB* incorporating the methods identified in the previous sections. The calculation methods of the individual components may be seen in Appendix A.

The VPP iterates ship speed (V_s), leeway angle (λ) and heel angle (ϕ) until the equilibrium conditions are met, which in this case is the balance of resistance with thrust, hydrodynamic side force with aerodynamic side force, and righting moment with heeling moment. The iteration size varies depending on the magnitude of the difference between the forces. This increases the speed of the calculation, particularly in more extreme wind conditions. A summary of iteration sizes is given in Table 13.

Table 13: Iteration sizes used in the VPP

Value	Maximum Iteration Size	Minimum Iteration Size
V_s	0.1 m/s	0.01 m/s
λ	1°	0.01°
ϕ	0.2°	0.1°

The hydrostatic input for the VPP is a table of data that may be generated for each individual vessel. An example of this with data for *Cutty Sark* is shown in Table 14. The advantage of this is that data unique to the vessel may be easily updated without the need to change parameters individually within the input dialogue. Five of these parameters are related to appendages such as bulbous bows and rudders and so may not be required for the analysis depending on the available data. These values are highlighted in grey.

Table 14: Hydrostatic input for the VPP with data for *Cutty Sark*

Parameter	Parameter Name	Unit	Value
L	Length	m	64.37
B	Beam	m	10.94
T	Draft (Amidships)	m	6.10
∇	Displacement Volume	m^3	2087.99
C_p	Prismatic Coefficient		0.628
LCB	Longitudinal Centre of Buoyancy	m (+ve fwd from amidships)	1.14
C_{stern}	Stern Coefficient (See Appendix A.1)		0
i_E	1/2 Angle of Entry	°	16.80

Development of a Velocity Prediction Program

A_{BT}	Bulbous Bow Area	m^2	0
T_F	Draft Forward	m	6.10
h_B	Depth of Bulbous Bow	m	0
A_T	Transom Area	m^2	0
C_M	Midship Section Coefficient		0.780
A_{APP}	Appendage Surface Area	m^2	0
k_2	Appendage Form Factor		0
C_B	Block Coefficient		0.489
WSA	Wetted Surface Area	m^2	1058.32
$A_{Windage}$	Area of Hull For Windage	m^2	250.63
A_{Jib}	Area of Jibs	m^2	597.45
A_{Driver}	Area of Driver (Gaff) Sails	m^2	237.98
A_{Main}	Area of Main Sails	m^2	1227.69
A_{Mizzen}	Area of Mizzen Sails	m^2	390.61
IHP	Input Horse Power	HP	0
CE	Centre of Effort above WL	m	17.89
FB	Freeboard	m	1.44

The output of the VPP is therefore V_s , λ and ϕ for a given wind speed and angle (V_T , γ) and bracing angle of the yards (θ). Under each iteration, the sail forces need to be calculated. These are based on the lift and drag estimations derived from experiments with *HMS Victory* (Leszcynski *et al*, 2005), which are given in Appendix A.4. For these, α is calculated based on the apparent wind speed, V_A , and angle (β). The angles are measured from the bow as opposed to the direction of travel, with the effect of leeway included at a later stage. These dimensions are defined in Figure 46. As heel will need to be calculated from a lookup table of righting moments, a table generated from *MAXSURF Stability* is also needed for each ship.

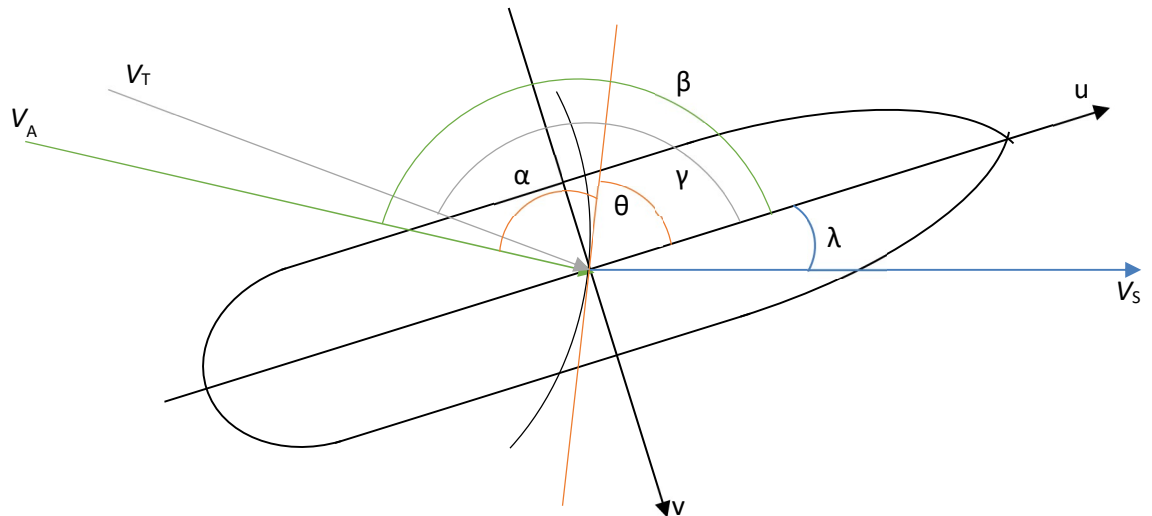


Figure 46: Diagram showing sail angles used in the VPP

The hydrodynamic side force calculation method assessment discussed in Section 4.4.4 is inconclusive over which method would be more suitable. Initial indications from the VPP are that leeway angle is generally less than 10°, and so in response to the previous analysis, the Kijima (1990) estimation method is adopted as this provided the nearer match below 10°.

In order to allow for the inclusion of steam propulsion, the thrust generated by the sails is added to the thrust from the engine. This is calculated using the EHP generated by the engine, which is equal to the IHP multiplied by an efficiency (η). This is then converted into thrust.

If a range of wind angles are included in the input, there is also an option for a polar performance diagram to be generated. A break point is also provided to prevent the freeboard from being exceeded, as at this point the vessel is in danger of flooding, and due to the shape of the deck the results of the VPP would no longer be reliable. For cases where it is uncertain which bracing angle to choose, it is possible to apply an extra loop to carry out the calculation for a variety of angles and select an optimum value for each wind angle. A flow chart describing the process used by the VPP is given in Figure 47.

Development of a Velocity Prediction Program

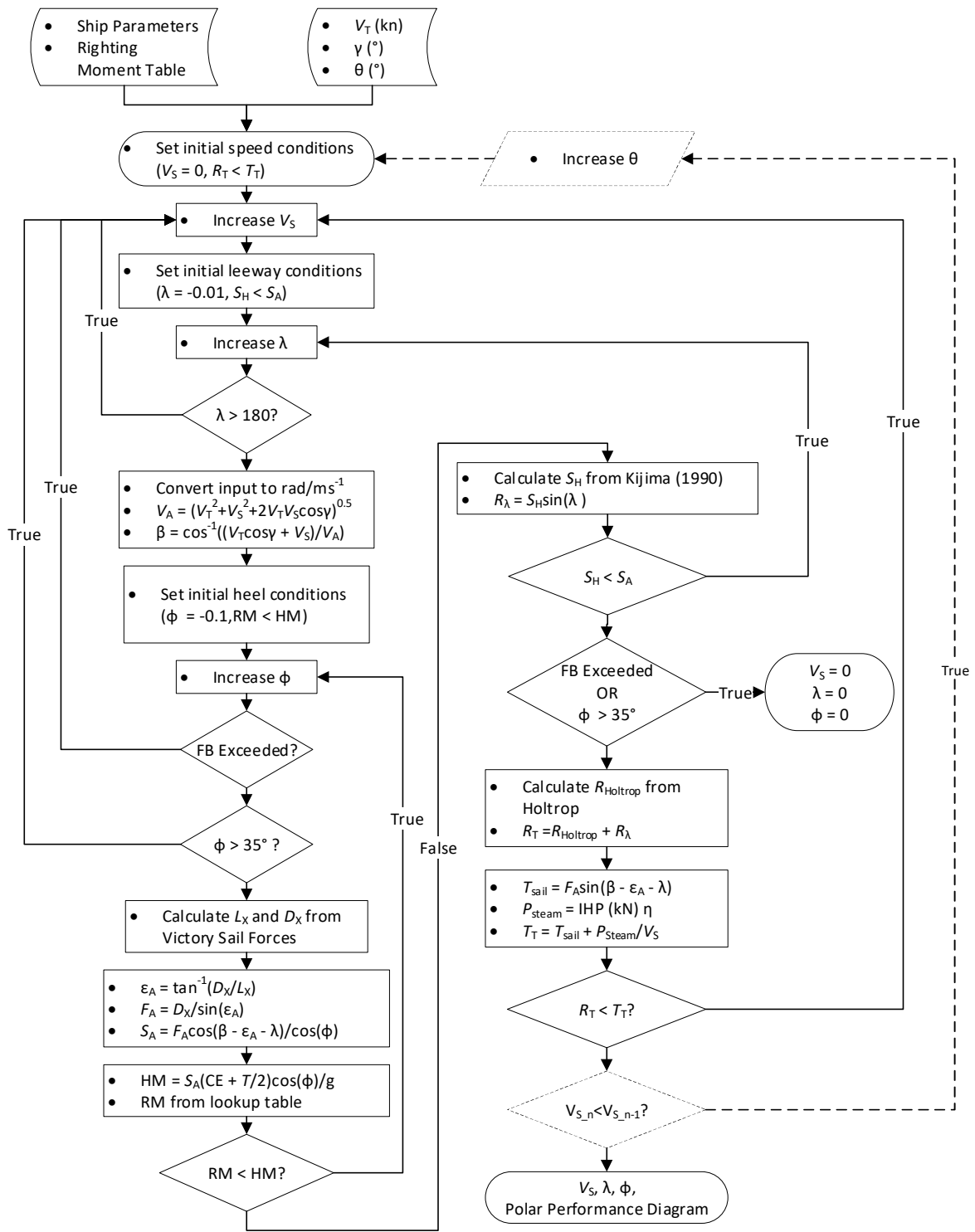


Figure 47: Flow Chart describing the VPP

An example of the output for *Cutty Sark* at $V_T = 20$ kn and $\theta = 50^\circ$ off the bow can be seen in Figure 48. These are arbitrary values that personal experience shows are good conditions for a square rigged vessel. It is expected that the speed estimates will be higher than the actual maximum speed, as effects such as hull roughness and resistance due to waves have been omitted. Examples of the variation in leeway and heel are shown in Figure 49 and Figure 50

Development of a Velocity Prediction Program

respectively. Under the conditions that the ship would be operating under, these outputs are what would be expected of a square rig vessel, with the peak leeway and heel occurring at the point of maximum ship speed. Reports and logs of the *Cutty Sark* indicate a maximum achievable speed of around 17.5 kts, which is shown to be possible by the polar diagram (Lubbock, 1924, p. 11). The polar diagram also shows that the ship is capable of sailing about 60° off the wind under these conditions, which agrees with literature, suggesting that a close-hauled vessel is capable of sailing between 56 to 67° from the wind direction (MacGregor, 1980b, pp. 15–16).

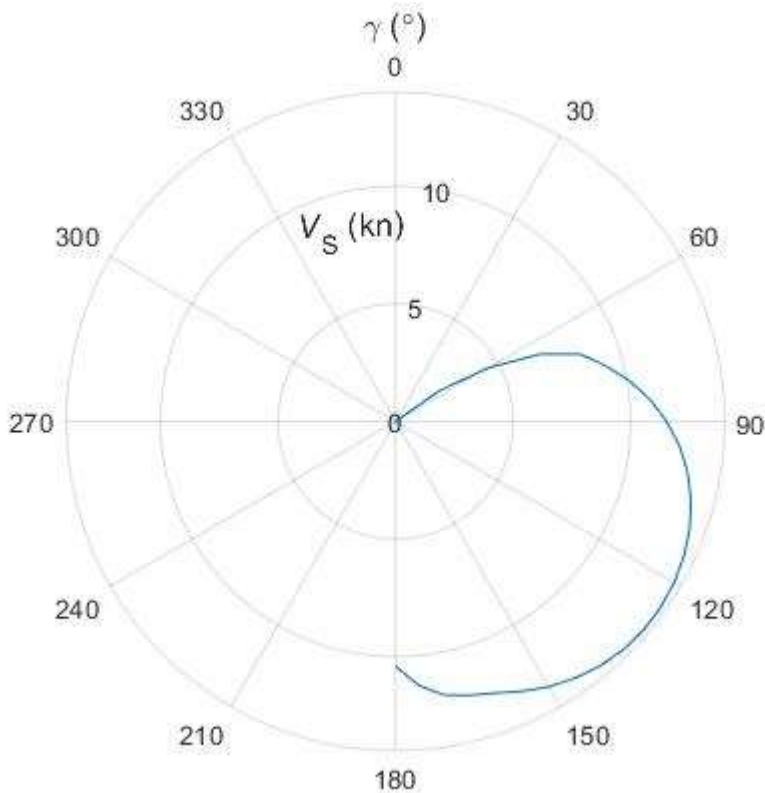


Figure 48: Polar performance diagram for *Cutty Sark* at $V_T=20$ kn, $\theta=50^\circ$

Development of a Velocity Prediction Program

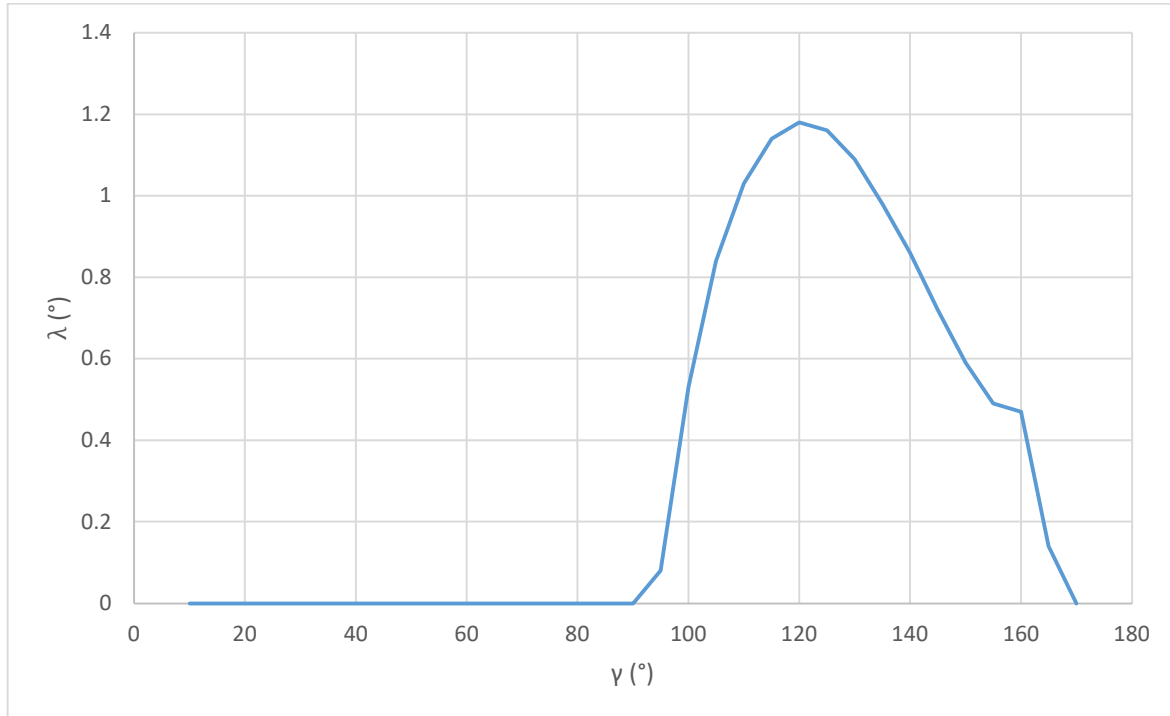


Figure 49: Variation in λ with γ for Cutty Sark at $V_T=20$ kn, $\theta=50^\circ$

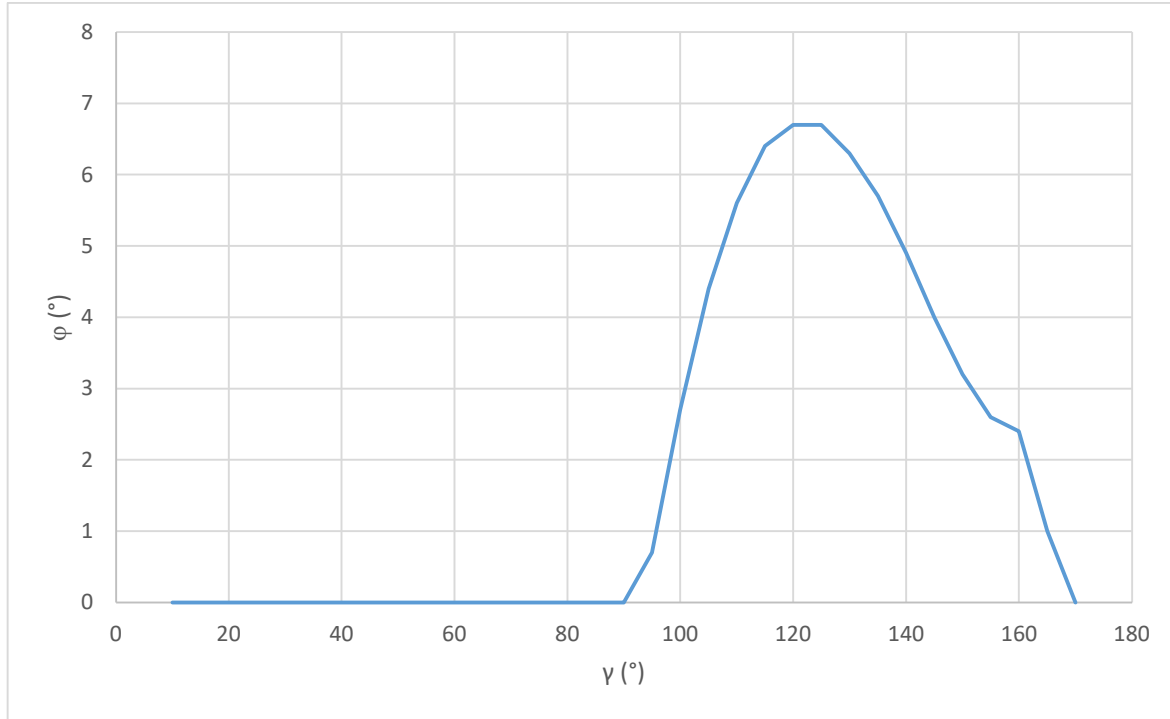


Figure 50: Variation in ϕ with γ for Cutty Sark at $V_T=20$ kn, $\theta=50^\circ$

4.6.1 VPP Sensitivity

It is possible that in combining the individual components of the VPP, some of parameters highlighted in the previous analysis do not have as large an effect on the overall VPP as in the individual components. A sensitivity analysis has therefore also been carried out on the VPP as a whole. In accordance with the previous findings, length, beam, draught, volumetric displacement and WSA were changed. C_B , and C_P were adjusted accordingly to obtain an estimate of the overall effect. Sailing conditions where the speed is near the maximum were chosen: $V_T = 25$ kn, $\gamma = 140^\circ$,

Development of a Velocity Prediction Program

$\theta = 50^\circ$. This produces a ship speed of around 16.3 kn. For lower speeds the effect of 10% parameter changes were found to remain less than 2.5%. The results are shown in Figure 51. This analysis shows that the length has the greatest effect on speed. A heavy reliance on the accuracy of the displacement is also indicated. However, although there is often no data to confirm the accuracy of this particular, if length, beam, draught and WSA are carefully controlled, there should not be too much error within the displacement. Figure 51 indicates that in order to keep the error in ship speed below 5%, the parameters including length, should be within 8% of the actual value. As length is the easiest to control, the total error is likely to be smaller. Trim was found to have a negligible effect relative to the change in draught. It may be noted that the curves produced by this analysis are not smooth. This is due to the precision of the VPP itself as the iteration of ship speed, leeway and heel can only be done to a certain number of decimal places in order to speed up the calculation, meaning that the matching of hull forces must allow a small margin to accommodate this. The minimum increments used are 0.01 ms^{-1} , 0.01° leeway and 0.1° heel.

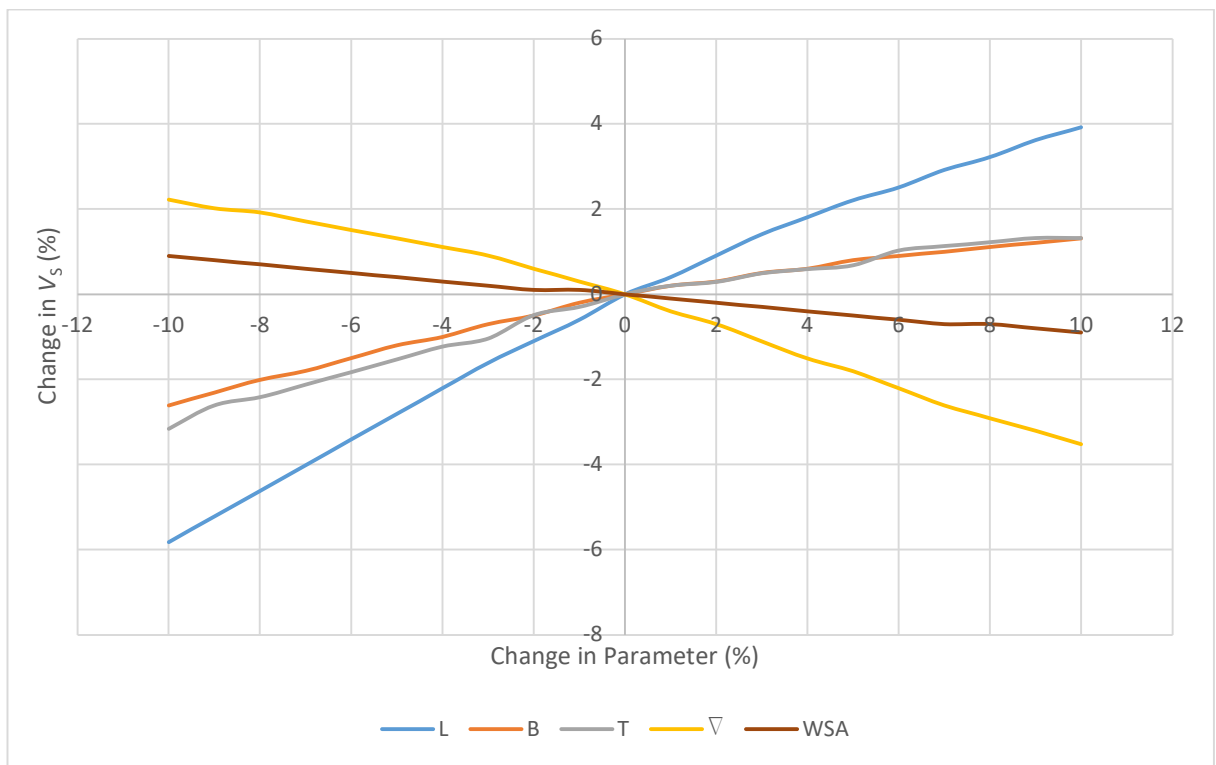


Figure 51: Variation of V_s with changes in parameter ($V_T = 25 \text{ kn}$, $\gamma = 140^\circ$, $\theta = 50^\circ$)

The most important outcome of the sensitivity analysis carried out on the VPP, is an understanding of how accurate the digital models need to be. The parameters that were shown to have the most effect on the results were length, draught and WSA. As the length of the ship is generally one of the known parameters, it is suggested that where possible this dimension should be used as the primary reference for scaling. This should minimise the error associated with it and hence improve the accuracy of the results. Similarly, draught can be set as a constant where it is

recorded, or scaled from the lines plan where a waterline is given. WSA will provide the greatest challenge in obtaining enough accuracy, as literature has only provided one example where it has been recorded as a comparison. The best way of ensuring maximum accuracy therefore, is by attempting to ensure that the lines generated from the digital model are as close to those on the plan as possible. Where there is no lines plan available, a judgement should be made based on other parameters, such as displacement, which are likely to drive WSA. Experience of using a 3D scanner in conjunction with a lines plan will also prove to be invaluable.

4.7 Summary

The use of regression equations for estimating hydrodynamic forces operating on historic ships has been investigated using the *Cutty Sark* as a base model, with additional verification using an alternative vessel, *Storm Cloud*. The Holtrop and Fung methods were identified as the most suitable for resistance calculation, although each provided significantly different predictions. These were compared with contemporary data found for *HMS Greyhound*, which gave inconclusive results for validating either method, despite following the trend of the Holtrop method. CFD was run for a model of *Cutty Sark*, which showed a good correlation with the Holtrop resistance prediction method. A similar analysis was carried out for hydrodynamic side force, identifying the Inoue and Kijima methods as most suitable, depending on the magnitude of the leeway angle. As the leeway angle was shown to remain relatively low by both the VPP and contemporary literature, it is proposed that the Kijima (1990) method is used as the primary method. The effect of heel angle on resistance was shown to be negligible through a series of CFD simulations.

A sensitivity analysis has been carried out for the individual hydrodynamic components, showing that length, draught and wetted surface area are the most likely parameters to have a significant effect on performance results. Of these, wetted surface area is the most challenging to control, highlighting the need for reasonably accurate modelling of the hull forms. A sensitivity analysis on the effect of the accuracy of calculating the VCG shows that this has a large effect on the heeling moment produced by the VPP, but a negligible effect on the speed and leeway.

The VPP has been written to combine the estimation methods that were found to be suitable. A sensitivity analysis has also been carried out on the program as a whole, which indicates that the effects of errors indicated by the individual components are reduced in the finished product. According to the sensitivity analysis on the VPP, to keep the speed error to within 5%, the error in the parameters should not exceed around 8%.

Development of a Velocity Prediction Program

As it was created with 19th Century British merchant ships as a focus, it is unlikely that the VPP developed here would be suitable for all historic ships. In its current form it is suggested that the VPP is only suitable for European and American ships dating from the mid-16th Century. However, given additional information on propulsive forces it is possible to adapt the program to allow for alternative rigs and hull forms. The VPP presented here would also produce an overestimate of ship speed as there are certain resistance components that may not be easily calculated, for example resistance due to waves, which is dependent on sea state, and resistance due to surface roughness. The assumption that the yaw moment is zero would also have a small effect on the hull resistance, as in reality there would be some resistance generated by the rudder in order to balance the moment.

Despite these limitations, the VPP provides a tool that is capable of estimating the sailing performance in a variety of wind conditions. The output includes the ability to produce a polar performance diagram and estimates of leeway and heel based on between 20 and 25 parameters, depending on the level of detail required. Where this had only previously done for individual vessels, it is now possible to quickly obtain an estimate of sailing performance for a large number of ships. The remaining challenges lie with the identification of the input variables. A majority of these are possible to extract from digital models, with a few details such as the sail areas and righting moments requiring additional sources or estimation based on other vessels. The methods of creating the digital models and obtaining estimates for the other inputs are discussed in the next chapter.

Development of a Velocity Prediction Program

Chapter 5: Selection and Digitisation of Primary Data

Chapters 3 and 4 showed that a knowledge of ship geometry is required for estimating or inferring performance, whether that is through a parametric analysis or the use of a VPP. It was shown in Chapter 3 that there was not enough existing data to achieve this. In order to increase the dataset, therefore, a set of digital models will need to be created to extract the parameters. The selection of ships to be incorporated in the performance analysis is important to consider when discussing methods of modelling ships. This chapter will cover the reasoning behind the selection of ships, along with methods of creating the digital model and providing estimates of other details that are required for the VPP, such as VCG and sail area.

As discussed in Section 2.3, much of the material required for modelling 19th Century ships is held by maritime museums. Lines plans and builders' half models are amongst the more common sources and so a method of extracting this information is required. The *Cutty Sark* digital model employed in Section 4 will be used for demonstrating the method of creating a digital model from a lines plan. For the purpose of comparing 3D scanning techniques and determining the effect of errors on performance prediction results, a 1:48 scale half model of the *Cutty Sark* was also constructed using the digital model for the design. This was to examine differences in accuracy between alternative scanning and post processing techniques, and to establish if scanning accuracy will have a significant impact on the estimated performance of a ship. These aspects will be discussed in Section 5.2.

In addition to the hull form, an estimate of the sail forces and VCG needs to be provided. This involves the calculation of sail areas and major weights and centres. For some vessels in the dataset this information is not always available, and so methods of estimating propulsion and structural details based on other ships from the dataset will be discussed in Sections 5.3 and 5.4. A summary of the mass estimates will be provided at the end of the chapter.

5.1 Selection of Ships for Analysis

In order to examine the evolution of ships, it is important that there are enough vessels in the dataset, spanning the full period under investigation. Employing the same criteria as in Chapter 3, it was decided that the selection of vessels considered should consist of ocean-going vessels only. The ships used must also have some form of hull data available, and where possible this has been extended to include a sail plan and survey report. In addition to this, where a lines plan is used, it also had to be of sufficient quality and half models had to be available to scan. Some models were unavailable to scan for a range of reasons, such as being on display at the time of data collection. Because of the limitations of the sail force calculation discussed in Section 4.4, only vessels that

Selection and Digitisation of Primary Data

are primarily square-rigged have been included. The exception to this is for steam ships, where it was more common to have a fore-and-aft rig and there are very few square-rigged examples.

The final selection of 61 ships and the source of the hull data is displayed in Table 15. Those marked with (*) are steam vessels and those marked with (+) are auxiliary steamers. The latter of these will be treated as sailing ships as they are fitted with full rigs. All of the steam ships in this dataset are single screw, as none of the paddle steamers with hull data that were identified met the criteria of ocean-going. It should be noted that the hull model for *Vision* was on display at the time of data collection and so was not scanned. For those vessels with “N/A” listed, it does not necessarily mean that the source does not exist; only that it had not been located at the time of writing.

Table 15: Final selection of ships (NMM=National Maritime Museum Greenwich, BI=Brunel Institute, GRM=Glasgow Riverside Museum, LRF=Lloyd's Register Foundation)

Name	Date	Model	Lines	Survey Report	Sail Plan
Acasta	1845	N/A	BI	LRF	BI
Afon Alaw	1891	N/A	(Greenhill, 1980)	N/A	N/A
Alexandra*	1863	NMM	N/A	LRF	N/A
Anaces*	1897	GRM	N/A	N/A	N/A
Ancona	1893	NMM	N/A	LRF	N/A
Ann Duthie	1868	N/A	(MacGregor, 1984b)	LRF	(MacGregor, 1984b)
Aphrodita	1858	N/A	(MacGregor, 1984b)	N/A	(MacGregor, 1984b)
Arab	1839	N/A	(MacGregor, 1984a)	N/A	(MacGregor, 1984a)
SS Arab*	1879	GRM	N/A	LRF	N/A
Australia	1826	N/A	BI	LRF	N/A
Balfour	1809	N/A	BI	N/A	N/A
Belle of Lagos	1868	N/A	(MacGregor, 1984b)	LRF	(MacGregor, 1984b)
Belle of the Clyde	1865	N/A	(MacGregor, 1984b)	LRF	(MacGregor, 1984b)
Blenheim	1848	N/A	(MacGregor, 1984a)	LRF	(MacGregor, 1984a)
Cairngorm	1853	N/A	(MacGregor, 1988)	LRF	(MacGregor, 1988)
Camertonian	1848	N/A	(MacGregor, 1988)	N/A	(MacGregor, 1988)
Carnatic	1859	N/A	BI	LRF	BI
Cedarbank	1892	NMM	N/A	N/A	N/A
City of Adelaide	1864	N/A	BI	LRF	BI
Cumberland	1800	N/A	BI	LRF	N/A
Cutty Sark	1869	Lines	(Lubbock, 1924)	LRF	BI
Dunbar	1853	N/A	(MacGregor, 1984b)	LRF	(MacGregor, 1984b)
Eastern Monarch	1856	GRM	BI	LRF	N/A
Edmund Preston	1858	N/A	(MacGregor, 1984b)	LRF	(MacGregor, 1984b)
Elissa	1877	N/A	BI	LRF	BI
Elizabeth	1832	N/A	NMM	LRF	N/A
Farquharson	1820	N/A	BI/NMM	Lines	BI
Fusi Yama	1865	N/A	(MacGregor, 1988)	LRF	(MacGregor, 1988)

Name	Date	Model	Lines	Survey Report	Sail Plan
SS Great Britain*	1844	N/A	(Corlett, 1975)	(Corlett, 1975)	N/A
Hurricane	1853	NMM	(MacGregor, 1988)	LRF	(MacGregor, 1988)
Hydaspes*	1872	NMM	NMM (?)	N/A	NMM (?)
Indian Empire	1896	NMM	N/A	N/A	N/A
John Garrow	1840	N/A	BI	LRF	N/A
John Lidgett	1862	GRM	N/A	LRF	BI
Loch Broom	1885	NMM	N/A	LRF	N/A
Mabel Young	1877	N/A	BI	LRF	BI
Maitland	1865	N/A	(MacGregor, 1988)	LRF	(MacGregor, 1988)
Marpesia	1866	GRM	BI	LRF	BI
Mermerus	1872	N/A	BI	LRF	(MacGregor, 1988)
Morayshire	1875	NMM	N/A	LRF	N/A
Neilson	1824	N/A	(MacGregor, 1988)	N/A	(MacGregor, 1988)
Norham Castle	1869	NMM	BI	LRF	BI
Princess Royal	1841	N/A	NMM	LRF	N/A
Samaria*	1868	GRM	N/A	N/A	N/A
Schomberg	1855	GRM	BI	N/A	BI
Sea King ⁺	1863	GRM	BI	N/A	BI
Seringapatam	1837	N/A	BI	N/A	N/A
Servia*	1881	GRM	N/A	N/A	N/A
Sindia	1887	N/A	(Lubbock, 1953b)	N/A	(Lubbock, 1953b)
Spindrift	1867	N/A	(MacGregor, 1988)	LRF	(MacGregor, 1988)
Storm Cloud	1854	N/A	(MacGregor, 1988)	LRF	(MacGregor, 1988)
Stornoway	1850	GRM	BI	LRF	BI
Sunfoo*	1871	GRM	N/A	LRF	N/A
Taeping	1863	NMM	BI	LRF	N/A
Thalia	1818	N/A	(MacGregor, 1988)	N/A	N/A
Thermopylae	1868	N/A	(MacGregor, 1988)	LRF	(MacGregor, 1988)
Titania	1866	NMM	(MacGregor, 1988)	N/A	(MacGregor, 1988)
Tszru*	1869	N/A	BI	LRF	BI
Vision	1853	GRM	(MacGregor, 1988)	LRF	(MacGregor, 1988)
Wendur	1884	NMM	N/A	LRF	N/A
Zeta ⁺	1865	N/A	BI	LRF	BI

5.2 Creation of Digital Hull Models

5.2.1 Modelling from a Lines Plan

A vessel may be digitally reconstructed from a lines plan using specialist software, such as the *MAXSURF* design suite. For the digital model of the *Cutty Sark*, described in Section 4.1, a lines plan was located and scanned as a high-resolution digital image. This was then adjusted in a photo editor to ensure that the axes would be correctly aligned, before being input into *MAXSURF Modeler*. In this software, the image may be scaled using known reference points, with an image for each viewpoint: body, plan and profile. Following this, the locations of the sections, buttock

lines and waterlines can be set. For working with some earlier plans, it is also possible to set diagonal lines. Marker points were placed on the body plan at each intersection between the sections, buttock lines and waterlines to define the basic hull shape. Additional points were added where the curvature was particularly great on the sections. In this way a simple, but structured point cloud is created, as shown in Figure 52.

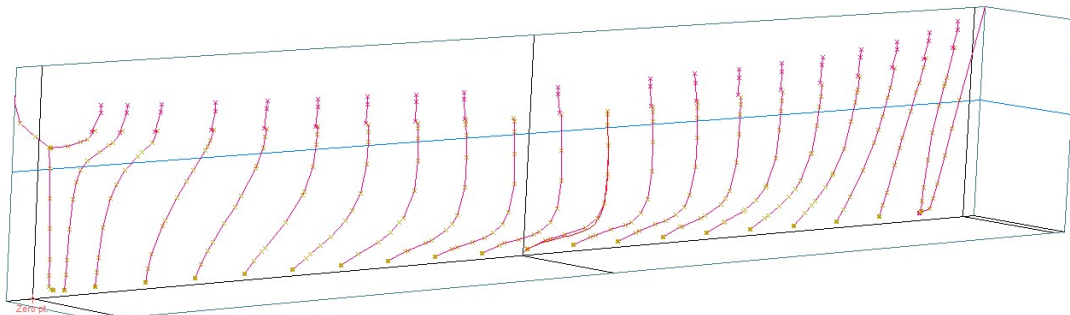


Figure 52: Structured point cloud with curves constructed from the lines of *Cutty Sark*

With markers as a starting point, there are several ways in which a surface may be fitted. Genetic algorithms are available within the software to fit both edges and the entire surface. These run through a series of iterations to fit a surface as closely as possible to the markers. With enough experience, it is possible to estimate the required surface stiffness and number of control points. Without a good estimate, the algorithms may not produce the best fit first time. It is also possible to loft a surface through station curves determined by the markers, such as the ones shown in Figure 52. The downside of this method is that, although it creates a good surface match, the control point web is often complex and so it is very difficult to make minor manual adjustments. The most accurate results will come from manually manipulating the control points on a surface to match the plan. However, as this can be very time consuming, it is better to initially utilise the genetic algorithm tools to obtain the general shape of the vessel in question (Couser, 2016). For the ships modelled in this research, it was found that the most efficient method was to use an existing model with a comparable hull shape and manually adjust it to fit the new plan. This means that only a few vessels had to be modelled using the genetic algorithm as a starting point.

For the digital model of *Cutty Sark*, it transpired that there was some discrepancy in each of the views on the lines plan, meaning that the markers were not necessarily in the correct position. Bearing this in mind, the surface was fitted to match the lines as closely as possible, and then adjusted in small increments so that the hydrostatic data was matched to within 0.5% of known hydrostatics in most cases. As this was not always possible for some vessels, other examples where there are significant discrepancies have not been used. The fit of the modelled sections compared to the original body plan is displayed in Figure 53. Curvature was checked to ensure that the surface was fair and there were no abnormalities on the surface. The final model rendered with Gaussian curvature is shown in Figure 54.

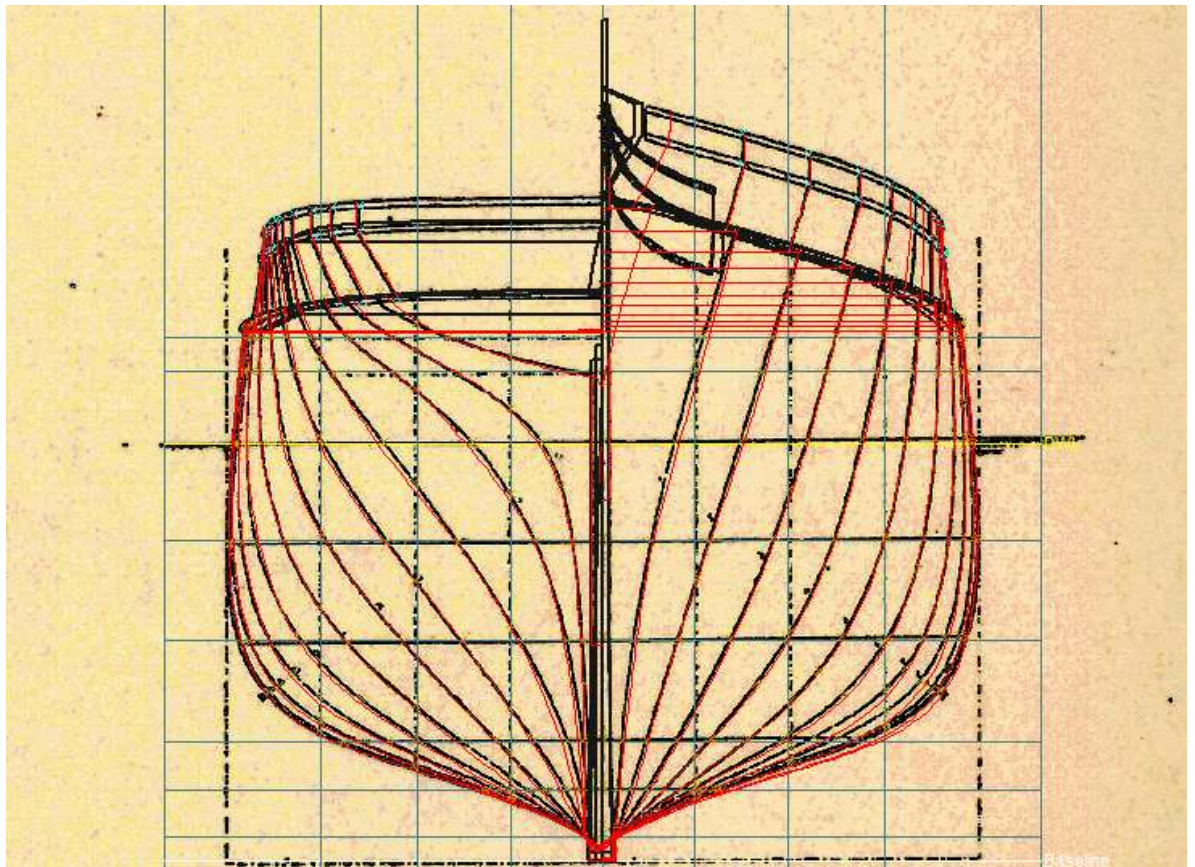


Figure 53: Comparison between modelled sections (red) and original lines plan (black)

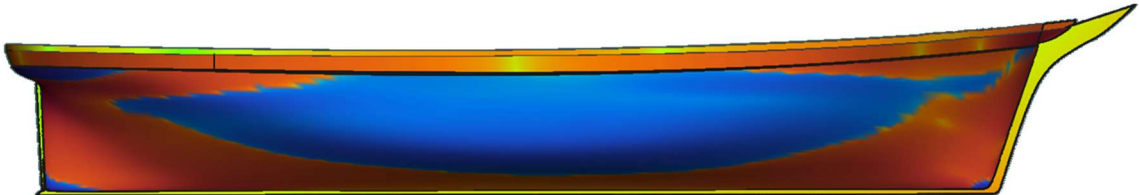


Figure 54: Model rendered with Gaussian curvature to indicate hull fairness

5.2.2 Modelling from a Half-Model

As some of the hull forms considered in this research were only available in the form of builder's half models, a procedure for digitising these ships was required. 3D scanning was selected as the method to be used. This allows the most detail to be incorporated in a short space of time, compared to manual measurements, which would have traditionally been the method of extracting dimensions.

To determine the best practice for scanning half models, a scale half model of *Cutty Sark* was created using the digital model for the design, with a backboard fitted to resemble other half models. The size was limited by the maximum length of material available (1.5 m), meaning that a short section of the stem had to be removed. As this is well above the waterline, this is purely cosmetic and should not make any difference to hydrostatics or any performance results. As models would traditionally have been scaled in imperial units, this was also done for the *Cutty Sark* model, using $\frac{1}{4}$ inch to a foot, or 1:48 scale. The design is shown in Figure 55. The *Cutty Sark*

Selection and Digitisation of Primary Data

half model was manufactured out of SIKA-M700 foam block using a 5-axis CNC machine. Due to the nature of the machining, a small radius was required to form sharp corners, and so there are small deviations from the computer model. An issue also arose during manufacture where the machine left a small ridge on the hull that runs parallel to the keel, meaning that it was necessary to fill the gap and fair it off by hand so as to not leave a sharp edge. This may cause a small error when scanning. However, it is estimated that any error will be less than ± 0.1 mm, which would scale to a total error of ± 4.8 mm and be negligible compared to scanner accuracy. The manufactured model is shown in Figure 56.

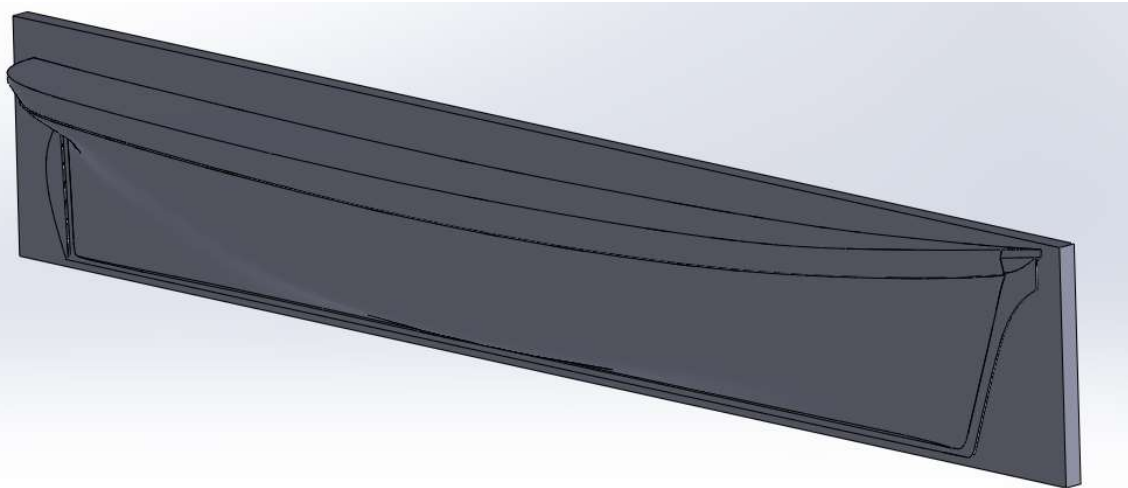


Figure 55: Half model design for *Cutty Sark*



Figure 56: *Cutty Sark* half model

The scanner made available for this research was a first generation *Sense* handheld scanner from *3D Systems*. This is an entry level markerless scanner aimed at reproducing physical objects for 3D printing (3D Systems, 2014). The specification for the scanner gives a spatial resolution at 0.5 m from the surface of ± 0.9 mm, which defines the size of object that may be detected, and a depth resolution of ± 1.0 mm at 0.5 m, which defines the error between the points recorded and the actual surface. Considering that many of the models are in 1:48th scale, this may result in a significant potential measurement error of 48 mm. This scanner has previously been found to produce significantly larger errors than other, more expensive scanners (Dickinson *et al.*, 2016, p. 211). However, if the effect of scanning accuracy on performance estimation can be determined, this may not necessarily be a problem. The primary advantage of this scanner is its portability.

5.2.3 Post-processing of the Scanned Data

Tests were carried out using the *Cutty Sark* half model to determine the best practice when scanning and post-processing using the *Sense* 3D scanner. An example of the output of the scanner is shown in Figure 57. Scans were taken in both light and dark conditions, with minimal difference between the outputs, with the conclusion that lighting conditions have a negligible effect in this case.

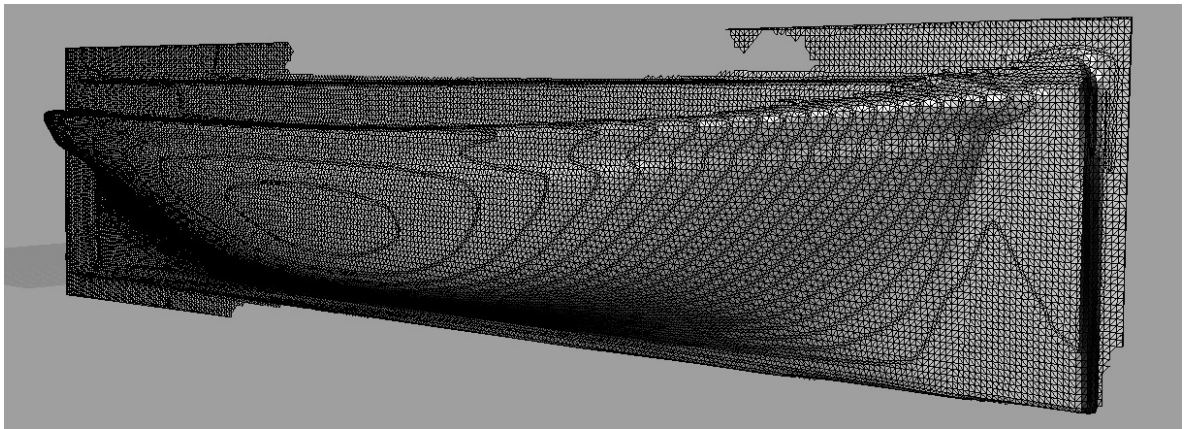


Figure 57: STL file from scanning the *Cutty Sark* half model in the dark using *Sense*TM scanner

It was noted at this stage that the scans struggle to capture finer details. This may be due to the scanner being unable to pick up sharp corners owing to reflections, particularly from the backboard. This causes problems when defining the baseline of the model as the keel is not well-defined by the mesh. As this is important in determining the location of the waterline, the hydrostatics can change significantly depending on where the baseline is taken. It was noted while testing the scanner that the larger the file, the less detailed the mesh was, and so a way of improving the detail picked up would be to scan the model in several parts. The issue with this comes from then combining multiple scans, particularly with the smooth surface typical of ships, which results in minimal reference points.

To extract the hydrostatics, a surface needs to be produced from the mesh. This cannot be done directly, so a surface fitting method is required. One such method is 'draping' a surface over the mesh. This provides a close match, but is heavily dependent on the direction in which the surface is applied. An alternative is to project curves onto the mesh and use these to guide a lofted surface. The issue with this method is that the complexity of a hull form means that the surface will often display distortions where the program is unsure where to apply the surface. If multiple lofted surfaces are used, this manifests itself by means of discontinuities in the surface.

In order to overcome some of the issues described above, if a lines plan for the vessel is available, the scan can be manually altered to ensure smooth surfaces, for example making the keel flat. There is, however, the possibility that this could change the shape of the model incorrectly, and

so this should only be done when there is a plan available. This result of using this technique is shown in Figure 58. This scan was made up of a series of smaller scans to enable a higher mesh resolution. Curves were then projected onto the mesh and a surface lofted through, before being exported to *MAXSURF* and adjusted using the lines plan as a guide. As can be seen, there is still a reasonable error at the bow and stern, which may be due to the large changes in geometry in these areas. The larger error at the bow could be accounted for by the fact that the surface lofting began at the stern.

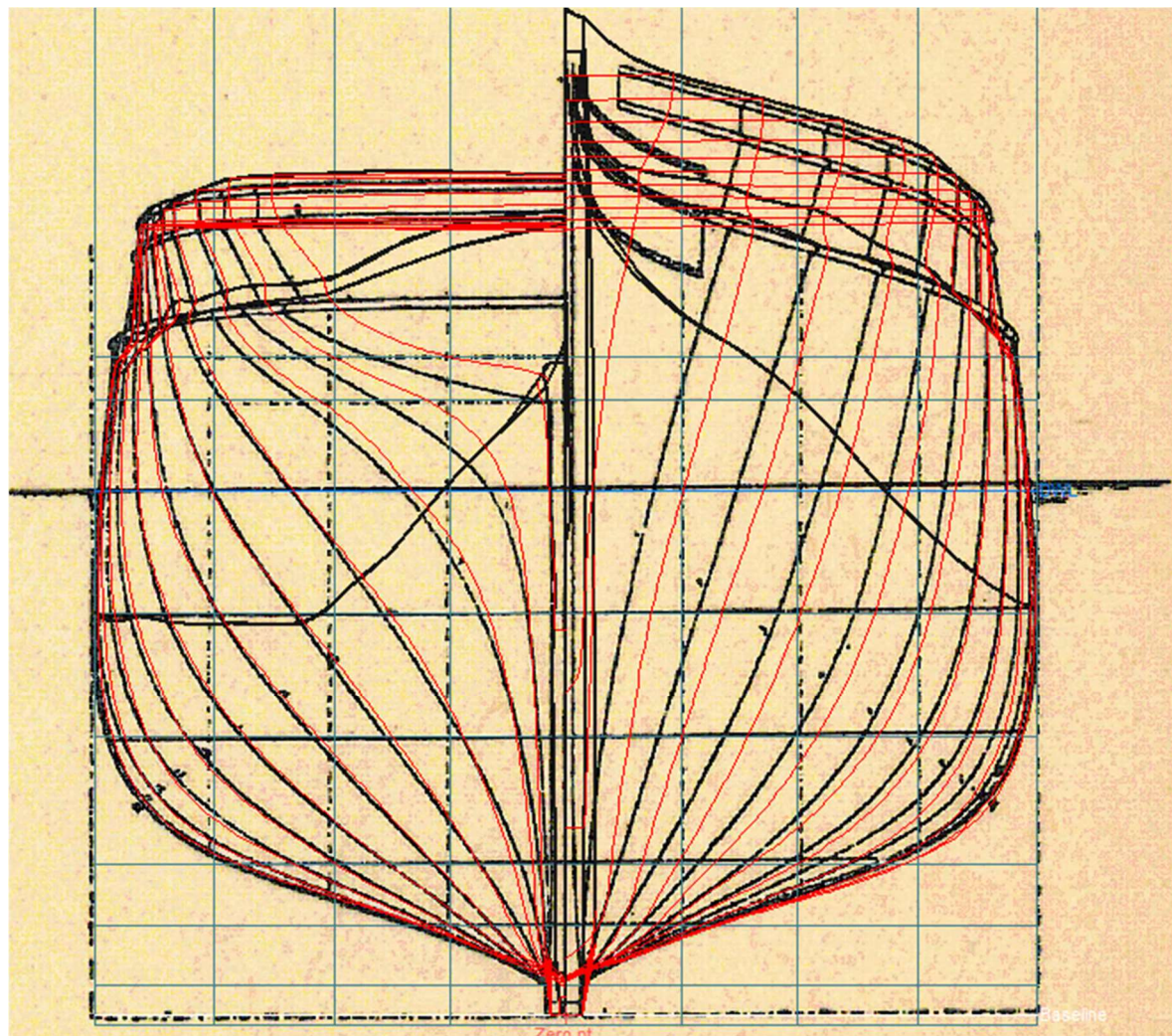


Figure 58: Scanned hull (red) adjusted to fit original lines plan (black)

An alternative method for reconstructing hull forms from a scan is by using a hybrid between the surface lofting method, and the method for generating a digital model from a lines plan. This involves projecting lines onto the scanned mesh as before, as shown in Figure 59. However, instead of lofting a surface through them, the projected curves are then imported into *MAXSURF Modeller*. The surface may then be modelled in *MAXSURF*, using the curves in place of a lines plan. This would reduce any potential errors that could be incurred during lofting and would allow a greater capability for scaling. To test this, the lines were scaled back up to the original length. The beam was then independently scaled to match the given register beam for the vessel, as the

Selection and Digitisation of Primary Data

scan was too narrow. It is not thought that this would make a significant difference to the scan geometry, as the error was minimal (around 20 cm after scaling). The result is a lines plan that fits the length and beam found in literature, with the comparison to the original digital model shown in Figure 60.

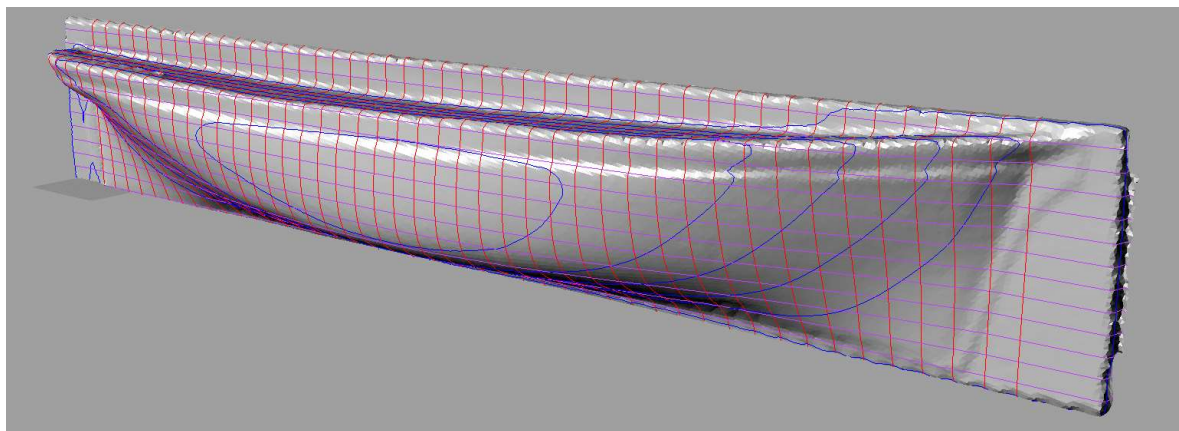


Figure 59: Lines projected onto the half model mesh

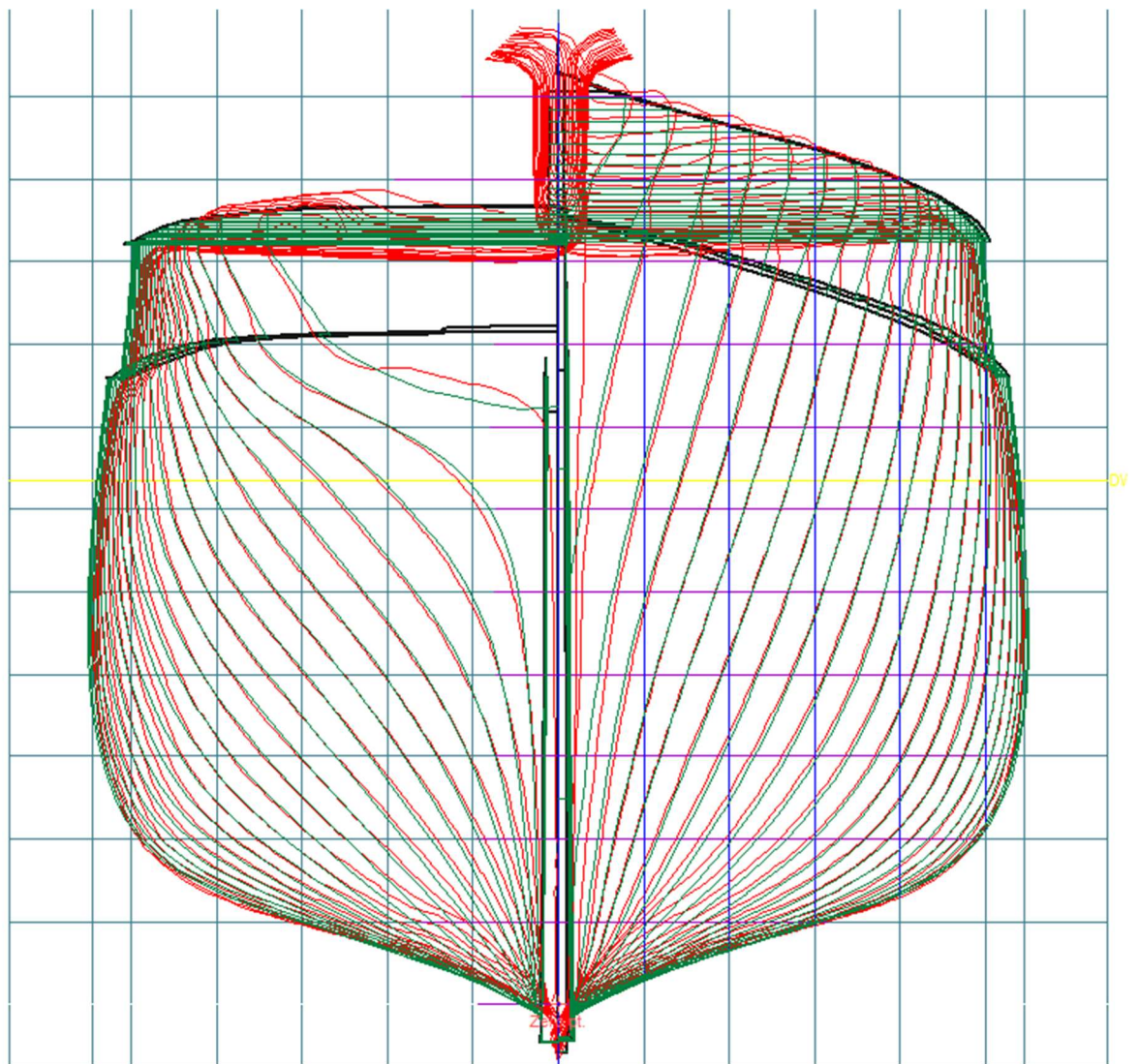


Figure 60: Comparison of *Cutty Sark* digital model (green) with scaled projected scan lines (red)

Selection and Digitisation of Primary Data

Some of the hydrostatics from the surface lofting and scanned lines based methods were compared with those from the original model. These are shown graphically in Figure 61. The closest method to the original is where a lines plan has been generated from the scan, as was indicated by the differences between Figure 58 and Figure 60. As with the surface lofting, it is difficult to define sharp hull details, such as the keel. In the case of the *Cutty Sark*, modelling the keel was made easier by having some knowledge of its dimensions beforehand. In some cases, this information may be available from survey reports or lines plans, highlighting the need for a variety of data sources to ensure data accuracy. It was also noted that knowledge of the principal dimensions, length and beam, are very important for this method, as when scaled the width of the model needed adjusting for *Cutty Sark*.

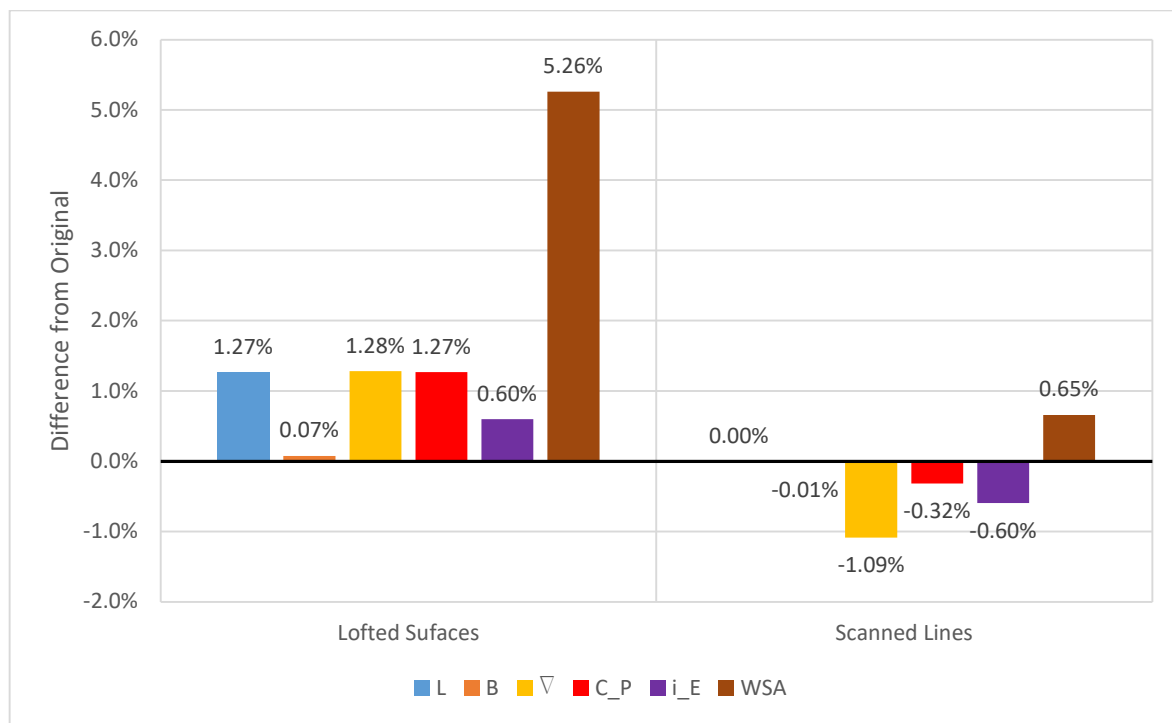


Figure 61: Comparison between particulars for scan post-processing methods

In relation to the sensitivity analyses carried out in Sections 4.2 to 4.6, as the scanned lines method shows the least variation in hydrostatics, it follows that the output ship speed from the VPP should be more accurate. Of the dimensions required for the VPP, the largest error was shown to be for the displaced volume, at 1.09%. The WSA has an error of only 0.65%, which would only have a negligible impact on the VPP output. In Section 4.6.1 it was shown that for an error of less than 5% for ship speed, the error in the dimensions should be less than 8%, indicating that this scanning method far exceeds that requirement.

5.2.4 Resistance Comparisons

Part of the reasoning behind trialling different scanning methods on a known half model was to assess how scan quality affects performance estimations. It is obviously ideal to obtain a perfect

Selection and Digitisation of Primary Data

scan of a model, as there is then little room for error in the performance predictions. However, the level of detail required to get an accurate idea of a ship's performance should be considered in order to reduce unnecessary cost and post-processing.

To quantify the potential effect of scanning and post-processing on overall resistance results, the hydrostatics of the models compared in the previous section were input into the module of the VPP used to calculate resistance with the Holtrop method. As regression methods are dependent on these parameters, it is expected that errors in hydrostatics would have an effect on the results. The difference between the scanned models and the original is shown in Figure 62 between 1 and 18 kn, which covers the expected range of attainable speeds for *Cutty Sark*. As would be expected with the much larger WSA, the lofted surfaces model displays a much higher error in resistance relative to the original, particularly at lower speeds where frictional resistance is dominant. The large "hump" visible in the lofted surface curve also indicates that there is a greater amount of wave-making resistance present for this model. The scanned lines model is slightly finer, as indicated by the C_p and half angle of entry, which will reduce the wave-making potential of the hull and hence shows less of a variation. It must be noted that the hump only constitutes around a 0.5% deviation from the expected trend, or around 0.5 kN in real terms and so is essentially negligible.

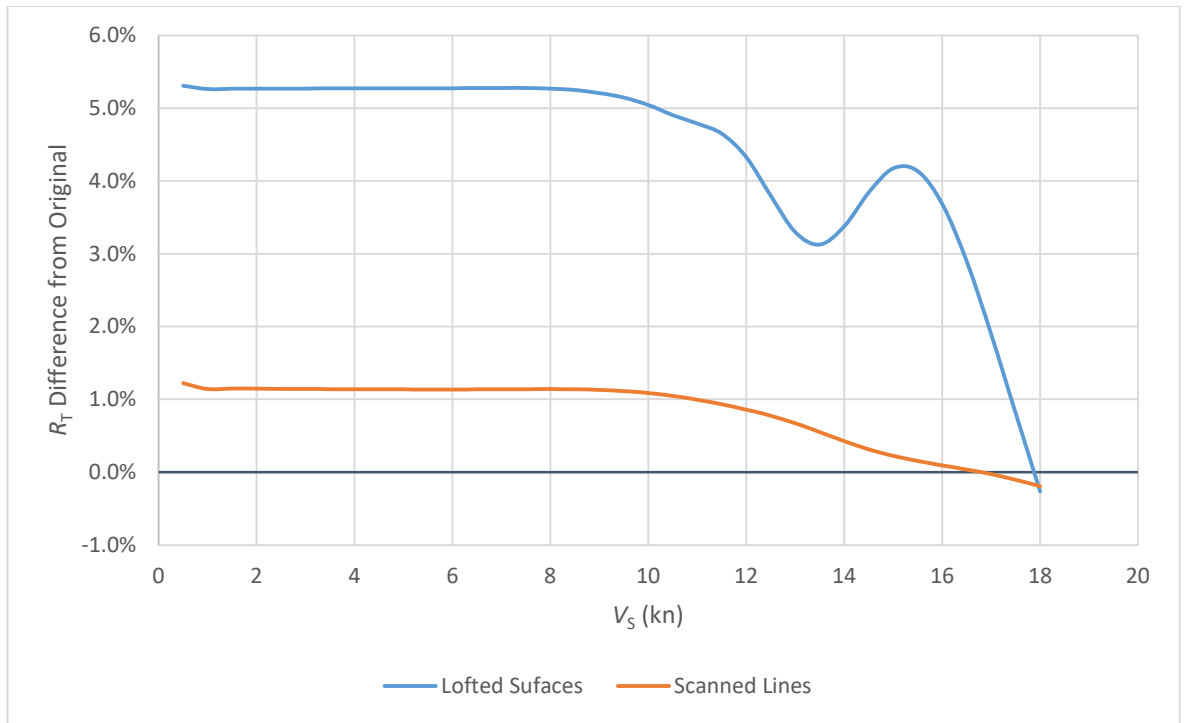


Figure 62: Comparison of R_T for the scanned models relative to the original

The speed output from the VPP for each digital model confirms this conclusion. This was analysed by considering nine different sailing conditions described in Table 16. All of these conditions have a fixed wind speed and angle, with the exception of condition 1, which calculates the optimum

wind angle for a given wind speed. All conditions are set to find the optimum bracing angle for the sails. Figure 63 shows clearly that the model based on lofted surfaces displays a much larger error than the one based on scanned lines relative to the original digital model. This is particularly true for the lower speed cases, indicating that the majority of the error is arising due to the WSA, which has the highest impact at low speed.

With the majority of the speeds generated from the scanned lines based model being within 0.5% of the original, it is clear that this is the best method for post-processing scans. However, as there is still some error, in the cases where there is a lines plan available these will be used to create the model in the final analysis. A comparison between the scans and lines for these ships will be given in Section 5.6.

Table 16: Wind conditions for comparing speeds of scans against original

	1	2	3	4	5	6	7	8	9
V_T (kn)	30	25	25	15	5	40	15	20	15
γ (°)	Free	130	150	130	130	170	70	140	90

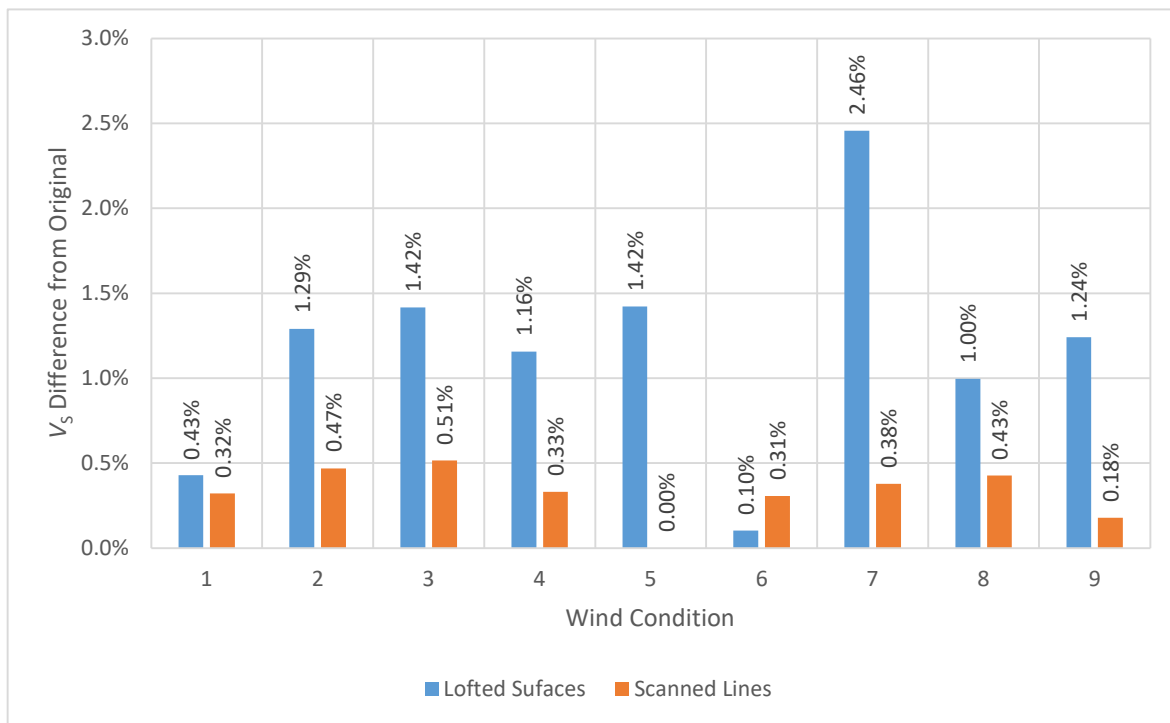


Figure 63: Difference between V_s of Cutty Sark between the original and the scanned models

5.2.5 Reliability of Scanned Hull Forms

A number of the ships to be investigated have both a lines plan and a half model available. These ships have been digitally modelled twice, using the lines plan and the scan separately. If it is assumed that the lines and the half model match, the error introduced by the scanner can be seen in both the dimensions and the speed output. This was done for nine ships in total.

One of the ships examined, *Schomberg*, produced a very large error, particularly in the beam, which was found to be over 10% smaller in the half model. MacGregor (1988, pp. 193–194) discusses this model in detail, comparing the lines traced from the builder's plan with dimensions taken off the half model. He also finds that the half model is a different shape, as shown in Figure 64, indicating that in this case it is the half model and not the scanner introducing the error. Therefore, this vessel is not included in the comparison between the lines and scans.

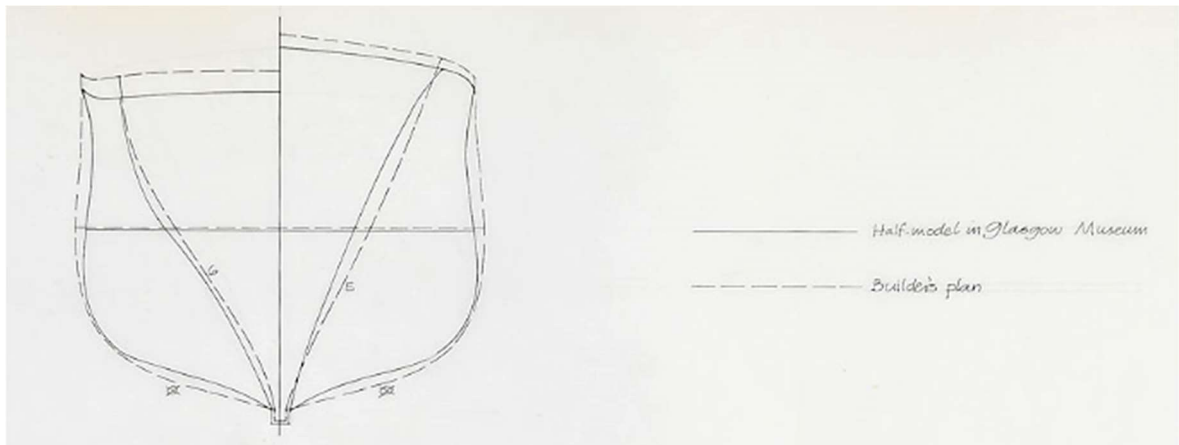


Figure 64: MacGregor's comparison of lines and model of *Schomberg* (Image: Brunel Institute)

Another of the half models that is potentially unreliable is that of *Sea King*, later known as *CSS Shenandoah*. Multiple designs were put forward for this ship, with the lines attributed to the designer William Rennie (MacGregor, 1988, pp. 222–223). The model is known to have come from the yard of Alexander Stephen & Sons, who built the ship, but it is unknown whether it is of Rennie's design, or Stephen's own suggestion. Stephen's design was supposedly sharper, but the difference between the scan and the digital model taken from the lines indicate that the lines are finer, with a C_p of 0.716 and 0.689, and half angle of entry of 20.5° and 20.4° respectively. This indicates that the model is probably of Rennie's design.

With these two vessels discounted due to the uncertainty about the relationship between the lines and the model, the remaining seven ships highlight areas in which the scan accuracy varies. The dimension with the least variation is the waterline length, L_{WL} , as might be expected since the length between perpendiculars, L_{BP} is used for scaling. The dimension that causes the biggest issues is the overall beam. This is consistently less by 1.5–6.3% for the scans. In Sections 4.2 to 4.6, the beam was shown to have a negligible effect on the hydrodynamic side force, with a minor effect on resistance and the overall ship speed. The other particulars that show a high difference are the C_p and WSA. Both of these were shown in Section 4.2 to have a large effect on the resistance. Despite this, the difference in speed between the two methods is small. The average percentage differences between particulars are shown in Table 17.

Table 17: Average difference between parameters of lines and scan based models

	Average	Standard Deviation
L_{WL}	-0.36%	0.77%
B	-2.91%	1.89%
∇	-0.07%	1.61%
C_p	1.10%	1.88%
i_E	-0.14%	4.01%
WSA	-0.69%	2.51%
V_s (Condition 1)	-0.70%	0.86%

A comparison of the maximum attainable ship speed in 30 kn of wind for each ship shows that the lines based digital model consistently gives a slightly higher speed, with a difference ranging between 0.1 and 2.1%, as shown in Figure 65. As the scan based model requires more steps to create and hence has more scope for error, in these cases the lines plan is considered the most reliable source. However, as the difference between the speeds is still relatively small (< 0.5 kn), it is still reasonable to use a scan for those ships that do not have a lines plan.

Another point to consider is the source of the lines plans. In at least four cases the lines were taken off the model. In the case of *Stornoway*, the origin of the lines are unknown, but the orientation of the plan indicates that they were taken from the model, which displays the port side, as opposed to the usual starboard side. Only the lines for *Norham Castle* and *Hurricane* are from the original or a trace of the builder's plan. These two vessels show the most similarity between the dimensions and the speeds, indicating that there may be an error introduced in the other ships when the lines were taken off. This is understandable as this would have been done by hand, and so only a certain level of accuracy can be achieved. In cases where the lines and models differ, there is also the potential for undocumented changes to the design between the model and the lines, similar to the case for *Sea King*, where two designs were proposed. Due to the uncertainties around these variations, it is impossible to quantify exactly how much error is introduced between a model and a plan.

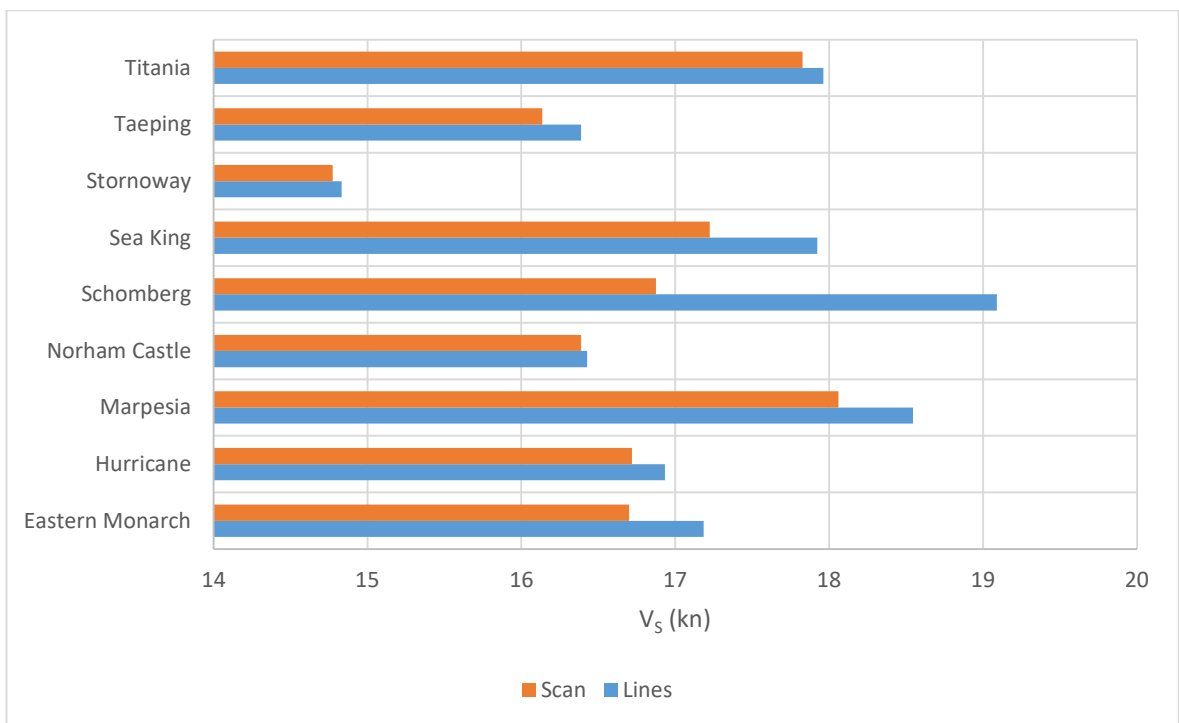


Figure 65: V_s for lines based models and scan based models in sailing condition 1

The effect of reflective surfaces was considered using a smaller half model of an unknown vessel. This was scanned with the *Sense* scanner, and with a *Faro Arm* which was temporarily made available for this research. The high precision *Faro Arm* scanner has been used previously for archaeological purposes (Tanner, 2013a, p. 137). For a 1.0 m model this will typically produce an error of around ± 0.076 mm (MacCarthaigh, 2008, p. 2), which would equate to a 3.65 mm total error. This is evidently much better than the *Sense* scanner, although given the size of the ships in question, and the sensitivity of the VPP as discussed in Section 4.7.1, it was decided that the *Sense* scanner would be the more cost effective solution.

The unknown half model, unlike the *Cutty Sark*, has been varnished and so has more potential for errors arising from reflections, which can form a “ghost surface” (Wang and Feng, 2016, p. 35). Both scans were post-processed and the hydrostatics compared on the same waterline. The majority of these were within 1% of each other; however, WSA and the midship sectional area, A_M were both over 2% different. The C_P also showed a difference of 1.77%. If we were to assume that the *Faro Arm* scan is a perfect representation, then this may be indicative of the error inherent in the *Sense* scanner, rather than error due to reflection as it is comparable with some of the errors given in Table 17. However, care should still be taken when scanning reflective surfaces.

5.3 Calculation of Sail Areas

In order to employ the regression equations developed by the *HMS Victory* simulation project (Leszczynski *et al.*, 2005), sail areas for the individual sail categories are required. Sail plans are available for a number of ships from throughout the century and so for these vessels this

Selection and Digitisation of Primary Data

calculation is relatively simple. In some cases the plan has been reconstructed based on spar dimensions or mast-making rules of the time, as drawn by experts such as MacGregor (1988, pp. 9–10). As a complete reconstruction of each sail plan would be very time consuming and require an intimate knowledge of rigging, this research will use a simpler method to estimate the areas and centres only.

Sails can be broken down into six main categories: driver, jib, mizzen, main, fore and stunsail. As equations are only provided for driver, jib, mizzen and main, the fore sails are treated as main sails. Stunsails, which are generally attached to the edge of the square sails on the fore and main masts, are typically only used in light winds (Uden and Cooper, 1980, p. 496) and are not considered for this research as there is currently no sail force data for them. Staysails between the masts are considered as jibs as their shape is usually similar. Where a quadrilateral fisherman staysail is used, this has also been considered as a jib. This is because as a fore-and-aft sail with no supporting booms, it was considered to be closest to a jib despite the difference in shape.

Once the sail types on a vessel have been identified, the total sail area and centre of each sail type may be calculated from the existing plans. Figure 66 shows the sail plan of *Cutty Sark* with the sails marked up in *AutoCad* to show how this process works. Each sail type is given a different colour and layer on the drawing for clarity, and by defining the individual sails as regions, an estimation of areas for each sail type and centre of effort (CE) may be extracted.

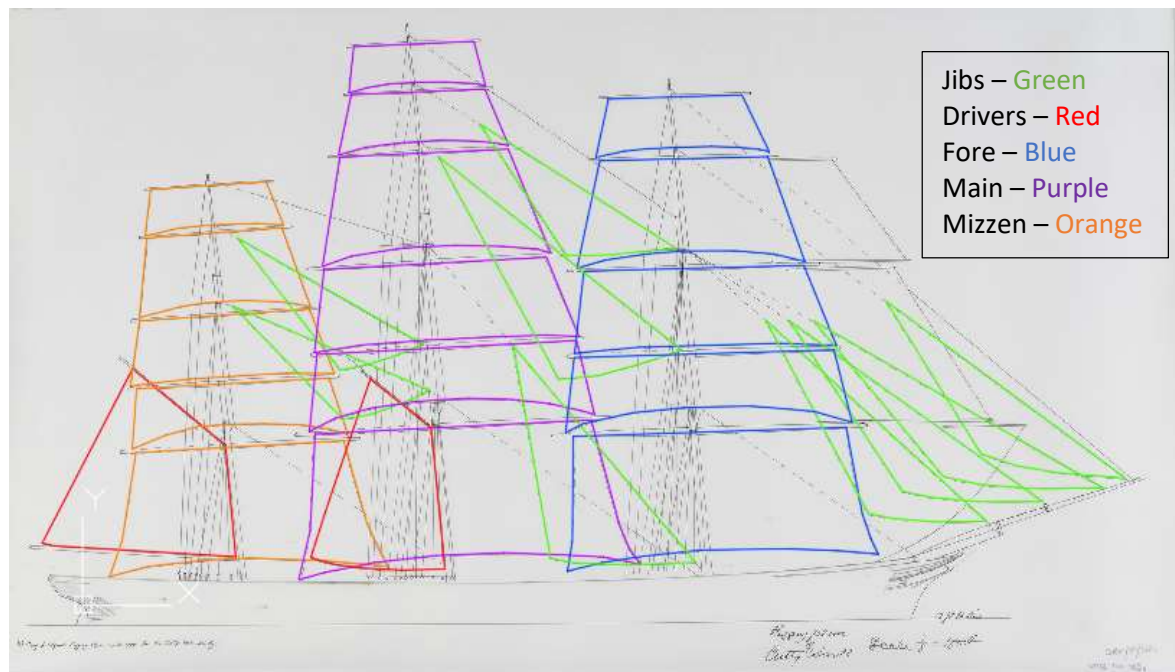


Figure 66: Marked up sail plan of the *Cutty Sark* (Sail Plan courtesy of the Brunel Institute)

For those vessels that do not have a sail plan available, a method of estimating the area and CE is required. This is achieved by assuming a relationship with certain ship parameters. The known sail

areas were therefore used to determine a suitable relationship. Total sail area is primarily dependent on the waterplane area (A_{WP}), as this determines the stability of the vessel (Oliver, 2007, p. 112). A naval architecture textbook from 1877 also indicates that it may have been common practice to base the sail area on the waterplane area (White, 1877, p. 488), although the text itself suggests using the displacement to scale the area from similar ships. The total sail area for a ship rigged vessel is given as between three and four times the waterplane area. However, based on the sail plan areas calculated for this research, it appears to be nearer 4.2. Total sail area is also dependent on the number of masts, which is a factor omitted in the above source, and also whether the vessel is sail or steam powered. A number of additional sail areas from plans with no corresponding model or lines were also calculated to increase the reliability of the estimation. These points have no method of extracting the waterplane area or the displacement, and so this has been simplified to a relationship between length between perpendiculars and beam, which are the main dimensions contributing to waterplane area. A measure related to L_{BP} , B and the number of masts (n) was proposed, giving:

$$f(L, B, n) = L^{1/2} B n^{1/4} \quad (12)$$

Plotting these values against the sail areas produces a good linear relationship, as shown in Figure 67. This indicates that this method will be suitable as a measure for estimating sail areas for those vessels without sail plans. A linear regression line was therefore fitted to the data, as shown in Figure 67, resulting in equations (13) to (16), which may be used for estimating the areas of the individual sail types.

The majority of the vessels considered for this analysis were ship-rigged, meaning that all of the masts are rigged with square sails, as opposed to barque rigged where the mizzen has fore-and-aft sails. It was found, however, that when plotted in the way previously described, the sail areas of a barque-rigged vessel are similar to those of a ship-rigged one. This means that the calculation may remain the same, with only the lack of mizzen sails on a barque needing consideration. It was also found that a closer relationship for the fore and main sails was created when they were combined. This does not cause any issues as they both use the same sail force calculation.

$$A_{S,Jib,Sail} = 6.3796f(L, B, n) - 141.02 \quad (13)$$

$$A_{S,Driver,Sail} = 12.381f(L, B, n) + 37.024 \quad (14)$$

$$A_{S,Mizzen,Sail} = 3.1496f(L, B, n) - 42 \quad (15)$$

$$A_{S,Main+For ,Sail} = 16.321f(L, B, n) - 649.93 \quad (16)$$

Selection and Digitisation of Primary Data

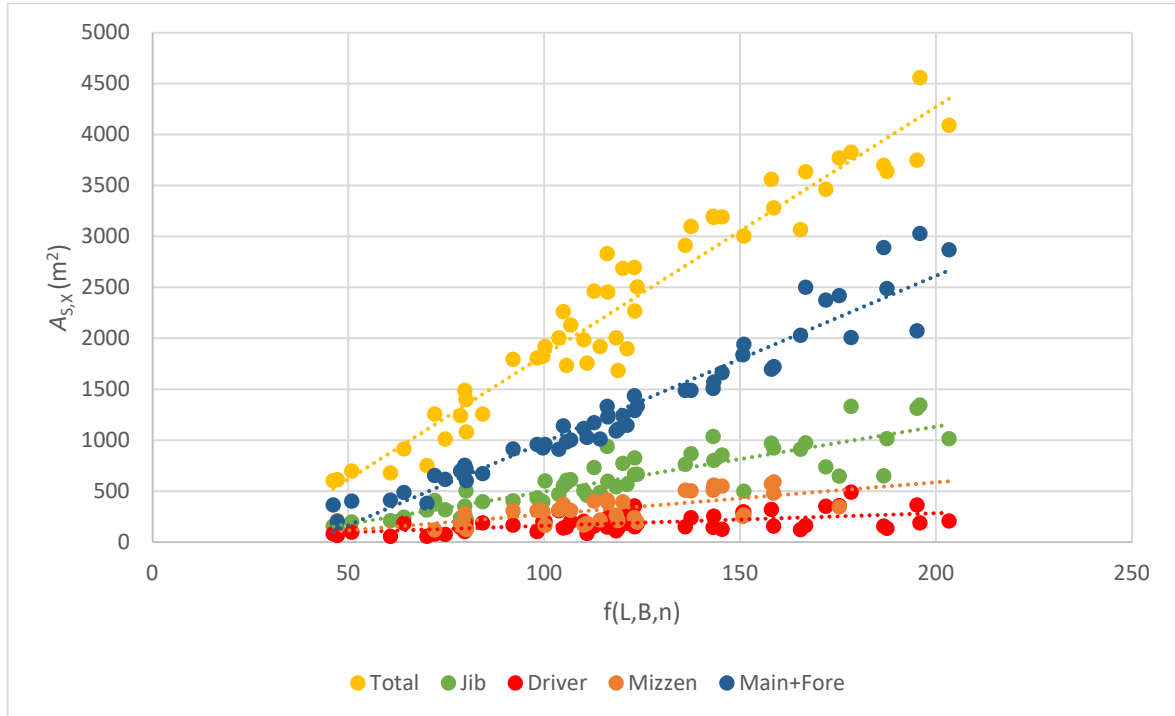


Figure 67: Sail area estimation of sailing vessels

Steam ships, however, are primarily fore-and-aft rigged, which as discussed in Section 2.10 should be treated with caution with the sail force calculations used. As there are so few square rigged examples, there have been no restrictions placed on the type of rig for steam ships. This means that a separate set of equations have been developed for estimating the sail areas of steam ships. It was found that for a good linear relationship in this case, it must be assumed that the sail area is only dependent on the ship length. These estimations are given in equations (17) to (20) and shown graphically in Figure 68.

$$A_{s,Jib,Steam} = 2.939L - 21.989 \quad (17)$$

$$A_{s,Driver,Steam} = 5.7162L - 45.496 \quad (18)$$

$$A_{s,Mizzen,Steam} = 0.5006L + 53.426 \quad (19)$$

$$A_{s,Main+Fore,Steam} = 3.8037L - 50.61 \quad (20)$$

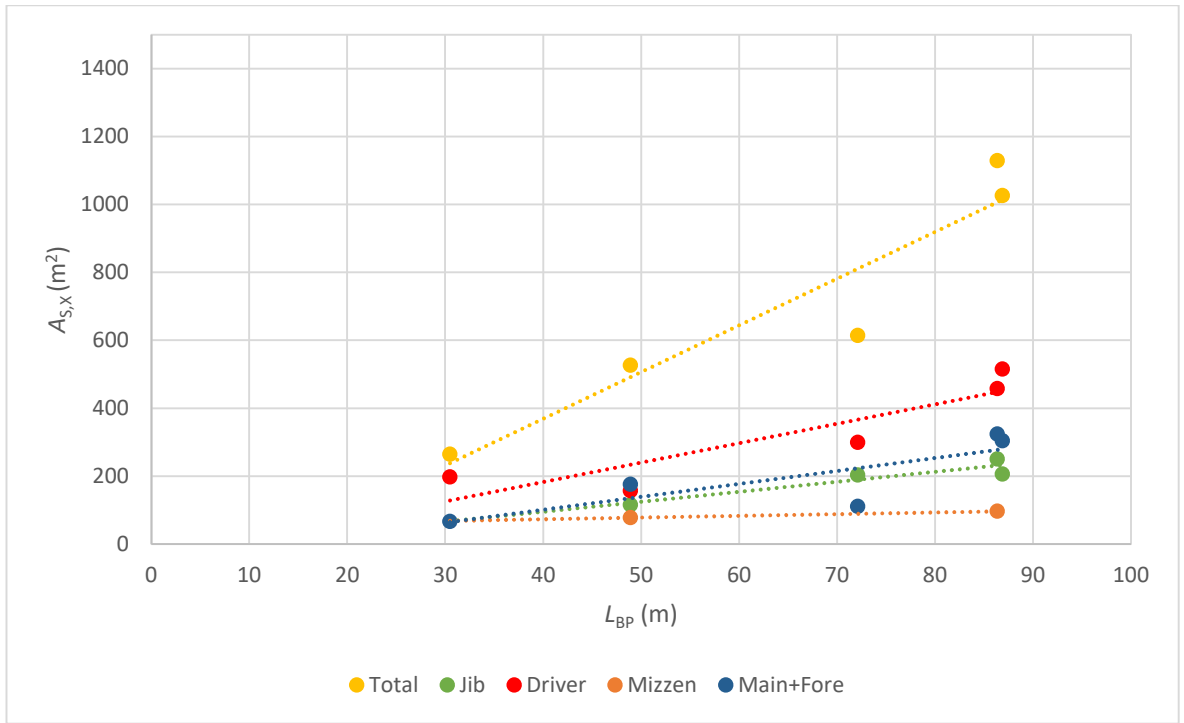


Figure 68: Sail area estimation of steam-powered vessels

The centre of area of the sails, which are required for calculating the heeling moment as well as the VCG of the vessel, are given in Figure 69 and Figure 70. The equations required for the estimate are presented in equations (21) to (24).

$$CE_{Vertical,Sail} = 0.0798f(L, B, n) + 9.0088 \quad (21)$$

$$CE_{Vertical,Steam} = 0.0813f(L, B, n) + 6.3443 \quad (22)$$

$$CE_{Long,Sail} = 0.248f(L, B, n) + 5.8282 \quad (23)$$

$$CE_{Long,Steam} = 0.4121f(L, B, n) - 2.3659 \quad (24)$$

Selection and Digitisation of Primary Data

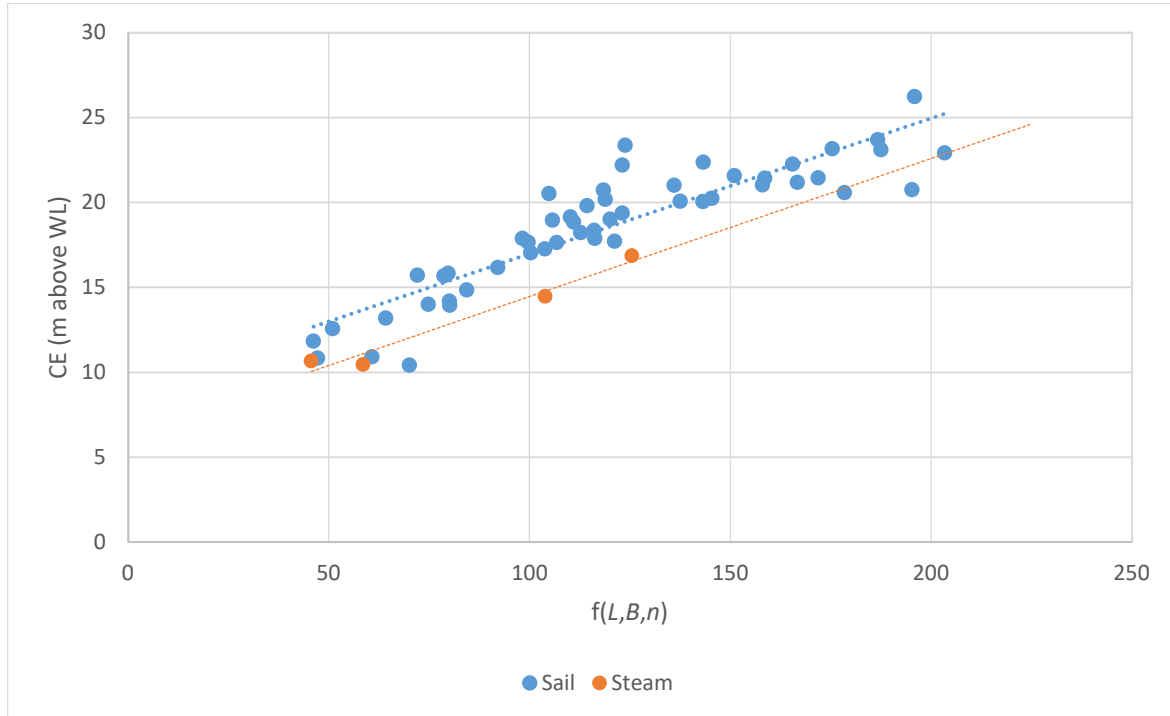


Figure 69: Vertical centre of sail area above load waterline

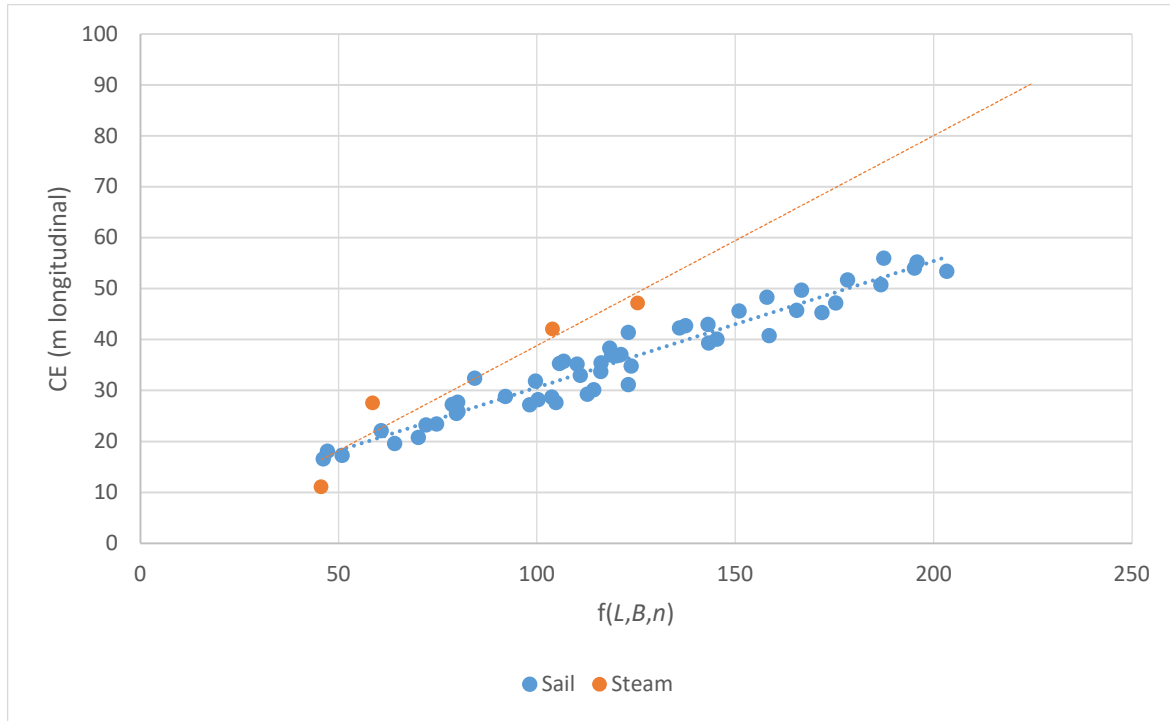


Figure 70: Longitudinal centre of sail area from aft perpendicular

5.4 Estimate of Centre of Gravity

The VPP requires the balance of heeling moment with righting moment. This is used in estimating heel angle under sail, and has a small effect on aerodynamic side force. Heeling moment is calculated by multiplying aerodynamic side force by the distance between the centre of area of the sails and the centre of lateral resistance of the hull. The centre of area of the sails can be found based on the area calculations described in Section 5.3, and the centre of lateral resistance

is assumed to be positioned at half of the load draught, as this was found to consistently be the approximate location for the vessels in question. In order to obtain righting moment, the VCG is required. This is dependent on the distribution of masses in the ship and may not be found in literature and so a method of calculation is required.

As described in Section 2.11, there are two main ways in which the VCG of a ship may be determined: through an inclining experiment, or through calculation of individual masses and centres within the vessel (Tanner, 2013b, p. 87). Due to the nature of this research, inclining experiments are not possible, as they would require an accurate full-scale reconstruction of each vessel. A detailed survey of weights and centres would also be challenging for vessels of this size, as this would normally involve creating a digital model with a high level of detail, which would only be practical for investigating a small number of ships. In addition to being time consuming, for most of the vessels numerous assumptions are required where the literature does not provide enough detail. In order to overcome these issues, it is proposed that estimates for some of the larger weights are produced. The methods adopted for obtaining these estimations are discussed in Sections 5.4.1 to 5.4.4.

It should be noted that many of the masses considered are estimates and so the overall VCG might not be an accurate representation of the original vessel. However, by treating each vessel in the same manner, a direct comparison is possible. In addition to this, it was also noted in Section 4.5.3 that errors in the estimation of VCG had a negligible effect on ship speed, meaning that only the heel angle output must be treated with caution in relation to the VCG.

5.4.1 Structure

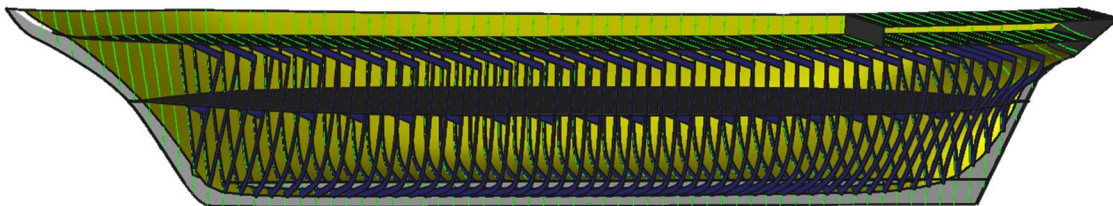
The structure of a ship makes up a majority of the lightship mass. Where possible, an estimation of hull weights and centres can be calculated based on data from survey reports. If the structural mass from enough ships can be obtained from these, then it is possible to estimate the weights and centres of those ships with little or no information available, in a similar way to the sail area estimations discussed in Section 5.3.

To utilise the information from survey reports, a structural model of each ship was created using *MAXSURF Structure*. Part of one such report for the ship *Acasta* (1845) and the corresponding digital model are shown in Figure 71 and Figure 72 respectively. This method allows some of the larger masses to be calculated, including frames, stringers, decks and hull plating or timber. As the survey reports provide details such as frame spacing, thickness and size of the flange and web, a reasonably detailed model may be produced. The total mass and centre of these is calculated by assigning materials to the individual components, many of which are listed in the report.

No. 1024 Survey held at	Shetland	Date 21 st February 1845	Reg. 26 Feb 1845
on the	Shetland	Master	Robert Webster
Tonnage 385 ^{1/4}	Built at	Shetland	When built 1845 Launched 23 rd Jan 1845
327 ^{1/4}			
By whom built Alexander Hall in C.		Owners	Benjamin Mair
Port belonging to Shetland		Destined Voyage	Cape of Good Hope
If Surveyed Afloat or in Dry Dock		At	At Building

Scantlings of Timber.	Length aloft	Feet. Inches.	Extreme Breadth	Feet. Inches.	Depth of Hold	Feet. Inches.
Timber and Space	each	24				
Floors	sided	10 ^{1/2}	Moulded	11 9		
1 st Foothooks	"	10	"	9 ^{1/2} 8		
2 nd Ditto	"	9 ^{1/2}	"	8 1 ^{1/2}		
3 rd Ditto	"	"	"			
Top Timbers	"	8 ^{1/2}	"	7 ^{1/2} 5 ^{1/2}		
Deck Beams ... N°. of 28	"	9 ^{1/2}	"	9 ^{1/2} 5 ^{1/2}		
Hold Beams ... N°. of 19	"	12	"	12 8 ^{1/2}		
Keel	"	12	"	13		
Kelsons	"	12	"	18		

Thickness of Plank.	Outside.	Inside.	Thickness.
Keel to Bilge	3 ^{1/2}	Foot Waling	3
Bilge Planks	5	Bilge Planks	4 ^{1/2}
Bilge to Wales	3 ^{1/2}	Ceiling in Flat	3
Wales	5	Ditto Bilge to Clamp	3
Topsides	2 ^{1/2}	Hold Beam Clamps	5
Sheer Strakes	2 ^{1/2}	Deck Beam Ditto	4
Plank Sheers	3 ^{1/2}	Ceiling 'twixt Decks	2 ^{1/2}
Water-Ways	7	Hold Beam Shelves	5
Upper Deck	3 ^{1/2}	Deck Beam Ditto	5

 Figure 71: Principal scantlings for *Acasta* (1845) (Courtesy of Lloyd's Register)

 Figure 72: Structural model of *Acasta* based on the Lloyd's Register survey report

The downside of the survey reports is that, although they supply nearly all of the scantlings required, they do not provide locations of parts. For example, a report will list the number of decks, but not deck height. This issue may only be solved where there is a midship section drawing available, as the height of the decks may be scaled off this. The same applies for longitudinal stringers. The exact location or number of frames is also not usually provided, however it is assumed that one will lie at amidships, therefore the locations and number of other frames can be calculated from the frame spacing. It is also assumed that the frames will begin and end on a deck beam, unless otherwise specified, which for iron or steel framed ships are normally placed periodically on frames. In the *Cutty Sark*, for example, there is a deck beam on every third frame. For wooden ships this has also been assumed to be the case, although as the frames and beams are thicker it is unlikely to be completely accurate. In some cases, like in Figure 71, the number of beams has been specified. In this case it is also assumed that the beams are equally spaced on frames unless otherwise specified.

For two steam ships, a structural mass was found to have already been calculated: *SS Great Britain* and *Alexandra*. *SS Great Britain* was modelled according to the lines plan and the structure

modelled. As *SS Great Britain* was not classed by LR, there is no survey report, but structural details can be found in literature (Corlett, 1975, pp. 44–51). The digital model for *Alexandra* was based on a half model. As the structural modelling does not contain all details and is focused on frame, stringer, hull shell and deck masses, the estimate produced should be below the actual lightship mass, which includes details such as fastenings. This means that an estimate of additional masses can be calculated as a percentage using the difference between the estimated and actual mass of these ships. Due to time limitations for this research, calculating the exact location of the centre of the additional masses is not possible. It is therefore proposed that they will be evenly distributed throughout the vessel and the centre will be equivalent to the centre of volume of the hull.

Modelling the structure of *SS Great Britain* gives a total lightship mass of 1250 tons, which gives a 12.8% difference to the actual value of 1410 tons. For *Alexandra*, the difference was 13.9%. In addition to these values, a lightship mass estimate was produced for the wooden sailing ship *Australia*, which had the draught marks at launch marked on the plan. If this is assumed to be the lightship condition without most of the rigging, then the ratio between the calculated weight and the actual weight would be 11.6%. Although these make up a small sample of the dataset, it appears that there is a relatively consistent variation of around 13% between the calculated structural mass and the actual structural mass. It is therefore proposed that an extra 13% should be added onto the structural mass to account for fittings and fastenings.

For those vessels where there is no survey report or structural data available, an estimation may be made based on other vessels. This was achieved by means of a linear regression line based on the L_{BP} and moulded depth (D_M) of the vessel, which were found to be most representative of a ship's structure. The calculated masses have been split into different materials and are shown in Figure 73. As there was only one data point for a steel ship, the estimations for steel vessels are based on the iron equation. The lightship mass estimates are therefore given as:

$$M_{Wood} = 2.9113x - 45.824 \quad (25)$$

$$M_{Composite} = 4.2197x - 313.73 \quad (26)$$

$$M_{Iron} = 4.5563x - 322.9 \quad (27)$$

Where:

$$x = L_{BP} D_M^{0.5} \quad (28)$$

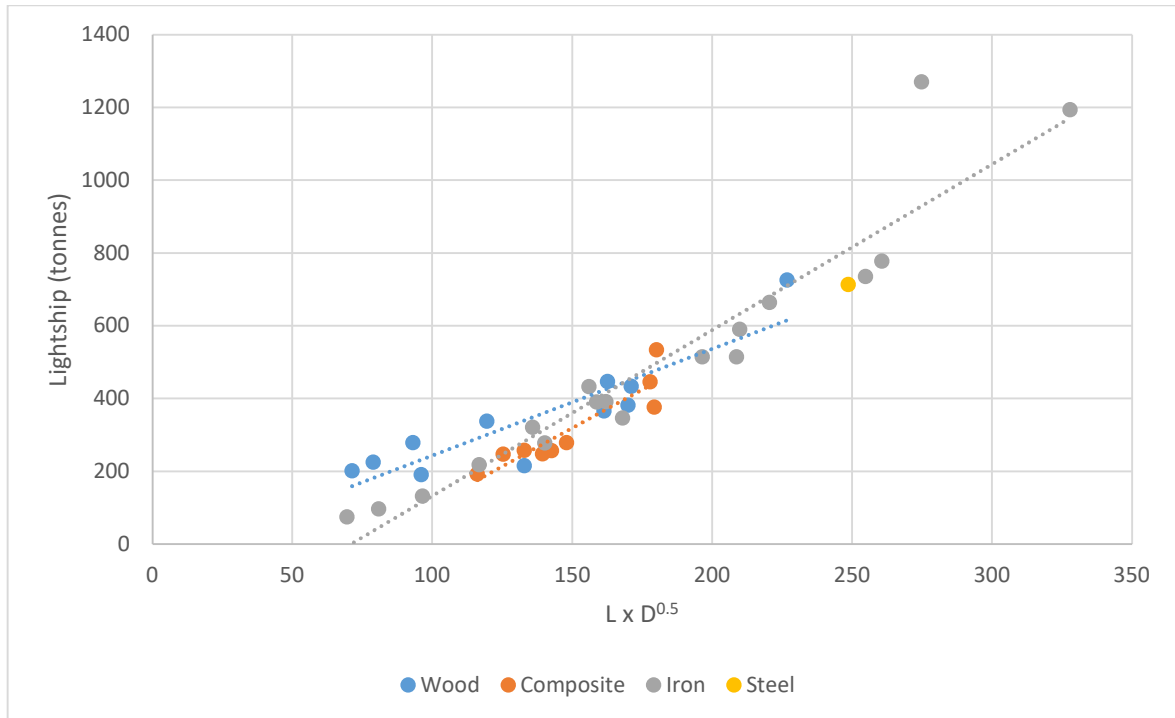


Figure 73: Structural weight estimations based on survey reports

The position of the centre of mass for the structural weights was found to be independent of construction material. With a linear relationship these can be estimated by:

$$VCG = 0.5631D_M + 0.3803 \quad (29)$$

$$LCG = 0.5007L_{BP} - 0.7491 \quad (30)$$

The survey reports also provide details on the anchors carried. Although this is a comparatively small mass item, not exceeding 10 tonnes, these are included in the mass calculation as it is a known mass. In the cases where there is no data, the anchor weight is estimated relative to ship length. The anchors will be positioned at the stem on the main deck.

5.4.2 Rig

The mass of the rig has been based off the sail plan where possible, with supplementary information from survey reports. A generic mass of sail cloth has been assumed from canvas masses given by White Stevens (1894, p. 103) of 38 lb/yd² (14.41 kg/m²). The volume and surface area of masts has been calculated where possible from the sail plan and a generic density and thickness applied where appropriate. In a couple of instances, mast and spar dimensions were included in the survey report, and so these have been used accordingly. The assumed plate thickness for iron and steel masts are based on these reports. Wooden masts were assumed to be made of pine with a density of 0.51 tonnes/m³ (Engineering Toolbox, 2004). Iron and steel masts were assigned thicknesses of 11.0 mm and 7.6 mm respectively based on information found in survey reports, with densities of 7.352 tonnes/m³ and 7.850 tonnes/m³ (Benham, Crawford and

Selection and Digitisation of Primary Data

Armstrong, 1996, p. 613). The mass of masts for those ships without a plan has been estimated based on the total sail area ($A_{S,T}$), as shown in equations (31) to (33) and Figure 74. The centre of mass for the masts and sails combined is based on the centre of areas from the sail plans given in equations (21) to (24), and is assumed to lie on the centreline of the ship. An allowance of 20% has been added to both masses to account for rigging and other masses that have potentially been missed, as well as spare spars that would typically have been carried in case of emergency (Stevens, 1894, pp. 622–623).

$$M_{Rig,Wood} = 0.0159A_{S,T} - 5.3115 \quad (31)$$

$$M_{Rig,Iron} = 0.0147A_{S,T} + 5.0384 \quad (32)$$

$$M_{Rig,Steel} = 0.0049A_{S,T} + 20.304 \quad (33)$$

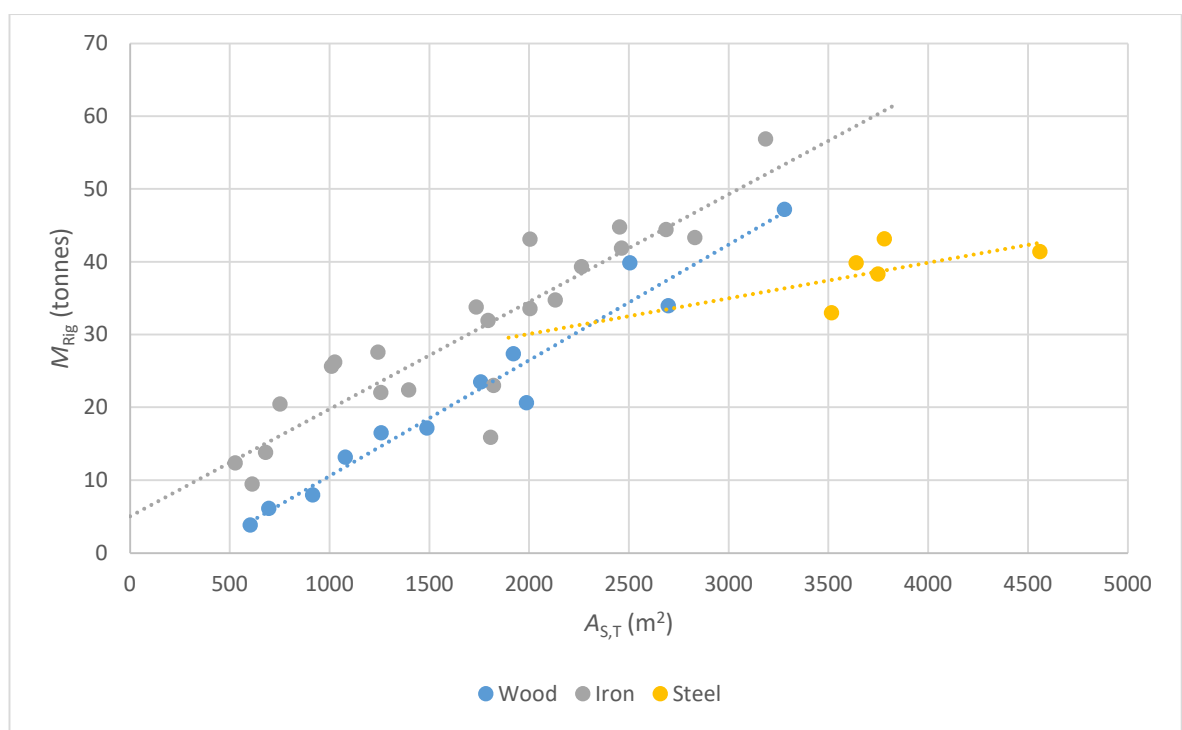


Figure 74: Estimates of mast mass based on plans and survey reports

5.4.3 Machinery and Coal

In a few cases, the masses of the machinery and coal for steam ships have been given in literature. Where this information has not been given, these masses have been interpolated based on the values from literature for ocean going vessels set against the nominal horsepower, NHP. Although NHP is based on the cylinder size and so is not a representation of actual horsepower, it does give some idea of the engine size. Unfortunately, even with a selection of over 1000 ships, this dataset is very limited, with only three points for machinery mass and only 16 for coal. These points are shown in Figure 75. It has been assumed that the relationships are linear. Using these points the relationships are as follows:

$$M_{Coal} = 1.0431NHP + 370.17 \quad (34)$$

$$M_{Machinery} = 0.4395NHP + 112.29 \quad (35)$$

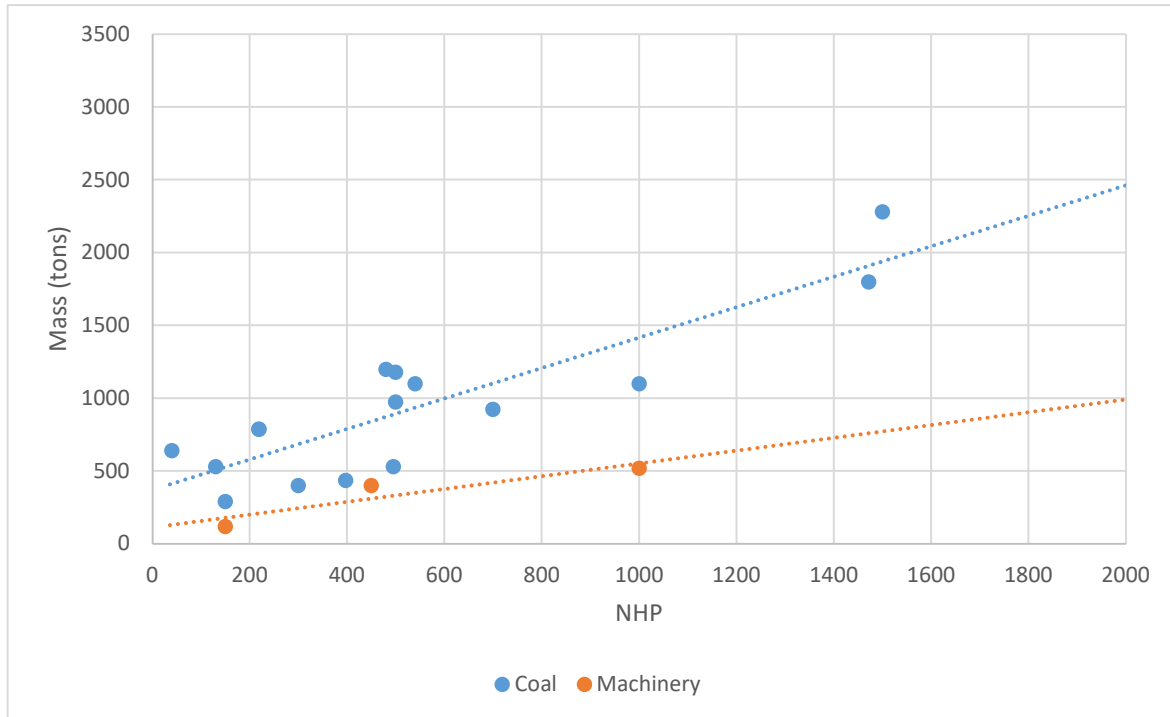


Figure 75: Machinery mass from literature compared to NHP

5.4.4 Cargo, Crew and Ballast

The stowage rates of many cargo types can be found from contemporary literature on the subject (Stevens, 1894), in some cases even giving the stowage method. For this research, in order to compare vessels more evenly, each ship will be modelled with the same type of cargo, in this case tea, with the stowage rates based on those given in *On the Stowage of Ships and their Cargoes* by Robert White Stevens (1894, p. 666). In this text the average stowage rate of tea is given as 1,200 lbs per 50 ft², which is equal to 384 kg/m³.

Without individually modelling the exact placing of the cargo, it is difficult to estimate an accurate cargo carrying capacity. Fortunately, the tonnage system introduced alongside the Merchant Shipping Act 1854, was designed to provide an estimate of the space available for cargo (*Tonnage Act (17 & 18 Vict. C.104)*, 1854; White, 1877, p. 51; MacGregor, 1988, p. 151). The Net Register Tonnage (NRT) is derived from the useful volume of a ship in cubic feet, divided by a factor of 100 (*Tonnage Act (17 & 18 Vict. C.104)*, 1854; White, 1877, p. 21; MacGregor, 1988, p. 151). If this is taken as the cargo space and a stowage rate is known, then theoretically the cargo mass can be calculated. However, for those ships built or registered before the 1854 Act, there may be no NRT available. In this case, NRT has been estimated from the relative mass displacement of the other vessels using the relationships shown in Figure 76 and equations (36) and (37).

$$NRT = 0.4738\Delta \quad (36)$$

$$NRT = 0.3254\Delta \quad (37)$$

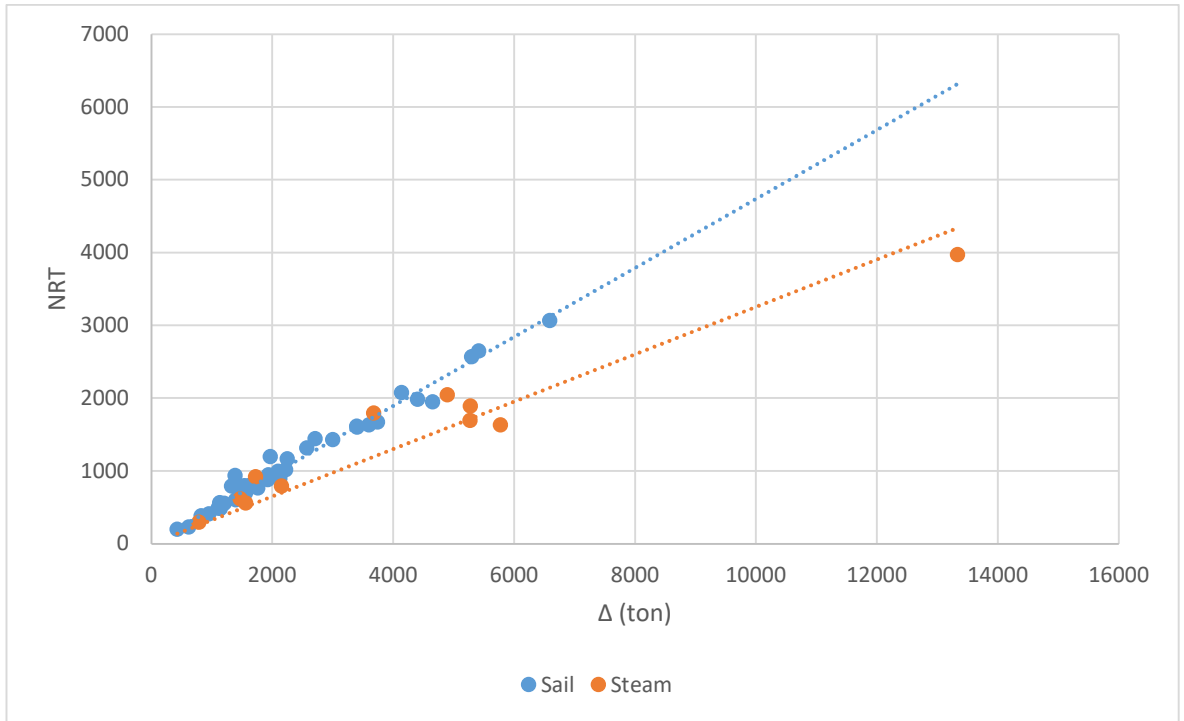


Figure 76: Relationship between Δ and NRT for cargo estimate

In order to verify this method, an effort was also made to calculate the capacity of the hulls in relation to a cargo of tea, which being stored in chests of a known size, may be modelled within *MAXSURF Modeler*. This allows the mass of tea in the main hold and corresponding ballast, which surrounds the chests, to be estimated, based on the stowage method shown in Figure 77. The remaining weight from the displacement has been assumed to be further cargo positioned on the upper deck at a height of 2/3 of the moulded depth. It has been found that this calculated mass has an average difference of 4.34 tonnes (7.83%) more cargo compared to the NRT estimate, with a standard deviation of 182.68 tonnes (28.81%). This variation can be partially accounted for by a lack of knowledge about the interior arrangement of many of the ships. Given this, it would appear that the NRT estimate is a better method as it automatically accounts for the unused space.

Ballast is assumed to be gravel with a specific gravity of 1500 kg/m³ and is calculated to bring the vessel to its load waterline where required. Where the mass of the cargo causes the vessel to exceed its load displacement, cargo has been deducted and no ballast is present. This method is considered with caution, as it would have often been considered normal to add some form of permanent ballast, at least to the top of the keelson (Stevens, 1894, p. 670). In most cases where this correction was made, the vessel was steam powered and so could have used coal as ballast.

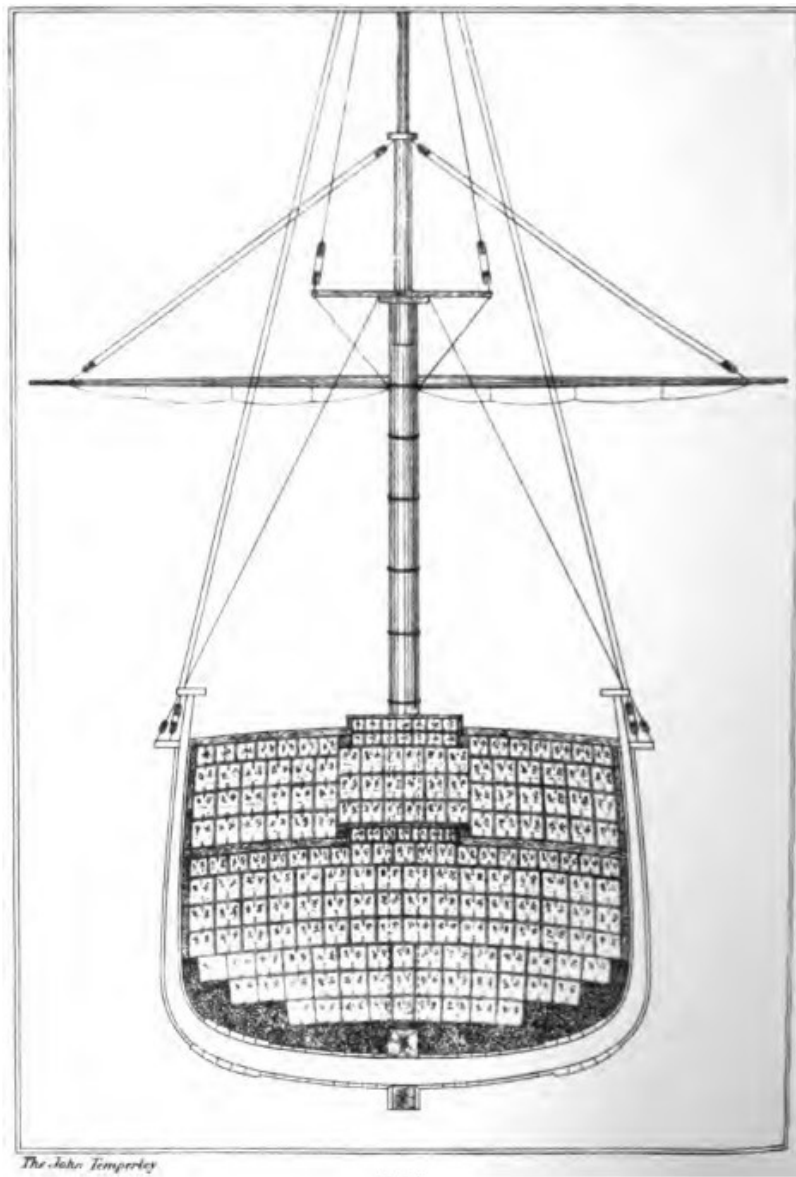


Figure 77: Stowage of Tea (Stevens, 1894, p. 669)

For the majority of masses, the longitudinal centre of gravity (LCG) has been positioned at the longitudinal centre of flotation (LCF) in an attempt to reduce the trim. The VCG for cargo and ballast is based on the modelled tea cargo, where it has been assumed that the ballast will be positioned around the tea chests. This gives a cargo VCG of 56.60% of the moulded depth, and for ballast 28.67%.

An allowance of 80 ft³ (2.27 m³) has been assigned per passenger in accordance with the 1828 Passenger Vessels Act, in which it is stated that no more than three people may be carried per ton burthen, which would equal 75 ft³ (2.12 m³) per person (*Passenger Vessels Act (Geo. IV C.21)*, 1828). This value also corresponds to the volume given per person on an Atlantic crossing by the USA, although this was largely ignored by ship owners who wanted to increase profits (*Carriage of Passengers Act, 1855*; Maddocks, 1981, p. 145). The crew and passengers have been assigned a weight of 75 kg each. A contemporary study from 1835 gives the average clothed 25 year old male

in Britain as between 151 and 155 lbs (68.5-70 kg) so this is a reasonable assumption, as the passenger weight includes an allowance for personal belongings (Quetelet, 1842, p. 114). The number of crew is based on suggestions by White Stevens (1894, p. 166) unless otherwise given in literature. This value does not take into account technological advances that may change the number of required crew, so this is an estimation that may be improved on. In a number of cases this estimate is considerably higher than the actual number of crew, but no alternative relationship could be found.

An American manual on seamanship gives 100 lbs (45.36 kg) each of salted beef and bread, and 60 gallons (0.227 m³) of water per person as the provisions required for an Atlantic crossing (Dana, 1873, p. 178). If we assume this to be equal to a month's supply, then scaling this up to a journey of 3 months, it would indicate that around 0.95 tonnes of provisions per man would be required. This would cover a journey by a tea clipper from China, or the journey to South Africa by an East Indiaman, after which they would be likely to take on fresh supplies (Northcote Parkinson, 1948, p. 153). Stores are therefore estimated at 1 tonne per crew member and are positioned a third of the moulded depth below the main deck.

A summary of the masses and their origins is given in Table 18. It is important to note that the estimated masses, particularly for the consumable items, may not be representative of what was actually used on each individual ship. The advantage of using the estimations described above are that each ship is loaded under the same conditions, making the VPP results more comparable.

Table 18: Summary of mass items

Item	Number	Mass/Item (tonne)	LCG (m)	VCG (m)
Lightship	1.13	Survey/estimate	Survey/estimate	Survey/estimate
Rig	1.2	Plan/survey/estimate	Plan/estimate	Plan/estimate
Cargo	1	NRT	LCF	0.5660 D_M
Ballast	1	Remaining mass	LCF	0.2876 D_M
Crew	Literature/estimate	0.075	LCF	0.66 D_M
Stores	Crew + Passengers	1.0	LCF	0.66 D_M
Passengers	Literature	0.075	LCF	0.66 D_M
Engine	0/1	Literature/estimate	0.4 L_{WL}	0.5 D_M
Coal	0/1	Literature/estimate	0.3 L_{WL}	0.5 D_M
Anchor	1	Survey/estimate	L_{WL}	D

5.5 Summary

The selection of ships to expand the dataset for both a new parametric analysis and for use in the VPP has been considered. The selection of 61 ships covers a range of ocean-going cargo and passenger ships from across the 19th Century. Difficulties with sourcing data on steam ships

Selection and Digitisation of Primary Data

means that a majority of the analysis will be based on sailing ships, which make up most of the new dataset. However, the steam ships will still provide an important comparison.

Methods for extracting data from both lines plans and half models have been discussed using *Cutty Sark* as a base model. A scaled half model of *Cutty Sark* was manufactured to test different scanning methods. Initial results show that creating a surface directly from the mesh produced by the *Sense* 3D scanner is not a suitable method for digitising half models, as there is a large variation between different scanning and post-processing methods. The effect of this variation on Holtrop resistance was investigated, and it was found that this produced a significant difference from the original model results. An alternative method where a lines plan is produced by projecting lines onto the mesh proved to be much more successful, with minimal differences in hull geometry and resistance shown between the scanned model of *Cutty Sark* and the original model. A similar result was found for the speed output from the VPP. Based on the results of the sensitivity analysis in Sections 4.2 to 4.6, this last method has been shown to be adequate for use with the VPP. The effect on scanning on geometry has also been examined using a number of vessels for which both a lines plan and half model were available. This showed that despite some consistent errors, the output of the VPP was not significantly different. This validates the use of half models as a source of data alongside lines plans.

Details of the procedures for estimating the sail areas of the ships have been discussed, with methods for ships with varying levels of source data. Where the source data is unavailable, linear relationships have been determined using basic hull dimensions to provide an estimate. A similar procedure has been taken for estimating the structural mass based on survey reports. Additional masses for steam ships such as coal and machinery have been calculated based on information from the larger, original dataset. Cargo is considered to be tea, with the mass based on the net tonnage where available, or an estimate of tonnage based on displacement, with the centres coming from a number of cases in which it was calculated directly. The mass estimates are perhaps the least reliable estimation compared to real-life cases. However, as the ships are being compared to each other, it is appropriate that the loading conditions use the same procedures to allow a true comparison of the performance.

With the modelling techniques discussed in this chapter, the methodology is now in place for examining the evolution of historic ships. The procedures for creating digital models enables a reanalysis of the parametric data, considering narratives that were previously impossible. The ability to estimate speed using this data and the VPP also allows a view of the evolution of 19th Century merchant ships that has not been examined before. Combined with the background and literature discussed in Chapter 2, the causes and effects of this evolution can be considered.

Chapter 6: Modelled Data and Case Studies

One of the objectives of this research is to use the data generated to improve our understanding of the evolution of 19th British Merchant ships. To achieve this, the parametric data originally presented in Chapter 3 has been re-analysed using dimensions and performance characteristics calculated from the digital models described in Chapter 5. In addition to this, a number of case studies have been identified to test the limitations of the methodology. By combining literature and the results from the parametric and performance analyses, it is possible to identify trends and provide potential explanations within these case studies. This chapter covers the new parametric analysis and investigates the case studies, examining the factors driving change and challenging the understanding of these changes relating to individual ship types.

6.1 Re-analysis of Data

In Chapter 3, a requirement for more data was identified to obtain a complete understanding of the evolution of ship design and performance. Using the methods developed in Chapters 4 and 5, it is now possible to obtain this data and investigate trends that would otherwise have been impossible. It is important to ensure that the 61 British ships modelled for this research are representative of their time. This can be achieved by comparing the modelled length-beam ratio with the data obtained from literature, as shown in Figure 78. This shows that the majority of both modelled sailing and steam ships lie within the expected range for their types, indicating that they are a suitable selection for examining the evolution of ocean going British ships.

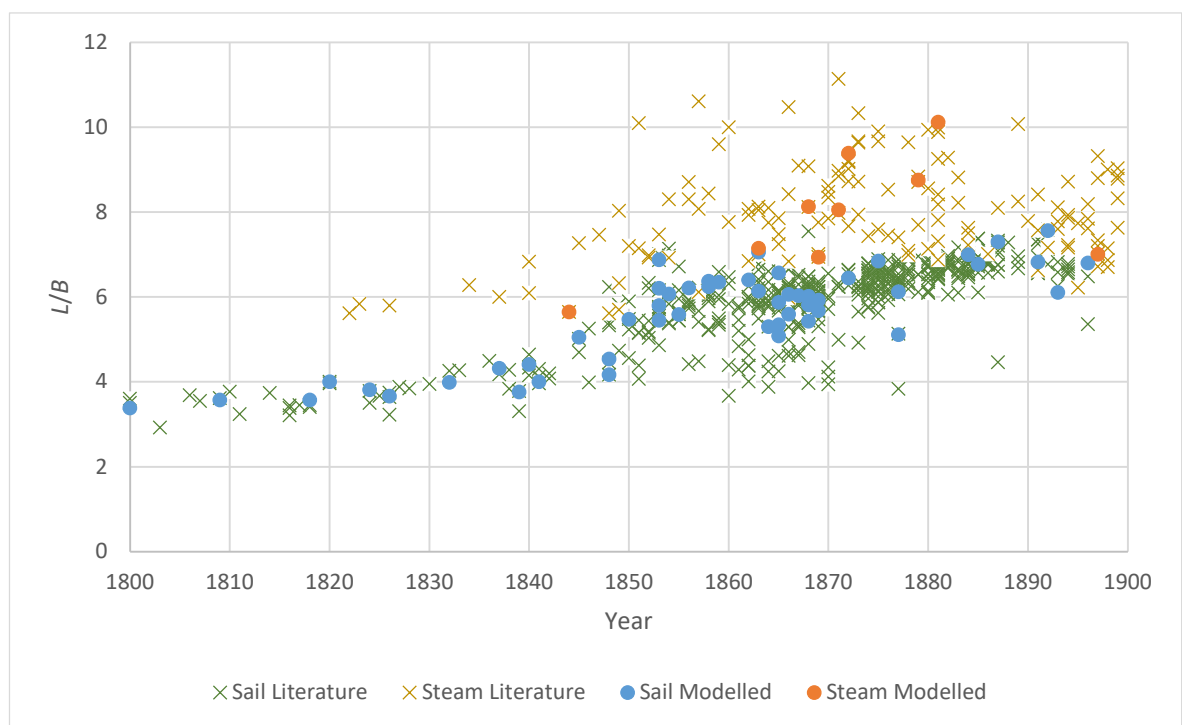


Figure 78: Modelled L/B compared with literature

Modelled Data and Case Studies

This is confirmed by considering the averages of the length-beam ratio for sailing ships for both the data from literature and the modelled data, which are 5.49 with a standard deviation (σ) of 1.03, and 5.59 with a σ of 1.05 respectively, a difference of less than 2%. The beam-draught ratios returns values of 1.91 average and 0.24 σ for literature and 1.81 average and 0.18 σ for the modelled data, which is a 5% difference, although this larger difference may be due to some of the original draughts not being measured in the load condition, which is the case for the modelled data.

Once it has been confirmed that the ships modelled are representative of the overall data set, those parameters for which there was previously limited data can be examined. One particularly important dimension that can be calculated from the digital ship models is the displacement. In Chapter 3 this was identified as an important factor in inferring the performance of ships from their dimensions as, when compared to other parameters, it can show something about the shape of a ship. One such ratio is the length-displacement ratio, which should follow a similar pattern to the length-beam ratio, with an overall increase throughout the century. Figure 79 compares the modelled data with the values from literature. The new values clearly follow a similar trend to the length-beam ratio, indicating that ships were becoming finer, a feature that would have a detrimental effect on cargo capacity, but a positive effect on ship speed.

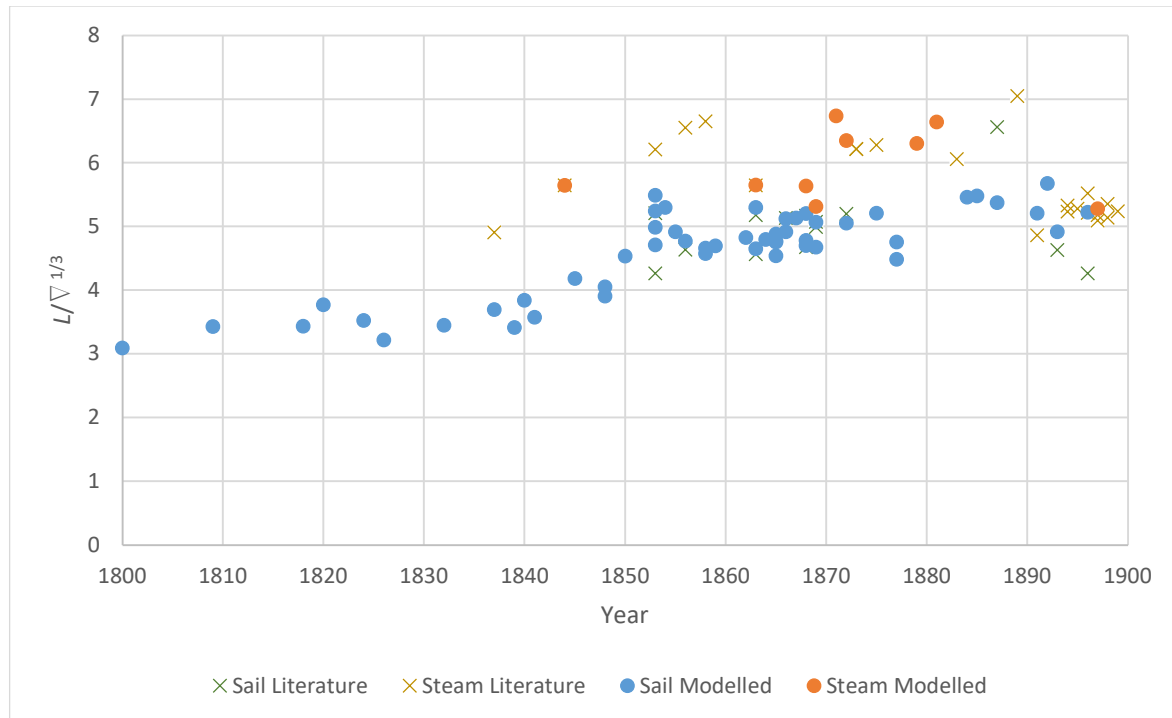


Figure 79: Variation of $L/V^{1/3}$ ratio with time including modelled data

The fineness of the hull can also be seen by considering the C_P , a value that cannot be calculated without the displacement or the midship section area. Figure 80 shows how the C_P developed over time. It is impossible to define any overall trend, especially as there is so much variation in

the middle of the century. What this variation does show is that there was a wider variety of hull forms being built between 1840 and 1860. This coincides with the number of experimental hull forms that appeared around this time, potentially in response to changing tonnage laws or new theories being developed by naval architects at the time, especially between 1850 and 1860. During this era there were a number of significant changes to shipping, including the repeal of the Navigation Acts in 1849 (MacGregor, 1984a, p. 11) and the introduction of the 1854 Merchant Shipping, including an update to the tonnage law (MacGregor, 1984b, p. 16, 1988, p. 151).

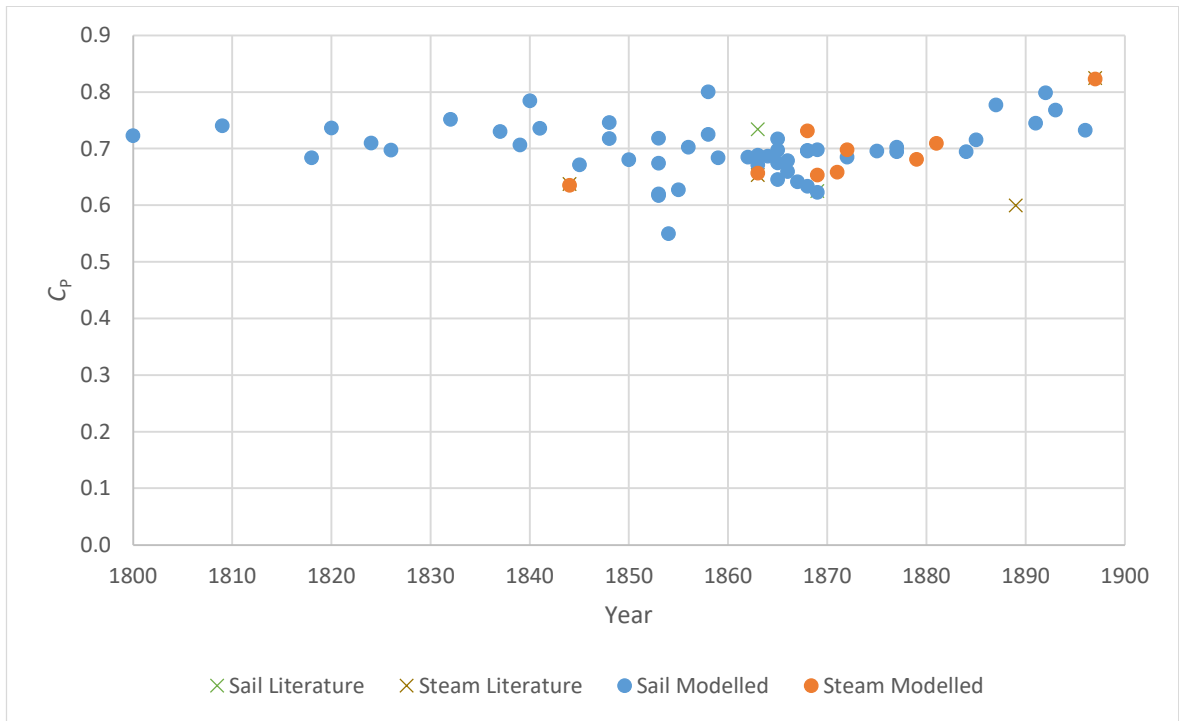


Figure 80: Variation of C_p with time using modelled data

Another set of data that required the digital models is WSA. In the original dataset, there were only four instances where WSA was given. As the calculation of WSA by hand is difficult, the accuracy of these values is called into question. The value from the digital models is calculated by dividing the surface into triangular elements, which is more accurate than alternative estimations, for example integrating the girth of the sections (Bentley Systems Incorporated, 2017). As WSA is dependent on ship size, in order to examine the changes to ships over time, this analysis implements a non-dimensional form using the square root of the volumetric displacement multiplied by the length (Molland, Turnock and Hudson, 2011, p. 21). This coefficient (C_{ws}) is therefore defined as:

$$C_{ws} = \frac{WSA}{(\nabla L)^{0.5}} \quad (38)$$

This value is plotted against time in Figure 81. It becomes clear from this graph that there are three steps to the variation of WSA. Over the first forty years there is little change, followed by a

period where there is a great deal more scatter, but the average appears to remain constant, finally ending with a lower average for the final 30 years. Overall, there seems to be a reduction in WSA relative to ship size, although it appears to be less significant than might be expected considering the radical change to the appearance of the ships. Throughout the century there are still ships with the same C_{ws} value, for example *Cumberland* (1800) and *Indian Empire* (1896), which are visibly very different, with the latter having an length-beam ratio of more than twice the former. This indicates that any significant changes to ship performance were not due to WSA. Another feature that may be noticed from Figure 81 is the reduction in variation at around 1870. Similarly to other measures, this may be indicative of a reduction in the number of experimental hull forms driven by a lack of understanding of the science behind ship design. As will be discussed in Section 6.2.2, the change at around 1870 may be due to advances developed by people such as Froude and Rankine, in what has been termed the “modern” phase in this research.

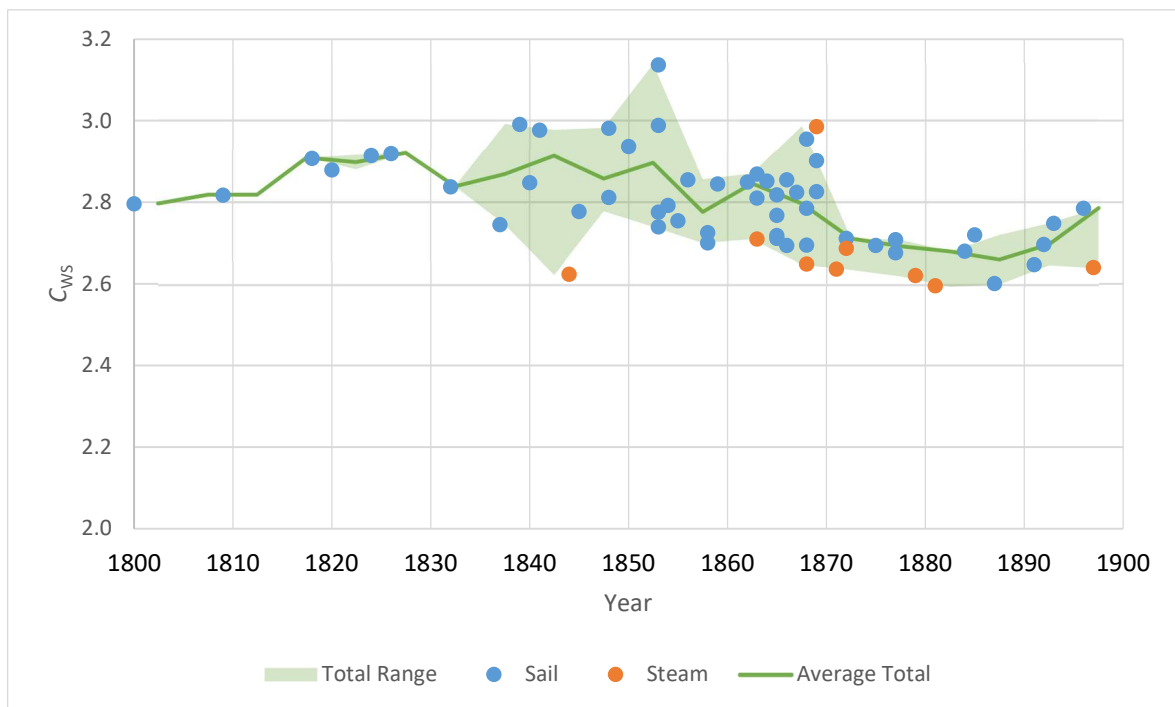


Figure 81: Change in C_{ws} with time

Using the data presented in Chapter 3, it was impossible to use ship speed as a performance metric, owing to the variation in the data sources. Using the VPP developed in Chapter 4, speeds can be generated which are comparable to each other. Figure 82 shows an example of this, with the modelled ship speed given as the maximum attainable speed in a 30 kn wind. The assumptions made in the creation of the VPP mean that these values will be slightly overestimated, but there is a clear trend for sailing ships showing that the potential speed increased over the course of the century. The values for steam ships do not show a clear trend. This will be due to both the lack of hull forms that could be found for this research, and also the

lack of information on engine efficiency, which is a key factor in determining the speed under power. For speed under sail, there is also a potential error with the sail force calculation, which was intended for a square-rigged ship, whereas the majority of steam ships shown here operated with a fore-and-aft schooner-rig. As discussed in Section 2.10, this may affect the results.

The upwards trend in the speed of sailing ships can be clearly seen by examining five year averages, as shown in Figure 83. Although there is not enough data to obtain the average for some intervals, the upward trend in speed from around 1830 is clear. The following five years are associated with several major events that may have had an impact on the design of ships, including changes to smuggling and tonnage laws and the end of the EIC monopoly in China. This is followed by a less significant increase following the repeal of the Navigation Acts in 1849. The increase in speed continues for around 50 years before dropping off again, although still around 6 kn faster than in 1800. The final turning point comes as steam power has dominated all but a few markets, leaving sailing ships to engage in bulk trades. In these trades the capacity of a vessel was more important than speed (Lubbock, 1953b; Geels, 2002). Without specifically designing for speed, any increase in ship size would normally have a negative effect on speed.

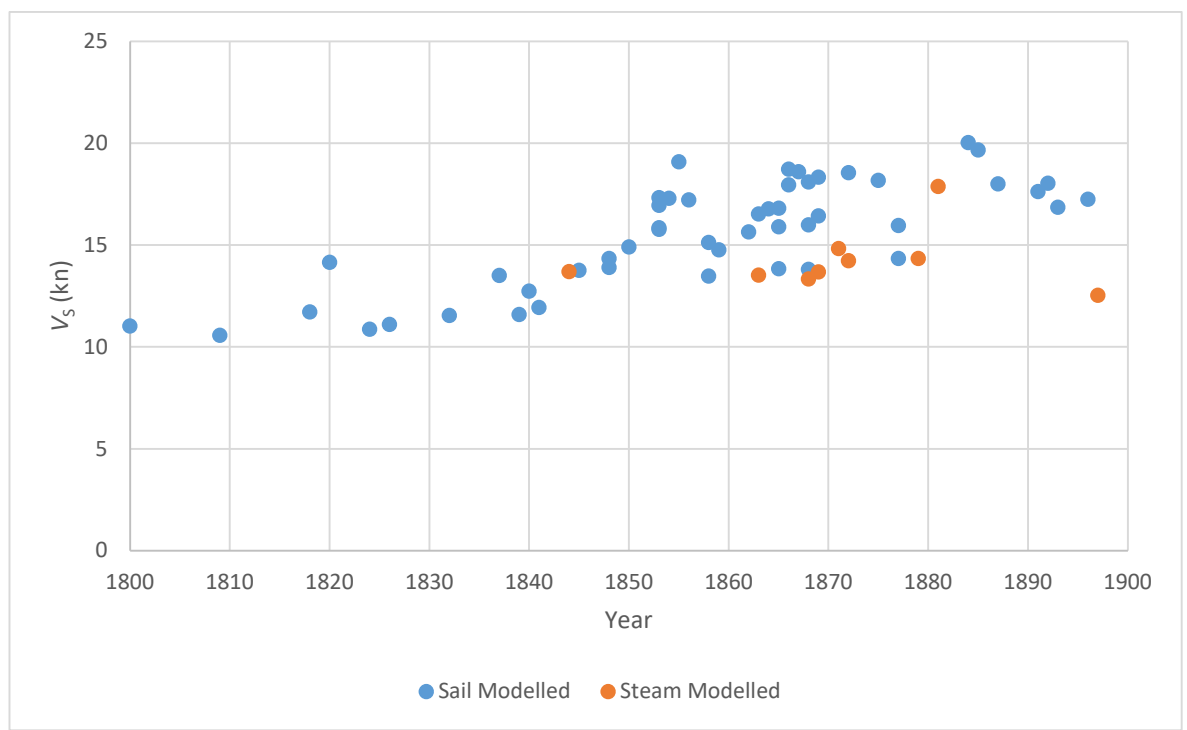


Figure 82: Maximum V_s in a 30 kn wind

Modelled Data and Case Studies

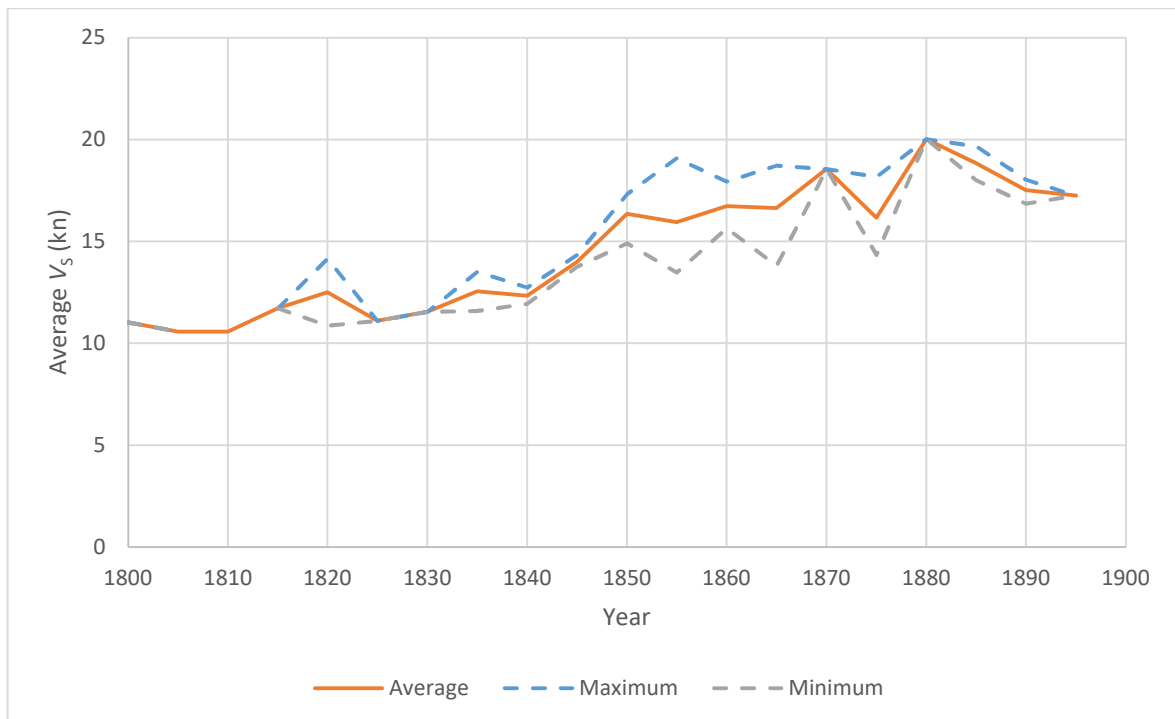


Figure 83: Average speeds for sailing vessels in a 30 kn wind at 5-year intervals

As discussed in Section 3.1, it is important to consider the Froude Number, F_n , when discussing ship speed so as to extract the effect that ship length has. Figure 84 shows the F_n for the selected ships based on the maximum speed in a 30 kn wind. The indistinct variation would indicate that the ship speed increases with time based primarily on the length. Further investigation into the driving forces behind performance changes will assist in clarifying this.

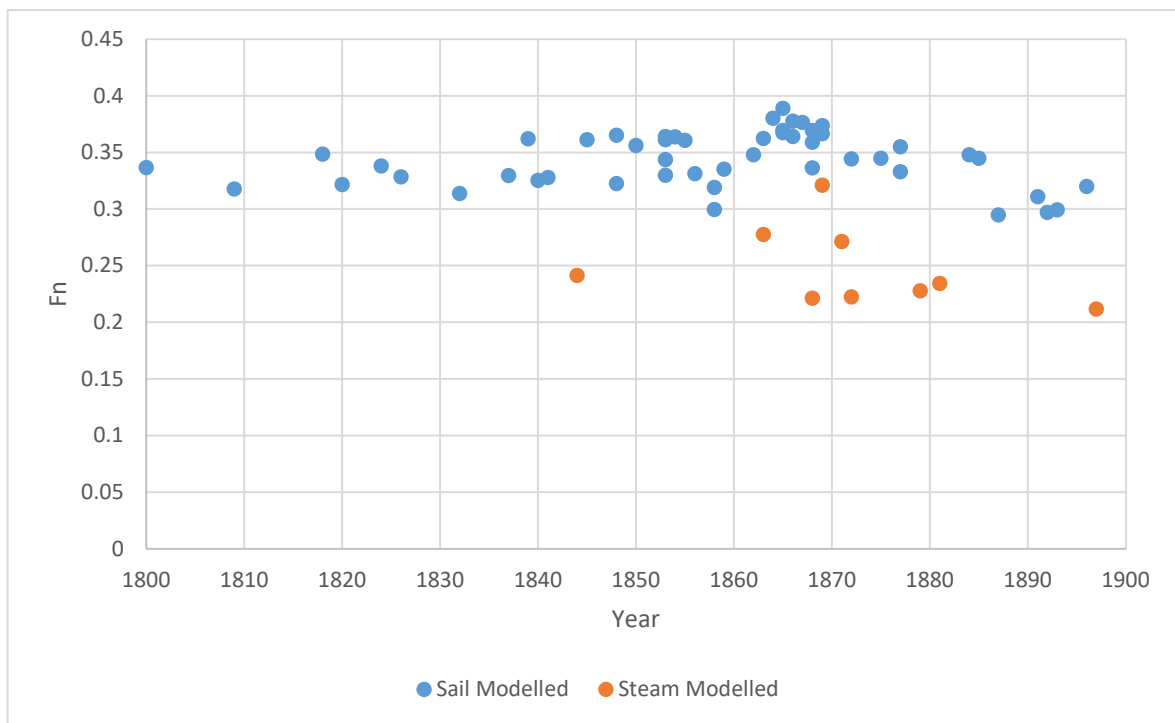


Figure 84: Maximum F_n in a 30 kn wind

The stability of ships is a factor that must also be considered when looking at performance. With such a variety of ship types, it would be impossible to compare this simply by considering the VCG or even the righting moment at any given heel angle. Instead it is proposed to use a simplified measure derived from the estimation of sail areas in Section 5.3. In this case the sail area, which is limited by the stability of the vessel, was linked to the waterplane area by means of the square root of the length and beam. This method should give an indication of the stability potential of the vessel, as the sail area is limited by stability, although it is not necessary in this case to include the number of masts in the estimation. Plotting this measure against time produces the relationship shown in Figure 85. As the size of ship grows, it follows that this measure should increase as the relative parameters increase. The key point to note is that the beam has a greater impact on stability than the length, and so the increase in L/B should have a negative impact on the stability. Despite the relative reduction in beam compared to length, however, according to this measure the overall stability still increases. This will be because the overall size of the ship is still increasing, which would also have a beneficial effect on the stability.

The second point to note in Figure 85 is the large amount of scatter up until the late 1870s. This is around the time in which greater focus was being given on the safety of ships in relation to stability, following the high profile capsizing of *HMS Captain* in 1870 and lobbying in parliament by Samuel Plimsoll on the subject of load lines. The eventual reduction in scatter could indicate that actions taken following these examples were successfully implemented.

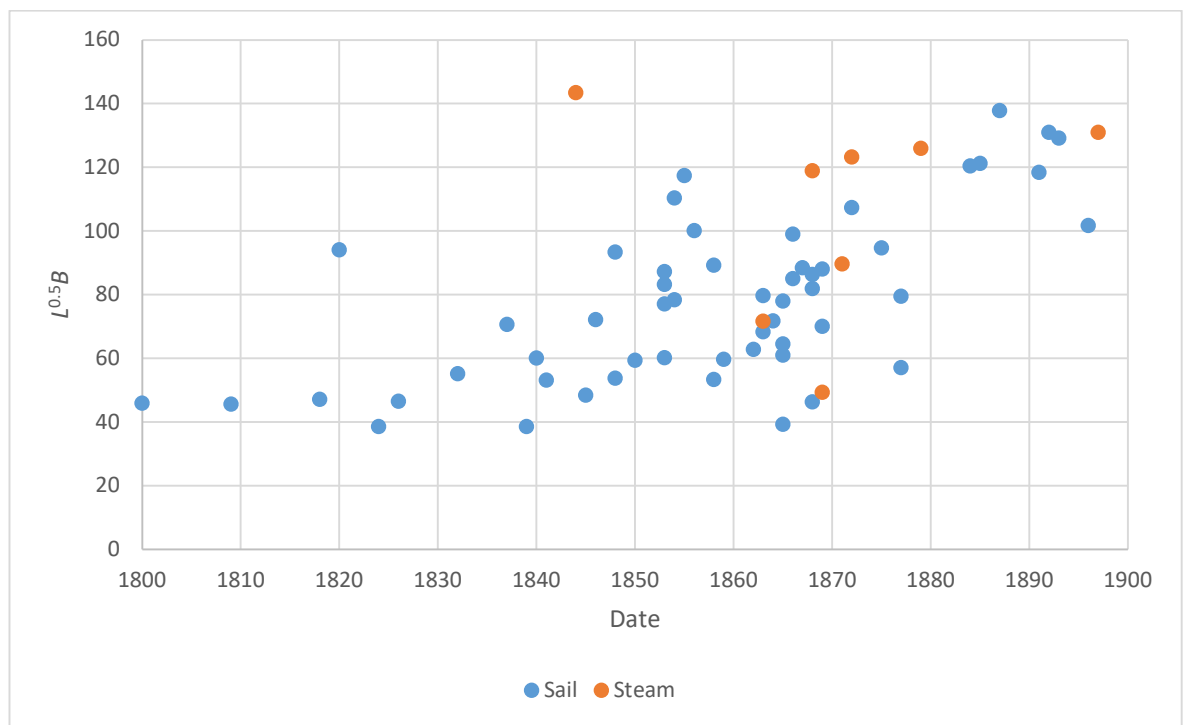


Figure 85: Measure of stability with time

This overview of the modelled data indicates that there was a significant and measurable change to ship design and performance over the course of the 19th Century, specifically with ships becoming finer and faster over time. The literature review in Chapter 2 provides some indication of the reasons behind this change, but to obtain a more complete story, the literature needs to be compared with the data generated. To achieve this, the remainder of this chapter will cover a series of case studies identified in the literature review, and examine how narratives can be considered in relation to the parametric and performance data calculated from the digital models.

6.2 The Driving Forces behind Change

To explain the evolution of ships, it is important to understand the driving force behind any change and the context in which change occurred (Adams, 2013, p. 63). It is clear from the data generated in this research that there was a distinct change to ship dimensions, with an associated increase in speed. In the 19th Century, there are a number of reasons why ship performance may have improved with time. Once it is understood what was changing, it is possible to tell the stories of ship design with respect to scientific knowledge, legislation and international influences.

6.2.1 Hull vs. Sails

The data generated in this research shows that there was a clear increase in ship speed over the course of the 19th Century. The main question that arises in relation to this was whether this was due to improvement in hull efficiency, propulsive efficiency or a combination of both. Since the VPP is based on individual force components, it is possible to investigate this aspect. The key components that determine ship speed are resistance, R_T , and the thrust generated by sails (T_S). As the thrust generated by engines (T_E) is estimated for some of the steam ships, it is not possible to consider engine efficiency at this stage, although the improvements in engine technology are generally well documented (Craig, 1980; Gardiner and Greenhill, 1993b).

As both R_T and T_S are dependent on the size of the ship, each has been converted into a non-dimensional form: R_T using WSA, and T_S using the total sail area ($A_{S,T}$). The coefficient of total hull resistance (C_{RT}) and coefficient of sail thrust (C_T) are defined by the following equations:

$$C_{RT} = \frac{R_T}{1/2 \rho_W WSA \cdot V_S^2} \quad (39)$$

$$C_T = \frac{T_S}{1/2 \rho_A A_{S,T} V_S^2} \quad (40)$$

C_{RT} is shown plotted against time in Figure 86 at a ship speed of 5 kn. In addition to sail and steam ships, an indication of the C_{RT} of a modern ship is also given. This ship is based on the data used as an example of how to use the Holtrop (1984) method ($L/B = 4.17$, $B/T = 3.75$). A five-year average

for sailing ships displayed on the graph shows that there is a distinct decrease in resistance with time, indicating that hull forms do indeed become more efficient with time. A small number of steam ships in the 1870s and 1880s even approach the value calculated for the modern ship.

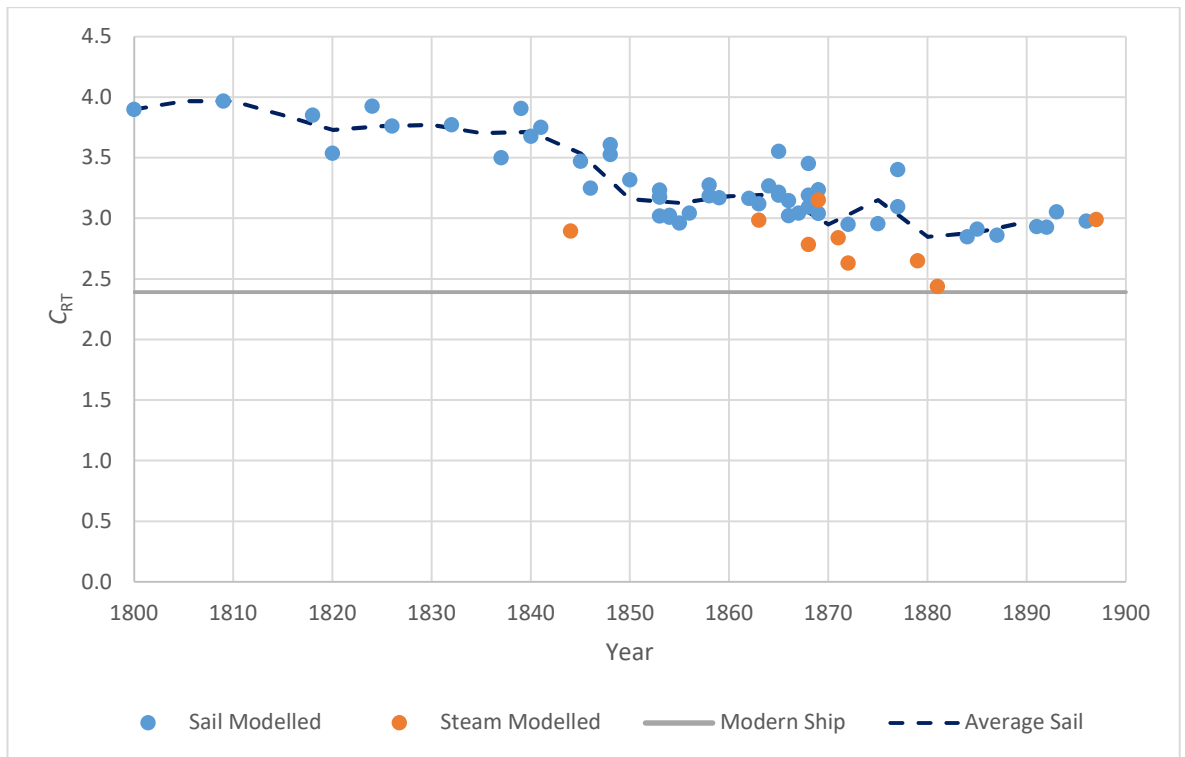


Figure 86: Changes to C_{RT} against time at a V_s of 5 kn

At higher speeds, it becomes clear what prevented earlier vessels from reaching the higher speeds of their successors. Figure 87 shows the change in C_{RT} at a ship speed of 10 kn, where there is a significant difference between the earlier and the later vessels. For a high percentage of the ships in the first 40 years, the C_{RT} values are so high that these vessels would struggle to reach 10 kn. It is still clear, however, that the hull forms become more efficient with time.

In contrast with the hydrodynamic efficiency of the hulls, when we consider C_T , there is not such an obvious effect. Figure 88 shows that at $V_T = 20$ kn, $\gamma = 130^\circ$ and $\theta = 40^\circ$, there is only a minor overall improvement in the efficiency of the rig. A five year average for the sail data has been included for clarity. Similar results were found for different wind conditions. Because the same base sail data was used for each vessel, this chart does not indicate any improvements in individual sail efficiency, but only the rig design as a whole. This would account for the small change even though there are acknowledged advances in sail design at the time, although these are generally aimed at improving the handling of the vessel (MacGregor, 1980b, p. 12). Despite this, it is apparent that the increase in speed displayed over the course of the 19th Century is due primarily to an improvement in hull design rather than the rig, which in turn can be linked to the increase in length.

Modelled Data and Case Studies

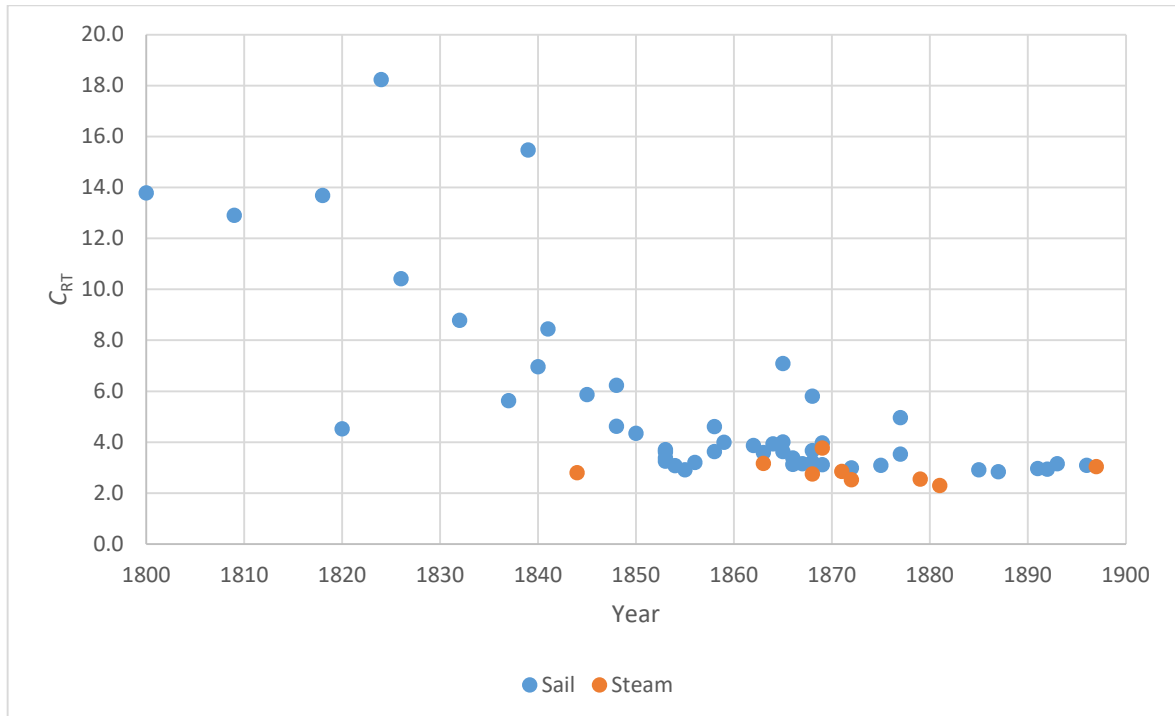


Figure 87: Changes to C_{RT} against time at a V_s of 10 kn

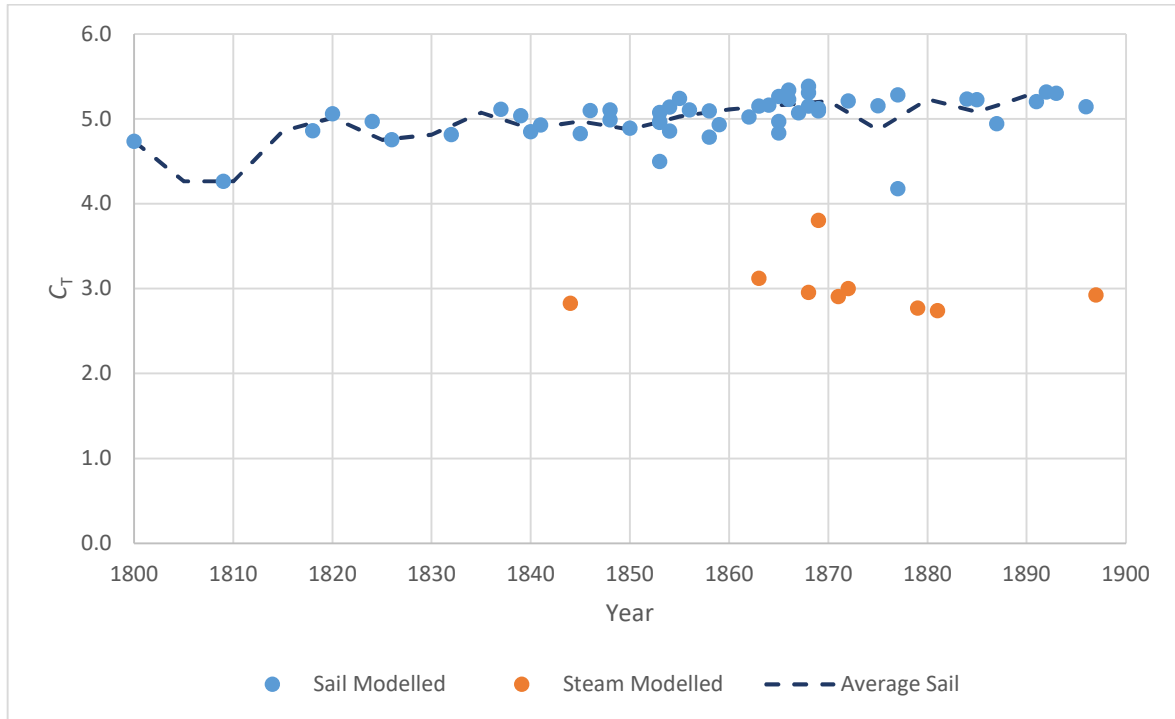


Figure 88: Changes to C_T against time ($V_s = 10$ kn, $\gamma = 130^\circ$, $\theta = 40^\circ$)

6.2.2 Changes to Understanding Hydrodynamics

A large part of the development of naval architecture as a science took place in the 19th Century (Molland, Turnock and Hudson, 2011, pp. 1–2). Understanding the hydrodynamic properties of hull forms was a key part of this. Documentary evidence shows how this understanding developed through technical papers and textbooks aimed at educating this new type of ship designer. However, the question remains as to how this knowledge actually affected real-world ship design. The data produced during the course of this research can give an indication of this.

Based on the literature examined in Section 2.2 on the development of naval architecture in the 19th Century, it would appear that the century may be divided into three sections: the empirical phase, the developmental phase and the modern period. The “empirical” phase refers to the time when ships were designed primarily on experience, sometimes even going against science, which had not at that point done much to improve ship performance. This phase may be associated with cultural limitations, including the potential influence of the *L/B* restriction in the early part of the century as discussed in Section 3.1. The second, the “developmental” phase, covers the period between 1835 and 1870, when there were increasing numbers of theories on ship design, culminating in the formation of the INA in 1860. The third phase has been entitled the “modern” phase to reflect the fact that many of the discoveries within this phase form the basis of naval architecture. This final phase begins at the time when William Froude was most active in his theories regarding the resistance of ships. In reality there is an overlap between the phases and it is impossible to apply exact dates, and so those stated here are more of a guideline to aid in the examination of the results from this research.

The first concept that can be examined is the importance of the location of the point of maximum beam. The further aft this point is, the finer the bow will be, assuming there are no other major changes to the design. The other hydrostatic particular that would be affected by this is the position of the LCB. The half angle of entry, i_E , which indicates the fineness of the bow, and the LCB have been plotted against time in Figure 89 and Figure 90 respectively. Although i_E may be calculated directly from a lines plan, the LCB may only be easily calculated using the digital models produced in this research.

The figures indicate that in the empirical phase the bows are relatively bluff, with an LCB around 1-3% forwards of amidships. This corresponds with literature, notably those suggestions that the maximum beam should be as far forwards as possible (Steel, 1805, p. 152; Chapman, 1968, p. 81). Data from Chapman, based on ships from a variety of countries including Britain, indicate that the LCB should be between 1/50th and 1/100th of the length from the middle of the load waterline (1-2% forwards of amidships) (Wildish, 1872, p. 69). This also agrees with the data plotted for the first 35 years.

Modelled Data and Case Studies

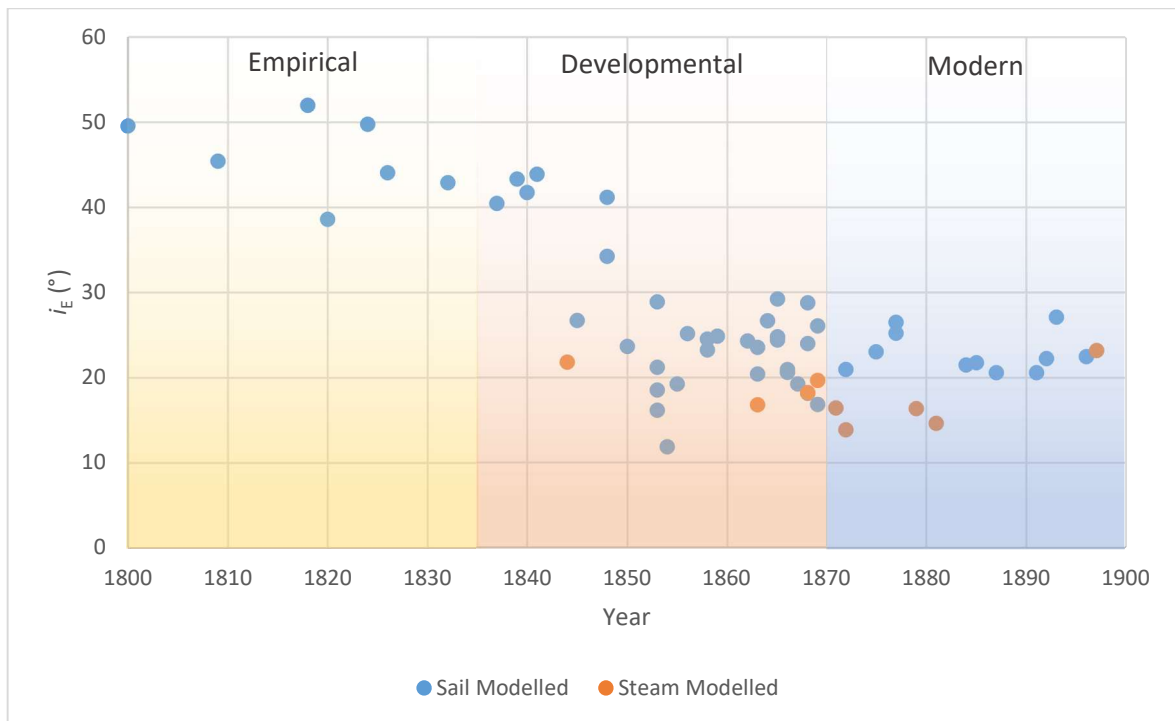


Figure 89: i_E with time

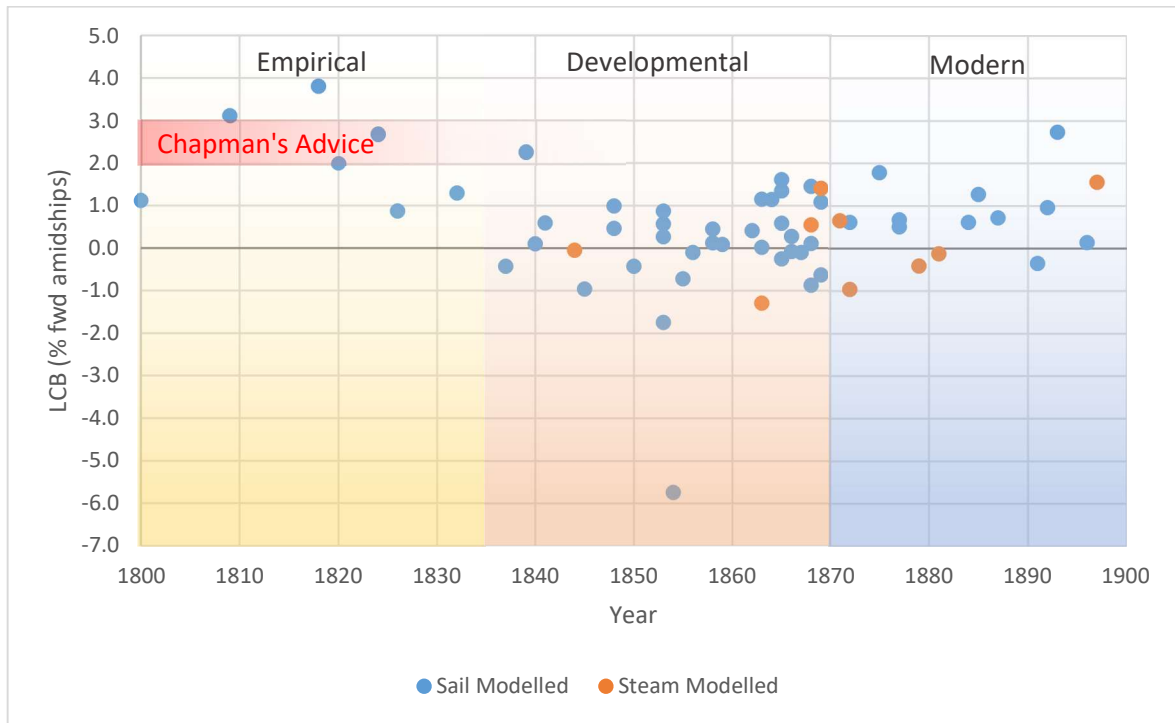


Figure 90: Change in position of LCB with time

In the second phase, there is a rapid increase in the sharpness of the bow, with an associated movement of the LCB aft. This indicates that ships were becoming finer and more symmetrical fore-and-aft. The positioning of the LCB reflects Maudslay's (1860) description of a hull form that had been around since the 1830s, where the point of maximum beam should be aft of amidships, although the maximum near the base of the ship should be further forwards, effectively creating a diagonal section of maximum beam. At the load draught this would lead to the LCB being moved further aft than it previously was. The influence of Scott Russell's wave-line theory is also evident;

by incorporating a long hollow bow with a shorter stern, this would have the effect of moving the LCB aft. This is particularly prominent in the ship *Storm Cloud*, whose lines were based on wave-line theory (Ferreiro and Pollara, 2016, p. 431), producing an LCB of 5.4% aft of amidships.

In the third phase, the LCB moves forwards again, although it appears that the sharpening of the bow has levelled off. There are two main reasons that this plateau could have occurred: firstly, it was found that narrowing the bow any further was detrimental to the cargo carrying capacity of a vessel; secondly, research into stability had shown that the long, narrow ships that had previously been thought to be the best design, were potentially unsafe (Barnaby, 1871, p. 62). In addition to this, work by William Froude and his son, Robert Edmund Froude, showed that a wider beam was not necessarily detrimental to hull resistance. A paper by R. E. Froude (1881) expanding his father's work suggests that the best hull form to reduce wave-making resistance has a "U" shaped section in the forebody and a "V" shaped section in the afterbody. This would have the effect of moving more volume, and consequently the LCB, forwards. Although there are not many data points after 1880, this effect can still be seen. As by this point shipbuilders were working closely with naval architects (Froude, 1881), this movement of the LCB could realistically be attributed to Froude's research. It is noted that the fineness of the bow does not increase at this point, as the importance of a sharp entrance to reduce wave-making was beginning to be realised (Kemp, 1891, p. 140).

As many of the changes noted above are attributed to the understanding of resistance, it would follow that there would be a change to the hull resistance as attitudes change. In order to examine this, the breakdown of the non-dimensional resistance components can be examined. The frictional resistance, R_F , was the first component to be understood to some degree (Bourne, 1867). It was not until W. Froude's tank tests in the 1870s that the wave-making resistance, R_W , began to be understood, although there were theories relating to it previously (Chapman, 1968, p. 80). Consequently there should be a reduction in frictional resistance before any reduction in wave-making resistance. In relation to the phases described previously this would mean that the non-dimensional value of R_F , C_F , should show a greater decrease in the developmental stage and the coefficient of R_W , C_W , should be reduced in the modern phase. These coefficients are defined as follows:

$$C_{F,W} = \frac{R_{F,W}}{1/2 \rho_W A_{WS} V^2} \quad (41)$$

Figure 91 shows this effect to some extent at a V_s of 5 kn, although it would appear that there was a large decline in C_W in around 1850, which would be too early if the variation was entirely dependent on the hydrodynamic understanding. However, in the process of reducing frictional

resistance, it is likely that the hull forms were also inadvertently designed to reduce wave-making (Ferreiro and Pollara, 2016, p. 426). This effect could be attributed to the conviction that the midship area, A_M , was critical to frictional resistance (Bourne, 1867, p. 22), meaning that in order to increase the cargo capacity of a vessel, length was the only dimension that could be increased without a significant penalty on ship speed. This would have reduced the comparative wave-making resistance, although not for the reasons that naval architects of the time believed. Scott Russell's wave line theory also helped to reduce wave-making, through understanding that the length of the entrance and run were responsible for the waves generated, although he failed to comprehend the mechanism behind the decrease in resistance (Kemp, 1891, p. 116).

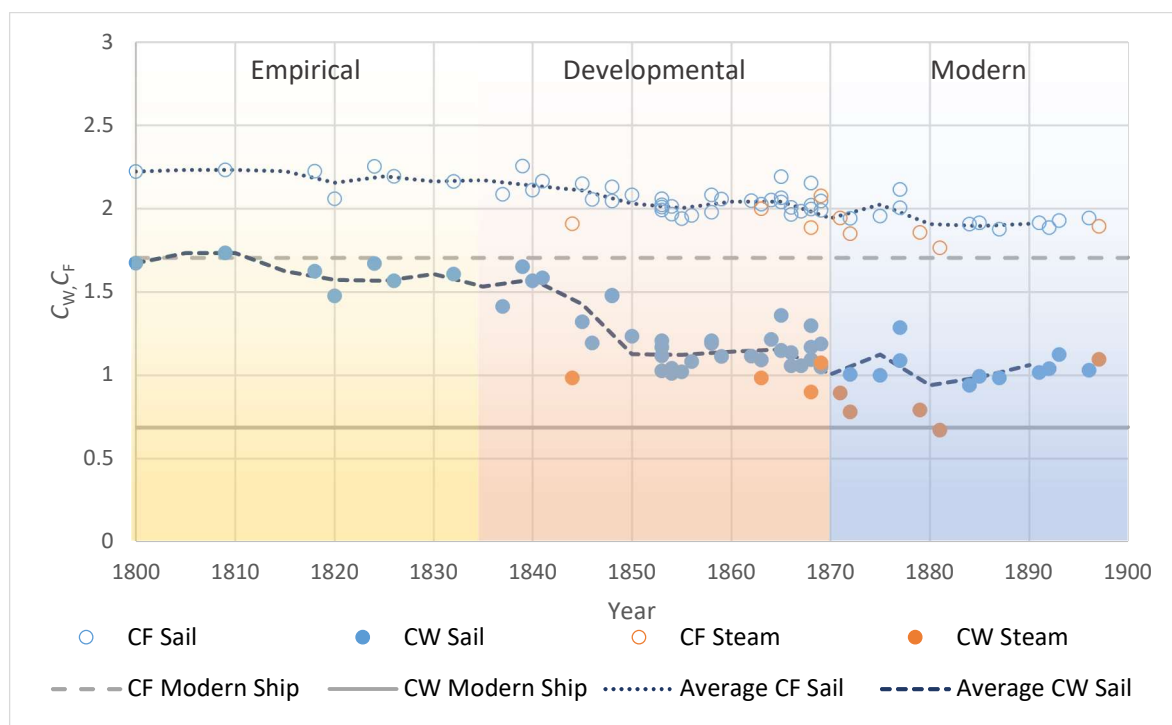


Figure 91: Variation in C_F and C_w with time at $V_s = 5$ kn

The results shown in Figure 91 are for a low speed, where friction is dominant. Figure 92 shows the results for C_w at $V_s = 10$ kn between 1840 and 1870, which gives a clearer view of the changes between the developmental and the modern phase. In this figure it is evident that there is some improvement to the wave-making features of the hull around the beginning of the modern phase, as shown by the reduction in scatter between the developmental and modern phases. It is clear that there are fewer cases where the wave-making is causing a large increase in resistance as a majority of ships adopted a finer hull form, indicating that shipbuilders could have been applying scientific knowledge to reduce wave-making resistance by this time, an impression which is echoed in the discussion of R.E. Froude's (1881) paper.

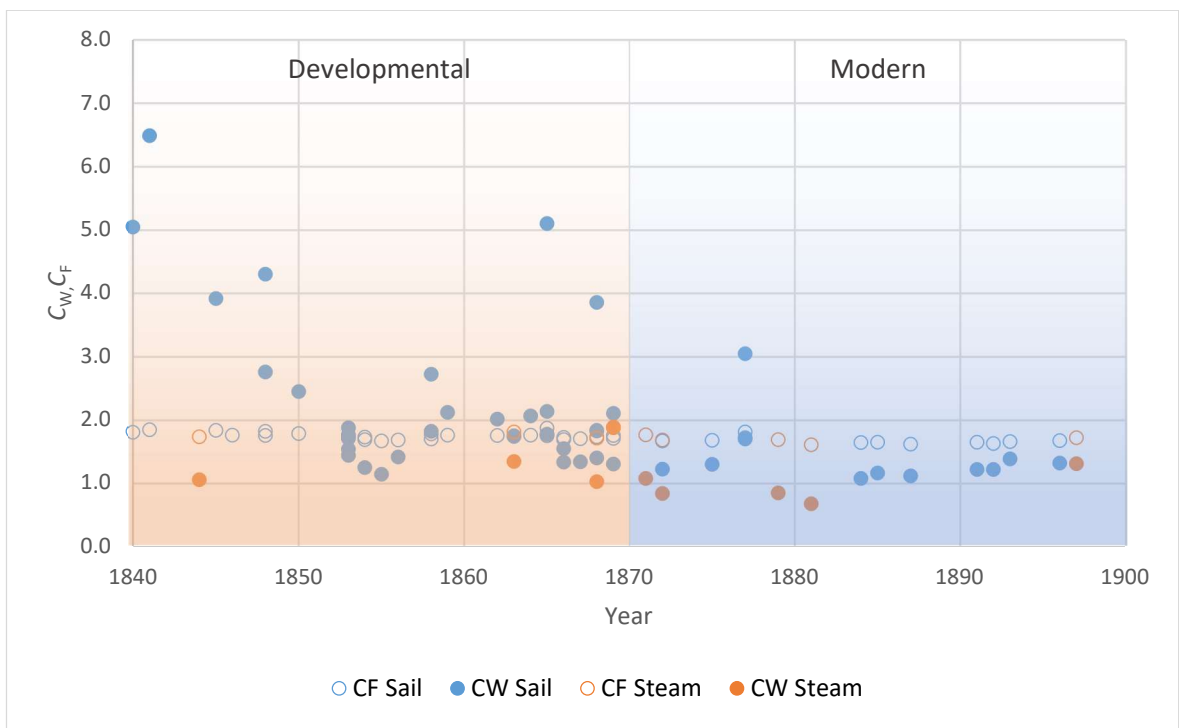


Figure 92: Variation in C_F and C_w with time at $V_s = 10$ kn between 1840 and 1900

An appreciation of the stability of ships also would have had an effect on ship design. Following the disaster of *HMS Captain* in which 480 lives were lost due to inadequate stability in 1870, there was much discussion on how to improve the stability of ships amongst British naval architects (Barnaby, 1871; Wildish, 1872). Although there was clearly an issue related to the stability of ships, there were differing opinions on how it could be improved. Barnaby (1871) argued that increasing freeboard was the most economical solution, more than increasing the beam as suggested by others. Wildish (1872) also supported an increase in freeboard over an assumption that an increase in the metacentric height, which would be achieved by an increase in beam, would increase the stability sufficiently. These discussions coincide with the arguments by Samuel Plimsoll in parliament, asking for regulations on the freeboard for merchant shipping to prevent the overloading of ships (Churchill *et al.*, 2018). In addition to these discussions, W. Froude's (1877) research into the effect of ship length on wave-making resistance found that the effect of beam on resistance was not as significant as some had feared. This was a piece of knowledge that came as a relief for shipbuilders who had been striving to make their ships longer and narrower and were struggling with some of the practical aspects of this (R.E. Froude, 1881, pp. 239–240).

Using the data generated by this research, the impact of these discussions on merchant shipping are examined. There are two main dimensions identified by contemporary naval architects to affect the stability; beam and freeboard. Changes to beam can be seen through comparing the beam-depth (B/D) and length-beam ratios. These are shown in Figure 93 and Figure 94 respectively for 1850 to 1900 for sailing ships, which have a greater reliance on stability in terms of safety. Although there is no clear change in B/D in reaction to the *HMS Captain* disaster, it

Modelled Data and Case Studies

remains consistently higher than 20 years prior to the disaster. The same is true for the L/B .

Considering that a long, thin ship was understood to be hydrodynamically more efficient (Bourne, 1867, p. 23), this indicates that by this point ship designers were prepared to accept the research of W. Froude in regards to ship rolling and resistance, indicating that a wide beam was not necessarily detrimental to ship performance (Froude, 1881).

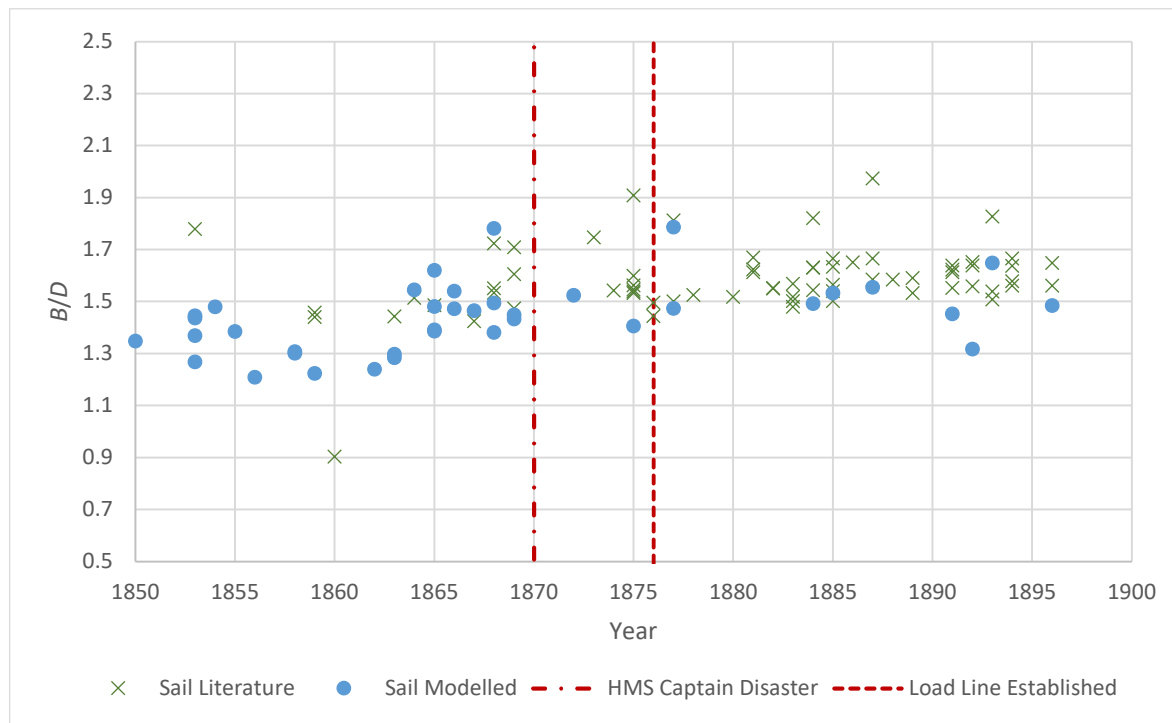


Figure 93: Variation of B/D ratio with time for sailing ships

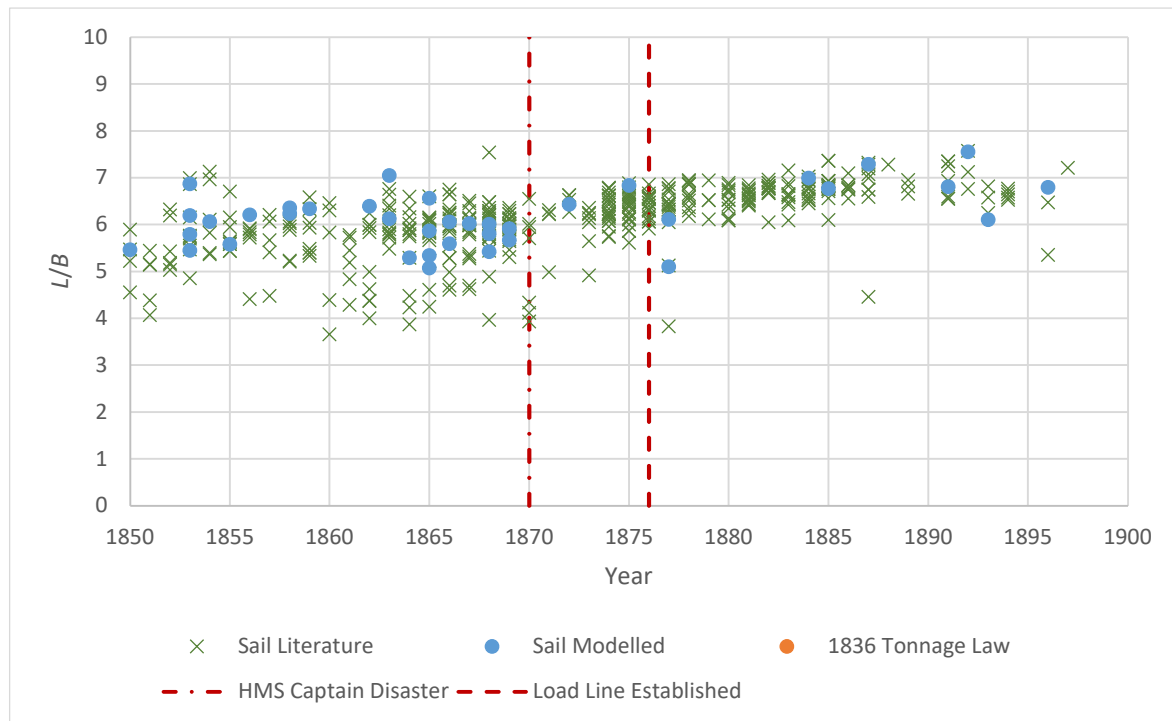
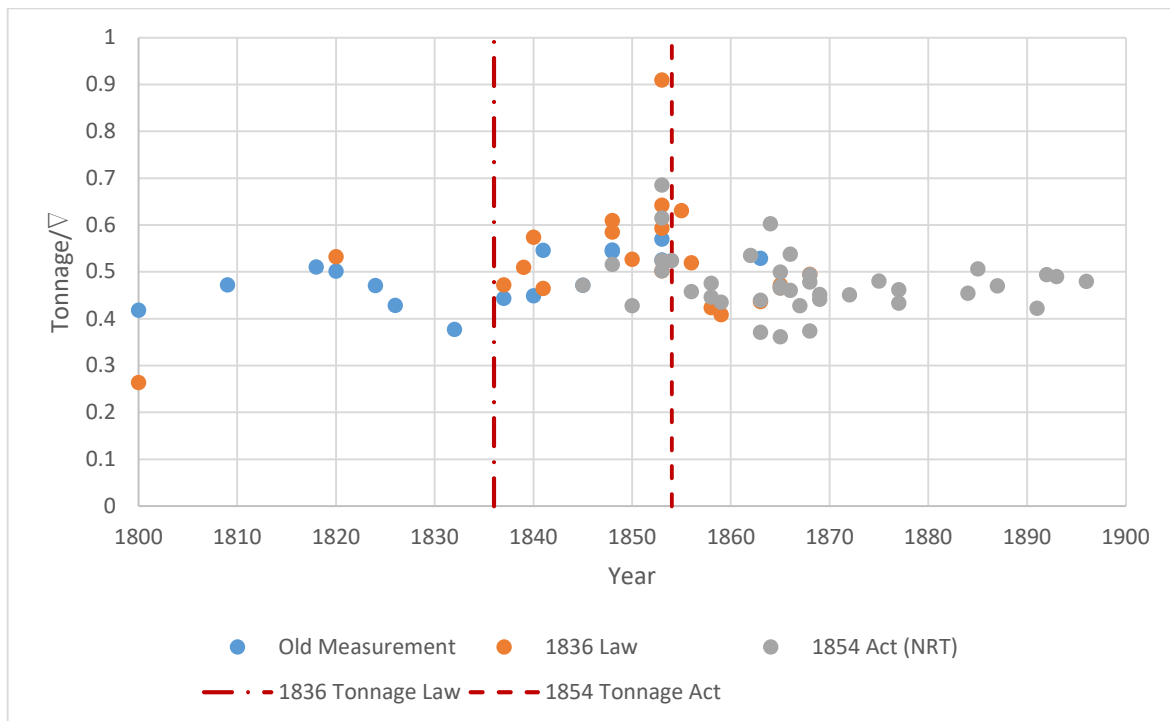


Figure 94: Variation of L/B ratio with time for sailing ships

6.2.3 Impact of the Tonnage Laws

The tonnage laws are often credited with influencing the design of ships (Northcote Parkinson, 1948, pp. 145–146; Corlett, 1975, pp. 2–3; Miller, 1980, p. 125; Geels, 2002, p. 1264). Prior to 1836, the tonnage calculation assumed that the draught of the ship was equal to half of the beam, which was approximately correct when the rule was created (White, 1877, p. 45). As tonnage was used as a means of obtaining tax from a ship, it was desirable to keep the tonnage value as low as possible while maximising cargo carrying capacity. This supposedly encouraged ship designers to build very deep ships with a relatively narrow beam, as any draught above half of the beam was effectively free cargo space (Salisbury, 1966, p. 338). After 1836 the tonnage calculation was based on the cross sectional area at three points along the ship, leading the way for ships to be designed with fine ends to reduce the apparent overall volume (MacGregor, 1988, p. 98). These points are often quoted as one of the reasons why ships before 1836 did not reach the same speeds as their successors (White, 1877, p. 47; MacGregor, 1988, p. 24). However, it has already been shown that the understanding of hydrodynamics may have played a significant part in this, which leaves the question of how much effect the 1836 tonnage law really had.

The ratio between the tonnage of ships and the displacement volume, ∇ , gives an indication of how ship builders managed to keep the tonnage low while maintaining cargo capacity. This relationship is shown in Figure 95 for sailing ships only. Both the 1836 and 1854 laws were adjusted to keep the value comparable with the pre-1836 “old measurement”, although this was not always the case and so for some ships there are multiple tonnage values. Overall, however, the tonnage remains at approximately half of the volumetric displacement in cubic metres. This indicates that the intention to keep the values constant was successful. This is an important point, as previous studies on the development of ship design in the 19th Century have used the variation in tonnage as a measure, which means that multiple methods were needed (Hughes and Reiter, 1958; Mendonça, 2013). Those ships with lower tonnage-displacement ratios would have been better for ship owners as these ships would have been able to carry more cargo with lower taxes. Variation in the pre-1836 “old measurement” clearly shows the tendency to design ships with a lower tonnage, as after 1836 the value from this calculation increases. The post-1836 tonnage law appears to have been harder evade as the ratio increases until after 1854. After this point NRT, which represents the useful cargo carrying capacity of the ships, remains reasonably constant in relation to displacement.


 Figure 95: Variation of tonnage/ ∇ ratio with time for sailing ships

The variation of the tonnage in relation to displacement indicates that ship design was influenced by tonnage laws to some degree. It is impossible to see from the beam-depth ratio shown in Figure 96 the supposed deep draught and relatively narrow beam of ships prior to 1836 discussed in Section 3.1 (White, 1877, p. 47; Salisbury, 1966, p. 338). The same trend is true in the beam-draught ratio, which would have more of an impact on V_s . It is noted by William Salisbury (1966, p. 338) that the beam-draught ratios seen before the introduction of the 1836 law can be found after the change in law too. This is shown clearly in Figure 97, which shows the variation in average B/D and B/T modelled in this research compared with the pre-1836 average value for B/D given by Salisbury (1966, p. 338). It is not until about 30 years after the calculation method was changed that higher ratios are seen, possibly due to the 1854 law. After 1836, however, there was an increase in the length-beam ratio, meaning that although there appears to have been little change of draught and depth compared to the beam, there would have been a decrease relative to the length, as shown by the L/D ratio in Figure 98. This may give the impression of ships becoming shallower, indicating that the correct description for ships built before the 1836 law is that they “were too deep for their length” (Salisbury, 1966, p. 338).

Modelled Data and Case Studies

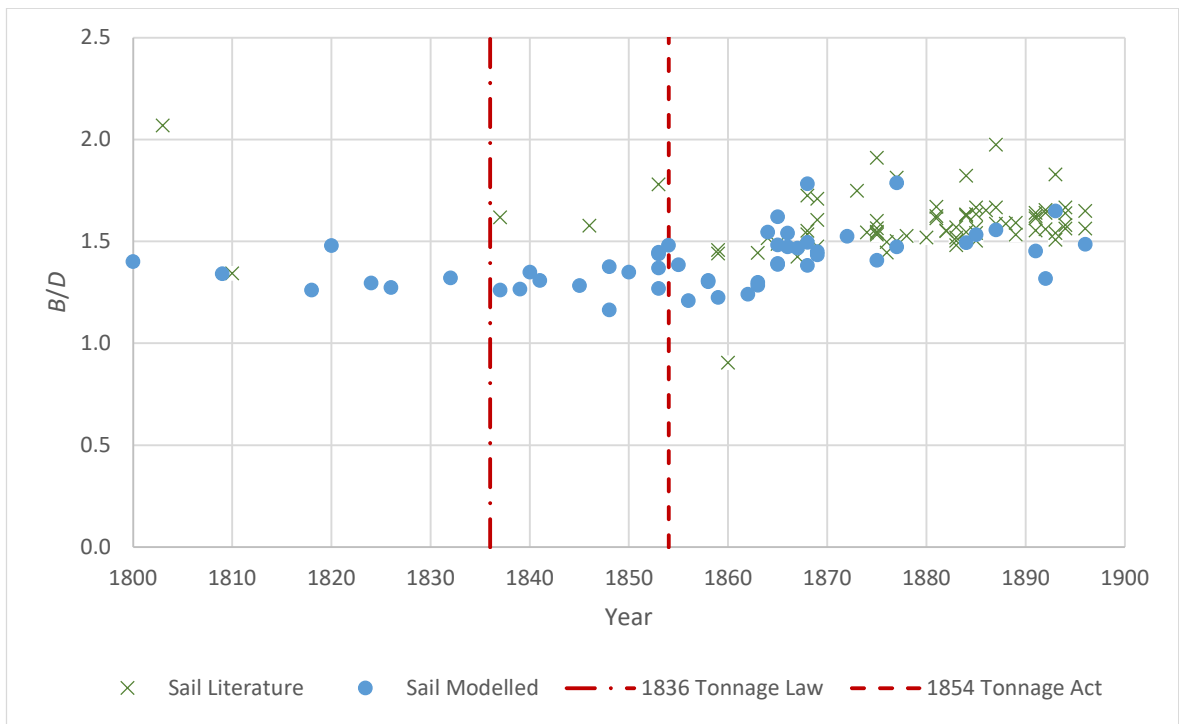


Figure 96: Effect of tonnage laws on B/D

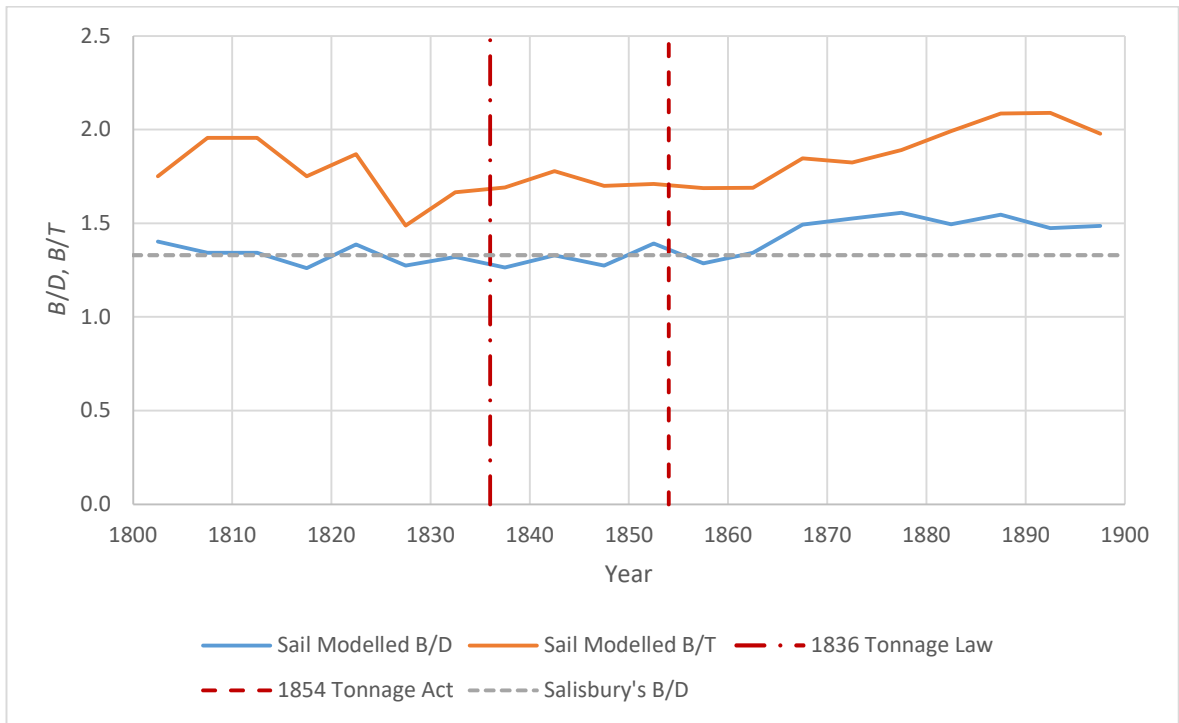


Figure 97: Average B/T and B/D ratios for sailing ships compared with Salisbury's value (Salisbury, 1966, p. 338)

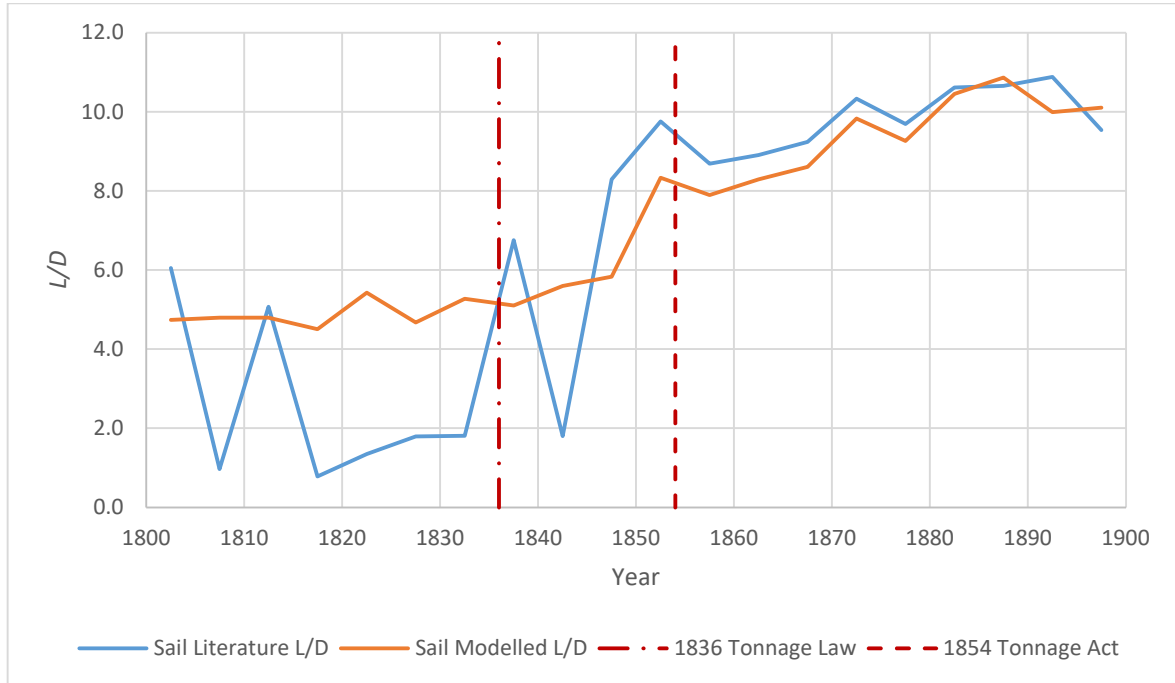


Figure 98: Effect of tonnage laws on L/D

The 1854 Tonnage Act, which came as part of the 1854 Merchant Shipping Acts, also had a potential influence on the form of ships, although the difference in measurement with the previous law was more subtle and so there is less commentary on the subject. The move from an estimate of volume based on three points, as given in the 1836 law, to a more comprehensive estimate reduces the potential ways in which the calculation could be exploited. If ship design was entirely dependent on tonnage laws, then following the 1854 Act, ships would no longer require the fine ends that they had adopted in the preceding years. Figure 99 shows the effect of both tonnage laws on the angle of the bow. Although there is not an instant increase in the fineness of the bow, there is a definite increase in the rate of change after the 1836 law. This may be in part due to the understanding of hydrodynamics, as discussed previously, but the tonnage law can be said to have played a part, as sources from the time indicate. The strong evidence that the “Aberdeen bow” was invented by the shipbuilder Alexander Hall as a method of bypassing the tonnage laws supports this (MacGregor, 1988, pp. 105–108). Post-1854 there is less evidence, but Figure 99 indicates that the bow shape remained reasonably constant from this point. Attributing this phenomenon solely to the Tonnage Act is difficult, as there are so many other considerations behind bow shape. For example, the practical side of having a narrow bow must be considered, as cargo space is necessarily limited and construction becomes difficult.

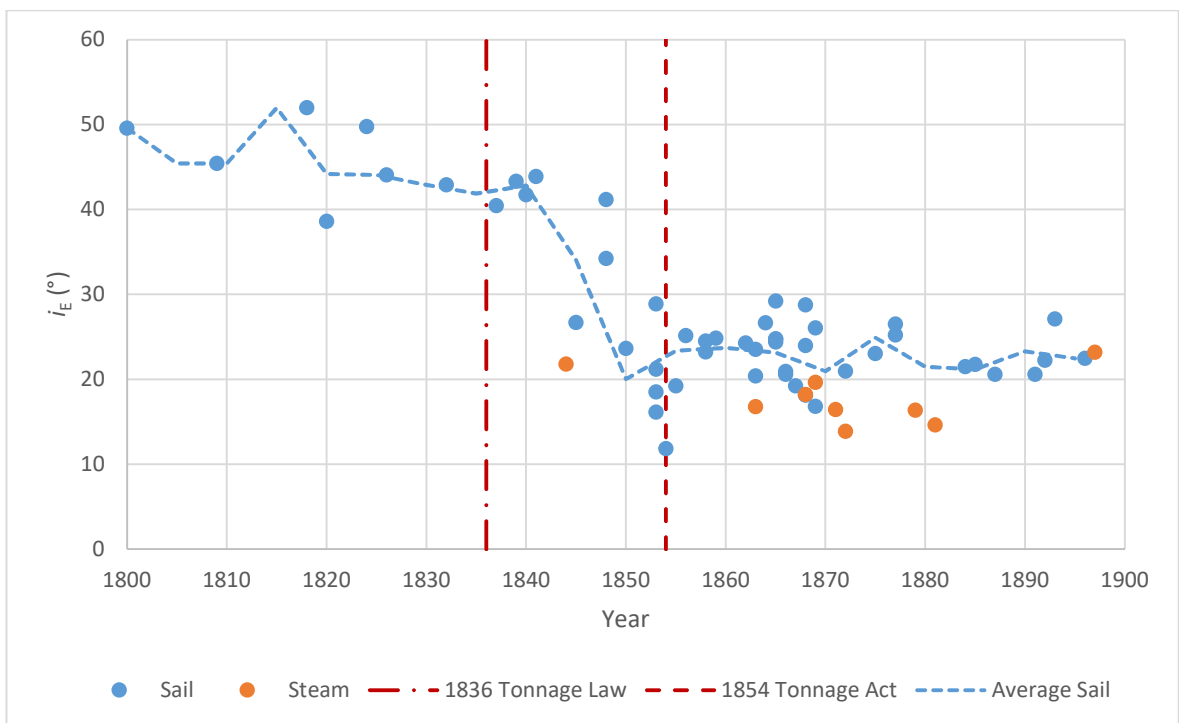


Figure 99: Effect of tonnage laws on i_E with a 5-year average line for sailing ships

These results show that the impact of tonnage calculations was not as straightforward as is often supposed. Although there is evidence to support that they had an effect on the design process, the impact is a lot more complicated and perhaps less significant than it is often made out to be. For example, the removal of the assumption of depth appears to have little instantaneous effect, even with those ships which were measured by the 1836 law. It is not until after the 1854 Tonnage Act that any variation in depth relative to the beam occurs. It is possible that any earlier appearance of reduced depth relates to the relationship with length, as ships did indeed become shallower relative to length. One of the other design factors associated with the tonnage, i_E , does appear to have been influenced by the 1836 law, although as described in Section 6.2.2, there are additional reasons for the narrowing of the bow.

6.2.4 International Influence

Another common belief is that British ship design remained stagnant until exposed to new and better designs from other nations (Lubbock, 1914, pp. 108–109; McDowell, 1952, p. 110; Kemp, 1978, p. 199; Jefferson, 2014, p. 5). These effects would be shown by an increase in overall ship speed, as foreign nations were adopting faster, clipper style hull forms (MacGregor, 1988, p. 38). Owing to the strict navigational laws and protectionist policies in place in the first half of the century, it is reasonable to assume that this was the case (Geels, 2002, p. 1264). However, the evidence produced in this research indicates that this was not necessarily the most significant influence. The USA is often considered as the nation that had the greatest influence on British ship design, owing to their history of building fast ships with the purpose of blockade running

(Kemp, 1978, p. 199; Rinman and Brodefors, 1983, pp. 22–23; Geels, 2002, p. 1264; Davis, 2009, p. 181).

Figure 100 shows the variation in maximum ship speed of British ships in 30 kn of wind in relation to the repeal of the Navigation Acts. When compared with the American clipper *Sea Witch* (1846) it is clear that she was faster than her British counterparts were. Although it is difficult to draw any definitive conclusions from one ship, the speed of *Sea Witch* indicates that some American ships were capable of achieving higher speeds than British vessels. However, when considering the period shortly after the lifting of the Navigation Acts, it would appear that British and American designs could easily compete with each other. This is shown by the extreme clipper *Lightning* (1854). *Lightning* was British owned, but built in New York by Donald McKay to an American design (MacGregor, 1988, p. 189). Although amongst the fastest of the ships shown in Figure 100, the similarity between the speed of *Lightning* and the British *Schomberg*, launched a year later shows that there were definitely comparable designs, although as they were owned by the same person there may have been some crossover in the design despite the use of an “Aberdeen bow” in *Schomberg* (MacGregor, 1988, p. 194). It should be noted that although *Schomberg* appears marginally faster, at these speeds *Lightning* exceeded her freeboard in the VPP and so is not sailing as close to the wind. However, even without this limitation there is only a very small margin between the two.

The myth that the British clipper only came into existence after the lifting of the Navigation Acts in 1849 would only be supported if there was a sudden and distinct change to ship dimensions and performance. Contrary to this, it appears instead that there was a gradual change to ship design that had begun some 20 years previously, indicated by the period of improvement shown in Figure 100. There is a slight improvement in performance shortly after 1850, which may be credited to the increased competition between British and American ships, but there is also enough evidence to question how much influence international ship design actually had on British ships. Following from the discussions on other influences, it is possible that the improvement in British ship design may have followed the same trend without international influences.

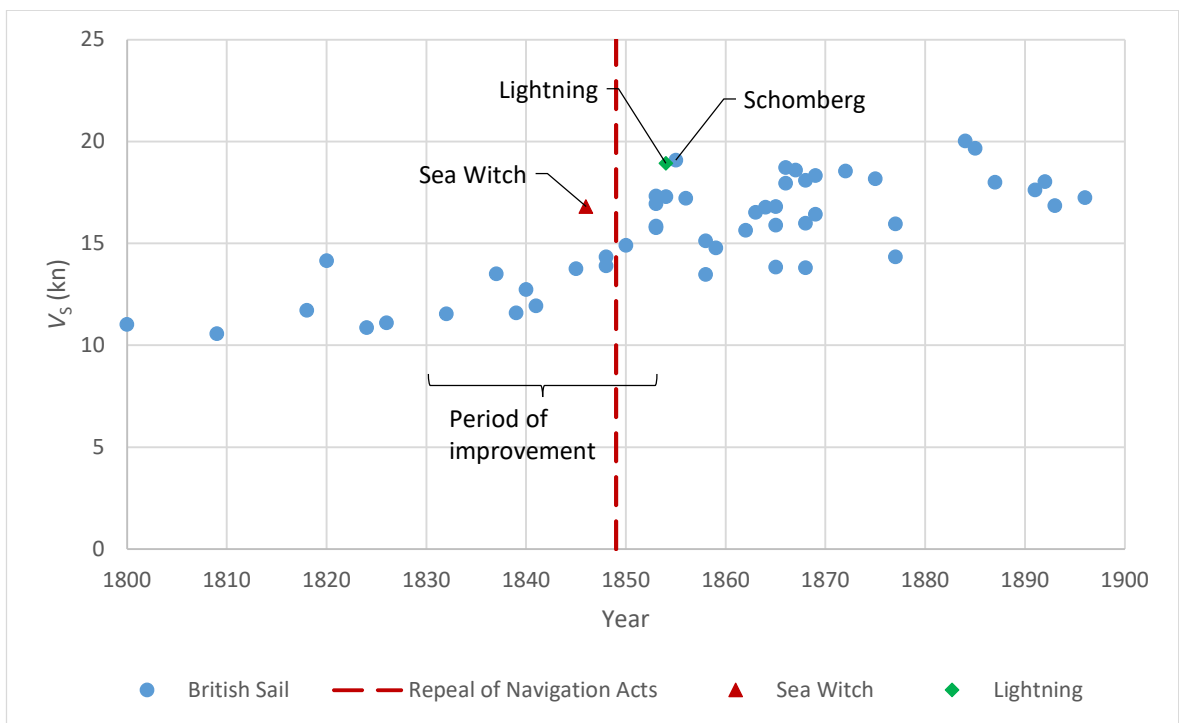


Figure 100: Increasing V_s of British ships in relation to American clippers ($V_T = 30$ kn)

6.3 Technical Impact

In addition to the causes behind evolution, it is also possible to see individual changes on technical aspects relating to 19th Century British merchant shipping. Quantitative evidence relating to ship design and performance enables common beliefs to be challenged, in particular those beliefs relating to certain ship types and uses.

6.3.1 The Effect of Rigs

The question of how the intended purpose of a ship affects its performance is a complicated one, due to the many different factors that may influence the performance. Because of this, it is difficult to determine the effect that the route or trade of a merchant ship may have on design. Instead, the focus needs to be on the individual factors, for example a vessel's ability to sail in different wind conditions. Any variation between the performance under a given wind angle will be due to either the sails or the hull. It has been shown by the force coefficients that the majority of the change to speed over the 19th Century was caused by the developing hull designs, but there is still a potential to determine if the type of rig has an effect on performance.

The two most common rigs in the dataset are ship and barque rigs. These are both primarily square-rigs; however, a barque does not have square sails on the mizzen mast. Historically a barque rig was preferred as it required fewer crew to obtain a similar performance (Allen, 1980, p. 22; McGowan, 1980, pp. 30–31; Bennet, 2005, p. 24), which is a cost saving. This can be examined by comparing speed between the two rigs. Figure 101 and Figure 102 show this comparison for downwind and upwind conditions respectively. Despite claims that the performance can be

Modelled Data and Case Studies

maintained by switching to a barque rig, this is clearly not the case, with the barque-rigged vessels achieving a consistently lower speed than the ship-rigged vessels. This indicates that there was some loss in performance when going between the two rig types, equating to 1 to 2 kn.

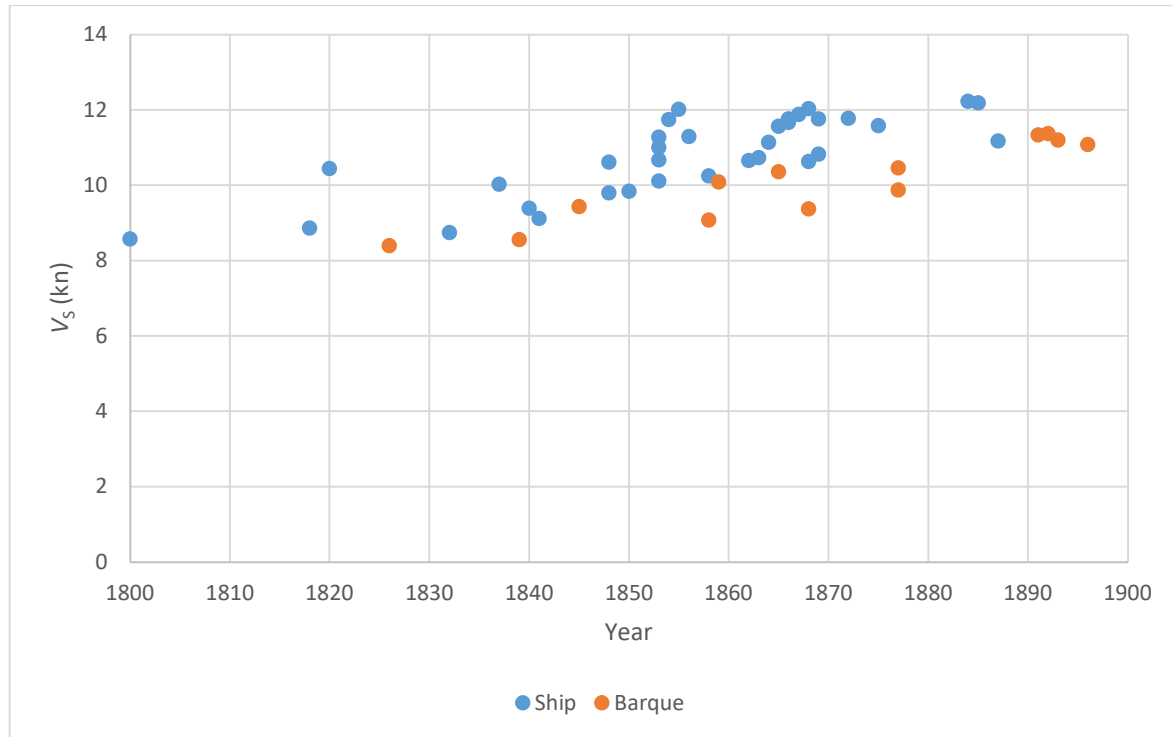


Figure 101: V_s of ship-rigged vessels relative to barque-rigged downwind ($V_T = 15$ kn, $\gamma = 130^\circ$)

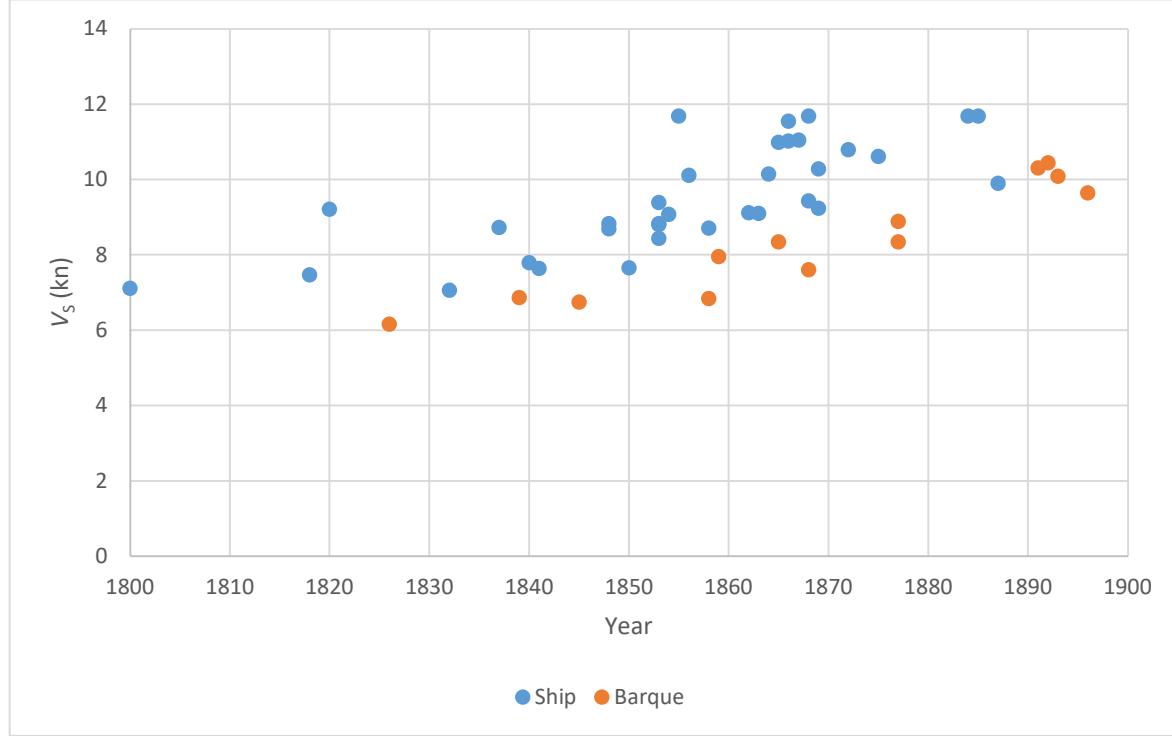


Figure 102: V_s of ship-rigged vessels relative to barque-rigged upwind ($V_T = 15$ kn, $\gamma = 70^\circ$)

In order to see what effect this would have on an individual vessel, where, for example, the rig has been changed at some point, an estimate of the sail areas for both rig types can be obtained to create a polar diagram. Figure 103 shows this for the 4-mast iron ship *Wendur* (1884) which

was reduced to a barque rig in 1906 (Caledonian Maritime Research Trust, 2019). The wind conditions selected were for a 15 kn wind with sails set to the optimum angle within 2.5°, which gives a maximum ship speed of about 12.4 kn in the original ship-rig, and approximately 0.7 kn less for the barque-rig. Given methods of measuring speed at the time, this difference may have gone unnoticed; however, it would have resulted in the equivalent of two extra days of travel time on a three-month voyage, which is approximately the time taken by a clipper to sail home to the UK from China (Lubbock, 1924, p. 85). Depending on the cargo carried, it is possible that the cost saving in crew numbers would outweigh the cost of a two-day delay, particularly later in the century when speed was not so important (Allen, 1980, p. 22; Bennet, 2005, p. 24). In addition to the decrease in speed, there is also a small increase in leeway, with a maximum difference of 0.5°.

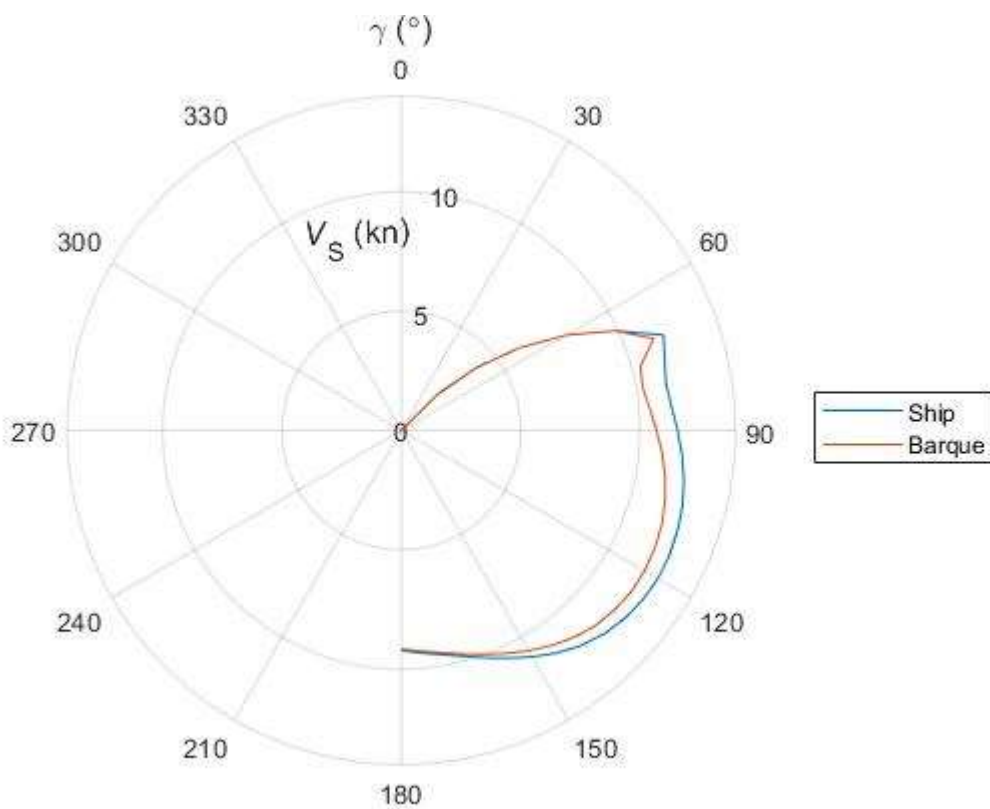


Figure 103: Comparison between ship and barque-rigs for *Wendur* (1884) ($V_T = 15$ kn, $\theta = \text{Variable}$)

The difference between the two rigs in terms of ship speed is surprisingly distinct. The reasons behind this may be determined by examining the force coefficients for each rig type. The downwind C_T at 10 kn is shown in Figure 104. These results are a lot closer than for overall ship speed, especially in the second half of the century, even though the barque-rigged vessels have around 200 m² less sail area than the ship-rigged vessels. This equates to a 15% difference in a three-mast vessel with a length of 50 m and a length-beam ratio of 5.0.

The C_{RT} for forwards resistance shown in Figure 105 indicates that the barque-rigged ships have slightly less efficient hulls than the ship-rigged vessels, supporting the idea that the hull influences

Modelled Data and Case Studies

the sailing ability of each rig type. This is again surprising, as in several instances vessels had their rig changed over the course of their lives. As the ships in this dataset are considered in the as-launched condition, with their original rigs, this may be the reason that the hull forms are showing a difference.

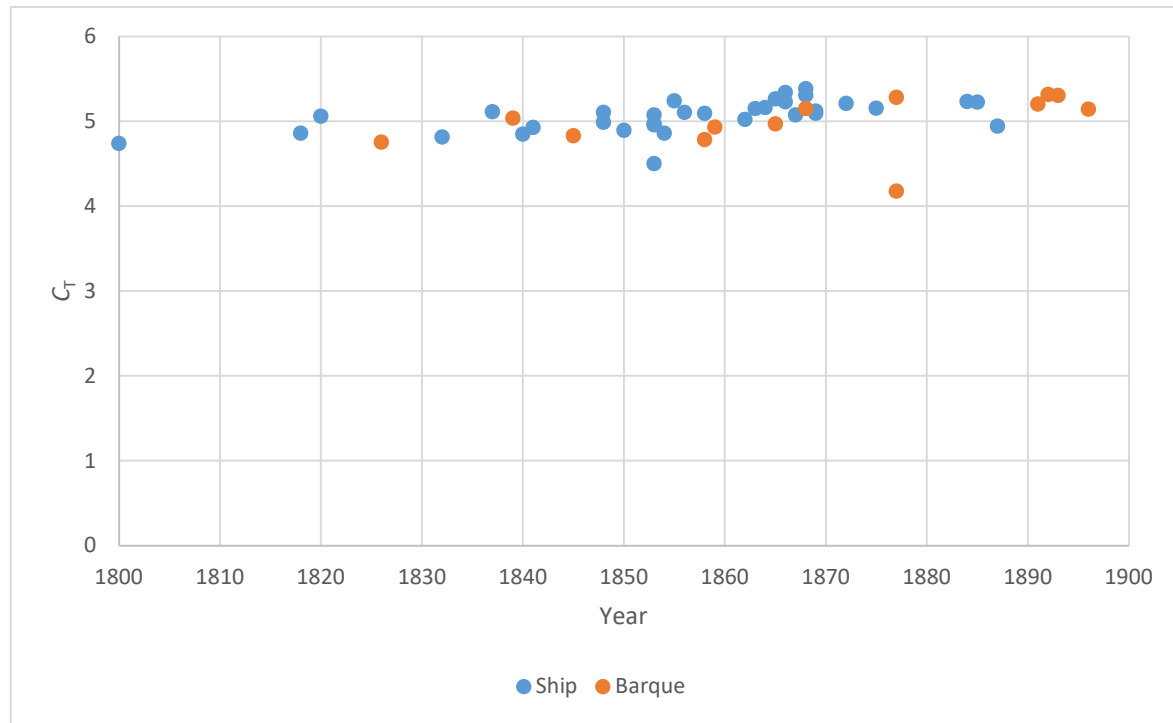


Figure 104: Differences in C_T between ship and barque-rigged vessels ($V_S = 10 \text{ kn}$, $V_T = 15 \text{ kn}$, $\gamma = 130^\circ$, $\theta = 40^\circ$)

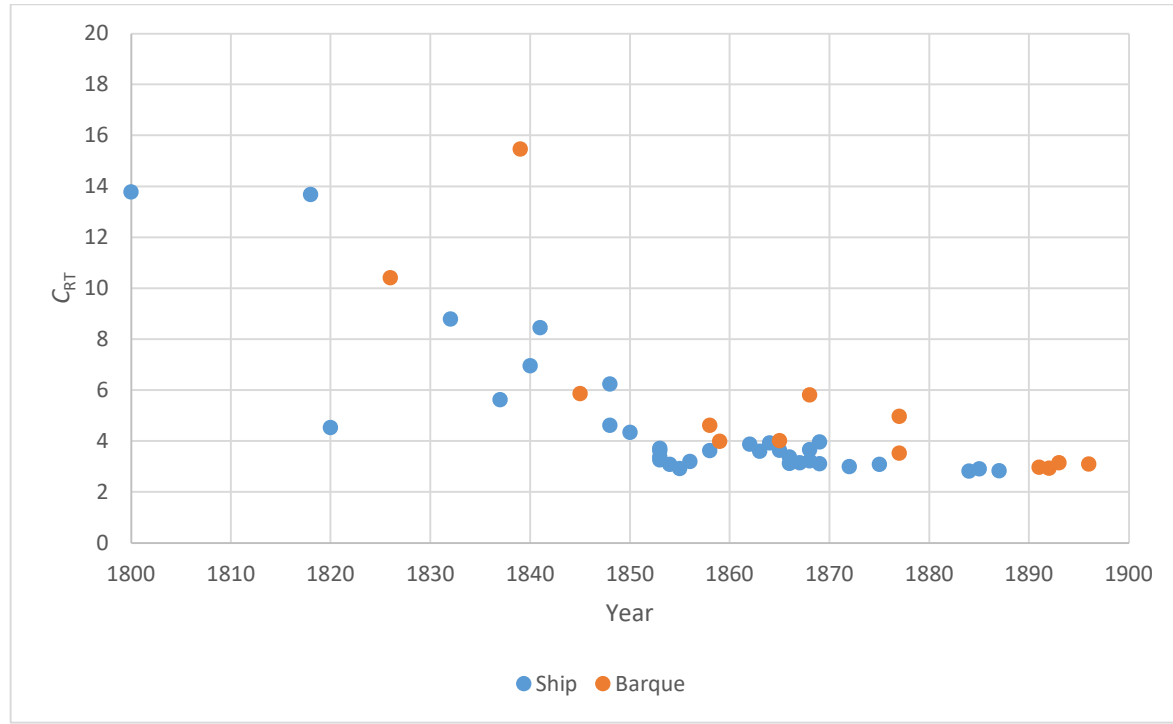


Figure 105: Differences in C_{RT} between ship and barque-rigged vessels at $V_S = 10 \text{ kn}$

It is still possible that there were some features of a hull that lent it to being barque-rigged. As barques are fore-and-aft rigged on the mizzen mast, this would suggest that they are more prone

to leeway, as there is a greater lateral force (Palmer, 2009b, p. 314). This means that the hull would need to have a larger underwater lateral area to counter the wind, which would increase the added resistance due to leeway. This is shown by the coefficient of hydrodynamic side force (C_{HS}) and the coefficient of aerodynamic side force (C_{AS}), defined by:

$$C_{HS} = \frac{S_H}{1/2 \rho_W WSA \cdot V^2} \quad (42)$$

$$C_{AS} = \frac{S_A}{1/2 \rho_A A_{S,T} V^2} \quad (43)$$

These values are shown in Figure 106 and Figure 107. These show that the barque-rigged vessels have both a higher aerodynamic and hydrodynamic side force than the ship-rigged vessels. This accounts for the other reason given for choosing a barque-rig over a ship-rig: the manoeuvrability (Allen, 1980, p. 22). The increased aerodynamic side force of the barque would enable a ship to come about faster when required, although the hydrodynamic side force would also need to be greater to prevent excessive leeway while under sail.

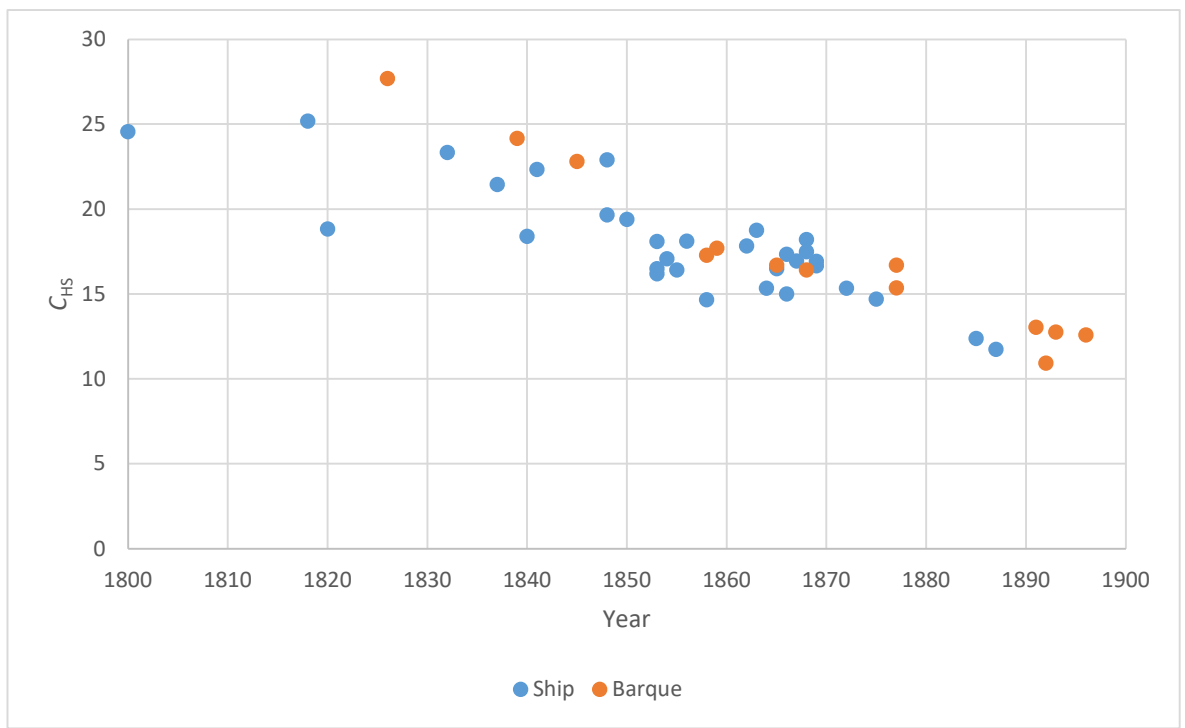


Figure 106: C_{HS} of ship-rigged vessels relative to barque-rigged at $\lambda = 5^\circ$

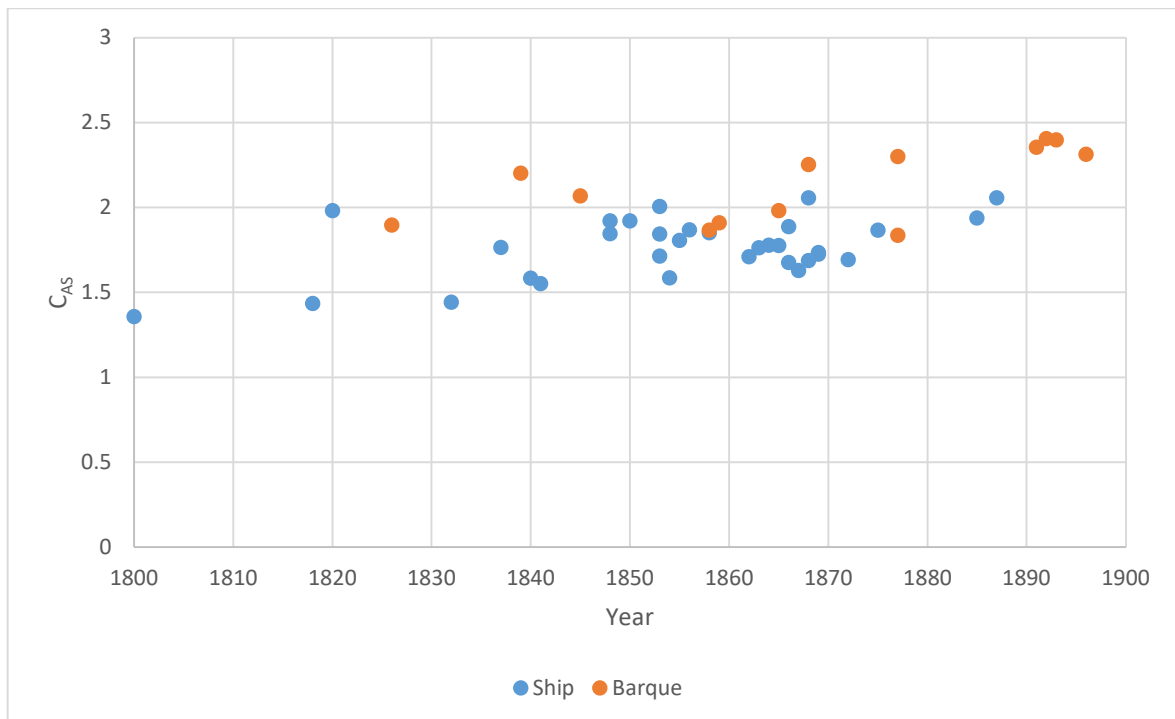


Figure 107: C_{AS} of ship and barque-rigged vessels at $V_s = 5 \text{ kn}$ ($V_f = 20 \text{ kn}$, $\gamma = 130^\circ$, $\theta = 40^\circ$)

From this data it appears that ship rigged vessels were better at sailing both upwind and downwind than barques of the time. The implications of this are that as much as 2 kn of speed could be lost through having the wrong rig. However, this section highlights that for merchant ships performance was not necessarily based solely on how fast the largest amount of cargo can be moved between two places, but how cheaply. The cost saving from reducing the crew number may have been enough to outweigh potential loss from arriving a few days late, particularly for low-value cargoes.

6.3.2 The Decline of the East India Company

“[East Indiamen] were of quite as bad a type as the ships of the more humble merchant marine” (Clark, 1970). This claim by Captain Arthur H. Clark, an American merchant captain of both sail and steam ships, is rather bold considering that it stems from ship particulars he had at his disposal (Clark, 1970). Although the ships on which he based this conclusion on are unknown, the data produced from this research allows the claim to be tested. The question is whether they are in fact representative of merchant ships at the time, and if not, why do they perform differently?

The East Indiamen were perhaps the most famous merchant ships at the beginning of the 19th Century. The EIC held the monopoly on trade to India and China until 1823 and 1834 respectively, meaning that their ships were responsible for a significant portion of British overseas trade (MacGregor, 1980a, p. 171). The ships themselves were amongst the largest in use at the time and were heavily armed, meaning that they are sometimes considered alongside warships rather than merchantmen (McGowan, 1980, p. 23). A significant number of them were actually bought

by the navy later in their lives (Hackman, 2001). Even after the termination of the EIC monopoly in 1834, a number of ship owners continued to build ships in the same vein as the East Indiamen, known as the “Blackwall Frigates” after the area in London in which many of them were built (Clark, 1970; MacGregor, 1984a).

Out of the ships considered in this research, three are counted as East Indiamen or Blackwall Frigates. Although they are often compared to the tea clippers and treated as old, obsolete ship designs (Tonry *et al.*, 2014), the results of this analysis suggest otherwise. Returning to Clark’s (Clark, 1970) suggestion based on the ship particulars that East Indiamen were no better than standard merchantmen, it can be seen by Figure 108 how this conclusion may have been drawn. Examination of the length-beam ratio, which is usually considered to be one of the primary drivers behind ship performance, shows that there is little to distinguish the East Indiamen from other ships at the time. Similarly, for B/T there is no distinguishing difference between the ship types. In the results for speed, however, shown in Figure 109, the East Indiamen are shown to be capable of achieving speeds higher than their contemporaries achieve. Another point to note is that, where the speed of ordinary ships appears to increase, the East Indiamen appear to be making little or no improvement.

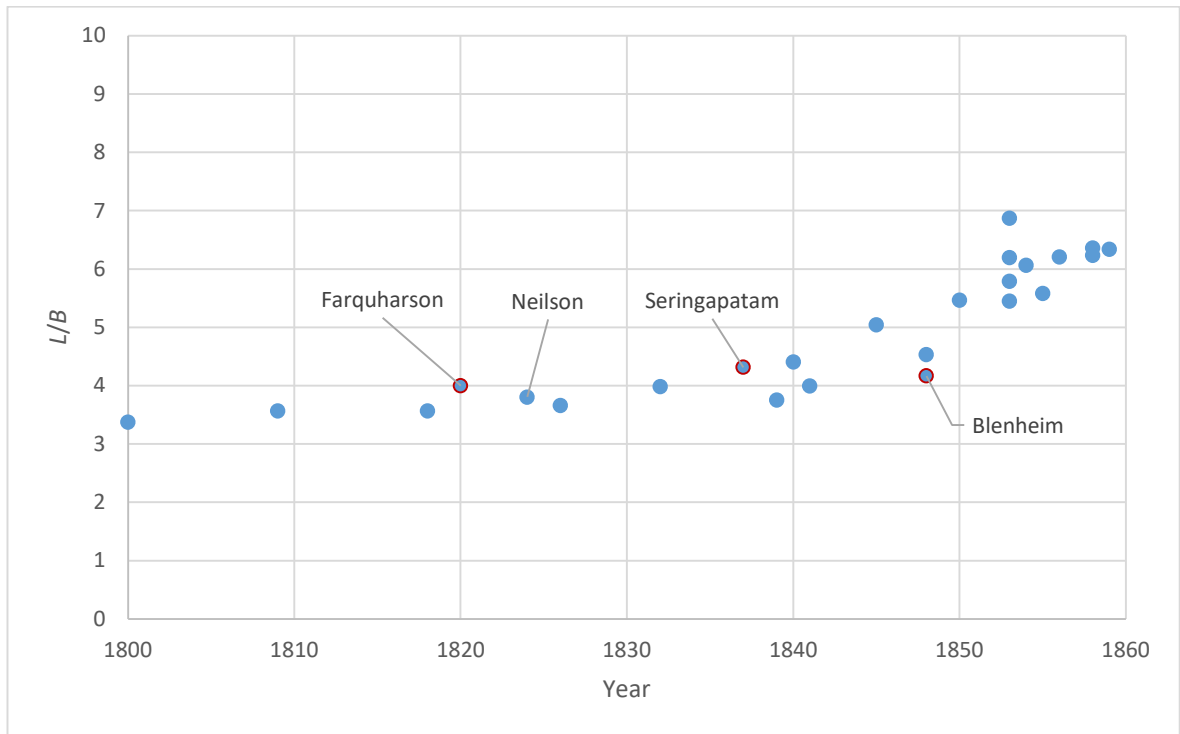


Figure 108: L/B ratio comparison between East Indiamen and other sailing merchant ships

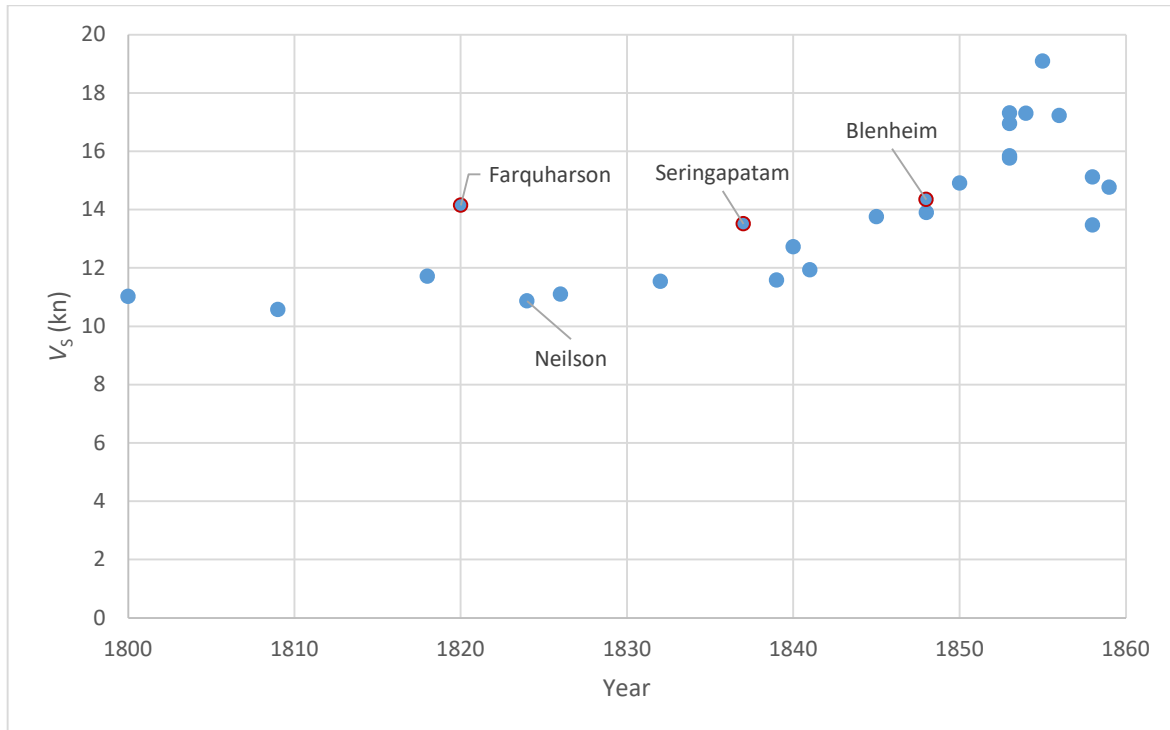


Figure 109: V_s of East Indiamen compared to other merchant ships ($V_T = 30$ kn)

This apparent stagnation in performance is shown more clearly when considering resistance.

Figure 110 shows that C_{RT} remains constant for East Indiamen, even when other ships have improved to match them. This is further revealed when data for an earlier East Indiaman, *Sir Edward Hughes*, is included. *Sir Edward Hughes* was built in India in 1784 (Hackman, 2001, p. 192) and gives a value of C_{RT} similar to the other three, much later ships. This may be due to differences between Indian and British shipbuilding methods, but as a ship built specifically for the EIC, it is unlikely that there would be any major design differences with their other vessels (Northcote Parkinson, 1948, p. 144; MacGregor, 1980a, p. 185, 1988, p. 64).

The fact that the C_{RT} of East Indiamen were significantly lower than other merchantmen indicates that, despite the similar principal particulars, there was something about the hull forms of the East Indiamen that led to an improved performance compared to the other earlier ships. There are two dimensions that have been identified as the possible cause of this: sharpness of the bow and displacement. As these ships were amongst the largest sailing at the time, this meant that they had a significantly larger capacity. As there is little difference in the basic dimensions, this indicates that the improved performance lies in the distribution of this displacement. Although there appears to be no explanation of why, it seems that the bows of the East Indiamen were slightly finer than others, positioning more of this displacement aft and consequently reducing the wave-making properties of the ship.

Figure 111 shows a comparison between the body plan of the East Indiaman *Farquharson* (1820) and the West Indiaman *Neilson* (1824). Although *Neilson* is about half the length of *Farquharson*,

the distinct differences in the form of the lines can be seen. The bow of *Farquharson* is considerably finer than that of *Neilson*, which in turn supports a much narrower stern. In addition to this the overall form of *Farquharson* appears to be finer, an impression supported by the length-displacement ratio.

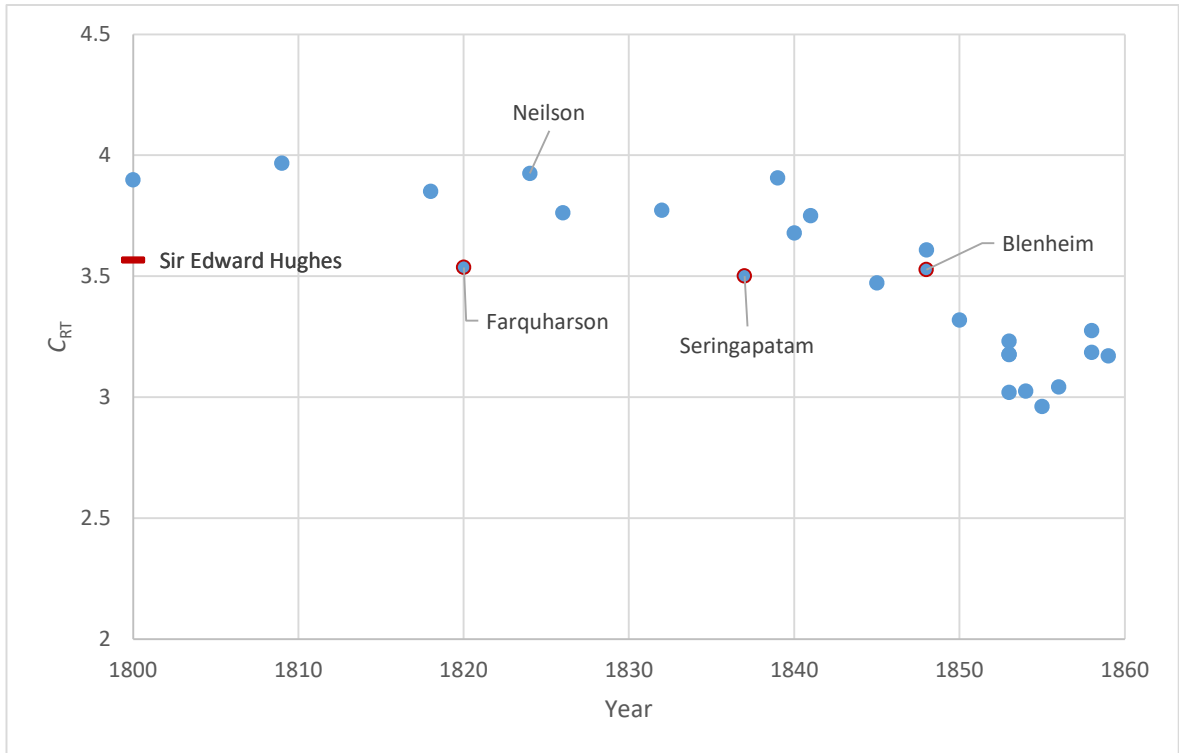


Figure 110: C_{RT} of East Indiamen compared to other sailing merchantmen

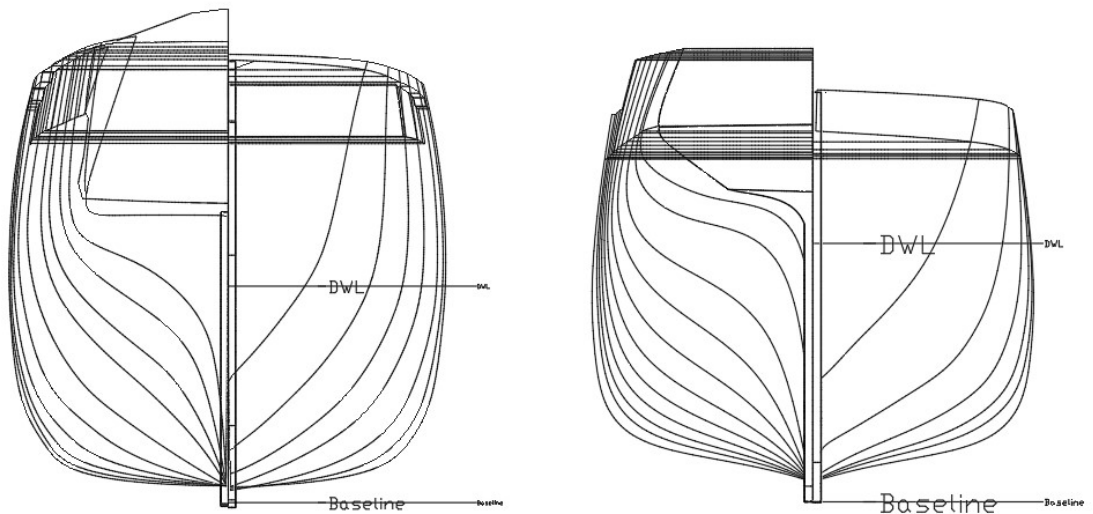


Figure 111: Comparison of the East Indiaman, *Farquharson* (Left), and the West Indiaman, *Neilson* (Right) – Not to scale

The ratio between the length and displacement appears to be the key to the differences between the East Indiamen and other ships. This is shown by Table 19, which compares the length-displacement ratio and half angle of entry of the East Indiamen, with those of *Neilson* and the average for other modelled sailing ships from between 1800 and 1840. These indicate that the

19th Century East Indiamen were a great deal finer than average. *Sir Edward Hughes* shows the same trend for the length-displacement ratio, although the fineness of the bow is equivalent to that of the later merchantmen.

Table 19: Parameter differences between East Indiamen and other ships prior to 1840

	$L/\nabla^{1/3}$	i_E
Average (1800-1840)	3.425725	46.09935
Neilson	3.523816	49.77248
Sir Edward Hughes	3.753733	48.1
Farquharson	3.768971	38.59283
Seringapatam	3.693573	40.43725
Blenheim	3.906406	41.18235

These results suggest that the design of East Indiamen may have been more advanced than they are credited with, and that they followed similar design conventions. The reasons to why this may be could lie with the differences in use between an East Indiaman and a standard merchantman. The EIC ships were generally larger and more heavily armed (Northcote Parkinson, 1948, pp. 144–145). They were exempt from the smuggling laws limiting L/B to 3.5 (*Smuggling Act (Geo. III C.47)*, 1782), although they were still subject to the tonnage laws that supposedly favoured deep, narrow vessels (Miller, 1980, p. 125). As the EIC began to lose their monopoly in 1813 and the measurement rule did not change until 1836, this may still have been a design consideration. In addition to this, the advantages of having a bluffer bow on cargo capacity may have been less important economically on a ship that size. It is noted by Clark that no one really knew what speeds the East Indiamen were capable of because they were never pushed in the way that perhaps a clipper was (Clark, 1970). This makes it seem unlikely that the hydrodynamic advantage was caused by a desire for greater speed.

Based on this research, it appears that East Indiamen should not be considered as typical merchantmen, although there are not enough plans of East Indiamen available to draw definitive conclusions about the ship type as a whole. Considering the ships were almost exclusively chartered to the EIC rather than owned by them (MacGregor, 1980a, pp. 171–172), it is also difficult to say if there were any particular design rules that could separate them from other merchant ships. What is evident, however, is that there is a need to establish what is “typical” when running a comparison between ships, and that examining the principal hull dimensions is not enough to infer performance. Care must also be taken when comparing ships from different time frames, as the definition of “good” performance will vary. This case study highlights the strength of the VPP for aiding performance comparisons, particularly in cases where there is little

or no data. Without the speeds calculated, it would have been very difficult to determine the difference between East Indiamen and standard merchantmen.

6.3.3 Clippers and Windjammers

There is a tendency for narratives on the development of ships to describe the opening of the Suez Canal in 1869 as the final nail in the coffin for sailing ships (McDowell, 1952, p. 114). Even the most complete works on the development of merchant sailing ships in the 19th Century fail to consider ships beyond 1875 (MacGregor, 1984b, 1988), meaning that the later ships are discounted from the discussion. The opening of the Suez Canal may have been the beginning of the end for the China tea clippers, but on certain routes sailing ships continued to be a viable option and the construction of large steel sailing ships continued until 1897 (Greenhill, 1993, p. 92). These later vessels are often overshadowed by their smaller, finer lined predecessors. The class of sailing ship that reigned from the 1880s until the end of viable commercial sailing were known as the “windjammers”. These ships were larger than the clippers, with full bodies designed for carrying cargo over speed (Lubbock, 1953a). Because of this they are often considered to be slower (McDowell, 1952, p. 117). It could be that in this case the appearance and popularity of the clippers has contributed to the belief that they were the superior ships of the 19th Century, although that in itself is subjective.

Literature varies so much on its opinion of windjammers and clippers that it is difficult to compare them. The “zenith” of sail has been used separately to describe both (McDowell, 1952, p. 114; Allen, 1980, p. 22), which asks the question if one was truly superior to the other. Each type was built with a different focus on performance; the clippers favoured speed over capacity owing to their high value cargo of things like tea (Geels, 2002, p. 1266), whereas windjammers were forced to survive with bulk cargoes such as nitrate or grain (Greenhill, 1980, p. 45) and so capacity was more important (Lubbock, 1953b, pp. 9–10; Geels, 2002, p. 1270). In this case, it is therefore important to consider both speed and capacity when determining performance.

Figure 112 shows a comparison between these two factors using the average downwind ship speed ($V_T = 15 \text{ kn}$, $\gamma = 130^\circ$), upwind ship speed ($V_T = 15 \text{ kn}$, $\gamma = 70^\circ$) and cargo capacity at five year intervals between 1840 and 1900. The speeds are based on the output of the VPP, and the cargo is based on the tonnage as described in Section 5.4.4.

There are two points that are in agreement with literature. First, that on average the ships in the final 25 years have a greater cargo capacity than their predecessors; second, that the upwind sailing capability of the windjammers was superior to the clipper ships. There is no support, however for the claim that windjammers were slower overall. Even if the apparent difference between the later clippers and the windjammers is due to the vessel selection, it appears that the

Modelled Data and Case Studies

windjammers were at least equal in downwind sailing speed to the ships in the clipper era, and in terms of performance had the potential to be better, as they were capable of carrying more cargo. In terms of profitability of the ships, this would have been more important for the bulk cargoes of the windjammers. For clipper ships, however, which relied on low-volume, high-value cargoes, extra capacities were not necessary, which accounts to some extent for the lower capacities in the clipper era. Even if ship owners had attempted to increase the capacity of the clippers, however, given the technology and understanding of hydrodynamics at the time, as described in Section 6.2.2, this may have served only to decrease the speed and increase build and crew costs.

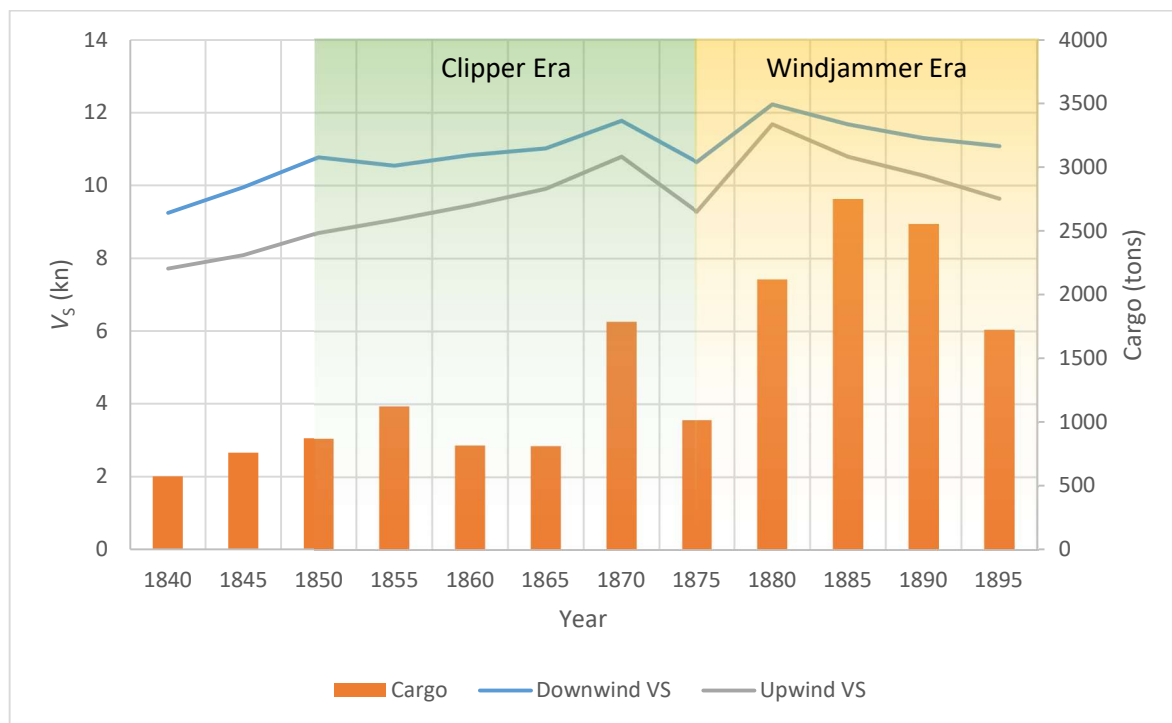


Figure 112: Comparison between average upwind V_s , downwind V_s and cargo capacity

It must be noted that the average speed should be considered with caution, particularly for this dataset where there is occasionally a lack of data for the given time interval. For example in Figure 112 there appears to be a sudden drop in speed during the period between 1875 and 1880. However, the main reason for the appearance of this significant change is due to the amount of data in the previous interval, where there is only one ship representing the data. This ship, *Mermerus* (1872), was amongst the narrowest ships in this time period, whereas the three vessels in the 1875-1880 period represent a range covering the expected variation of the time. This is shown in Figure 113, which indicates that, if speed is proportional to the length-beam ratio, then the average speed of the ships in the clipper era should be slightly lower.

Despite potential anomalies within the data, it appears that the so-called windjammers of the last 25 years of the 19th Century performed better than the clipper ships, which have been referred to as the “thoroughbreds of the sea” (Lubbock, 1914, p. 216). Even though they were built under different conditions, it would not be unreasonable to assume that if steel and the accompanying technology were available earlier, the windjammers would have been able to play a significant role in the China tea trade.

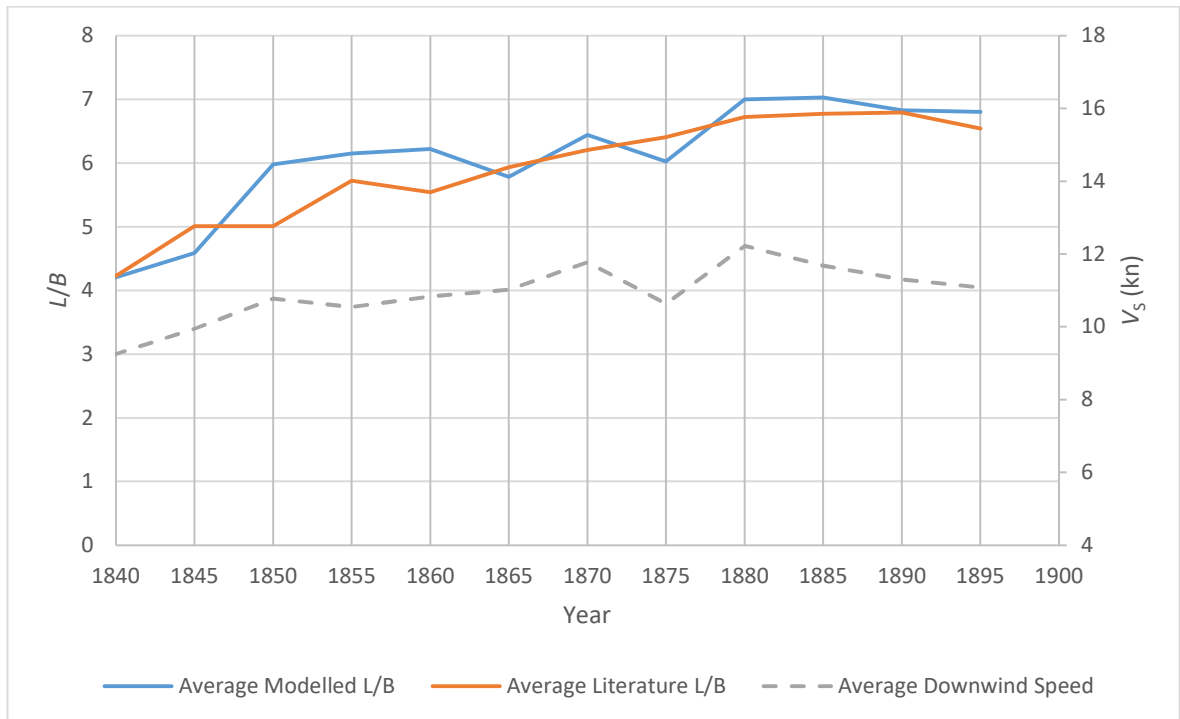


Figure 113: *L/B* averages from literature and modelled data in relation to downwind *V_s*

In order to determine the efficiency of each ship type, non-dimensional factors need to be considered. This may be achieved using two measures: the Froude number to determine speed, and the coefficients of total resistance and thrust to determine the individual effect of each sail. Figure 114 shows the variation of the Froude number in the upwind and downwind conditions compared to the corresponding speed. This indicates that there was actually a drop in performance with time, especially in the downwind condition. This may be due to the increasing use of the barque rig discussed in Section 6.3.1, which would have had a larger impact on downwind sailing than upwind, due to the loss of the square sails on the mizzen mast.

In Section 6.2.1, it was shown that the greater impact on speed was caused by improvements to hull efficiency. In the case of the windjammers however, it appears that the minor change to rig efficiency that occurs throughout the century may have had a greater impact on the overall speed than any improvement to hull efficiency. It can be seen from Figure 115 that there is a gradual decrease in the coefficient of total resistance, likely to be driven by an increase in length. At the

Modelled Data and Case Studies

same time there is a much larger increase in the coefficient of thrust, signifying that the layout of the rig would have driven the increase in speed achieved by the windjammers.

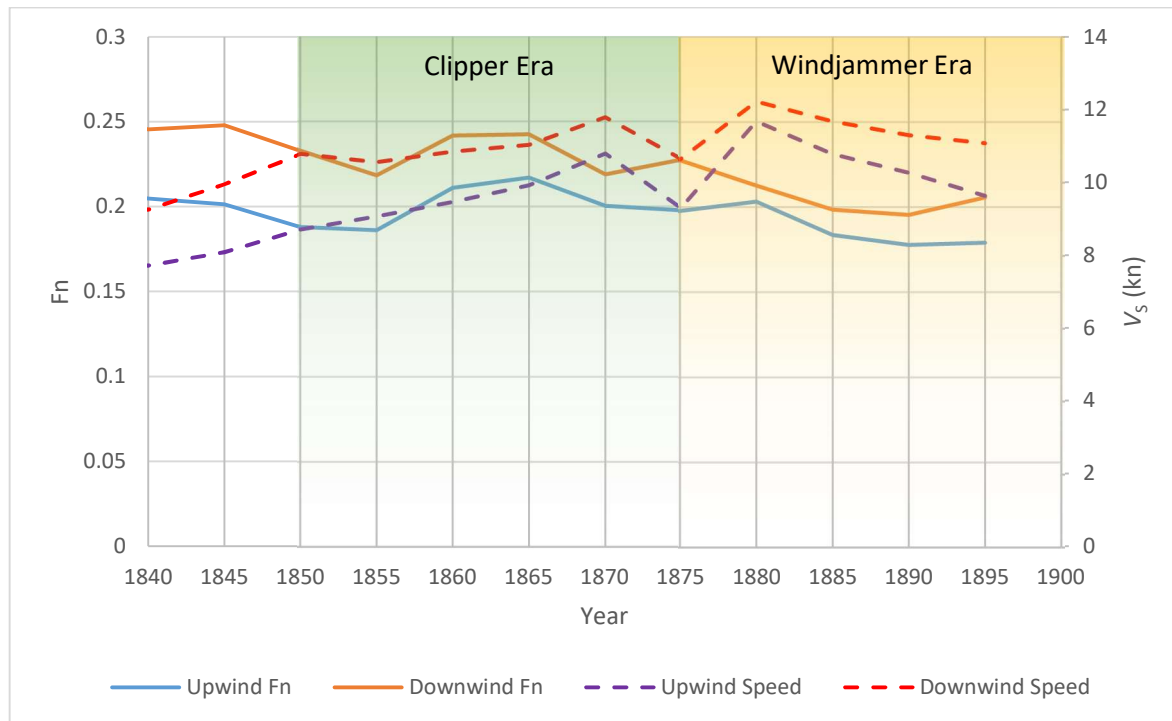


Figure 114: Variation of Fn and speed during the clipper and windjammer eras

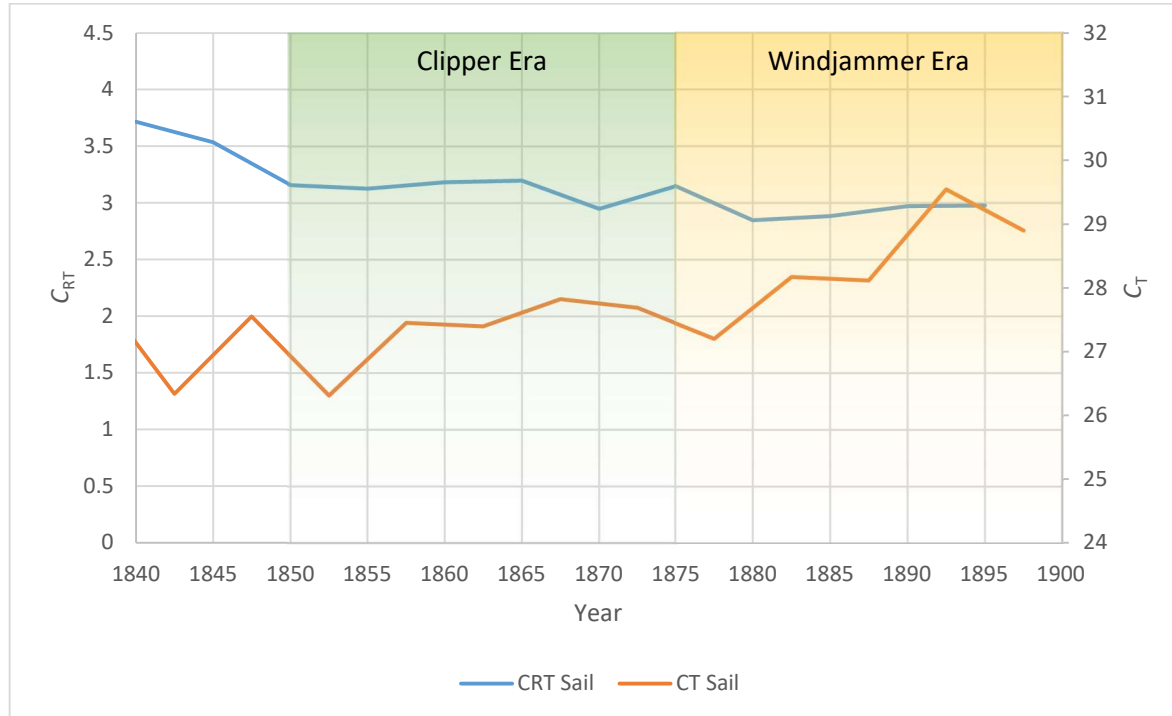


Figure 115: Variation of C_{RT} and downwind C_T during the clipper and windjammer eras at 5 kn

In terms of stability, changes in performance can be seen using the variable discussed in Section 6.1. As illustrated in Figure 116, it can be seen that the overall stability in the windjammer era would have been higher than in the clipper era. This can be explained primarily by the increase in

length, demonstrated by the red line, which shows that the windjammers were on average around 50% longer than the clippers. The result is that overall the ships were much larger and so their potential stability would have been greater. In the clipper era, however, it is noted that the stability measure does not follow the absolute length as closely, indicating that these ships may have been less stable relative to their length. This agrees with the purpose of these vessels, which were primarily built for speed and hence may have had cause for a compromise between speed and stability by reducing the beam.

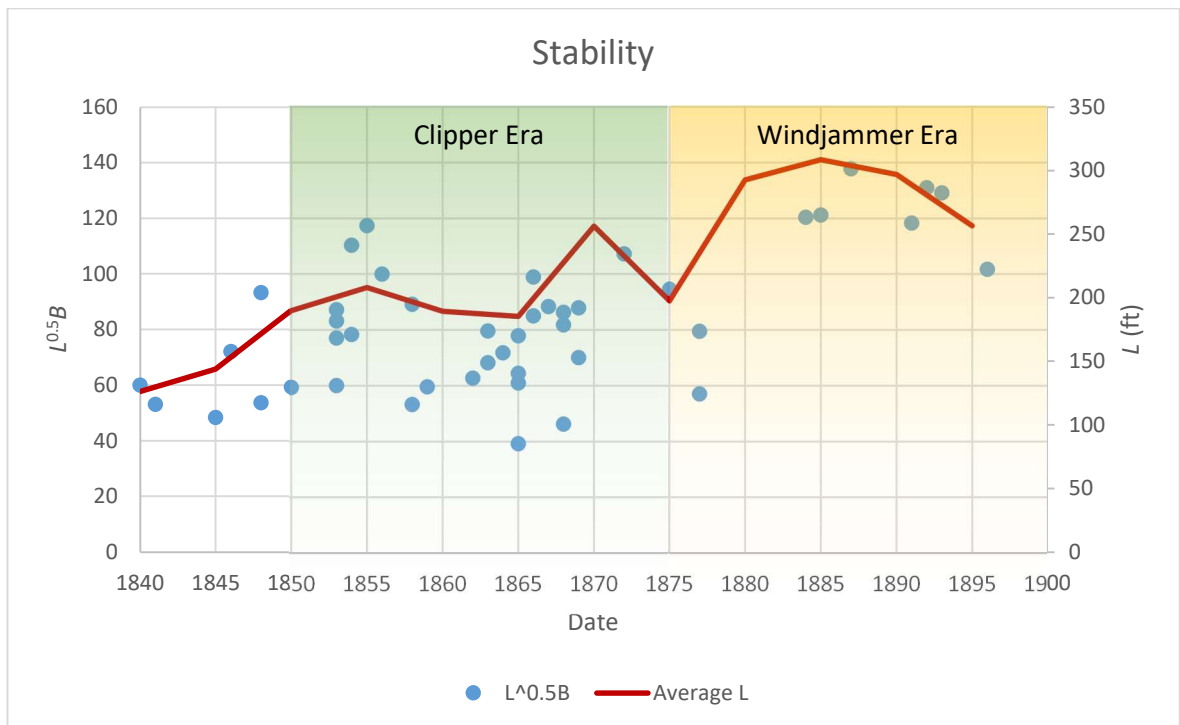


Figure 116: Variation of stability relative to length

These results show that hydrodynamically there was little difference between the two ship types. In terms of the ability to carry more cargo faster, the windjammers would have been the superior merchant ship. However, relative to their size, as indicated by the Froude number, the clippers had a marginal advantage. There are also considerable differences between the stability potential of the ship types, which is likely to have been driven by the priority that speed held in the design. Considering the major uses of the two ship types, with the clippers designed to carry low-volume, high-value goods and the windjammers designed to carry high-volume, low-value goods, it is clear that each ship type was suited to its market.

6.4 Summary

New data has been generated using the methodologies and data sources previously described. This has allowed for a parametric analysis of ships in the 19th Century to be carried out where there was previously not enough information. The results show that there was a marked increase

in ship speed over the course of the century, with the length-beam ratio and the length-displacement ratio being the most significant changes to ship design. Alternative parameters linked to ship speed such as prismatic coefficient and wetted surface area were shown to have less of an effect.

The case studies show how the methodologies developed during this research can be used to increase the understanding of the evolution of ship design. The reasons behind the evolution of ships in the 19th Century is heavily dependent on the understanding of hydrodynamics, with only small improvements in rig efficiency. The influence of tonnage legislation appears to play a lesser part than has previously been described, with the reduction in depth of hull relative to beam not being apparent until around 30 years after the change that was supposed to have caused it. The international influence on ship design is also less significant than some sources claim, as there appears to have been a gradual increase in British ship performance prior to the lifting of the protectionist Navigation Acts.

When considering the differences between different ships and ship types, the data generated can provide new insights into established beliefs. Despite a belief that a barque rig could be used with fewer crew for a negligible reduction in performance (Allen, 1980, p. 22), it appears that up to 2 kn of speed could be lost as a result. Without further knowledge of the economics, however, this could still represent a cost saving in terms of crew reduction.

The parametric data also indicates that the East Indiamen may have been more advanced than previously thought, and their decline towards the middle of the century was probably due to a lack of development, having maintained the previously good design. This questions why they are often considered as a typical ship of the age. An attempt has also been made to clarify the opinions given in literature on the sailing ships of the second half of the century, often categorised as clippers and windjammers. It has been found that the supposedly slow, bulky windjammers were capable of speeds similar to the clippers, and better when travelling upwind. In addition to the speed, an increased cargo capacity would make an argument that the windjammers were the more useful cargo carrier.

These case studies have shown that it is possible to use the methodology developed in Chapters 3 to 5 to challenge the understanding of ship design and performance in the 19th Century. The ability to visualise how ships change in a diachronic manner allows trends to be seen where there was previously little quantitative evidence. In addition to this, the ability to calculate the ship speeds and forces on the hull shows how the changes in ship design relate to performance.

Chapter 7: Conclusions and Future Work

7.1 Conclusions

The evolution of 19th Century British merchant ships is a topic in which there had previously been little quantitative analysis, particularly in relation to performance. The research covered in this thesis shows that it is possible to generate the required quantitative data and use it to show trends that have previously only been discussed in a qualitative manner. The methods developed have been tested for their suitability for use with historic ships and enables ship performance to be analysed with a minimal level of data, making it an easily accessible tool for understanding historic ship performance. This structured engineering performance analysis has not previously been attempted on such a large scale.

Existing data on the form of 19th Century British merchant ships was found to be limited, with the most common hull dimensions being length, beam, depth of hold and the tonnage. A parametric analysis in Chapter 3 showed that these are not enough to reliably show how performance changed with time; more hull data was required, along with the ability to estimate ship speed, one of the most important components of performance for a merchant ship. To determine these, a new dataset of ship particulars had to be generated using digital models, and a new VPP needed to be written and tested. Unlike other VPPs aimed at historic ships, which are usually aimed at only one ship or ship type, this one needed to be designed to accommodate a wide variety of vessels. Modern VPPs, however, are generally aimed at yachts, and so are incapable of handling the larger sailing ships seen in history. The process of creating digital models described in Chapter 5 not only allowed the hydrostatics required for the VPP to be generated, but also enabled a new parametric analysis to be carried out on data that was otherwise inaccessible.

The development of the VPP in Chapter 4 allowed a large set of ship speeds to be generated. By plotting these speeds and the hull parameters against the year in which the ship was built, the evolution of ship design and performance can be seen in a graphical form. When combined with previous studies on cargo capacity, it is clear that British merchant ships in the 19th Century not only became larger, but also faster overall, confirming general perception of design in that era. It is also clear that the evolution was not a linear process, but there were a number of external factors influencing the rate of change. At the beginning of the century, while Britain was subject to a number of protectionist laws and experience-based design, there was little change in the design and performance of ships. A combination of improving understanding of hydrodynamics and the removal of regulations that were potentially stifling design, such as the pre-1836 Tonnage law and the 1784 Smuggling Act, led to a sharp increase in performance between around 1830

and 1855. This rapid increase then reduced, until around 1880 when there was little increase in the speed of sailing ships, due to the increasing demand to reduce operational costs over speed.

It has been shown in Chapters 3 and 6 that hull parameters can, to some extent, be used infer performance, but their greatest impact is showing why and by what means performance changed. The ability to tie hull dimensions and sailing performance to a narrative has been demonstrated, showing the power of science in ship design and how legislation such as tonnage laws can influence design and performance in subtle ways. It has been shown that improvements in speed over the century were driven primarily by improved hull efficiency. A study of different ship types based on speed and hull data indicates that there are misconceptions about the abilities of some ships. For example, it appears that East Indiamen, although slow compared to more modern ships, were hydrodynamically better designed than their counterparts, meaning that the tendency to treat them as typical ships of the time is misleading. The differences between clippers and windjammers has also been highlighted in reference to their operational requirements.

This research has created a new, structured methodology for approaching the analysis of historic ship performance and evolution. In addition to this, a new dataset has been established through the creation of digital models based on lines plans and half models. This has allowed the evolution of 19th Century British merchant ships to be measured using quantitative data in a new manner, providing evidence both for and against existing hypotheses.

7.2 Future Work

There are two primary directions in which the research covered in this thesis could be extended: the expansion of the dataset, and improvements to the VPP. This research has covered the evolution of 19th Century British merchant ships, but the methodology developed could apply to any historic ship. A number of other categories could therefore be covered, including the examination of naval vessels, a different time period or a different country. The further back in time, however, the fewer hull data sources there will be. This means that additional reconstruction work may need to be carried out to create a large enough dataset for a meaningful analysis. The ability to estimate the speed of historic ships in a standardised manner also gives the potential to determine capabilities of individual vessels without the need to build replicas or undertake expensive model testing.

There is scope to strengthen the VPP in its current form with the use of model testing. As the validation of the hydrodynamic forces is based on CFD only, it would be ideal to carry out towing tank tests to confirm its suitability. The weakest point of the VPP is the sail force calculation. This was developed for only one square-rigged ship, meaning that it may not be suitable for others. It would therefore be prudent to create a new estimation method based on wind tunnel tests. This

Conclusions and Future Work

would allow for a wider variety of rigs and sail shapes to be considered. In addition to this, with a more reliable sail force calculation it would be possible to examine the evolution of sail propulsion in more detail. This was hinted at in Section 6.3.1 with the comparison of ship and barque-rigged vessels, where the ship-rig appeared to improve vessel performance by a noticeable margin.

For some ship types, small additions to the VPP would be required. For example, in its current form, the VPP would be unsuitable for narrow rowing craft. However, with the inclusion of a resistance estimation method such as thin ship theory and a knowledge of the power generated by oars, it would be possible to calculate the speed of such a craft. In addition to examples not included in this research, the results from this thesis would likely be strengthened by an increase in the steam ship dataset, which would require a more detailed investigation into steam engine efficiencies and outputs.

Overall, the research carried out for this thesis has shown the possibility of identifying how ships evolved with time in a diachronic manner. The interdisciplinary approach of combining naval architecture with archaeology and history has highlighted how we can use a limited amount of data to aid the understanding of a critical period in the development of maritime technology, globalisation and the modern world.

Conclusions and Future Work

References

3D Systems (2014) 'Sense™ 3D Scanner User Guide'. Available at: http://cubify.s3.amazonaws.com/Scanners/Sense/sense_userguide_pc.pdf.

Adams, J. (2013) *A Maritime Archaeology of Ships: Innovation and Social Change in Medieval and Early Modern Europe*. 1st edn. Oxford: Oxbow Books.

Allen, O. E. (1980) *The Seafarers: The Windjammers*. Edited by G. G. Daniels. Time-Life Books.

Allington, G. P. (2004) 'Sailing Rigs and Their Use on Ocean-going Merchant Steamships, 1820-1910', *International Journal of Maritime History*, XVI(1), pp. 125–152.

Barnaby, N. (1871) 'On the Relative Influence of Breadth of Beam and Height of Freeboard in Lengthening Out the Curves of Stability', *Transactions of the Institution of Naval Architects*, XII, pp. 62–76. doi: 10.3940/rina.trans.1871.06.

Benham, H. (1986) *The Smuggling Century: The story of smuggling on the Essex Coast 1730-1830*. Chelmsford: Essex Record Office.

Benham, P. P., Crawford, R. J. and Armstrong, C. G. (1996) *Mechanics of Engineering Materials*. 2nd edn. Harlow, Essex: Pearson Education Ltd.

Bennet, J. (2005) *Sailing Rigs. An Illustrated Guide*. London: Chatham Publishing.

Bentley Systems Incorporated (2013) 'Maxsurf Resistance User Manual'. Bentley Systems Incorporated, p. 3.

Bentley Systems Incorporated (2017) 'Maxsurf Modeler Manual'.

Bischoff, V. et al. (2014) 'Post-excavation documentation, reconstruction and experimental archaeology applied to clinker-built ship-finds from Scandinavia', in Carlo Betrami (ed.) *Archaeology of Post-Medieval Shipwrecks*. All'Insegna del Giglio, pp. 21–29.

Du Bosque, F. L. (1896) 'Speed Trials of a Screw-Propelled Ferryboat', in *Fourth General Meeting of the Society of Naval Architects and Marine Engineers*. New York, USA: Society of Naval Architects and Marine Engineers, pp. 93–104.

Bourne, J. (1867) 'On the Proper Form of Ships', *Transactions of the Institution of Naval Architects*, VIII, pp. 21–26. doi: 10.3940/rina.trans.1867.03.

Bristol Record Society (1950) *Records of Bristol Ships 1800-1838 (Vessels over 150 tons)*. Edited by G. E. Farr. Bristol: J. W. Arrowsmith Ltd. doi: 10.1017/CBO9781107415324.004.

Brock, P. W. and Greenhill, B. (1973) *Steam and Sail in Britain and North America*. Guildford: David & Charles (Holdings) Limited.

Caledonian Maritime Research Trust (2019) *The Clyde Built Ships*. Available at: clydeships.co.uk (Accessed: 16 April 2019).

Carriage of Passengers Act (1855). US.

Çengel, Y. A. and Cimbala, J. M. (2010) 'Introduction to Computational Fluid Dynamics', in Kanoglu, M. (ed.) *Fluid Mechanics - Fundamentals and Applications*. 2nd edn. New York, USA, USA: McGraw-Hill Higher Education, pp. 853–920.

References

Chapman, F. H. af (1968) *Architectura Navalis Mercatoria: A Facsimile of the classic Eighteenth Century Treatise on Shipbuilding*. Edited by J. Inman. London: Allard Coles Ltd.

Chatfield (1946) 'President's Address', *Transactions of the Institution of Naval Architects*, 88, pp. xxxvii–xxxix.

Churchill, N. et al. (2018) *200 Stories from the Sea*. Sailor's Society.

Clark, A. H. (1970) *The Clipper Ship Era*. 2nd edn. London: Patrick Stephens Limited.

Clarke, D., Gelding, P. and Hine, G. (1983) 'The Application of Manoeuvring Criteria in Hull Design Using Linear Theory', *Transactions of RINA*, 125, pp. 45–68.

Claughton, A. R., Wellicome, J. F. and Shenoi, R. A. (eds) (1998) *Sailing Yacht Design: Theory*. Harlow, Essex: Addison Wesley Longman Limited.

CLIWOC (no date) *An English-Spanish-Dutch-French Dictionary of Wind Force Terms Used by Mariners from 1750 to 1850*.

Clowes, G. S. L. (1962) *Sailing Ships: Their History and Development Part I*. 5th edn. London: Science Museum.

Corlett, E. (1975) *The Iron Ship*. Bradford-on-Avon: Moonraker Press.

Couser, P. (2016) 'Modeling Existing Vessels in MAXSURF, Part 2'. Bentley Systems Incorporated.

Couser, P., Ward, C. and Vosmer, T. (2009) 'Hypothetical Reconstruction of an Ancient Egyptian Sea Going Vessel from the Reign of Hatshepsut, 1500BCE', in *International Conference on Historic Ships*. The Royal Institution of Naval Architects, pp. 86–139.

Craig, R. (1980) 'Steam Tramps and Cargo Liners', in *The Ship*. London: Her Majesty's Stationery Office.

Customs Act (3 & 4 Will. IV C.55) (1833). UK.

Dana, R. H. (1873) *The Seaman's Friend: A Treatise on Practical Seamanship*. Edited by 13. Boston, US: Thomas Groom & Co.

Davis, A. (2009) 'The Pride of Baltimore', in Bennett, J. (ed.) *Sailing into the Past: Learning from Replica Ships*. Barnsley: Seaforth Publishing, pp. 179–190.

Day, A. H. and Doctors, L. (1997) 'Resistance optimization of displacement vessels on the basis of principal parameters', *Journal of ship research*, 41(4), pp. 249–259.

Deakin, B. (1997) 'Model Tests in Support of the Design of a 50 Meter Barque', in *The 13th Chesapeake Sailing Yacht Symposium*, pp. 65–75.

Delftship Marine Software (2016) 'DELFTship Manual'. Hoofddorp.

Dickinson, A. S. et al. (2016) 'Registering a methodology for imaging and analysis of residual-limb shape after transtibial amputation', *Journal of Rehabilitation Research and Development*, 53(2), pp. 207–218. doi: 10.1682/JRRD.2014.10.0272.

Dolwick, J. S. (2008) 'In search of the social: Steamboats, square wheels, reindeer and other things', *Journal of Maritime Archaeology*, 3(1), pp. 15–41. doi: 10.1007/s11457-008-9027-9.

Emam, S. M., Khatibi, S. and Khalili, K. (2014) 'Improving the Accuracy of Laser Scanning for 3D Model Reconstruction Using Dithering Technique', *Procedia Technology*. Elsevier, 12, pp. 353–

References

358. doi: 10.1016/j.protcy.2013.12.498.

Engineering Toolbox (2004) *Densities of Wood Species*. Available at: https://www.engineeringtoolbox.com/wood-density-d_40.html (Accessed: 24 June 2019).

Ferreiro, L. D. (2007) *Ships and Science: the birth of naval architecture in the scientific revolution 1600-1800*. Cambridge, MA: The MIT Press.

Ferreiro, L. D. (2011) 'The Social History of the Bulbous Bow', *Technology and Culture*, 52(2), pp. 335–359. doi: 10.1353/tech.2011.0055.

Ferreiro, L. D. and Pollara, A. (2016) 'Contested Waterlines: The Wave-Line Theory and Shipbuilding in the Nineteenth Century', *Technology and Culture*, 57(2), pp. 414–444. doi: 10.1353/tech.2016.0039.

Finney, B. R. (1977) 'Voyaging Canoes and the Settlement of Polynesia', *Science*, 196(4296), pp. 1277–1285.

Fletcher, M. E. (1958) 'The Suez Canal and World Shipping, 1869-1914', *Journal of Economic History*, 18, pp. 556–573. doi: 10.1017/S0022050700107740.

Fossen, T. I. (2011) *Handbook of Marine Craft Hydrodynamics and Motion Control*, Thor I. Fossen. John Wiley & Sons, Ltd.

Froude, R. E. (1881) 'On the Leading Phenomena of the Wave-Making Resistance of Ships', *Transactions of the Institution of Naval Architects*, XXII, pp. 220–245. doi: 10.3940/rina.trans.1881.11.

Froude, W. (1874) 'On Experiments with H.M.S. "Greyhound"', *Transactions of the Institution of Naval Architects*, XV, pp. 36–73. doi: 10.3940/rina.trans.1874.03.

Froude, W. (1877) 'On Experiments upon the Effect Produced on the Wave-making Resistance of Ships by Length of Parallel Middle Body', *Transactions of the Institution of Naval Architects*, XVIII, pp. 77–97. doi: 10.3940/rina.trans.1877.06.

Fujiwara, T. et al. (2005) 'Steady sailing performance of a hybrid-sail assisted bulk carrier', *Journal of Marine Science and Technology*, 10(3), pp. 131–146. doi: 10.1007/s00773-004-0189-3.

Fung, S. C. (1987) 'Resistance predictions and parametric studies', *Naval Engineers Journal*, (March), pp. 64–80.

Fung, S. C. and Leibman, L. (1995) 'Revised Speed-Dependant Powering Predictions for High-Speed Transom Stern Hull Forms', in Kruppa, C. F. L. (ed.) *3rd International Conference on High-Speed Sea Transportation (FAST' 95)*. Lubeck-Travemunde, Germany: Schiffbautechnische Gesellschaft, Germany, pp. 151–164.

Fyfe, C. F. A. (1907) *Steamship Coefficients, Speeds and Powers: A Pocket Book*. 1st edn. London, England: E. & F.N. Spon Ltd.

Gardiner, R. and Greenhill, B. (eds) (1993a) *Sail's Last Century: The Merchant Sailing Ship 1830-1930*. London: Conway Maritime Press.

Gardiner, R. and Greenhill, B. (1993b) *The Advent of Steam - The Merchant Steamship before 1900*. London: Conway Maritime Press.

Geels, F. W. (2002) 'Technological transitions as evolutionary reconfiguration processes: a multi-level perspective and a case-study', *Research Policy*, 31(8), pp. 1257–1274. doi: 10.1016/S0048-

References

7333(02)00062-8.

Gifford, E. (1995) 'The sailing characteristics of Saxon ships as derived from half-scale working models with special reference to the Sutton Hoo ship', *The International Journal of Nautical Archaeology*, 24(2), pp. 121–131. doi: 10.1006/ijna.1995.1016.

Glasgow Herald (1868) 'The Ocean Race with China Tea Clippers', 5 September, p. 5.

Grant, H. et al. (2001) 'Schooner Brilliant Sail Coefficients and Speed Polars', in *The 15th Chesapeake Sailing Yacht Symposium*. Annapolis, pp. 118–134.

Greenhill, B. (1980) *Life and death of the Merchant Sailing Ship 1815-1965, The Ship*.

Greenhill, B. (1993) 'The Merchant Sailing Vessel in the Twentieth Century', in Gardiner, R. and Greenhill, B. (eds) *Sail's Last Century: The Merchant Sailing Ship 1830-1930*. London: Conway Maritime Press, pp. 98–117.

Griffiths, D. (1985) *Brunel's 'Great Western'*. Wellingborough: Patrick Stephens Limited.

Hackman, R. (2001) *Ships of the East India Company*. Gravesend, Kent: World Ship Society.

Hersh, J. S. and Voth, H.-J. (2011) 'Sweet Diversity: Colonial Goods and the Rise of European Living Standards after 1492', *SSRN Electronic Journal*. doi: 10.2139/ssrn.1443730.

Holtrop, J. (1984) 'A statistical re-analysis of resistance and propulsion data', *International Shipbuilding Progress*, 31(363), pp. 272–276.

Holtrop, J. and Mennen, G. G. (1982) 'An Approximate Power Prediction Method', *International Shipbuilding Progress*, 29(July), pp. 166–170. doi: 10.1007/s13398-014-0173-7.2.

Horn, J. R. (2000) *The Influence of Stern Vortices on Ship Manoeuvring*. University of Newcastle upon Tyne.

Hughes, J. R. T. and Reiter, S. (1958) 'The First 1945 British Steamships', *Journal of the American Statistical Association*, 53(282), pp. 360–381.

Inoue, S., Hirano, M. and Kijima, K. (1981) 'Hydrodynamic Derivatives on Ship Manoeuvring', *International Shipbuilding Progress*, (May), pp. 112–125.

ITTC (2008) 'The Maneuvering Committee: final report and recommendations to the 25th ITTC', in *Proceedings of 25th ITTC*, pp. 143–208.

Jefferson, S. (2014) *Clipper Ships and the Golden Age of Sail: Races and Rivalries on the 19th Century High Seas*. 1st edn. London: Bloomsbury.

Jiang, Q. et al. (2016) *Reverse modelling of natural rock joints using 3D scanning and 3D printing*, *Computers and Geotechnics*. doi: 10.1016/j.compgeo.2015.11.020.

De Jong, P. (2008) 'The Development of a Velocity Prediction Program for Traditional Dutch Sailing Vessels of the Type Skûtsje', in *20th HISWA Symposium*, pp. 1–18.

Kelly, M. and Ó Gráda, C. (2018) 'Speed under Sail during the Early Industrial Revolution.', *CEPR Discussion Papers*, 12576. doi: 10.1111/ehr.12696.

Kemp, D. (1891) *Yacht Architecture*. 2nd edn. London: Horace Cox.

Kemp, P. (1978) *The History of Ships*. London: Orbis Publishing.

References

Kijima, K. *et al.* (1990) 'On the manoeuvring performance of a ship with the parameter of loading condition', *Autumn Meeting of the Society of Naval Architects of Japan*. doi: 10.2534/jjasnaoe1968.1990.168_141.

Lavery, B. (2019) 'Steam and Emigration', in Wilkes, A. (ed.) *A Short History of Seafaring*. 2nd edn. London: Dorling Kindersley Ltd., pp. 192–282.

Lavery, B. and Stephens, S. (1995) *Ship Models: Their Purpose and Development from 1650 to the Present*. London.

Lee, H.-Y. and Shin, S.-S. (1998) 'The Prediction of Ship's Manoeuvring Performance in Initial Design Stage', *PRADS Practical Design of Ships and Mobile Units*, pp. 633–639.

Leszczynski, R. *et al.* (2005) *Virtual Trafalgar*. Southampton.

Lloyd's Register Foundation (2016) 'Lloyd's Register Infosheet No. 10'. London: Lloyd's Register Foundation.

Lloyd's Register Foundation (2017) 'Lloyd's Register Infosheet No. 31'. London: Lloyd's Register Foundation.

Longo, J. and Stern, F. (2002) 'Effects of drift angle on model ship flow', *Experiments in Fluids*, 32, pp. 558–569. doi: 10.1007/s00348-001-0397-0.

Lubbock, B. (1914) *The China Clippers*. 2nd edn. Glasgow, Scotland: James Brown & Son, Publishers.

Lubbock, B. (1921) *The Colonial Clippers*. 2nd edn. Glasgow: James Brown & Son, Nautical Publishers.

Lubbock, B. (1922) *The Blackwall Frigates*. 1st edn. Glasgow: James Brown & Son, Nautical Publishers.

Lubbock, B. (1924) *The Log of the 'Cutty Sark'*. 1st edn. Glasgow: James Brown & Son, Nautical Publishers.

Lubbock, B. (1953a) *The Last of the Windjammers Vol. I*. Glasgow: Brown, Son & Ferguson Ltd. Nautical Publishers.

Lubbock, B. (1953b) *The Last of the Windjammers Vol. II*. Glasgow: Brown, Son & Ferguson Ltd. Nautical Publishers.

Lyon, D. (1975) *The Denny List Volume I*. Greenwich: National Maritime Museum.

Macarthur, A. (2009) 'HM Bark Endeavour', in Bennett, J. (ed.) *Sailing into the Past: Learning from Replica Ships*. Barnsley: Seaforth Publishing, pp. 163–177.

MacCarthaigh, C. (2008) 'Traditional Boats of Ireland Project Scanning Procedure', *History, Folklore and Construction (Cork, 2008)*.

MacGregor, D. (1979) *Clipper Ships*. Watford, UK: Argus Books Ltd.

MacGregor, D. (1980a) *Merchant Sailing Ships 1775–1815*. 1st edn. Watford, UK: Argus Books Ltd.

MacGregor, D. (1980b) *Square Rigged Sailing Ships*. 2nd edn. Watford, UK: Argus Books Ltd.

MacGregor, D. (1984a) *Merchant Sailing Ships 1815–1850*. London: Conway Maritime Press.

References

MacGregor, D. (1984b) *Merchant Sailing Ships 1850-1875*. London: Conway Maritime Press.

MacGregor, D. (1988) *Fast Sailing Ships: Their Design and Construction 1775-1875*. 2nd edn. London: Conway Maritime Press.

Maddocks, M. (1981) *The Seafarers: The Atlantic Crossing*. Edited by A. Horan. Amsterdam: Time-Life Books.

Marchaj, C. A. (2000) *Aero-Hydrodynamics of Sailing*. 3rd edn. London: Alard Coles Nautical.

MARIN (2010) 'Holtrop-Mennen founders reveal the secret of method's long-lasting success', *MARIN Report*, August, pp. 6-7.

Maudslay, J. (1860) 'An Improvement in the Form of Ships', *Transactions of the Institution of Naval Architects*, I, pp. 54-56. doi: 10.3940/rina.trans.1860.03.

McDowell, W. (1952) *The Shape of Ships*. 2nd edn. London: Hutchinson & Co. Ltd.

McGowan, A. (1980) 'The Century Before Steam', in *The Ship*. London: Her Majesty's Stationery Office.

McGrail, S. (2009) 'Experimental Archaeology: Replicas and Reconstructions', in Bennett, J. (ed.) *Sailing into the Past: Learning from Replica Ships*. Barnsley: Seaforth Publishing, pp. 16-23.

Mctaggart, K. (2016) 'Literature Review for Design and Assessment of Directional Stability and Turning Performance of Naval Destroyers', (February).

Mendonça, S. (2013) 'The "Sailing ship effect": Reassessing history as a source of insight on technical change', *Research Policy*, 42(10), pp. 1724-1738. doi: 10.1016/j.respol.2012.12.009.

Menna, F., Nocerino, E. and Scamardella, A. (2011) 'Reverse Engineering and 3D Modelling for Digital Documentation of Maritime Heritage', *International Archives of the Photogrammetry, Remote Sensing and Spatial Information Sciences*, XXXVIII(5/W16), pp. 245-252.

Miller, R. (1980) *The East Indiamen*. Edited by J. Hicks. Amsterdam: Time-Life Books.

Mitchell, B. R. and Deane, P. (1971) *Abstract of British Historical Statistics*. Cambridge: Cambridge University Press.

Molland, A. F., Turnock, S. R. and Hudson, D. A. (2011) *Ship Resistance and Propulsion*. Cambridge: University of Cambridge Press.

Moody, R. D. (1996) *Preliminary power prediction during early design stages of a ship*, Cape Peninsula University of Technology. Cape Technikon.

Muckelroy, K. (1978) 'Maritime Archaeology'. Cambridge: Cambridge University Press.

Murray, W. M. et al. (2017) 'Cutwaters Before Rams: an experimental investigation into the origins and development of the waterline ram', *International Journal of Nautical Archaeology*, 46(1), pp. 72-82. doi: 10.1111/1095-9270.12209.

Noor, C. W. M. (2009) *Manoeuvring Prediction of Offshore Supply Vessel*. Universiti Teknologi Malaysia.

Northcote Parkinson, C. (1948) 'The East India Trade', in Northcote Parkinson, C. (ed.) *The Trade Winds*. London: George Allen and Unwin Ltd, pp. 141-156.

Oliver, J. C. (2007) 'Hull Design and Evaluation', in Claughton, Wellcome, and Shenoi (eds) *Sailing*

References

Yacht Design Practice, pp. 101–125.

Van Oortmerssen, G. (1971) 'A Power Prediction method and Its Application to Small Ships', *International Shipbuilding Progress*, 18(207), pp. 397–415.

Owens, P. (2015) *CLIP - Ships by official number*. Available at: <http://www.crewlist.org.uk/data/vesselsnum.php> (Accessed: 26 October 2017).

Palmer, C. (2009a) 'Measuring Performance Under Sail', in Bennett, J. (ed.) *Sailing into the Past: Learning from Replica Ships*. Barnsley: Seaforth Publishing, pp. 24–32.

Palmer, C. (2009b) 'Windward sailing capabilities of ancient vessels', *International Journal of Nautical Archaeology*, 38(2), pp. 314–330. doi: 10.1111/j.1095-9270.2008.00208.x.

Passenger Vessels Act (Geo. IV C.21) (1828). UK.

Pokorný, L. (2017) *Sails for La Grace*. Available at: http://www.lagrace.eu/new_sails (Accessed: 6 April 2018).

Porter, N. E. (1879) 'On the Legal Load Line and some Remarks Relating to the Principles of Safe Freeboard', *Transactions of the Institution of Naval Architects*, XX, p. 196. doi: 10.3940/rina.trans.1879.12.

Poveda, P. (2012) 'Hypothetical Reconstruction of Dramont E Shipwreck', in N. Güsenin (ed.) *Between Continents. Proceedings of the Twelfth Symposium on Boat and Ship Archaeology*. Istanbul, pp. 331–336.

Quetelet, M. A. (1842) *A Treatise on Man and the Development of his Faculties*. Edited by T. Smibert. Edinburgh: William and Robert Chambers.

Radhakrishnan, V. (1997) 'From Square Sails to Wing Sails: The Physics of Sailing Craft', *Current Science*, 73(6), pp. 503–516.

Rankine, W. J. M. (1870) 'On Stream-Line Surfaces', *Transactions of the Institution of Naval Architects*, XI, pp. 175–181. doi: 10.3940/rina.trans.1870.16.

Ransley, J. et al. (eds) (2013) *People and the Sea: A Maritime Archaeological Research Agenda for England*. York. doi: 10.11141/RR171.

Rawson, K. J. and Tupper, E. C. (2001a) *Basic Ship Theory Volume 1*. 5th edn. Oxford: Butterworth-Heinemann. doi: 10.1016/B978-075065398-5/50017-0.

Rawson, K. J. and Tupper, E. C. (2001b) *Basic Ship Theory Volume 2*. 5th edn. Oxford: Butterworth-Heinemann. doi: 10.1016/B978-075065398-5/50017-0.

Reed, E. J. (1885) *A Treatise on the Stability of Ships*. London: Charles Griffin and Company.

Registry Act (5 & 6 Will. IV C.56) (1835). UK.

De Ridder, E. J., Vermeulen, K. J. and Keuning, J. A. (2004) 'A Mathematical Model for the Tacking Maneuver of a Sailing Yacht', in *The International HISWA Symposium on Yacht Design and Yacht Construction*, pp. 1–34.

Rinman, T. and Brodefors, R. (1983) *The Commercial History of Shipping*. Edited by P. Hogg. Gothenburg: Rinman & Linden AB.

Royal Museums Greenwich (no date) *Research guide H6: Lloyd's*. Available at: <http://www.rmg.co.uk/discover/researchers/research-guides/research-guide-h6-lloyd's-lloyd's>

References

register-survey-reports (Accessed: 16 October 2017).

Salisbury, W. (1966) 'Early Tonnage Measurement in England Part III', *The Mariner's Mirror*, 52(4), pp. 329–340. doi: 10.1080/00253359.1966.10659347.

Sandler, S. (1973) "In deference to public opinion" the loss of H.M.S. Captain', *Mariners Mirror*, 59(1), pp. 57–68. doi: 10.1080/00253359.1973.10657874.

Schneekluth, H. and Bertram, V. (1998) *Ship Design for Efficiency and Economy*. Butterworth-Heinemann. doi: 10.1016/B978-075064133-3/50005-0.

Science and Art Department (1878) *Catalogue of Ship Models and Marine Engineering in the South Kensington Museum*. London: George E. Eyre and William Spottiswoode.

Scott Russell, J. (1860a) 'The Wave-Line Principle of Ship-Construction Part I', *Transactions of the Institution of Naval Architects*, I, pp. 184–195.

Scott Russell, J. (1860b) 'The Wave-Line Principle of Ship-Construction Part II', *Transactions of the Institution of Naval Architects*, I, pp. 196–211.

Scott Russell, J. (1861) 'The Wave-Line Principle of Ship Construction Part III - Conclusion', *Transactions of the Institution of Naval Architects*, II, pp. 230–245.

Scott Russell, J. (1864) *The Modern System of Naval Architecture*. London: Day & Son.

Sichko, C. (2011) 'The Influence of the Suez Canal on Steam Navigation'. Available at: http://scholar.colorado.edu/cgi/viewcontent.cgi?article=1873&context=honr_theses.

Siemens PLM Software (2016) 'EHP v11.06 User Guide'.

Skogman, A. (1985) 'The Practical Meaning of Lateral Balance for a Sail-assisted Research Vessel', *Journal of Wind Engineering and Industrial Aerodynamics*, 20(1–3), pp. 201–226. doi: 10.1016/0167-6105(85)90019-4.

Smith, E. W. (1978) *Passenger Ships of the World: Past and Present*. 2nd edn. Boston, MA: George H. Dean Company.

Smuggling Act (Geo. III C.47) (1782). Cambridge, UK.

Steel, D. (1805) *The Shipwright's Vade Mecum*. London.

Steffy, J. R. (1994) 'Interpretation and Dissemination', in *Wooden Shipbuilding and the Interpretation of Shipwrecks*. London: Chatham Publishing, pp. 235–250.

Stevens, R. W. (1894) *On the Stowage of Ships and their Cargoes*. 7th edn. London: Longmans, Green and Co.

Stoot, W. F. (1959) 'Some Aspects of Naval Architecture in the Eighteenth Century', *Transactions of the Institution of Naval Architects*, pp. 31–42. doi: 10.3940/rina.trans.1959.03.

Tanner, P. (2013a) '3D Laser Scanning for the Digital Reconstruction and Analysis of a 16th-Century Clinker Built Sailing Vessel', in *ACUA Underwater Archaeology Proceedings*. Advisory Council on Underwater Archaeology, pp. 137–150.

Tanner, P. (2013b) *Digital Reconstruction and Analysis of the Newport Ship*. Cork, Ireland.

Tanner, P. (2018) 'The Testing and Analysis of Hypothetical Ship Reconstructions', in Litwin, J. (ed.) *Baltic and Beyond. Continuity and Change in Shipbuilding: Proceedings of the Fourteenth*

References

International Symposium on Boat and Ship Archaeology. Gdansk: National Maritime Museum, pp. 143–150.

Tezdogan, T. et al. (2015) ‘Full-scale unsteady RANS CFD simulations of ship behaviour and performance in head seas due to slow steaming’, *Ocean Engineering*, 97, pp. 186–206. doi: 10.1016/j.oceaneng.2015.01.011.

The Pall Mall Gazette (1866) ‘Occasional Notes’, 11 June, p. 9.

Toby, A. S. (1997) ‘U.S. High Speed Destroyers, 1919–1942: Hull Proportions (To the Edge of the Possible)’, *Naval Engineers Journal*, (May).

Tonnage Act (17 & 18 Vict. C.104) (1854). UK. Available at: https://laws.parliament.na/cms_documents/merchant-shipping-act-1854---part-1-f0c07d081e.pdf.

Tonry, C. E. H. et al. (2014) ‘Digital Modelling in the Performance Evaluation of 19th Century Clipper Ships: the Thermopylae and the Cutty Sark’, in *RINA Historic Ships*. London: Royal Institution of Naval Architects. doi: 10.3940/rina.hist.2014.05.

Tonry, C. E. H. et al. (2016) ‘Digital Modelling in the Evaluation of the Sinking of the HMS Victory (1737)’, in *RINA Historic Ships*. London: Royal Institution of Naval Architects, pp. 31–35.

Turnock, S. R. et al. (2006) ‘Application of simulation technology to the performance evaluation of HMS Victory as an exemplar of the ships at the battle of Trafalgar’, in *Technology of the Ships of Trafalgar*. Southampton.

Uden, G. and Cooper, R. (1980) *A Dictionary of British Ships and Seamen*. 1st edn. Harmondsworth: Allen Lane/Kestrel Books (Penguin Books Ltd).

Ville, S. (1993) ‘The Transition to Iron and Steel Construction’, in *Sail’s Last Century: The Merchant Sailing Ship 1830–1930*. London: Conway Maritime Press, pp. 52–72.

Wang, Y. and Feng, H.-Y. (2016) ‘Effects of scanning orientation on outlier formation in 3D laser scanning of reflective surfaces’, *Optics and Lasers in Engineering*, 81, pp. 35–45. doi: 10.1016/j.optlaseng.2016.01.003.

Watson, D. G. M. (1998) *Practical Ship Design (Elsevier Ocean Engineering)*. Oxford: Elsevier.

Watson, D. and Gilfillan, A. W. (1977) ‘Some Ship Design Methods’, *Transactions RINA*, p. 46.

Webster, C., Sims, C. and Means, B. (2015) ‘3D Scanning and Printing - Episode 19’. Archaeotech Podcast. Available at: <https://www.mixcloud.com/archaeotechpodcast-archaeology/3d-scanning-and-printing-episode-19/>.

Weymouth, G. D., Wilson, R. V. and Stern, F. (2005) ‘RANS Computational Fluid Dynamics Predictions of Pitch and Heave Ship Motions in Head Seas’, *Journal of ship research*, 49(2), pp. 80–97.

Whipple, A. B. C. (1980) *The Seafarers: The Clipper Ships*. Edited by J. Hicks. Amsterdam: Time-Life Books.

White, W. H. (1877) *A Manual of Naval Architecture*. London: John Murray.

Whitewright, J. (2011) ‘The Potential Performance of Ancient Mediterranean Sailing Rigs’, *International Journal of Nautical Archaeology*, 40(1), pp. 2–17. doi: 10.1111/j.1095-9270.2010.00276.x.

References

Wildish, J. G. (1872) 'The elements of Design affecting the Sailing Qualities of Ships, with Special Reference to the Ships of our Navy', *Transactions of the Institution of Naval Architects*, XIII, pp. 67–82. doi: 10.3940/rina.trans.1872.09.

Wilkinson, C. (2009) *British Logbooks in UK Archives 17th –19th Centuries: A survey of the range, selection and suitability of British logbooks and related documents for climatic research*.

Wolfson Unit (2016) 'Wolfson Suite 2016 PowerPrediction'. Wolfson Unit.

Woolley, J. (1860) 'On the Present State of the Mathematical Theory of Naval Architecture', *Transactions of the Institution of Naval Architects*, I, pp. 10–38.

Zou, L., Larsson, L. and Orych, M. (2010) 'Verification and validation of CFD predictions for a manoeuvring tanker', *Journal of Hydrodynamics*. Publishing House for Journal of Hydrodynamics, 22(5 SUPPL. 1), pp. 421–428. doi: 10.1016/S1001-6058(09)60233-X.

Appendix A VPP Calculations

A.1 Holtrop Resistance Estimation

$$R_T = R_F(1 + k_1) + R_{APP} + R_W + R_B + R_{TR} + R_A \quad (44)$$

$$1 + k_1 = 0.93 + 0.487118c_{14}(B/L)^{1.06806}(T/L)^{0.46706}(L/L_R)^{0.121563} \\ (L^3/\nabla)^{0.36486}(1 - C_P)^{-0.604247} \quad (45)$$

$$L_R = L(1 - C_P + 0.06C_P lcb/(4C_P - 1)) \quad (46)$$

$$C_{14} = 1 + 0.011C_{Stern} \quad (47)$$

Afterbody Form	C_{Stern}
Pram with gondola	-25
V-shaped sections	-10
Normal section shape	0
U-shaped sections with Hogner stern	10

For $F_n > 0.55$:

$$R_{W-B} = c_{17} c_2 c_5 \nabla \rho_W g \exp\{m_3 F_n^d m_4 \cos(\lambda F_n^{-2})\} \quad (48)$$

Where:

$$c_{17} = 6919.3 C_M^{-1.3346} (\nabla/L^3)^{2.00977} (L/B - 2)^{1.40692} \quad (49)$$

$$m_3 = -7.2035(B/L)^{0.326869}(T/B)^{0.605375} \quad (50)$$

$$c_2 = \exp(-1.89\sqrt{c_3}) \quad (51)$$

$$c_5 = (1 - 0.8 A_T/(BT C_M)) \quad (52)$$

$$\begin{aligned} \lambda &= 1.446C_P - 0.03L/B \\ &\text{when } L/B > 12 \\ \lambda &= 1.446C_P - 0.36 \\ &\text{when } L/B > 12 \end{aligned} \quad (53)$$

$$d = -0.9 \quad (54)$$

$$c_3 = 0.56 A_{BT}^{1.5} / \{BT(0.31\sqrt{A_{BT}} + T_F - h_B)\} \quad (55)$$

$$m_4 = c_{15} 0.4 \exp(-0.034F_n^{-3.29}) \quad (56)$$

Appendix A

$$\begin{aligned}
c_{15} &= -1.69385 \\
\text{when } L^3/\nabla &< 512 \\
c_{15} &= -1.69385 + (L/\nabla^{1/3} - 8)/2.36 \\
\text{when } 512 &< L^3/\nabla < 1726.91 \\
c_{15} &= 0 \\
\text{when } L^3/\nabla &> 1726.91
\end{aligned} \tag{57}$$

For $F_n < 0.4$:

$$R_{W-A} = c_1 c_2 c_5 \nabla \rho_W g \exp\{m_1 F_n^d m_4 \cos(\lambda F_n^{-2})\} \tag{58}$$

Where:

$$c_1 = 2223105 c_7^{3.78613} (T/B)^{1.07961} (90 - i_E)^{-1.37565} \tag{59}$$

$$\begin{aligned}
c_7 &= 0.229577 (B/L)^{0.33333} \\
\text{when } B/L &< 0.11 \\
c_7 &= B/L \\
\text{when } 0.11 &< B/L < 0.25 \\
c_7 &= 0.5 - 0.0625 L/B \\
\text{when } B/L &> 0.25
\end{aligned} \tag{60}$$

$$m_1 = 0.0140407 L/T - 1.75254 \nabla^{1/3}/L - 4.79323 B/L - c_{16} \tag{61}$$

$$\begin{aligned}
c_{16} &= 8.07981 C_P - 13.8673 C_P^2 + 6.984388 C_P^3 \\
\text{when } C_P &< 0.8 \\
c_{16} &= 1.73014 - 0.7067 C_P \\
\text{when } C_P &> 0.8
\end{aligned} \tag{62}$$

For $0.4 < F_n < 0.55$:

$$R_W = R_{W-A_{0.4}} + (10F_n - 4) (R_{W-B_{0.55}} - R_{W-A_{0.4}})/1.5 \tag{63}$$

A.2 Fung Resistance Estimation

$$R_T = R_F + R_R \tag{64}$$

$$R_R = C_R^{-1} / 2 \rho_W WSAV_S^2 \tag{65}$$

$$C_R = \exp \left\{ \sum_{i=1}^n \left[B_i \prod_{j=1}^9 \left(x_j^{c_{ij}} \right) \right] \right\} \tag{66}$$

Where:

$$x_1 = F_n^{-0.7} \tag{67}$$

$$x_2 = \cos(\lambda F_n^{-1.93}) \exp(-0.2/F_n^2) \tag{68}$$

$$x_3 = \{0.034977 [\Delta/(L_{WL}/100)^3]\}^{0.5} \tag{69}$$

Appendix A

$$x_4 = A_{20}/A_M \quad (70)$$

$$x_5 = C_P^2 \quad (71)$$

$$x_6 = B_{20}/B_M \quad (72)$$

$$x_7 = B_M/T_M \quad (73)$$

$$x_8 = \ln(90 - i_E) \quad (74)$$

$$x_9 = C_M \quad (75)$$

$$\lambda = 0.75C_P + 0.035\Delta/(L_{WL}/100)^3 \quad (76)$$

Regression Coefficients:

n	B _i	x ₁	x ₂	x ₃	x ₄	x ₅	x ₆	x ₇	x ₈	x ₉
0	-0.076885	0	0	0	0	0	0	0	0	0
1	-5.38179	1	0	0	0	0	0	0	0	0
2	-7.3172	0	1	0	0	0	0	0	0	0
3	4.0212	0	0	1	0	0	0	0	0	0
4	-3.01541	0	0	0	1	0	0	0	0	0
5	-3.30347	0	0	0	0	0	1	0	0	0
6	-0.356016	0	0	0	0	0	0	1	0	0
7	-0.78642	0	0	0	0	0	0	0	1	0
8	0.521915	2	0	0	0	0	0	0	0	0
9	3.67289	1	1	0	0	0	0	0	0	0
10	-0.526597	1	0	1	0	0	0	0	0	0
11	3.66578	1	0	0	1	0	0	0	0	0
12	2.98649	1	0	0	0	1	0	0	0	0
13	2.98314	1	0	0	0	0	1	0	0	0
14	0.322491	1	0	0	0	0	0	1	0	0
15	1.30663	1	0	0	0	0	0	0	0	1
16	2.19508	0	2	0	0	0	0	0	0	0
17	6.39624	0	1	0	1	0	0	0	0	0
18	3.35822	0	1	0	0	1	0	0	0	0
19	0.303679	0	1	0	0	0	0	1	0	0
20	-1.4792	0	1	0	0	0	0	0	0	1
21	-0.937577	0	0	2	0	0	0	0	0	0
22	0.865737	0	0	1	1	0	0	0	0	0
23	-0.554399	0	0	1	0	1	0	0	0	0
24	0.588584	0	0	1	0	0	1	0	0	0
25	-0.139506	0	0	1	0	0	0	1	0	0
26	0.693635	0	0	1	0	0	0	0	0	1
27	-7.49626	0	0	0	1	0	1	0	0	0
28	-0.619228	0	0	0	1	0	0	1	0	0
29	2.03959	0	0	0	0	1	1	0	0	0
30	0.34546	0	0	0	0	1	0	1	0	0

Appendix A

n	B _i	x ₁	x ₂	x ₃	x ₄	x ₅	x ₆	x ₇	x ₈	x ₉
31	-5.49323	0	0	0	0	1	0	0	0	1
32	0.251484	0	0	0	0	0	1	1	0	0
33	-0.946722	0	0	0	0	0	1	0	0	1
34	0.666034	0	0	0	0	0	0	0	0	2
35	-0.635371	2	0	0	1	0	0	0	0	0
36	-0.25757	2	0	0	0	0	1	0	0	0
37	-0.021711	2	0	0	0	0	0	1	0	0
38	0.566362	1	2	0	0	0	0	0	0	0
39	-0.438407	1	1	1	0	0	0	0	0	0
40	-2.17903	1	1	0	1	0	0	0	0	0
41	-0.11578	1	1	0	0	0	0	1	0	0
42	0.179566	1	0	2	0	0	0	0	0	0
43	-0.429466	1	0	1	1	0	0	0	0	0
44	-0.279766	1	0	1	0	0	1	0	0	0
45	0.0317788	1	0	1	0	0	0	1	0	0
46	-0.343553	1	0	1	0	0	0	0	0	1
47	-2.27502	1	0	0	2	0	0	0	0	0
48	3.63388	1	0	0	1	0	1	0	0	0
49	-0.108805	1	0	0	1	0	0	1	0	0
50	-2.5626	1	0	0	0	1	1	0	0	0
51	-0.118863	1	0	0	0	0	1	1	0	0
52	-0.18464	1	0	0	0	0	0	1	0	1
53	-0.261647	0	2	1	0	0	0	0	0	0
54	-3.81958	0	2	0	0	1	0	0	0	0
55	0.122566	0	1	2	0	0	0	0	0	0
56	-0.280095	0	1	1	0	0	1	0	0	0
57	-0.033813	0	1	1	0	0	0	1	0	0
58	0.328726	0	1	1	0	0	0	0	0	1
59	-5.60445	0	1	0	1	1	0	0	0	0
60	0.403458	0	1	0	0	0	2	0	0	0
61	0.780698	0	1	0	0	0	1	0	0	1
62	0.361519	0	0	2	1	0	0	0	0	0
63	0.0332259	0	0	2	0	0	0	1	0	0
64	-0.973847	0	0	1	2	0	0	0	0	0
65	-0.161135	0	0	1	1	0	0	1	0	0
66	4.18896	0	0	0	2	1	0	0	0	0
67	0.76225	0	0	0	2	0	0	1	0	0
68	1.59206	0	0	0	1	0	2	0	0	0
69	0.776198	0	0	0	1	0	0	1	0	1

A.3 Kijima (1990) Side Force Estimation

$$Y_\lambda = (0.5\pi k + 1.4C_B B/L) \left(\frac{1+2t}{3T} \right) \quad (77)$$

$$Y_{\lambda\lambda} = 2.5(1 - C_B)^T B + 0.5 \quad (78)$$

$$S = 0.5\rho LTV_S^2 (Y_\lambda \lambda + Y_{\lambda\lambda} \lambda |\lambda|) \quad (79)$$

Where:

$$k = \frac{2T}{L} \quad (80)$$

A.4 Victory Sail Force Estimations

$$Windage C_L = -0.1762\alpha^4 + 1.15\alpha^3 - 2.3662\alpha^2 + 1.5418\alpha + 0.0145 \quad (81)$$

$$Windage C_D = -0.2429\alpha^4 + 1.5308\alpha^3 - 2.8875\alpha^2 + 1.7616\alpha + 0.0179 \quad (82)$$

$$Jib C_L = -2.794\alpha^2 + 7.5172\alpha - 3.0915 \quad (83)$$

$$Jib C_D = -2.1744\alpha^2 + 6.6501\alpha - 3.726 \quad (84)$$

$$Driver C_L = -0.4698\alpha^2 + 1.173\alpha - 0.1077 \quad (85)$$

$$Driver C_D = -0.6115\alpha^3 - 3.0175\alpha^2 - 3.5805\alpha + 1.4662 \quad (86)$$

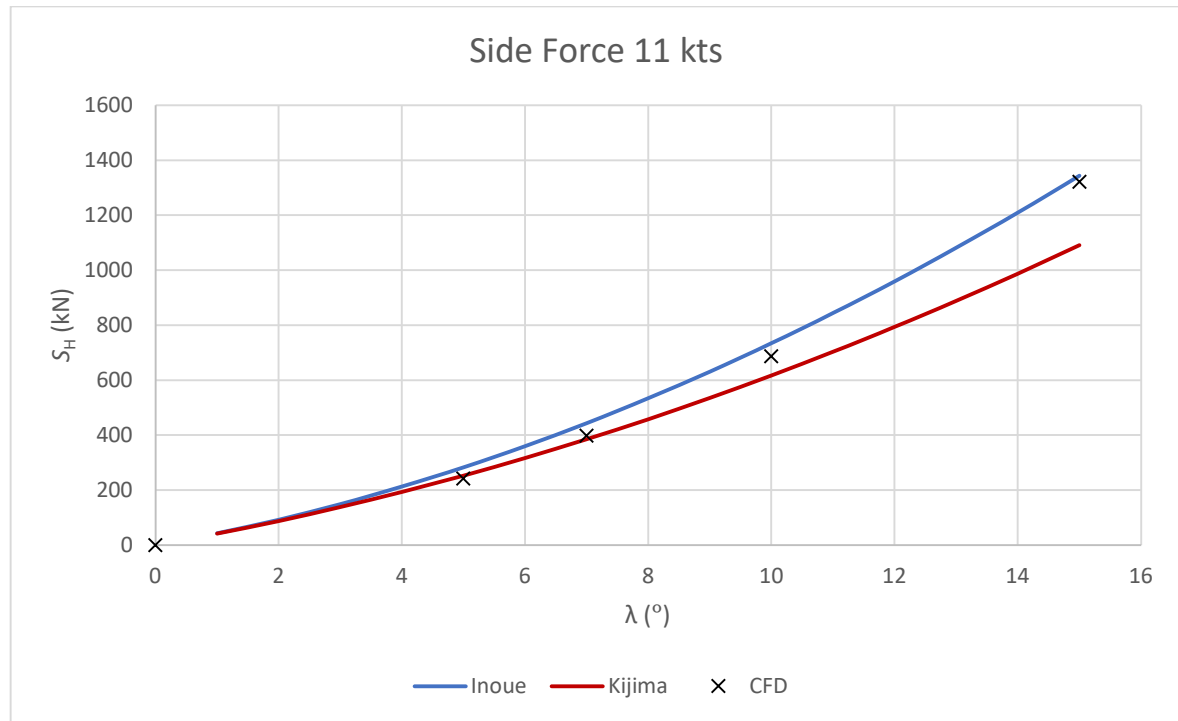
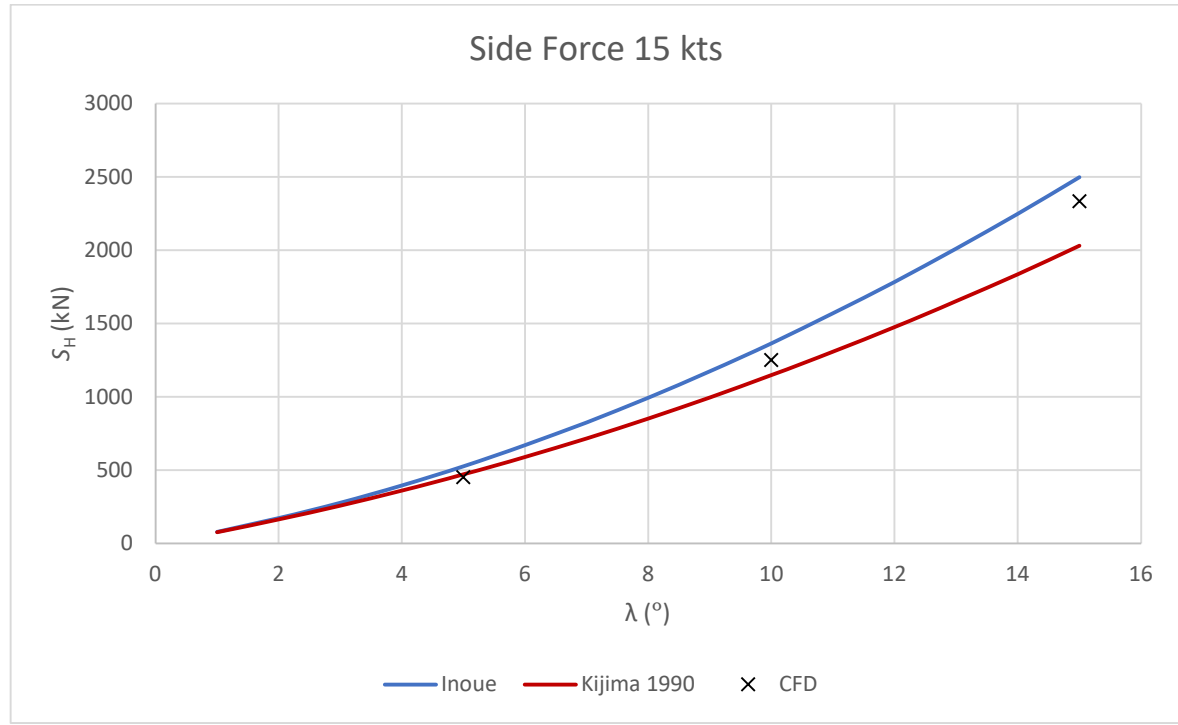
$$Main C_L = -2.5528\alpha^2 + 3.7977\alpha + 0.5674 \quad (87)$$

$$Main C_D = -0.0141\alpha^3 - 0.7776\alpha^2 + 3.2405\alpha + 0.0793 \quad (88)$$

$$Mizzen C_L = -2.745\alpha^2 + 5.3629\alpha - 0.6103 \quad (89)$$

$$Mizzen C_D = +1.5308\alpha^3 - 2.8875\alpha^2 + 1.7616\alpha - 0.8899 \quad (90)$$

$$C_L, C_D = \frac{L_X, D_X}{\frac{1}{2} \rho_A A_S V_A^2} \quad (91)$$

A.5 *Storm Cloud Validation*Figure 117: Comparison of S_H from CFD with estimated S_H for *Storm Cloud* at $V_s = 11$ knFigure 118: Comparison of S_H from CFD with estimated S_H for *Storm Cloud* at $V_s = 15$ kn

Appendix A

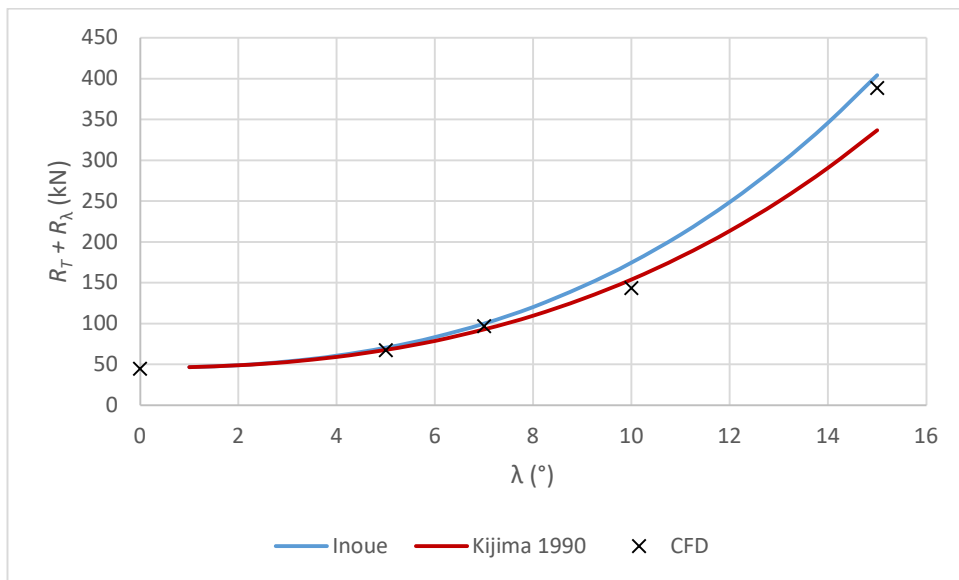


Figure 119: Estimated $R_T + R_\lambda$ compared to $R_T + R_\lambda$ for Storm Cloud at $V_s = 11$ kn

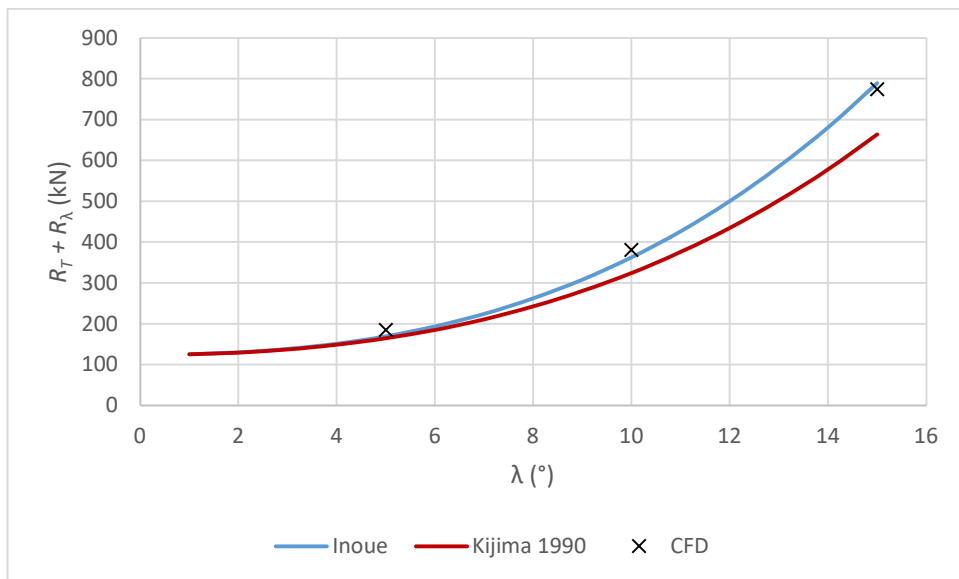


Figure 120: Estimated $R_T + R_\lambda$ compared to $R_T + R_\lambda$ for Storm Cloud at $V_s = 15$ kn

Appendix B Ship Data

Ship Name:	Acasta		Year:	1845	No.	23018
Builder:	Alexander Hall & Sons		Model:	N/A		
Owner:	Benjamin Moir		Lines:	BI		
Reg. Port:	Aberdeen		Structure Report:	LRF		
Material:	Wood		Sail Plan:	BI		
Use:	Cargo		Engine Details	Literature	Estimated	
Engine:	Sail		Total Sail Area (m ²)			915.54
Sail Type:	Barque		Engine IHP (HP)			
Propeller:	-		Engine NHP			
Particulars	Literature	Measured	Tonnage			
L _{BP} (m)	39.11	39.11	GM (pre-1836):	385.16		
L _{LWL} (m)		38.14	nm (pre-1854):			
D _M (m)		6.04	GRT:	385.00		
B _{WL} (m)	7.80	7.75	NRT:	385.00		
T _{Load} (m)		4.98	Weight (tonnes)	Literature	Estimated	
▽ (m ³)		816.57	Cargo			418.64
WSA (m ²)		490.16	Crew			0.90
LCB (m)		-0.29	Lightship			216.00
C _B		0.56	Machinery			
C _P		0.67	Notes: One of the first ships to have an Aberdeen Bow to reduce tonnage according to 1836 rules. Lines reconstructed from diagram on tonnage. Sail plan from spar dimensions.			
C _M		0.83				
C _{WP}		0.82				
A _M (m ²)		31.86				
A _{WP} (m ²)		242.22				
i _E (°)		26.69	Sources: (MacGregor, 1988), LR, clydeships.co.uk			
V _{S_VT30} (kn)		13.76				
V _{S_Steam} (kn)						

Appendix B

Ship Name:	Afon Alaw	Year:	1891	No.	99346
Builder:	Alexander Stephen & Sons	Model:		N/A	
Owner:	Hughes & Co. Menai Bridge	Lines:		(Greenhill, 1980)	
Reg. Port:	Liverpool	Structure Report:		N/A	
Material:	Steel	Sail Plan:		N/A	
Use:	Cargo	Engine Details	Literature	Estimated	
Engine:	Sail	Total Sail Area (m ²)			3185.08
Sail Type:	Barque	Engine IHP (HP)			
Propeller:		Engine NHP			
Particulars	Literature	Measured	Tonnage		
L _{BP} (m)	86.69	86.69	ton (pre-1836):		
L _{LWL} (m)		85.81	nm (pre-1854):		
D _M (m)	7.70	8.75	GRT:		2052.00
B _{BWL} (m)	12.50	12.71	NRT:		1947.00
T _{Load} (m)	6.07	6.40	Weight (tonnes)	Literature	Estimated
Δ (m ³)		4608.04	Cargo		2117.10
WSA (m ²)		1664.37	Crew		3.60
LCB (m)		-0.11	Lightship		955.15
C _B		0.66	Machinery		
C _P		0.75	Notes: Original lines plan. Sources: (Greenhill, 1980), clydeships.co.uk		
C _M		0.89			
C _{WP}		0.81			
A _M (m ²)		72.04			
A _{WP} (m ²)		877.47			
i _E (°)		20.60			
V _{S_VT30} (kn)		17.63			
V _{S_Steam} (kn)					

Appendix B

Ship Name:	Alexandra	Year:	1863	No.	47411
Builder:	Thames Ironworks and Shipbuilding Company	Model:		NMM	
Owner:	London & Mediterranean Steam Navigation Company	Lines:		N/A	
Reg. Port:	London	Structure Report:	LRF		
Material:	Iron	Sail Plan:	N/A		
Use:	Cargo	Engine Details	Literature	Estimated	
Engine:	Steam	Total Sail Area (m ²)			679.37
Sail Type:	Schooner	Engine IHP (HP)			634.10
Propeller:	Single Screw	Engine NHP	150		
Particulars	Literature	Measured	Tonnage		
L _{BP} (m)	64.01	64.01	ton (pre-1836):		
L _{WL} (m)		62.86	nm (pre-1854):		
D _M (m)	6.04	5.94	GRT:		813.00
B _{WL} (m)	9.14	8.96	NRT:		618.00
T _{Load} (m)		4.51	Weight (tonnes)	Literature	Estimated
▽ (m ³)	1458.78	1454.35	Cargo	510.06	525.36
WSA (m ²)		819.48	Crew	1.73	1.73
LCB (m)		-0.39	Lightship	492.78	488.74
C _B		0.57	Machinery	121.93	121.93
C _P	0.20	0.66	Notes: Details on the back of model. One of several ships of same name built that year. Sources: test.marinersmuseum.org, NMM, LR, Merchant Navy Lists (MNL)		
C _M		0.88			
C _{WP}		0.80			
A _M (m ²)	34.86	35.21			
A _{WP} (m ²)		451.69			
i _E (°)		16.76			
V _{S_VT30} (kn)	10.90	13.53			
V _{S_Steam} (kn)	10.90	10.75			

Appendix B

Ship Name:	Anaces	Year:	1897	No.	105579
Builder:	Russell & Co.	Model:	GRM		
Owner:	G. T. Soley & Co. Ltd.	Lines:	N/A		
Reg. Port:	Greenock	Structure Report:	N/A		
Material:	Steel	Sail Plan:	N/A		
Use:	Cargo	Engine Details	Literature	Estimated	
Engine:	Steam	Total Sail Area (m ²)			1057.98
Sail Type:	Schooner	Engine IHP (HP)			1353.8
Propeller:	Single Screw	Engine NHP		208	
Particulars	Literature	Measured	Tonnage		
L _{BP} (m)	94.40	94.40	ton (pre-1836):		
L _{LWL} (m)		93.07	nm (pre-1854):		
D _M (m)	6.96	8.14	GRT:		2535.00
B _{BWL} (m)	13.44	13.48	NRT:		1633.00
T _{Load} (m)	5.74	5.74	Weight (tonnes)	Literature	Estimated
Δ (m ³)		5720.59	Cargo		1775.67
WSA (m ²)		1926.55	Crew		1.80
LCB (m)		0.48	Lightship		1021.59
C _B		0.80	Machinery		202.65
C _P		0.82	Notes: Sources: clydeships.co.uk		
C _M		0.99			
C _{WP}		0.87			
A _M (m ²)		74.64			
A _{WP} (m ²)		1076.09			
i _E (°)		23.17			
V _{S_VT30} (kn)		12.54			
V _{S_Steam} (kn)		10.61			

Appendix B

Ship Name:	Ancona	Year:	1893	No.	102118
Builder:	Russell & Co.	Model:	NMM		
Owner:	The Ship Ancona Co Ltd	Lines:	N/A		
Reg. Port:	Liverpool	Structure Report:	LRF		
Material:	Steel	Sail Plan:	N/A		
Use:	Cargo	Engine Details	Literature	Estimated	
Engine:	Sail	Total Sail Area (m ²)		3518.26	
Sail Type:	Barque	Engine IHP (HP)			
Propeller:	-	Engine NHP			
Particulars	Literature	Measured	Tonnage		
L _{BP} (m)	85.40	85.40	ton (pre-1836):		
L _{WL} (m)		81.46	nm (pre-1854):		
D _M (m)	7.47	8.47	GRT:		2852.00
B _{WL} (m)	13.66	13.98	NRT:		2570.00
T _{Load} (m)	6.52	6.52	Weight (tonnes)	Literature	Estimated
▽ (m ³)	6273.60	5244.65	Cargo		2794.53
WSA (m ²)		1796.26	Crew		4.88
LCB (m)		0.83	Lightship		806.52
C _B		0.71	Machinery		
C _P		0.77	Notes: Sources: NMM, clydeships.co.uk, LR		
C _M		0.93			
C _{WP}		0.85			
A _M (m ²)		83.74			
A _{WP} (m ²)		966.29			
i _E (°)		27.11			
V _{S_VT30} (kn)		16.84			
V _{S_Steam} (kn)					

Appendix B

Ship Name:	Ann Duthie	Year:	1868	No.	60686
Builder:	Duthie, Sons & Co.	Model:		N/A	
Owner:	John Duthie and Sons and Company	Lines:		(MacGregor, 1984b)	
Reg. Port:	Aberdeen	Structure Report:	LRF		
Material:	Wood	Sail Plan:		(MacGregor, 1984b)	
Use:	Cargo	Engine Details	Literature	Estimated	
Engine:	Sail	Total Sail Area (m ²)			1756.93
Sail Type:	Ship	Engine IHP (HP)			
Propeller:	-	Engine NHP			
Particulars	Literature	Measured	Tonnage		
L _{BP} (m)	61.77	60.96	ton (pre-1836):		
L _{LWL} (m)		58.48	nm (pre-1854):		
D _M (m)	6.22	7.01	GRT:		993.00
B _{WL} (m)	10.73	10.49	NRT:		993.00
T _{Load} (m)		5.94	Weight (tonnes)	Literature	Estimated
▽ (m ³)		2075.53	Cargo		1079.76
WSA (m ²)		970.39	Crew		1.80
LCB (m)		0.03	Lightship		413.67
C _B		0.57	Machinery		
C _P		0.70	Notes: Lines from half model. Sail plan reconstructed. Sources:(MacGregor, 1984a, 1988), LR aberdeenships.com		
C _M		0.82			
C _{WP}		0.81			
A _M (m ²)		50.95			
A _{WP} (m ²)		494.38			
i _E (°)		23.96			
V _{S_VT30} (kn)		16.00			
V _{S_Steam} (kn)					

Appendix B

Ship Name:	Aphrodita	Year:	1858	No.	21497
Builder:	Josiah Jones Jnr	Model:		N/A	
Owner:	Jones, Palmer & Co.	Lines:		(MacGregor, 1984b)	
Reg. Port:	Liverpool	Structure Report:		N/A	
Material:	Iron	Sail Plan:		(MacGregor, 1984b)	
Use:	Cargo	Engine Details	Literature	Estimated	
Engine:	Sail	Total Sail Area (m ²)			2004.50
Sail Type:	Ship	Engine IHP (HP)			
Propeller:	-	Engine NHP			
Particulars	Literature	Measured	Tonnage		
L _{BP} (m)	66.05	68.58	om (pre-1836):		
L _{WL} (m)		68.05	nm (pre-1854):		1427.00
D _M (m)		8.23	GRT:		1663.00
B _{WL} (m)	11.06	10.77	NRT:		1601.00
T _{Load} (m)		6.10	Weight (tonnes)	Literature	Estimated
▽ (m ³)		3366.92	Cargo		1740.87
WSA (m ²)		1292.52	Crew		3.00
LCB (m)		0.04	Lightship		610.68
C _B		0.76	Machinery		
C _P		0.80	Notes: Original register length probably length of keel. Designed to carry cargo over speed (MacGregor 1988, p.150). Lines and sail plan copies of original. Sources: (MacGregor, 1984a, 1988), LR, NMM, MNL		
C _M		0.96			
C _{WP}		0.85			
A _M (m ²)		61.77			
A _{WP} (m ²)		614.13			
i _E (°)		23.23			
V _{S_VT30} (kn)		15.12			
V _{S_Steam} (kn)					

Appendix B

Ship Name:	Arab	Year:	1839	No.	-
Builder:	James Geddie	Model:	N/A		
Owner:	Wemyss	Lines:	(MacGregor, 1984a)		
Reg. Port:	Fraserburgh	Structure Report:	N/A		
Material:	Wood	Sail Plan:	(MacGregor, 1984a)		
Use:	Cargo	Engine Details	Literature	Estimated	
Engine:	Sail	Total Sail Area (m ²)		696.21	
Sail Type:	Barque	Engine IHP (HP)			
Propeller:	-	Engine NHP			
Particulars	Literature	Measured	Tonnage		
L _{BP} (m)	27.79	27.58	ton (pre-1836):		
L _{WL} (m)		27.70	nm (pre-1854):	269.00	
D _M (m)		5.79	GRT:		
B _{WL} (m)	7.34	7.34	NRT:		
T _{Load} (m)		4.42	Weight (tonnes)	Literature	Estimated
Δ (m ³)		527.87	Cargo		274.57
WSA (m ²)		361.64	Crew		0.75
LCB (m)		0.69	Lightship		164.15
C _B		0.59	Machinery		
C _P		0.71	Notes: Sources: (MacGregor, 1984a), LR		
C _M		0.84			
C _{WP}		0.86			
A _M (m ²)		26.95			
A _{WP} (m ²)		173.17			
i _E (°)		43.32			
V _{S_VT30} (kn)		11.59			
V _{S_Steam} (kn)					

Appendix B

Ship Name:	SS Arab	Year:	1879	No.	76846
Builder:	J & G Thomson	Model:	GRM		
Owner:	Union Steam Ship Co.	Lines:	N/A		
Reg. Port:	Southampton	Structure Report:	LRF		
Material:	Iron	Sail Plan:	N/A		
Use:	Cargo	Engine Details	Literature	Estimated	
Engine:	Steam	Total Sail Area (m ²)			1211.02
Sail Type:	Schooner	Engine IHP (HP)			2650.45
Propeller:	Single Screw	Engine NHP	500		
Particulars	Literature	Measured	Tonnage		
L _{BP} (m)	106.68	106.68	ton (pre-1836):		
L _{WL} (m)		106.62	nm (pre-1854):		
D _M (m)	9.45	9.45	GRT:		3170.00
B _{WL} (m)	12.25	12.19	NRT:		2044.00
T _{Load} (m)		6.10	Weight (tonnes)	Literature	Estimated
▽ (m ³)		4850.70	Cargo		2222.58
WSA (m ²)		1884.22	Crew		3.23
LCB (m)		-0.13	Lightship		1348.93
C _B		0.62	Machinery		396.75
C _P		0.68	Notes: Beam scaled independently Sources: (Smith, 1978), clydeships.co.uk, LR		
C _M		0.91			
C _{WP}		0.79			
A _M (m ²)		66.72			
A _{WP} (m ²)		1017.60			
i _E (°)		16.35			
V _{S_VT30} (kn)	13.00	14.35			
V _{S_Steam} (kn)	13.00	13.72			

Appendix B

Ship Name:	Australia	Year:	1826	No.	
Builder:	Adams	Model:	N/A		
Owner:	Scott & Co.	Lines:	BI		
Reg. Port:	London	Structure Report:	LRF		
Material:	Wood	Sail Plan:	N/A		
Use:	Cargo	Engine Details	Literature	Estimated	
Engine:	Sail	Total Sail Area (m ²)		721.20	
Sail Type:	Barque	Engine IHP (HP)			
Propeller:	-	Engine NHP			
Particulars	Literature	Measured	Tonnage		
L _{BP} (m)	30.75	30.75	ton (pre-1836):	373.17	
L _{LWL} (m)		33.19	nm (pre-1854):		
D _M (m)		6.58	GRT:		
B _{BWL} (m)	8.44	8.39	NRT:		
T _{Load} (m)	5.18	5.64	Weight (tonnes)	Literature	Estimated
▽ (m ³)		871.44	Cargo		453.28
WSA (m ²)		496.48	Crew		0.90
LCB (m)		0.27	Lightship		254.75
C _B		0.56	Machinery		
C _P		0.70	Notes: Sources: (MacGregor, 1988), NMM, MNL, LR, Buckler's Hard Maritime Museum		
C _M		0.81			
C _{WP}		0.85			
A _M (m ²)		37.62			
A _{WP} (m ²)		234.55			
i _E (°)		44.08			
V _{S_VT30} (kn)		11.10			
V _{S_Steam} (kn)					

Appendix B

Ship Name:	Balfour	Year:	1809	No.	2275
Builder:	T & J Brocklebank	Model:		N/A	
Owner:		Lines:		Bl	
Reg. Port:		Structure Report:		N/A	
Material:	Wood	Sail Plan:		N/A	
Use:		Engine Details	Literature	Estimated	
Engine:	Sail	Total Sail Area (m ²)			527.39
Sail Type:	Brig	Engine IHP (HP)			
Propeller:	-	Engine NHP			
Particulars	Literature	Measured	Tonnage		
L _{BP} (m)	29.82	29.82	ton (pre-1836):		310.00
L _{WL} (m)		29.61	nm (pre-1854):		
D _M (m)		6.22	GRT:		
B _{WL} (m)	8.24	8.35	NRT:		
T _{Load} (m)	4.27	4.27	Weight (tonnes)	Literature	Estimated
▽ (m ³)		656.58	Cargo		341.52
WSA (m ²)		392.84	Crew		0.83
LCB (m)		0.95	Lightship		188.80
C _B		0.62	Machinery		
C _P		0.74	Notes: Sources: (MacGregor, 1980a), MNL, LR		
C _M		0.85			
C _{WP}		0.86			
A _M (m ²)		29.93			
A _{WP} (m ²)		211.84			
i _E (°)		45.42			
V _{S_VT30} (kn)		10.58			
V _{S_Steam} (kn)					

Appendix B

Ship Name:	Belle of Lagos	Year:	1868	No.	60092
Builder:	Alexander Stephen & Sons	Model:	N/A		
Owner:	George Eastee	Lines:	(MacGregor, 1984b)		
Reg. Port:	Liverpool	Structure Report:	LRF		
Material:	Iron	Sail Plan:	(MacGregor, 1984b)		
Use:	Cargo	Engine Details	Literature	Estimated	
Engine:	Sail	Total Sail Area (m ²)			680.02
Sail Type:	Barque	Engine IHP (HP)			
Propeller:	-	Engine NHP			
Particulars	Literature	Measured	Tonnage		
L _{BP} (m)	39.84	39.84	om (pre-1836):		
L _{LWL} (m)		37.79	nm (pre-1854):		
D _M (m)		4.11	GRT:		251.00
B _{BWL} (m)	7.32	7.34	NRT:		228.00
T _{Load} (m)	3.66	3.66	Weight (tonnes)	Literature	Estimated
V (m ³)	619.43	609.72	Cargo		247.92
WSA (m ²)		409.12	Crew		0.75
LCB (m)		0.44	Lightship		109.44
C _B		0.61	Machinery		
C _P		0.70	Notes: Lines and sail plan copies of original Sources: (MacGregor, 1984a), www.trytallshipping.co.uk , LR		
C _M		0.88			
C _{WP}		0.82			
A _M (m ²)		23.13			
A _{WP} (m ²)		223.54			
i _E (°)		28.76			
V _{S_VT30} (kn)		13.80			
V _{S_Steam} (kn)					

Appendix B

Ship Name:	Belle of the Clyde		Year:	1865	No.	51483					
Builder:	Alexander Stephen & Sons		Model:	N/A							
Owner:	George Eastee		Lines:	(MacGregor, 1984b)							
Reg. Port:	Liverpool		Structure Report:	LRF							
Material:	Iron		Sail Plan:	(MacGregor, 1984b)							
Use:	Cargo		Engine Details	Literature	Estimated						
Engine:	Sail		Total Sail Area (m ²)	611.52							
Sail Type:	Brig		Engine IHP (HP)								
Propeller:	-		Engine NHP								
Particulars	Literature	Measured	Tonnage								
L _{BP} (m)	35.05	34.14	ton (pre-1836):								
L _{WL} (m)		33.35	nm (pre-1854):	198.00							
D _M (m)		4.15	GRT:	199.00							
B _{WL} (m)	6.71	6.72	NRT:	199.00							
T _{Load} (m)		3.20	Weight (tonnes)	Literature	Estimated						
▽ (m ³)	426.17	424.62	Cargo	216.39							
WSA (m ²)		322.69	Crew	0.60							
LCB (m)		0.18	Lightship	84.64							
C _B		0.60	Machinery								
C _P		0.70	Notes: Lines and sail plan copies of original Sources: (MacGregor, 1984a), clydeships.co.uk, LR								
C _M		0.86									
C _{WP}		0.80									
A _M (m ²)		18.24									
A _{WP} (m ²)		178.45									
i _E (°)		29.21									
V _{S_VT30} (kn)		13.84									
V _{S_Steam} (kn)											

Appendix B

Ship Name:	Blenheim	Year:	1848	No.	23278
Builder:	T & W Smith	Model:	N/A		
Owner:	T & W Smith	Lines:	(MacGregor, 1984a)		
Reg. Port:	Newcastle	Structure Report:	LRF		
Material:	Wood	Sail Plan:	(MacGregor, 1984a)		
Use:	Cargo	Engine Details	Literature	Estimated	
Engine:	Sail	Total Sail Area (m ²)			2696.71
Sail Type:	Ship	Engine IHP (HP)			
Propeller:	-	Engine NHP			
Particulars	Literature	Measured	Tonnage		
L _{BP} (m)	53.34	53.34	ton (pre-1836):		1392.00
L _{LWL} (m)		53.67	nm (pre-1854):		1489.00
D _M (m)		9.30	GRT:		1314.00
B _{BWL} (m)	12.80	12.79	NRT:		1314.00
T _{Load} (m)		6.55	Weight (tonnes)	Literature	Estimated
▽ (m ³)		2545.82	Cargo		1428.80
WSA (m ²)		1039.36	Crew		2.40
LCB (m)		0.30	Lightship		504.87
C _B		0.57	Machinery		
C _P		0.75	Notes: East India Company. Lines from rigged model. Sail plan copy of original (?) Sources: (MacGregor, 1984a), tynedbuiltships.co.uk		
C _M		0.76			
C _{WP}		0.86			
A _M (m ²)		63.53			
A _{WP} (m ²)		585.44			
i _E (°)		41.18			
V _{S_VT30} (kn)		14.35			
V _{S_Steam} (kn)					

Appendix B

Ship Name:	Cairngorm	Year:	1853	No.	9971
Builder:	Alexander Hall & Sons	Model:		N/A	
Owner:	Jardine, Matheson & Co.	Lines:		(MacGregor, 1988)	
Reg. Port:	London	Structure Report:		LRF	
Material:	Wood	Sail Plan:		(MacGregor, 1988)	
Use:	Cargo	Engine Details	Literature	Estimated	
Engine:	Sail	Total Sail Area (m ²)			1920.56
Sail Type:	Ship	Engine IHP (HP)			
Propeller:	-	Engine NHP			
Particulars	Literature	Measured	Tonnage		
L _{BP} (m)	60.96	60.96	ton (pre-1836):		
L _{WL} (m)		58.02	nm (pre-1854):		1246.00
D _M (m)	6.25	7.77	GRT:		980.00
B _{WL} (m)	11.13	11.18	NRT:		939.00
T _{Load} (m)		5.91	Weight (tonnes)	Literature	Estimated
▽ (m ³)		1369.87	Cargo		874.11
WSA (m ²)		884.40	Crew		1.88
LCB (m)		0.17	Lightship		431.25
C _B		0.36	Machinery		
C _P		0.62	Notes: Lines from half model. Sail plan from spar dimensions. Sources: (MacGregor, 1988), clydeships.co.uk		
C _M		0.58			
C _{WP}		0.70			
A _M (m ²)		38.22			
A _{WP} (m ²)		450.73			
i _E (°)		18.51			
V _{S_VT30} (kn)		17.32			
V _{S_Steam} (kn)					

Appendix B

Ship Name:	Camertonian	Year:	1848	No.	-
Builder:	Peile, Scott & Co.	Model:	N/A		
Owner:	Isaac Scott	Lines:	(MacGregor, 1988)		
Reg. Port:	Workington	Structure Report:	N/A		
Material:	Wood	Sail Plan:	(MacGregor, 1988)		
Use:	Cargo	Engine Details	Literature	Estimated	
Engine:	Sail	Total Sail Area (m ²)			1258.11
Sail Type:	Ship	Engine IHP (HP)			
Propeller:	-	Engine NHP			
Particulars	Literature	Measured	Tonnage		
L _{BP} (m)	39.01	39.01	ton (pre-1836):		485.00
L _{LWL} (m)		40.57	nm (pre-1854):		543.00
D _M (m)		7.39	GRT:		
B _{BWL} (m)	8.76	8.60	NRT:		
T _{Load} (m)		5.41	Weight (tonnes)	Literature	Estimated
▽ (m ³)		891.21	Cargo		463.56
WSA (m ²)		566.91	Crew		1.13
LCB (m)		0.14	Lightship		293.19
C _B		0.49	Machinery		
C _P		0.72	Notes: Lines and sail plan from model Sources: (MacGregor, 1988), LR		
C _M		0.68			
C _{WP}		0.82			
A _M (m ²)		30.58			
A _{WP} (m ²)		277.78			
i _E (°)		34.25			
V _{S_VT30} (kn)		13.90			
V _{S_Steam} (kn)					

Appendix B

Ship Name:	Carnatic	Year:	1859	No.	27235
Builder:	Alexander Stephen & Sons	Model:	N/A		
Owner:	G. L. Munro	Lines:	BI		
Reg. Port:	London	Structure Report:	LRF		
Material:	Iron	Sail Plan:	BI		
Use:	Cargo	Engine Details	Literature	Estimated	
Engine:	Sail	Total Sail Area (m ²)			1242.39
Sail Type:	Barque	Engine IHP (HP)			
Propeller:	-	Engine NHP			
Particulars	Literature	Measured	Tonnage		
L _{BP} (m)	52.33	52.33	ton (pre-1836):		
L _{WL} (m)		51.64	nm (pre-1854):		566.00
D _M (m)		6.74	GRT:		604.00
B _{WL} (m)	8.26	8.25	NRT:		603.00
T _{Load} (m)		5.33	Weight (tonnes)	Literature	Estimated
▽ (m ³)		1384.55	Cargo		655.68
WSA (m ²)		760.61	Crew		1.28
LCB (m)		0.03	Lightship		363.05
C _B		0.61	Machinery		
C _P		0.68	Notes: Sources: clydeships.co.uk, LR		
C _M		0.89			
C _{WP}		0.82			
A _M (m ²)		39.18			
A _{WP} (m ²)		348.28			
i _E (°)		24.84			
V _{S_VT30} (kn)		14.77			
V _{S_Steam} (kn)					

Appendix B

Ship Name:	Cedarbank	Year:	1892	No.	99839
Builder:	Mackie & Thomson & Co.	Model:	NMM		
Owner:	A. Weir & Co.	Lines:	N/A		
Reg. Port:	Glasgow	Structure Report:	N/A		
Material:	Steel	Sail Plan:	N/A		
Use:	Cargo/Passenger	Engine Details	Literature	Estimated	
Engine:	Sail	Total Sail Area (m ²)			3669.06
Sail Type:	Barque	Engine IHP (HP)			
Propeller:	-	Engine NHP			
Particulars	Literature	Measured	Tonnage		
L _{BP} (m)	99.36	99.36	ton (pre-1836):		
L _{LWL} (m)		95.45	nm (pre-1854):		
D _M (m)	7.92	9.97	GRT:		2825.00
B _{WL} (m)	13.11	13.14	NRT:		2649.00
T _{Load} (m)	6.15	6.15	Weight (tonnes)	Literature	Estimated
Δ (m ³)		5359.76	Cargo	4877.03	2880.43
WSA (m ²)		1928.69	Crew	1.95	1.95
LCB (m)		0.29	Lightship		1250.24
C _B		0.70	Machinery		
C _P		0.80	Notes:		
C _M		0.88	Cargo from literature is coal		
C _{WP}		0.86	Sources: clydeships.co.uk, MNL, wrecksite.eu, LR, www.shippingtandy.com		
A _M (m ²)		70.27			
A _{WP} (m ²)		1066.59			
i _E (°)		22.23			
V _{S_VT30} (kn)		18.02			
V _{S_Steam} (kn)					

Appendix B

Ship Name:	City of Adelaide	Year:	1864	No.	50036
Builder:	Pile & Hay	Model:	N/A		
Owner:	Devitt & Moore	Lines:	BI		
Reg. Port:	London	Structure Report:	LRF		
Material:	Composite	Sail Plan:	BI		
Use:	Cargo/Passenger	Engine Details	Literature	Estimated	
Engine:	Sail	Total Sail Area (m ²)			1806.54
Sail Type:	Ship	Engine IHP (HP)			
Propeller:	-	Engine NHP			
Particulars	Literature	Measured	Tonnage		
L _{BP} (m)	53.89	52.49	ton (pre-1836):		
L _{WL} (m)		52.66	nm (pre-1854):		
D _M (m)	6.71	6.41	GRT:		807.00
B _{WL} (m)	10.17	9.91	NRT:		791.00
T _{Load} (m)	5.18	4.82	Weight (tonnes)	Literature	Estimated
▽ (m ³)		1311.97	Cargo		802.69
WSA (m ²)		749.57	Crew		1.58
LCB (m)		0.35	Lightship		291.19
C _B		0.52	Machinery		
C _P		0.69	Notes: Awaiting restoration in Adelaide, Australia. Tea clipper, supposedly faster than Cutty Sark. Sources: (Lubbock, 1921; MacGregor, 1984b), LR, sunderlandships.com, cityofadelade.org.au		
C _M		0.76			
C _{WP}		0.79			
A _M (m ²)		36.25			
A _{WP} (m ²)		409.52			
i _E (°)		26.65			
V _{S_VT30} (kn)		16.78			
V _{S_Steam} (kn)					

Appendix B

Ship Name:	Cumberland	Year:	1800	No.	-
Builder:	Daniel Brocklebank	Model:	N/A		
Owner:	John Hartley & Sons	Lines:	BI		
Reg. Port:		Structure Report:	LRF		
Material:	Wood	Sail Plan:	N/A		
Use:		Engine Details	Literature	Estimated	
Engine:	Sail	Total Sail Area (m ²)		831.48	
Sail Type:	Ship	Engine IHP (HP)			
Propeller:	-	Engine NHP			
Particulars	Literature	Measured	Tonnage		
L _{BP} (m)	30.02	28.90	ton (pre-1836):		340.96
L _{LWL} (m)		30.42	nm (pre-1854):		215.00
D _M (m)		6.10	GRT:		
B _{BWL} (m)	8.33	8.54	NRT:		
T _{Load} (m)	3.66	4.88	Weight (tonnes)	Literature	Estimated
Δ (m ³)		815.16	Cargo		424.01
WSA (m ²)		440.37	Crew		0.68
LCB (m)		0.34	Lightship		227.79
C _B		0.60	Machinery		
C _P		0.72	Notes: Sources: (MacGregor, 1980a), LR		
C _M		0.84			
C _{WP}		0.85			
A _M (m ²)		37.04			
A _{WP} (m ²)		222.17			
i _E (°)		49.57			
V _{S_VT30} (kn)		11.04			
V _{S_Steam} (kn)					

Appendix B

Ship Name:	Cutty Sark	Year:	1869	No.	63557
Builder:	Scott & Linton	Model:		From Lines	
Owner:	John & R D Willis	Lines:		(Lubbock, 1924)	
Reg. Port:	London	Structure Report:		LRF	
Material:	Composite	Sail Plan:		Bl	
Use:	Cargo	Engine Details	Literature	Estimated	
Engine:	Sail	Total Sail Area (m ²)	2972.90	2453.73	
Sail Type:	Ship	Engine IHP (HP)			
Propeller:	-	Engine NHP			
Particulars	Literature	Measured	Tonnage		
L _{BP} (m)	64.77	64.78	ton (pre-1836):		
L _{WL} (m)		65.21	nm (pre-1854):		
D _M (m)	6.83	7.54	GRT:		963.00
B _{WL} (m)	10.97	10.94	NRT:		921.00
T _{Load} (m)	6.10	6.10	Weight (tonnes)	Literature	Estimated
▽ (m ³)	2081.23	2088.00	Cargo	1168.45	1001.46
WSA (m ²)		1070.93	Crew	2.63	2.63
LCB (m)		-0.19	Lightship		503.81
C _B	0.48	0.49	Machinery		
C _P	0.19	0.62	Notes: Restored ship in dry dock in Greenwich, UK Sail driving force equivalent to 3000HP (The Clipper Ships - Seafarers). Lines from post-build survey in 1920s. Sources: (Lubbock, 1924), clydeships.co.uk, wikipedia.com, LR		
C _M	0.23	0.78			
C _{WP}	0.23	0.73			
A _M (m ²)	51.36	51.37			
A _{WP} (m ²)	525.92	517.35			
i _E (°)		16.83			
V _{S_VT30} (kn)	17.50	18.33			
V _{S_Steam} (kn)					

Appendix B

Ship Name:	Dunbar	Year:	1853	No.	-
Builder:	James Lang	Model:	N/A		
Owner:	Duncan Dunbar	Lines:	(MacGregor, 1984b)		
Reg. Port:	London	Structure Report:	LRF		
Material:	Wood	Sail Plan:	(MacGregor, 1984b)		
Use:	Cargo/Passenger	Engine Details	Literature	Estimated	
Engine:	Sail	Total Sail Area (m ²)			1987.09
Sail Type:	Ship	Engine IHP (HP)			
Propeller:	-	Engine NHP			
Particulars	Literature	Measured	Tonnage		
L _{BP} (m)	61.54	61.49	ton (pre-1836):		1171.00
L _{LWL} (m)		60.99	nm (pre-1854):		1321.00
D _M (m)		7.74	GRT:		1167.00
B _{BWL} (m)	10.67	10.61	NRT:		1167.00
T _{Load} (m)		5.82	Weight (tonnes)	Literature	Estimated
Δ (m ³)		2227.29	Cargo		1215.89
WSA (m ²)		1009.78	Crew	4.50	4.50
LCB (m)		0.27	Lightship		489.79
C _B		0.60	Machinery		
C _P		0.72	Notes: Lines from half model. Sail plan from spar dimensions. Sources: (MacGregor, 1984a), wrecksite.eu, sunderlandships.com, LR		
C _M		0.83			
C _{WP}		0.84			
A _M (m ²)		50.78			
A _{WP} (m ²)		538.74			
i _E (°)		28.89			
V _{S_VT30} (kn)		15.77			
V _{S_Steam} (kn)					

Appendix B

Ship Name:	Eastern Monarch	Year:	1856	No.	17553
Builder:	Alexander Stephen & Sons	Model:	GRM		
Owner:	Joseph Somes	Lines:	BI		
Reg. Port:	London	Structure Report:	LRF		
Material:	Wood	Sail Plan:	N/A		
Use:	Cargo/Passenger	Engine Details	Literature	Estimated	
Engine:	Sail	Total Sail Area (m ²)			2941.64
Sail Type:	Ship	Engine IHP (HP)			
Propeller:	-	Engine NHP			
Particulars	Literature	Measured	Tonnage		
L _{BP} (m)	72.85	72.85	ton (pre-1836):		
L _{WL} (m)		72.71	nm (pre-1854):		1849.00
D _M (m)		9.69	GRT:		1631.00
B _{WL} (m)	12.28	11.72	NRT:		1631.00
T _{Load} (m)		7.47	Weight (tonnes)	Literature	Estimated
▽ (m ³)		3562.57	Cargo		1773.5
WSA (m ²)		1452.97	Crew		2.93
LCB (m)		-0.03	Lightship		820.51
C _B		0.57	Machinery		
C _P		0.70	Notes: Largest wooden ship built in Britain at the time. Lines from half model. Sources: (MacGregor, 1984b), clydeships.co.uk, LR		
C _M		0.81			
C _{WP}		0.86			
A _M (m ²)		69.70			
A _{WP} (m ²)		712.88			
i _E (°)		25.16			
V _{S_VT30} (kn)		17.20			
V _{S_Steam} (kn)					

Appendix B

Ship Name:	Edmund Preston	Year:	1858	No.	26173
Builder:	Alexander Stephen & Sons	Model:	N/A		
Owner:	Edmund Preston	Lines:	(MacGregor, 1984b)		
Reg. Port:	Liverpool	Structure Report:	LRF		
Material:	Iron	Sail Plan:	(MacGregor, 1984b)		
Use:	Cargo	Engine Details	Literature	Estimated	
Engine:	Sail	Total Sail Area (m ²)			750.97
Sail Type:	Barque	Engine IHP (HP)			
Propeller:	-	Engine NHP			
Particulars	Literature	Measured	Tonnage		
L _{BP} (m)	46.94	48.04	om (pre-1836):		
L _{LWL} (m)		47.58	nm (pre-1854):		
D _M (m)		5.91	GRT:		489.54
B _{BWL} (m)	7.77	7.70	NRT:		489.00
T _{Load} (m)	4.72	4.72	Weight (tonnes)	Literature	Estimated
Δ (m ³)		1095.26	Cargo	1018.08	531.72
WSA (m ²)		622.22	Crew		1.05
LCB (m)		0.14	Lightship		246.57
C _B		0.63	Machinery		
C _P		0.73	Notes: Lines and sail plan copies of original Sources: (MacGregor, 1984a, 1984b), clydeships.co.uk, LR		
C _M		0.88			
C _{WP}		0.84			
A _M (m ²)		31.72			
A _{WP} (m ²)		308.38			
i _E (°)		24.51			
V _{S_VT30} (kn)		13.47			
V _{S_Steam} (kn)					

Appendix B

Ship Name:	Elissa	Year:	1877	No.	78726
Builder:	Alexander Hall & Co.	Model:		N/A	
Owner:	Henry Fowler Watt & Edward W Crossfield	Lines:		BI	
Reg. Port:	Liverpool	Structure Report:	LRF		
Material:	Iron	Sail Plan:	BI		
Use:	Cargo	Engine Details	Literature	Estimated	
Engine:	Sail	Total Sail Area (m ²)		1010.29	
Sail Type:	Barque	Engine IHP (HP)			
Propeller:	-	Engine NHP			
Particulars	Literature	Measured	Tonnage		
L _{BP} (m)	43.98	43.98	ton (pre-1836):		
L _{WL} (m)		42.67	nm (pre-1854):		
D _M (m)	4.72	4.82	GRT:	431.00	
B _{WL} (m)	8.56	8.61	NRT:	409.00	
T _{Load} (m)	4.27	4.27	Weight (tonnes)	Literature	Estimated
▽ (m ³)		943.72	Cargo		444.73
WSA (m ²)		543.44	Crew		0.98
LCB (m)		0.21	Lightship		148.73
C _B		0.60	Machinery		
C _P		0.70	Notes:		
C _M		0.87	Still seaworthy. Based in Galveston TX		
C _{WP}		0.79	Sources: clydeships.co.uk, wikipedia.com, LR		
A _M (m ²)		31.81			
A _{WP} (m ²)		291.09			
i _E (°)		26.50			
V _{S_VT30} (kn)		14.35			
V _{S_Steam} (kn)					

Appendix B

Ship Name:	Elizabeth	Year:	1832	No.	26645
Builder:	J M Hillhouse	Model:		N/A	
Owner:	Miles, Ford & Co.	Lines:		NMM	
Reg. Port:	Bristol	Structure Report:	LRF		
Material:	Wood	Sail Plan:		N/A	
Use:	Cargo	Engine Details	Literature	Estimated	
Engine:	Sail	Total Sail Area (m ²)			940.16
Sail Type:	Ship	Engine IHP (HP)			
Propeller:	-	Engine NHP			
Particulars	Literature	Measured	Tonnage		
L _{BP} (m)	35.03	36.45	ton (pre-1836):		445.47
L _{LWL} (m)		36.60	nm (pre-1854):		
D _M (m)		6.92	GRT:		
B _{BWL} (m)	8.23	9.14	NRT:		
T _{Load} (m)	5.49	5.49	Weight (tonnes)	Literature	Estimated
Δ (m ³)		1181.31	Cargo		614.46
WSA (m ²)		590.05	Crew		0.98
LCB (m)		0.39	Lightship		247.32
C _B		0.64	Machinery		
C _P		0.75	Notes: Not enough data for structural model in survey report. Sources: NMM, MNL, LR, (Bristol Record Society, 1950)		
C _M		0.85			
C _{WP}		0.89			
A _M (m ²)		42.91			
A _{WP} (m ²)		297.55			
i _E (°)		42.91			
V _{S_VT30} (kn)		11.55			
V _{S_Steam} (kn)					

Appendix B

Ship Name:	Farquharson		Year:	1820	No.	-			
Builder:	Gordon		Model:	N/A					
Owner:	EIC		Lines:	Bl/NMM					
Reg. Port:			Structure Report:	Lines					
Material:	Wood		Sail Plan:	Bl					
Use:	Cargo/Passenger		Engine Details	Literature	Estimated				
Engine:	Sail		Total Sail Area (m ²)	2378.24					
Sail Type:	Ship		Engine IHP (HP)						
Propeller:	-		Engine NHP						
Particulars	Literature	Measured	Tonnage						
L _{BP} (m)	52.12	52.12	ton (pre-1836):	1326.00					
L _{WL} (m)	51.97	51.41	nm (pre-1854):	1407.00					
D _M (m)		8.81	GRT:						
B _{BWL} (m)	13.03	13.03	NRT:						
T _{Load} (m)	6.57	6.43	Weight (tonnes)	Literature	Estimated				
▽ (m ³)		2644.63	Cargo	1191.19					
WSA (m ²)		1061.62	Crew	9.98	9.98				
LCB (m)		0.61	Lightship	453.27					
C _B		0.60	Machinery						
C _P		0.74	Notes: Modern half model to be found at the Cutty Sark in Greenwich. One of the last East Indamen to be built. Lines copy of original. Sail plan reconstructed by MacGregor. Sources: (MacGregor, 1980a), LR						
C _M		0.82							
C _{WP}		0.85							
A _M (m ²)		69.80							
A _{WP} (m ²)		571.96							
i _E (°)		38.59							
V _{S_VT30} (kn)	11.00	14.15							
V _{S_Steam} (kn)									

Appendix B

Ship Name:	Fusi Yama		Year:	1865	No.	52736			
Builder:	Alexander Stephen & Sons		Model:	N/A					
Owner:	Killick, Martin & Co.		Lines:	(MacGregor, 1988)					
Reg. Port:	London		Structure Report:	LRF					
Material:	Composite		Sail Plan:	(MacGregor, 1988)					
Use:	Cargo		Engine Details	Literature	Estimated				
Engine:	Sail		Total Sail Area (m ²)	1396.77					
Sail Type:	Barque		Engine IHP (HP)						
Propeller:	-		Engine NHP						
Particulars	Literature	Measured	Tonnage						
L _{BP} (m)	50.44	50.44	ton (pre-1836):						
L _{LWL} (m)		50.31	nm (pre-1854):						
D _M (m)		6.17	GRT:						
B _{BWL} (m)	8.56	8.59	NRT:						
T _{Load} (m)		4.88	Weight (tonnes)	Literature	Estimated				
Δ (m ³)		1194.82	Cargo	353.93	604.58				
WSA (m ²)		690.94	Crew	1.50	1.50				
LCB (m)		-0.08	Lightship	470.43	279.45				
C _B		0.58	Machinery						
C _P		0.68	Notes: Lightship given by MacGregor as 420 tons. Lines and sail plan traces of original. Sources: (MacGregor, 1988), wrecksite.eu, clydeships.co.uk, LR						
C _M		0.85							
C _{WP}		0.80							
A _M (m ²)		35.17							
A _{WP} (m ²)		339.07							
i _E (°)		24.38							
V _{S_VT30} (kn)		15.90							
V _{S_Steam} (kn)									

Appendix B

Ship Name:	SS Great Britain	Year:	1844	No.	25967
Builder:		Model:		N/A	
Owner:	Great Western Railway Company	Lines:		(Corlett, 1975)	
Reg. Port:	Bristol	Structure Report:		(Corlett, 1975)	
Material:	Iron	Sail Plan:		N/A	
Use:	Cargo/Passenger	Engine Details	Literature	Estimated	
Engine:	Steam	Total Sail Area (m ²)	1486.45	964.18	
Sail Type:	Schooner	Engine IHP (HP)	1800	1800.00	
Propeller:	Single Screw	Engine NHP	1000		
Particulars	Literature	Measured	Tonnage		
L _{BP} (m)	86.87	86.87	ton (pre-1836):		3443.00
L _{WL} (m)		87.36	nm (pre-1854):		1460.48
D _M (m)		10.01	GRT:		3270.00
B _{WL} (m)	15.39	15.39	NRT:		1795.00
T _{Load} (m)	5.49	5.49	Weight (tonnes)	Literature	Estimated
▽ (m ³)	3642.25	3640.87	Cargo	304.81	76.73
WSA (m ²)	1451.70	1479.79	Crew	9.75	9.75
LCB (m)	-0.01	-0.01	Lightship	1432.63	1435.16
C _B	0.51	0.50	Machinery	528.34	528.34
C _P	0.19	0.64	Notes:		
C _M	0.24	0.80	Restored Ship in dry dock in Bristol, UK		
C _{WP}	0.24	0.79	Sources: (Corlett, 1975), thegreatoceanliners.com, LR		
A _M (m ²)	66.88	65.53			
A _{WP} (m ²)	1056.31	1040.48			
i _E (°)	24.70	21.79			
V _{S_VT30} (kn)	13.67	13.71			
V _{S_Steam} (kn)	13.67	12.69			

Appendix B

Ship Name:	Hurricane	Year:	1853	No.	27179		
Builder:	Alexander Stephen & Sons	Model:	NMM				
Owner:	Clyde & Australian Shipping Co.	Lines:	(MacGregor, 1988)				
Reg. Port:	Glasgow	Structure Report:	LRF				
Material:	Iron	Sail Plan:	(MacGregor, 1988)				
Use:	Cargo/Passenger	Engine Details	Literature	Estimated			
Engine:	Sail	Total Sail Area (m ²)			1821.74		
Sail Type:	Ship	Engine IHP (HP)					
Propeller:	-	Engine NHP					
Particulars	Literature	Measured	Tonnage				
L _{BP} (m)	65.50	65.50	ton (pre-1836):		1110.00		
L _{LWL} (m)	64.01	64.67	nm (pre-1854):		979.00		
D _M (m)		6.58	GRT:		1198.00		
B _{WL} (m)	9.36	9.53	NRT:		1198.00		
T _{Load} (m)	5.72	5.72	Weight (tonnes)	Literature	Estimated		
V (m ³)	1989.12	1948.42	Cargo		1079.97		
WSA (m ²)		985.39	Crew		2.25		
LCB (m)		0.08	Lightship		392.03		
C _B		0.56	Machinery				
C _P		0.67	Notes:				
C _M		0.83	Lines and sail plan traces of original.				
C _{WP}		0.81					
A _M (m ²)		44.64	Sources: (MacGregor, 1988), clydeships.co.uk, LR				
A _{WP} (m ²)		490.25					
i _E (°)		21.20					
V _{S_VT30} (kn)	18.00	16.95					
V _{S_Steam} (kn)							

Appendix B

Ship Name:	Hydaspes	Year:	1872	No.	65730
Builder:	William Denny & Bros	Model:		NMM	
Owner:	Peninsular & Oriental Steam Navigation Company	Lines:		NMM (?)	
Reg. Port:	Glasgow	Structure Report:		N/A	
Material:	Iron	Sail Plan:		NMM (?)	
Use:	Cargo/Passenger	Engine Details	Literature	Estimated	
Engine:	Steam	Total Sail Area (m ²)		1254.37	
Sail Type:	Schooner	Engine IHP (HP)	2052	2052.00	
Propeller:	Single Screw	Engine NHP		450	
Particulars	Literature	Measured	Tonnage		
L _{BP} (m)	110.16	110.16	ton (pre-1836):		
L _{WL} (m)		110.31	nm (pre-1854):	2723.00	
D _M (m)	9.22	8.38	GRT:	2984.00	
B _{WL} (m)	11.99	11.74	NRT:	1891.00	
T _{Load} (m)	6.58	6.58	Weight (tonnes)	Literature	Estimated
▽ (m ³)		5225.31	Cargo		1893.54
WSA (m ²)		2040.30	Crew		3.00
LCB (m)		-0.29	Lightship		1277.18
C _B		0.62	Machinery		307.17
C _P		0.70	Notes: 2861m ³ for cargo Sister ship Cathay Sources: (Science and Art Department, 1878; Lyon, 1975), theshipslist.com		
C _M		0.89			
C _{WP}		0.79			
A _M (m ²)		67.83			
A _{WP} (m ²)		1021.56			
i _E (°)		13.86			
V _{S_VT30} (kn)	12.00	14.23			
V _{S_Steam} (kn)	12.00	12.56			

Appendix B

Ship Name:	Indian Empire	Year:	1896	No.	108154
Builder:	John Reid & Co.	Model:	NMM		
Owner:	George Duncan & Co. Empire Line	Lines:	N/A		
Reg. Port:	London	Structure Report:	N/A		
Material:	Steel	Sail Plan:	N/A		
Use:	Cargo	Engine Details	Literature	Estimated	
Engine:	Sail	Total Sail Area (m ²)		2609.73	
Sail Type:	Barque	Engine IHP (HP)			
Propeller:	-	Engine NHP			
Particulars	Literature	Measured	Tonnage		
L _{BP} (m)	78.24	78.24	ton (pre-1836):		
L _{LWL} (m)		76.70	nm (pre-1854):		
D _M (m)	7.32	7.74	GRT:		1738.00
B _{WL} (m)	12.07	11.50	NRT:		1614.00
T _{Load} (m)	5.82	5.82	Weight (tonnes)	Literature	Estimated
V (m ³)		3364.62	Cargo		1755.01
WSA (m ²)		1414.88	Crew	1.80	1.80
LCB (m)		0.04	Lightship		755.99
C _B		0.66	Machinery		
C _P		0.73	Notes: Length of model scaled by 55.68. Scanned with Morayshire Sources, NMM, wrecksite.eu, LR		
C _M		0.90			
C _{WP}		0.82			
A _M (m ²)		59.85			
A _{WP} (m ²)		724.70			
i _E (°)		22.45			
V _{S_VT30} (kn)		17.22			
V _{S_Steam} (kn)					

Appendix B

Ship Name:	John Garrow	Year:	1840	No.	34818
Builder:	John Ronalds & Co.	Model:	N/A		
Owner:	Anderson, Garrow & Co	Lines:	Bl		
Reg. Port:	Liverpool	Structure Report:	LRF		
Material:	Iron	Sail Plan:	N/A		
Use:	Cargo	Engine Details	Literature	Estimated	
Engine:	Sail	Total Sail Area (m ²)			1256.86
Sail Type:	Ship	Engine IHP (HP)			
Propeller:	-	Engine NHP			
Particulars	Literature	Measured	Tonnage		
L _{BP} (m)	39.65	41.27	ton (pre-1836):		556.00
L _{WL} (m)		43.22	nm (pre-1854):		711.00
D _M (m)		6.93	GRT:		
B _{BWL} (m)	9.14	9.36	NRT:		
T _{Load} (m)	5.03	5.03	Weight (tonnes)	Literature	Estimated
▽ (m ³)		1238.50	Cargo	1524.07	644.21
WSA (m ²)		658.91	Crew		1.43
LCB (m)		0.03	Lightship		172.75
C _B		0.60	Machinery		
C _P		0.78	Notes: One of the first completely iron sailing vessels. Draught of 9ft fwd, 10ft aft with 420 tons ballast. Not enough information for structural model. Lines from post-build extension. Sources: (MacGregor, 1984a), LR, MNL, wrecksite.eu		
C _M		0.77			
C _{WP}		0.89			
A _M (m ²)		36.51			
A _{WP} (m ²)		358.38			
i _E (°)		41.74			
V _{S_VT30} (kn)		12.73			
V _{S_Steam} (kn)					

Appendix B

Ship Name:	John Lidgett	Year:	1862	No.	45046
Builder:	Alexander Stephen & Sons	Model:	GRM		
Owner:	J Lidgett & Sons	Lines:	N/A		
Reg. Port:	London	Structure Report:	LRF		
Material:	Composite	Sail Plan:	BI		
Use:	Cargo	Engine Details	Literature	Estimated	
Engine:	Sail	Total Sail Area (m ²)			1617.94
Sail Type:	Ship	Engine IHP (HP)			
Propeller:	-	Engine NHP			
Particulars	Literature	Measured	Tonnage		
L _{BP} (m)	54.47	54.47	ton (pre-1836):		
L _{LWL} (m)		53.37	nm (pre-1854):		
D _M (m)		6.86	GRT:		770.00
B _{BWL} (m)	9.17	8.51	NRT:		770.00
T _{Load} (m)		5.46	Weight (tonnes)	Literature	Estimated
Δ (m ³)		1439.56	Cargo		837.27
WSA (m ²)		789.92	Crew	1.73	1.73
LCB (m)		0.13	Lightship		289.96
C _B		0.58	Machinery		
C _P		0.69	Notes: Sources: (MacGregor, 1984b), clydeships.co.uk, MNL, LR		
C _M		0.85			
C _{WP}		0.81			
A _M (m ²)		39.34			
A _{WP} (m ²)		366.17			
i _E (°)		24.27			
V _{S_VT30} (kn)		15.65			
V _{S_Steam} (kn)					

Appendix B

Ship Name:	Loch Broom	Year:	1885	No.	90017
Builder:	Barclay, Curle & Co.	Model:	NMM		
Owner:	General Shipping Co.	Lines:	N/A		
Reg. Port:	Glasgow	Structure Report:	LRF		
Material:	Iron	Sail Plan:	N/A		
Use:	Cargo	Engine Details	Literature	Estimated	
Engine:	Sail	Total Sail Area (m ²)			3851.13
Sail Type:	Ship	Engine IHP (HP)			
Propeller:	-	Engine NHP			
Particulars	Literature	Measured	Tonnage		
L _{BP} (m)	87.69	87.69	ton (pre-1836):		
L _{WL} (m)		85.50	nm (pre-1854):		
D _M (m)	7.77	8.44	GRT:		2128.00
B _{WL} (m)	12.95	12.95	NRT:		2075.00
T _{Load} (m)	6.11	6.11	Weight (tonnes)	Literature	Estimated
▽ (m ³)		4100.74	Cargo		2256.29
WSA (m ²)		1610.54	Crew		3.68
LCB (m)		0.39	Lightship		831.27
C _B		0.61	Machinery		
C _P		0.72	Notes: Sources: clydeships.co.uk, LR		
C _M		0.86			
C _{WP}		0.82			
A _M (m ²)		66.99			
A _{WP} (m ²)		895.62			
i _E (°)		21.75			
V _{S_VT30} (kn)		19.62			
V _{S_Steam} (kn)					

Appendix B

Ship Name:	Mabel Young	Year:	1877	No.	77050
Builder:	Alexander Stephen & Sons	Model:	N/A		
Owner:	Killick, Martin & Co.	Lines:	BI		
Reg. Port:	London	Structure Report:	LRF		
Material:	Iron	Sail Plan:	BI		
Use:	Cargo	Engine Details	Literature	Estimated	
Engine:	Sail	Total Sail Area (m ²)			1735.47
Sail Type:	Barque	Engine IHP (HP)			
Propeller:	-	Engine NHP			
Particulars	Literature	Measured	Tonnage		
L _{BP} (m)	61.87	61.87	ton (pre-1836):		
L _{LWL} (m)		61.52	nm (pre-1854):		
D _M (m)		6.86	GRT:		1046.00
B _{WL} (m)	10.21	10.11	NRT:		1016.00
T _{Load} (m)		5.49	Weight (tonnes)	Literature	Estimated
▽ (m ³)		2200.75	Cargo	1442.79	1103.89
WSA (m ²)		984.64	Crew	1.73	1.73
LCB (m)		0.16	Lightship		442.66
C _B		0.64	Machinery		
C _P		0.70	Notes: Lines and sail plan copies of original Sources: (MacGregor, 1984b), clydeships.co.uk		
C _M		0.91			
C _{WP}		0.83			
A _M (m ²)		50.89			
A _{WP} (m ²)		513.47			
i _E (°)		25.23			
V _{S_VT30} (kn)		15.96			
V _{S_Steam} (kn)					

Appendix B

Ship Name:	Maitland	Year:	1865	No.	53441
Builder:	William Pile	Model:		N/A	
Owner:	John R Kelso	Lines:		(MacGregor, 1988)	
Reg. Port:	North Shields	Structure Report:		LRF	
Material:	Composite	Sail Plan:		(MacGregor, 1988)	
Use:	Cargo	Engine Details	Literature	Estimated	
Engine:	Sail	Total Sail Area (m ²)			2203.47
Sail Type:	Ship	Engine IHP (HP)			
Propeller:	-	Engine NHP			
Particulars	Literature	Measured	Tonnage		
L _{BP} (m)	55.78	55.78	ton (pre-1836):		
L _{WL} (m)		54.67	nm (pre-1854):		754.60
D _M (m)		7.04	GRT:		798.20
B _{WL} (m)	10.67	10.44	NRT:		798.20
T _{Load} (m)		5.24	Weight (tonnes)	Literature	Estimated
▽ (m ³)		1598.02	Cargo		867.94
WSA (m ²)		818.08	Crew	1.65	1.65
LCB (m)		0.49	Lightship		315.12
C _B		0.54	Machinery		
C _P		0.65	Notes: Credited with achieving 15 kts, but apparently the master claimed 17 kts (MacGregor 1988, p.232). Lines from half model. Sail plan copy of original (?) Sources: (MacGregor, 1988), LR, sunderlandships.com		
C _M		0.83			
C _{WP}		0.77			
A _M (m ²)		45.24			
A _{WP} (m ²)		435.45			
i _E (°)		24.74			
V _{S_VT30} (kn)	17.00	16.82			
V _{S_Steam} (kn)					

Appendix B

Ship Name:	Marpesia	Year:	1866	No.	54960
Builder:	John Reid & Co.	Model:	GRM		
Owner:	Joseph Heap & Sons	Lines:	BI		
Reg. Port:	Liverpool	Structure Report:	LRF		
Material:	Iron	Sail Plan:	BI		
Use:	Cargo/Passenger	Engine Details	Literature	Estimated	
Engine:	Sail	Total Sail Area (m ²)			2729.48
Sail Type:	Ship	Engine IHP (HP)			
Propeller:	-	Engine NHP			
Particulars	Literature	Measured	Tonnage		
L _{BP} (m)	71.38	71.18	ton (pre-1836):		
L _{LWL} (m)		71.13	nm (pre-1854):		
D _M (m)		7.62	GRT:		1443.00
B _{BWL} (m)	11.70	11.74	NRT:		1443.00
T _{Load} (m)		5.91	Weight (tonnes)	Literature	Estimated
Δ (m ³)		2684.95	Cargo		1569.07
WSA (m ²)		1177.29	Crew		2.63
LCB (m)		0.08	Lightship		581.39
C _B		0.55	Machinery		
C _P		0.68	Notes: Sources: (MacGregor, 1984b, 1988), clydeships.co.uk, LR		
C _M		0.81			
C _{WP}		0.78			
A _M (m ²)		55.56			
A _{WP} (m ²)		646.26			
i _E (°)		20.94			
V _{S_VT30} (kn)		18.55			
V _{S_Steam} (kn)					

Appendix B

Ship Name:	Mermerus		Year:	1872	No.	67904
Builder:	Barclay, Curle & Co.		Model:	Private?		
Owner:	Golden Fleece Line		Lines:	BI		
Reg. Port:	Greenock		Structure Report:	LRF		
Material:	Iron		Sail Plan:	(MacGregor, 1988)		
Use:	Cargo		Engine Details	Literature	Estimated	
Engine:	Sail		Total Sail Area (m ²)	3251.33	3184.92	
Sail Type:	Ship		Engine IHP (HP)			
Propeller:	-		Engine NHP			
Particulars	Literature	Measured	Tonnage			
L _{BP} (m)	80.53	78.18	ton (pre-1836):			
L _{WL} (m)		77.37	nm (pre-1854):			
D _M (m)		7.96	GRT:	1750.00		
B _{WL} (m)	12.13	12.14	NRT:	1671.00		
T _{Load} (m)	6.65	6.65	Weight (tonnes)	Literature	Estimated	
▽ (m ³)	3716.59	3703.05	Cargo	2458.83	1816.99	
WSA (m ²)		1451.41	Crew		3.08	
LCB (m)		0.19	Lightship		750.42	
C _B	0.57	0.62	Machinery			
C _P		0.69	Notes:			
C _M		0.90	Lines copy of original. Sail plan copy of original (?)			
C _{WP}		0.81	Sources: (Lubbock, 1921; MacGregor, 1979, 1984a, 1988), clydeships.co.uk, LR			
A _M (m ²)		69.84				
A _{WP} (m ²)		727.11				
i _E (°)		20.96				
V _{S_VT30} (kn)		18.55				
V _{S_Steam} (kn)						

Appendix B

Ship Name:	Morayshire	Year:	1875	No.	73782
Builder:	Dobie & Co.	Model:	NMM		
Owner:	Thomas Law & Son	Lines:	N/A		
Reg. Port:	Glasgow	Structure Report:	LRF		
Material:	Iron	Sail Plan:	N/A		
Use:	Passenger	Engine Details	Literature	Estimated	
Engine:	Sail	Total Sail Area (m ²)			2706.03
Sail Type:	Ship	Engine IHP (HP)			
Propeller:	-	Engine NHP			
Particulars	Literature	Measured	Tonnage		
L _{BP} (m)	74.85	74.85	ton (pre-1836):		
L _{LWL} (m)		73.82	nm (pre-1854):		
D _M (m)		7.77	GRT:		1428.00
B _{WL} (m)	11.35	10.94	NRT:		1428.00
T _{Load} (m)	6.48	6.05	Weight (tonnes)	Literature	Estimated
Δ (m ³)		2972.90	Cargo		1552.76
WSA (m ²)		1261.95	Crew	1.95	1.95
LCB (m)		0.54	Lightship		581.51
C _B		0.63	Machinery		
C _P		0.70	Notes: Length of model scaled by 55.68 Scanned with Indian Empire. Sources: clydeships.co.uk, LR		
C _M		0.91			
C _{WP}		0.81			
A _M (m ²)		57.84			
A _{WP} (m ²)		630.81			
i _E (°)		23.02			
V _{S_VT30} (kn)		17.81			
V _{S_Steam} (kn)					

Appendix B

Ship Name:	Neilson	Year:	1824	No.	-
Builder:	Edward Adams	Model:	N/A		
Owner:	Laughton	Lines:	(MacGregor, 1988)		
Reg. Port:		Structure Report:	N/A		
Material:	Wood	Sail Plan:	(MacGregor, 1988)		
Use:	Cargo	Engine Details	Literature	Estimated	
Engine:	Sail	Total Sail Area (m ²)		602.64	
Sail Type:	Brig	Engine IHP (HP)			
Propeller:	-	Engine NHP			
Particulars	Literature	Measured	Tonnage		
L _{BP} (m)	27.84	27.84	ton (pre-1836):		232.01
L _{WL} (m)		27.78	nm (pre-1854):		
D _M (m)		5.64	GRT:		
B _{WL} (m)	7.36	7.31	NRT:		
T _{Load} (m)	4.27	4.27	Weight (tonnes)	Literature	Estimated
▽ (m ³)		493.05	Cargo		256.46
WSA (m ²)		341.10	Crew		0.68
LCB (m)		0.82	Lightship		161.63
C _B		0.57	Machinery		
C _P		0.71	Notes: Lines copy of original. Sail plan from spar dimensions. Sources: (MacGregor, 1984a, 1988), LR		
C _M		0.81			
C _{WP}		0.86			
A _M (m ²)		24.98			
A _{WP} (m ²)		172.46			
i _E (°)		49.77			
V _{S_VT30} (kn)		10.87			
V _{S_Steam} (kn)					

Appendix B

Ship Name:	Norham Castle		Year:	1869	No.	60427			
Builder:	Alexander Stephen & Sons		Model:	NMM					
Owner:	Thomas Skinner & Co.		Lines:	BI					
Reg. Port:	Glasgow		Structure Report:	LRF					
Material:	Composite		Sail Plan:	BI					
Use:	Cargo		Engine Details	Literature	Estimated				
Engine:	Sail		Total Sail Area (m ²)	1793.47					
Sail Type:	Ship		Engine IHP (HP)						
Propeller:	-		Engine NHP						
Particulars	Literature	Measured	Tonnage						
L _{BP} (m)	54.07	54.07	ton (pre-1836):						
L _{LWL} (m)		53.59	nm (pre-1854):						
D _M (m)	5.56	6.64	GRT:						
B _{BWL} (m)	9.51	9.53	NRT:						
T _{Load} (m)		5.33	Weight (tonnes)	Literature	Estimated				
Δ (m ³)		1546.00	Cargo						
WSA (m ²)		813.54	Crew						
LCB (m)		0.33	Lightship						
C _B		0.58	Machinery						
C _P		0.70	Notes: Original lines plan. Sail plan trace of original (?) Sources: clydeships.co.uk, LR, nzetc.victoria.ac.nz						
C _M		0.83							
C _{WP}		0.82							
A _M (m ²)		41.29							
A _{WP} (m ²)		413.19							
i _E (°)		26.04							
V _{S_VT30} (kn)		16.43							
V _{S_Steam} (kn)									

Appendix B

Ship Name:	Princess Royal	Year:	1841	No.	-
Builder:	J M Hilhouse	Model:	N/A		
Owner:	Hillhouse	Lines:	NMM		
Reg. Port:	Bristol	Structure Report:	LRF		
Material:	Wood	Sail Plan:	N/A		
Use:	Cargo	Engine Details	Literature	Estimated	
Engine:	Sail	Total Sail Area (m ²)		1118.33	
Sail Type:	Ship	Engine IHP (HP)			
Propeller:	-	Engine NHP			
Particulars	Literature	Measured	Tonnage		
L _{BP} (m)	35.66	35.66	ton (pre-1836):	543.00	
L _{WL} (m)		36.40	nm (pre-1854):	462.00	
D _M (m)		6.81	GRT:		
B _{WL} (m)	8.99	8.91	NRT:		
T _{Load} (m)		5.26	Weight (tonnes)	Literature	Estimated
▽ (m ³)		995.01	Cargo		517.56
WSA (m ²)		566.42	Crew		1.05
LCB (m)		0.18	Lightship		315.46
C _B		0.61	Machinery		
C _P		0.74	Notes: Sources: (MacGregor, 1984a), LR		
C _M		0.83			
C _{WP}		0.86			
A _M (m ²)		37.13			
A _{WP} (m ²)		264.39			
i _E (°)		43.89			
V _{S_VT30} (kn)		11.96			
V _{S_Steam} (kn)					

Appendix B

Ship Name:	Samaria		Year:	1868	No.	60370		
Builder:	J & G Thomson		Model:	GRM				
Owner:	The British & North American Royal Mail Steam Packet Company		Lines:	N/A				
Reg. Port:	Glasgow		Structure Report:	N/A				
Material:	Iron		Sail Plan:	N/A				
Use:	Cargo/Passenger		Engine Details	Literature	Estimated			
Engine:	Steam		Total Sail Area (m ²)	1099.37				
Sail Type:	Schooner		Engine IHP (HP)	1277.58				
Propeller:	Single Screw		Engine NHP	280				
Particulars	Literature	Measured	Tonnage					
L _{BP} (m)	97.72	97.72	Gross Tonnage (GRT):					
L _{LWL} (m)		95.99	Net Tonnage (NRT):					
D _M (m)	8.69	9.13	2602.00					
B _{WL} (m)	12.04	12.03	1694.00					
T _{Load} (m)	6.83	6.83	Weight (tonnes)					
Δ (m ³)		5220.51	Cargo:					
WSA (m ²)		1874.85	Crew:					
LCB (m)		0.17	Lightship:					
C _B		0.66	Machinery:					
C _P		0.73	1155.23					
C _M		0.91	191.24					
C _{WP}		0.83						
A _M (m ²)		74.28	Notes:					
A _{WP} (m ²)		953.50	Sources: (Smith, 1978), clydeships.co.uk, LR, theshipslist.com					
i _E (°)		18.23						
V _{S_VT30} (kn)	13.00	13.34						
V _{S_Steam} (kn)	13.00	10.87						

Appendix B

Ship Name:	Schomberg	Year:	1855	No.	26100
Builder:	Alexander Hall & Sons	Model:	GRM		
Owner:	James Baines & Co, Black Ball Line	Lines:	BI		
Reg. Port:	Liverpool	Structure Report:	N/A		
Material:	Wood	Sail Plan:	BI		
Use:	Cargo/Passenger	Engine Details	Literature	Estimated	
Engine:	Sail	Total Sail Area (m ²)		3279.27	
Sail Type:	Ship	Engine IHP (HP)			
Propeller:	-	Engine NHP			
Particulars	Literature	Measured	Tonnage		
L _{BP} (m)	75.50	75.50	ton (pre-1836):		
L _{WL} (m)		77.80	nm (pre-1854):	2284.00	
D _M (m)		9.75	GRT:		
B _{WL} (m)	13.87	13.51	NRT:		
T _{Load} (m)		7.01	Weight (tonnes)	Literature	Estimated
▽ (m ³)		3621.28	Cargo		1013.72
WSA (m ²)		1462.18	Crew	9.75	9.75
LCB (m)		-0.22	Lightship		720.25
C _B		0.49	Machinery		
C _P		0.63	Notes:		
C _M		0.79	Largest British Clipper (clipper ships). Wrecked on maiden voyage.		
C _{WP}		0.74	Half model does not match builder's plan (possibly an earlier version of the design)- MacGregor		
A _M (m ²)		74.10	Lines copy of original. Sail plan from spar dimensions.		
A _{WP} (m ²)		774.30			
i _E (°)		19.23			
V _{S_VT30} (kn)	15.50	19.09			
V _{S_Steam} (kn)			Sources: (MacGregor, 1988), clydeships.co.uk, MNL		

Appendix B

Ship Name:	Sea King	Year:	1863	No.	48547
Builder:	Alexander Stephen & Sons	Model:	GRM		
Owner:	Robertson & Co	Lines:	BI		
Reg. Port:	London	Structure Report:	N/A		
Material:	Composite	Sail Plan:	BI		
Use:	Cargo/Passenger	Engine Details	Literature	Estimated	
Engine:	Steam Aux	Total Sail Area (m ²)			2131.00
Sail Type:	Ship	Engine IHP (HP)	850		850.00
Propeller:	Single Screw	Engine NHP	200		
Particulars	Literature	Measured	Tonnage		
L _{BP} (m)	67.06	68.15	ton (pre-1836):		1126.48
L _{LWL} (m)	65.93	66.29	nm (pre-1854):		930.36
D _M (m)	6.86	7.44	GRT:		1018.00
B _{BWL} (m)	9.91	9.66	NRT:		790.00
T _{Load} (m)	6.02	5.94	Weight (tonnes)	Literature	Estimated
Δ (m ³)	2170.49	2130.99	Cargo		859.02
WSA (m ²)		1056.25	Crew	2.93	2.93
LCB (m)		0.35	Lightship		517.45
C _B	0.55	0.57	Machinery		127.24
C _P	0.22	0.69	Notes: Auxiliary Steamer. Lines and sail plan copies of original. Sources: (MacGregor, 1988), clydeships.co.uk, LR		
C _M	0.23	0.83			
C _{WP}	0.24	0.81			
A _M (m ²)	44.80	46.64			
A _{WP} (m ²)	510.93	509.71			
i _E (°)		20.40			
V _{S_VT30} (kn)	16.00	17.94			
V _{S_Steam} (kn)	9.00	10.77			

Appendix B

Ship Name:	Seringapatam	Year:	1837	No.	15867
Builder:	R&H Green	Model:	N/A		
Owner:	R&H Green	Lines:	Bl		
Reg. Port:	London	Structure Report:	N/A		
Material:	Wood	Sail Plan:	N/A		
Use:	Cargo/Passenger	Engine Details	Literature	Estimated	
Engine:	Sail	Total Sail Area (m ²)			1807.49
Sail Type:	Ship	Engine IHP (HP)			
Propeller:	-	Engine NHP			
Particulars	Literature	Measured	Tonnage		
L _{BP} (m)	45.29	45.29	ton (pre-1836):		818.00
L _{LWL} (m)		46.87	nm (pre-1854):		871.00
D _M (m)	6.71	8.32	GRT:		
B _{BWL} (m)	10.85	10.49	NRT:		
T _{Load} (m)		6.10	Weight (tonnes)	Literature	Estimated
▽ (m ³)		1844.00	Cargo		959.16
WSA (m ²)		807.00	Crew		1.65
LCB (m)		-0.13	Lightship		374.13
C _B		0.61	Machinery		
C _P		0.73	Notes: One of the first Blackwall Frigates. East India Company. Lines from model. Sources: (MacGregor, 1984a), MNL, LR, historic-shipping.co.uk		
C _M		0.84			
C _{WP}		0.85			
A _M (m ²)		53.84			
A _{WP} (m ²)		413.35			
i _E (°)		40.44			
V _{S_VT30} (kn)		13.49			
V _{S_Steam} (kn)					

Appendix B

Ship Name:	Servia	Year:	1881	No.	84172
Builder:	J & G Thomson	Model:	GRM		
Owner:	Cunard Steamship Co. Ltd.	Lines:	N/A		
Reg. Port:	Liverpool	Structure Report:	N/A		
Material:	Steel	Sail Plan:	N/A		
Use:	Passenger	Engine Details	Literature	Estimated	
Engine:	Steam	Total Sail Area (m ²)			1837.60
Sail Type:	Barque	Engine IHP (HP)	12000		12000.00
Propeller:	Single Screw	Engine NHP		1472	
Particulars	Literature	Measured	Tonnage		
L _{BP} (m)	156.97	156.97	ton (pre-1836):		
L _{LWL} (m)		156.02	nm (pre-1854):		
D _M (m)		12.34	GRT:		7392.00
B _{WL} (m)	15.88	15.52	NRT:		3971.00
T _{Load} (m)		8.53	Weight (tonnes)	Literature	Estimated
Δ (m ³)		13206.54	Cargo	4064.19	3404.55
WSA (m ²)		3725.64	Crew	18.90	18.90
LCB (m)		-0.04	Lightship		2474.66
C _B		0.65	Machinery		1796.29
C _P		0.71	Notes:		
C _M		0.92	Sources: theshiplist.com, clydeships.co.uk, LR, (Smith, 1978)		
C _{WP}		0.81			
A _M (m ²)		119.27			
A _{WP} (m ²)		1942.79			
i _E (°)		14.61			
V _{S_VT30} (kn)	17.80	17.88			
V _{S_Steam} (kn)	17.80	17.88			

Appendix B

Ship Name:	Sindia	Year:	1887	No.	93757
Builder:	Harland & Wolff	Model:		N/A	
Owner:	T & J Brocklebank	Lines:		(Lubbock, 1953)	
Reg. Port:	Liverpool	Structure Report:		N/A	
Material:	Steel	Sail Plan:		(Lubbock, 1953)	
Use:	Cargo	Engine Details	Literature	Estimated	
Engine:	Sail	Total Sail Area (m ²)			3748.30
Sail Type:	Ship	Engine IHP (HP)			
Propeller:		Engine NHP			
Particulars	Literature	Measured	Tonnage		
L _{BP} (m)	100.37	100.37	ton (pre-1836):		
L _{WL} (m)		99.48	nm (pre-1854):		
D _M (m)	8.69	8.84	GRT:		3067.00
B _{WL} (m)	13.78	13.76	NRT:		3067.00
T _{Load} (m)	6.71	6.71	Weight (tonnes)	Literature	Estimated
▽ (m ³)		6524.05	Cargo		3334.95
WSA (m ²)		2095.16	Crew		5.18
LCB (m)		0.22	Lightship		1171.52
C _B		0.70	Machinery		
C _P		0.78	Notes: Sources: (Lubbock, 1953b), theyard.info, LR		
C _M		0.93			
C _{WP}		0.84			
A _M (m ²)		84.32			
A _{WP} (m ²)		1133.36			
i _E (°)		20.60			
V _{S_VT30} (kn)		18.00			
V _{S_Steam} (kn)					

Appendix B

Ship Name:	Spindrift	Year:	1867	No.	58329
Builder:	Charles Connell & Co.	Model:		N/A	
Owner:	James Findlay	Lines:		(MacGregor, 1988)	
Reg. Port:	Glasgow	Structure Report:		LRF	
Material:	Composite	Sail Plan:		(MacGregor, 1988)	
Use:	Cargo	Engine Details	Literature	Estimated	
Engine:	Sail	Total Sail Area (m ²)			2685.34
Sail Type:	Ship	Engine IHP (HP)			
Propeller:	-	Engine NHP			
Particulars	Literature	Measured	Tonnage		
L _{BP} (m)	66.87	65.78	ton (pre-1836):		
L _{LWL} (m)	66.02	66.50	nm (pre-1854):		
D _M (m)		7.44	GRT:		
B _{BWL} (m)	11.16	10.91	NRT:		899.00
T _{Load} (m)	5.18	6.10	Weight (tonnes)	Literature	Estimated
Δ (m ³)		2103.53	Cargo		977.54
WSA (m ²)		1056.30	Crew	2.63	2.63
LCB (m)		-0.03	Lightship		425.93
C _B		0.49	Machinery		
C _P		0.64	Notes: Lines and sail plan from rigged model. Sources: (MacGregor, 1988), clydeships.co.uk, LR		
C _M		0.76			
C _{WP}		0.76			
A _M (m ²)		49.27			
A _{WP} (m ²)		542.53			
i _E (°)		19.21			
V _{S_VT30} (kn)		18.60			
V _{S_Steam} (kn)					

Appendix B

Ship Name:	Storm Cloud	Year:	1854	No.	23040
Builder:	Alexander Stephen & Sons	Model:		N/A	
Owner:	Alex Stephen	Lines:		(MacGregor, 1988)	
Reg. Port:	Glasgow	Structure Report:		LRF	
Material:	Iron	Sail Plan:		(MacGregor, 1988)	
Use:	Cargo	Engine Details	Literature	Estimated	
Engine:	Sail	Total Sail Area (m ²)			2003.75
Sail Type:	Ship	Engine IHP (HP)			
Propeller:	-	Engine NHP			
Particulars	Literature	Measured	Tonnage		
L _{BP} (m)	61.45	60.96	ton (pre-1836):		
L _{WL} (m)	59.53	59.87	nm (pre-1854):		
D _M (m)		6.78	GRT:		908.00
B _{WL} (m)	10.06	10.04	NRT:		797.00
T _{Load} (m)	4.80	5.49	Weight (tonnes)	Literature	Estimated
▽ (m ³)		1521.71	Cargo		866.63
WSA (m ²)		842.84	Crew		1.73
LCB (m)		-1.75	Lightship		441.32
C _B		0.44	Machinery		
C _P		0.55	Notes: Lines from offsets and plan. Sail plan trace of original. Sources: (MacGregor, 1979, 1988), clydeships.co.uk, LR		
C _M		0.81			
C _{WP}		0.70			
A _M (m ²)		46.17			
A _{WP} (m ²)		418.33			
i _E (°)		11.84			
V _{S_VT30} (kn)	17.00	17.30			
V _{S_Steam} (kn)					

Appendix B

Ship Name:	Stornoway	Year:	1850	No.	10520
Builder:	Alexander Hall & Sons	Model:	GRM		
Owner:	Jardine, Matheson & Co.	Lines:	BI		
Reg. Port:	London	Structure Report:	LRF		
Material:	Wood	Sail Plan:	BI		
Use:	Cargo	Engine Details	Literature	Estimated	
Engine:	Sail	Total Sail Area (m ²)			1079.58
Sail Type:	Ship	Engine IHP (HP)			
Propeller:	-	Engine NHP			
Particulars	Literature	Measured	Tonnage		
L _{BP} (m)	48.10	47.24	ton (pre-1836):		
L _{LWL} (m)		47.38	nm (pre-1854):		595.00
D _M (m)		6.40	GRT:		527.00
B _{BWL} (m)	8.78	8.64	NRT:		483.00
T _{Load} (m)		5.33	Weight (tonnes)	Literature	Estimated
Δ (m ³)		1129.51	Cargo		525.20
WSA (m ²)		679.33	Crew		1.13
LCB (m)		-0.13	Lightship		381.32
C _B		0.54	Machinery		
C _P		0.68	Notes: Sources: aberdeenships.com, (MacGregor, 1988), MNL, LR		
C _M		0.80			
C _{WP}		0.81			
A _M (m ²)		35.00			
A _{WP} (m ²)		315.79			
i _E (°)		23.66			
V _{S_VT30} (kn)		14.91			
V _{S_Steam} (kn)					

Appendix B

Ship Name:	Sunfoo		Year:	1871	No.	65572		
Builder:	Alexander Stephen & Sons		Model:	GRM				
Owner:	E M De Bussche		Lines:	N/A				
Reg. Port:	London		Structure Report:	LRF				
Material:	Iron		Sail Plan:	N/A				
Use:	Cargo/Passenger		Engine Details	Literature	Estimated			
Engine:	Steam		Total Sail Area (m ²)		884.82			
Sail Type:	Schooner		Engine IHP (HP)		1191.03			
Propeller:	Single Screw		Engine NHP	250				
Particulars	Literature	Measured	Tonnage					
L _{BP} (m)	80.50	80.50	ton (pre-1836):					
L _{WL} (m)		77.16	nm (pre-1854):					
D _M (m)		6.80	GRT:	1449.00				
B _{WL} (m)	10.09	10.00	NRT:	918.00				
T _{Load} (m)	3.96	3.96	Weight (tonnes)	Literature	Estimated			
▽ (m ³)		1704.95	Cargo		327.65			
WSA (m ²)		956.07	Crew	5.63	5.63			
LCB (m)		0.20	Lightship		666.63			
C _B		0.56	Machinery		178.29			
C _P		0.66	Notes: Sources: clydeships.co.uk, MNL, LR, trove.nl.gov.au, flotilla-australia.com					
C _M		0.86						
C _{WP}		0.76						
A _M (m ²)		33.54						
A _{WP} (m ²)		580.50						
i _E (°)		16.43						
V _{S_VT30} (kn)	9.43	14.83						
V _{S_Steam} (kn)	9.43	12.67						

Appendix B

Ship Name:	Taeping	Year:	1863	No.	47842
Builder:	Robert Steele & Co.	Model:		NMM	
Owner:	Richard Gilman of London, Alex Rodger, Glasgow & Charles Carnie, Blantyre	Lines:		BI	
Reg. Port:	Glasgow	Structure Report:	LRF		
Material:	Composite	Sail Plan:	N/A		
Use:	Cargo	Engine Details	Literature	Estimated	
Engine:	Sail	Total Sail Area (m ²)			1732.79
Sail Type:	Ship	Engine IHP (HP)			
Propeller:	-	Engine NHP			
Particulars	Literature	Measured	Tonnage		
L _{BP} (m)	55.99	55.99	ton (pre-1836):		
L _{WL} (m)		57.49	nm (pre-1854):		
D _M (m)		7.10	GRT:		767.00
B _{WL} (m)	9.48	9.13	NRT:		767.00
T _{Load} (m)		6.04	Weight (tonnes)	Literature	Estimated
▽ (m ³)		1744.92	Cargo	1253.80	834.01
WSA (m ²)		908.67	Crew	2.25	2.25
LCB (m)		0.01	Lightship		356.98
C _B		0.57	Machinery		
C _P		0.67	Notes:		
C _M		0.85	Tea clipper. Winner of 1866 Great Tea race.		
C _{WP}		0.82	Sources: (Science and Art Department, 1878; Clark, 1970), plimsoll.org, LR		
A _M (m ²)		45.15			
A _{WP} (m ²)		412.63			
i _E (°)		23.53			
V _{S_VT30} (kn)		16.52			
V _{S_Steam} (kn)					

Appendix B

Ship Name:	Thalia	Year:	1818	No.
Builder:	Balthazar Adams	Model:	N/A	
Owner:		Lines:	(MacGregor, 1988)	
Reg. Port:		Structure Report:	N/A	
Material:	Wood	Sail Plan:	N/A	
Use:	Cargo	Engine Details	Literature	Estimated
Engine:	Sail	Total Sail Area (m ²)		915.19
Sail Type:	Ship	Engine IHP (HP)		
Propeller:	-	Engine NHP		
Particulars	Literature	Measured	Tonnage	
L _{BP} (m)	30.18	30.48	ton (pre-1836):	357.00
L _{WL} (m)		30.23	nm (pre-1854):	
D _M (m)		6.77	GRT:	
B _{WL} (m)	8.74	8.54	NRT:	
T _{Load} (m)	4.88	4.88	Weight (tonnes)	Literature
▽ (m ³)		699.55	Cargo	363.87
WSA (m ²)		422.84	Crew	0.90
LCB (m)		1.16	Lightship	202.41
C _B		0.56	Machinery	
C _P		0.68	Notes: Lines copy of original. Sources: (MacGregor, 1984a, 1988), LR	
C _M		0.82		
C _{WP}		0.85		
A _M (m ²)		33.82		
A _{WP} (m ²)		218.11		
i _E (°)		51.99		
V _{S_VT30} (kn)		11.74		
V _{S_Steam} (kn)				

Appendix B

Ship Name:	Thermopylae		Year:	1868	No.	60688
Builder:	Walter Hood & Co.		Model:	N/A		
Owner:	George Thomson & Co.		Lines:	(MacGregor, 1988)		
Reg. Port:	Aberdeen		Structure Report:	LRF		
Material:	Composite		Sail Plan:	(MacGregor, 1988)		
Use:	Cargo		Engine Details	Literature	Estimated	
Engine:	Sail		Total Sail Area (m ²)	1627.66	2830.52	
Sail Type:	Ship		Engine IHP (HP)			
Propeller:	-		Engine NHP			
Particulars	Literature	Measured	Tonnage			
L _{BP} (m)	64.62	64.62	ton (pre-1836):			
L _{LWL} (m)	63.09	63.37	nm (pre-1854):			
D _M (m)	7.07	7.77	GRT:			
B _{BWL} (m)	10.97	10.74	NRT:			
T _{Load} (m)	5.94	6.32	Weight (tonnes)	Literature	Estimated	
Δ (m ³)	1952.45	1915.98	Cargo			
WSA (m ²)		1029.56	Crew			
LCB (m)		-0.26	Lightship			
C _B	0.46	0.46	Machinery			
C _P		0.63	Notes: Famous for racing against Cutty Sark in 1872. Lines from offsets. Sail plan copy of original. Sources: (White, 1877; Lubbock, 1924; MacGregor, 1988), clydeships.co.uk, aberdeenships.com			
C _M		0.73				
C _{WP}		0.75				
A _M (m ²)		47.69				
A _{WP} (m ²)		495.80				
i _E (°)		18.13				
V _{S_VT30} (kn)		18.10				
V _{S_Steam} (kn)						

Appendix B

Ship Name:	Titania		Year:	1866	No.	56745		
Builder:	Robert Steele & Co.		Model:	NMM				
Owner:	Richard H Shaw (Shaw, Lowther, Maxton & Phillipps)		Lines:	(MacGregor, 1988)				
Reg. Port:	London		Structure Report:	N/A				
Material:	Composite		Sail Plan:	(MacGregor, 1988)				
Use:	Cargo		Engine Details	Literature	Estimated			
Engine:	Sail		Total Sail Area (m ²)		2462.72			
Sail Type:	Ship		Engine IHP (HP)					
Propeller:	-		Engine NHP					
Particulars	Literature	Measured	Tonnage					
L _{BP} (m)	60.96	60.96	ton (pre-1836):					
L _{WL} (m)		61.30	nm (pre-1854):					
D _M (m)		7.39	GRT:					
B _{WL} (m)	10.97	10.89	NRT:					
T _{Load} (m)		5.94	Weight (tonnes)	Literature	Estimated			
▽ (m ³)		1907.90	Cargo		955.80			
WSA (m ²)		976.47	Crew		1.65			
LCB (m)		-0.02	Lightship		435.74			
C _B		0.50	Machinery					
C _P		0.66	Notes:					
C _M		0.76	Lines from half model. Sail plan from outline plan					
C _{WP}		0.77						
A _M (m ²)		47.16	Sources: clydeships.co.uk, LR					
A _{WP} (m ²)		496.25						
i _E (°)		20.60						
V _{S_VT30} (kn)		17.96						
V _{S_Steam} (kn)								

Appendix B

Ship Name:	Tszru	Year:	1869	No.	63558
Builder:	Alexander Stephen & Sons	Model:		N/A	
Owner:	Edward Munster de Bussche	Lines:		BI	
Reg. Port:	London	Structure Report:	LRF		
Material:	Composite	Sail Plan:		BI	
Use:	Cargo	Engine Details	Literature	Estimated	
Engine:	Steam	Total Sail Area (m ²)			526.80
Sail Type:	Schooner	Engine IHP (HP)			324.09
Propeller:	Single Screw	Engine NHP		70	
Particulars	Literature	Measured	Tonnage		
L _{BP} (m)	48.89	48.89	ton (pre-1836):		
L _{LWL} (m)		48.47	nm (pre-1854):		
D _M (m)		5.64	GRT:		431.00
B _{WL} (m)	7.04	7.05	NRT:		293.00
T _{Load} (m)	4.27	4.42	Weight (tonnes)	Literature	Estimated
Δ (m ³)		778.62	Cargo		318.60
WSA (m ²)		579.91	Crew		1.13
LCB (m)		0.43	Lightship		217.31
C _B		0.52	Machinery		48.51
C _P		0.65	Notes:		
C _M		0.80	Original lines and sail plan.		
C _{WP}		0.78	Sources: clydeships.co.uk, LR		
A _M (m ²)		24.57			
A _{WP} (m ²)		264.22			
i _E (°)		19.62			
V _{S_VT30} (kn)		13.69			
V _{S_Steam} (kn)		9.43			

Appendix B

Ship Name:	Vision		Year:	1853	No.	7068			
Builder:	Alexander Hall & Sons		Model:	GRM					
Owner:	J. Beazley		Lines:	(MacGregor, 1988)					
Reg. Port:	Liverpool		Structure Report:	LRF					
Material:	Wood		Sail Plan:	(MacGregor, 1988)					
Use:	Cargo		Engine Details	Literature	Estimated				
Engine:	Sail		Total Sail Area (m ²)	1487.88					
Sail Type:	Ship		Engine IHP (HP)						
Propeller:	-		Engine NHP						
Particulars	Literature	Measured	Tonnage						
L _{BP} (m)	51.82	51.82	ton (pre-1836):						
L _{WL} (m)		51.41	nm (pre-1854):	720.00					
D _M (m)		6.58	GRT:	563.00					
B _{WL} (m)	8.41	8.36	NRT:	563.00					
T _{Load} (m)		5.85	Weight (tonnes)	Literature	Estimated				
▽ (m ³)		1120.53	Cargo	612.19					
WSA (m ²)		717.31	Crew	1.20					
LCB (m)		-0.53	Lightship	243.61					
C _B		0.45	Machinery						
C _P		0.62	Notes:						
C _M		0.72	Model on display in Glasgow Riverside Museum						
C _{WP}		0.74	Lines from half model. Sail plan from spar dimensions						
A _M (m ²)		35.13	Sources: (MacGregor, 1988), clydeships.co.uk, aberdeenships.com						
A _{WP} (m ²)		317.66							
i _E (°)		16.12							
V _{S_VT30} (kn)		15.84							
V _{S_Steam} (kn)									

Appendix B

Ship Name:	Wendur	Year:	1884	No.	89956
Builder:	Charles Connell & Co.	Model:	NMM		
Owner:	Alexander MacKay & Co	Lines:	N/A		
Reg. Port:	Glasgow	Structure Report:	LRF		
Material:	Iron	Sail Plan:	N/A		
Use:	Cargo	Engine Details	Literature	Estimated	
Engine:	Sail	Total Sail Area (m ²)			3836.19
Sail Type:	Ship	Engine IHP (HP)			
Propeller:	-	Engine NHP			
Particulars	Literature	Measured	Tonnage		
L _{BP} (m)	89.21	89.21	ton (pre-1836):		
L _{LWL} (m)		88.44	nm (pre-1854):		
D _M (m)	7.85	8.53	GRT:		2045.00
B _{BWL} (m)	12.80	12.75	NRT:		1982.00
T _{Load} (m)		6.40	Weight (tonnes)	Literature	Estimated
Δ (m ³)		4360.27	Cargo	2942.47	2155.16
WSA (m ²)		1664.14	Crew	1.65	1.65
LCB (m)		0.19	Lightship		878.73
C _B		0.61	Machinery		
C _P		0.70	Notes: Steel Masts Sources: clydeships.co.uk, plimsoll.org, LR		
C _M		0.87			
C _{WP}		0.82			
A _M (m ²)		70.89			
A _{WP} (m ²)		917.31			
i _E (°)		21.50			
V _{S_VT30} (kn)		20.00			
V _{S_Steam} (kn)					

Appendix B

Ship Name:	Zeta	Year:	1865	No.	51109
Builder:	Alexander Stephen & Sons	Model:		N/A	
Owner:	Henry Bath & Sons	Lines:		Bl	
Reg. Port:	Swansea	Structure Report:		LRF	
Material:	Iron	Sail Plan:		Bl	
Use:	Cargo	Engine Details	Literature	Estimated	
Engine:	Steam Aux	Total Sail Area (m ²)			1256.61
Sail Type:	Barque	Engine IHP (HP)			392.54
Propeller:	Single Screw	Engine NHP	90		
Particulars	Literature	Measured	Tonnage		
L _{BP} (m)	56.39	56.39	ton (pre-1836):		
L _{WL} (m)		56.02	nm (pre-1854):		
D _M (m)		6.19	GRT:		734.00
B _{WL} (m)	8.53	8.59	NRT:		558.00
T _{Load} (m)		5.18	Weight (tonnes)	Literature	Estimated
▽ (m ³)		1543.76	Cargo		606.75
WSA (m ²)		799.43	Crew		1.43
LCB (m)		0.41	Lightship		314.13
C _B		0.63	Machinery		58.76
C _P		0.72	Notes: Auxiliary Steamer. Original Lines and sail plan. Sources: clydeships.co.uk, MNL, LR		
C _M		0.88			
C _{WP}		0.84			
A _M (m ²)		38.38			
A _{WP} (m ²)		394.18			
i _E (°)		24.77			
V _{S_VT30} (kn)		15.16			
V _{S_Steam} (kn)		9.12			

Appendix B

Appendix C Gantt Chart

